

**Time Series Analysis of High Resolution Remote Sensing Data  
to Assess Degradation of Vegetation Cover  
of the Island of Socotra (Yemen)**

**Dissertation**

To Fulfill the  
Requirements for the Degree of  
„Doctor of Philosophy“ (PhD)



---

**seit 1558**

**Submitted to the Council of the Faculty of Biology and Pharmacy  
of the Friedrich Schiller University Jena**

by

**M.Sc. Alhemiary, Abdulmaged**

born on 01.01.1968 in Taiz (Yemen)

Jena, October 2016

**Defense Date: 04.05.2017**

**PD Dr. Gottfried Jetschke**, Head of the Dendro Ecology Group, Institute of Ecology, Friedrich Schiller University Jena, Germany

**PD Dr. Sören Hese**, Head of the VHR Section, Institute for Geography, Department of Earth Observation, Friedrich Schiller University Jena, Germany

**Prof. Dr. Sebastian Schmidlein**, Heading the Vegetation Science and Biogeography Lab, Karlsruhe Institute of Technology, Institute of Geography and Geoecology

## Content

Introduction.....	III
Problem description .....	III
Objectives and aims of the study .....	V
Thesis Organization .....	VI
<b>Chapter 1: Theoretical background .....</b>	<b>1</b>
1.1. Characterization of ecosystems dynamics in semiarid regions .....	1
1.2. Vegetation changes and their explanatory factors based on remote sensing investigations .....	2
<b>Chapter 2: Study area and geographical location .....</b>	<b>7</b>
2.1 Physiographical characterisation and ecological zonation .....	8
2.2 Climatic characteristics .....	10
2.3 Soils Characteristics.....	11
2.4 Vegetation .....	12
2.5 Land use .....	14
<b>Chapter 3: Data used and data pre-processing .....</b>	<b>17</b>
3.1 Data collection.....	17
3.1 Rainfall data and pre-processing .....	17
3.2 Satellite data .....	19
3.3 Data pre-processing .....	24
3.3.1 Geometric corrections .....	25
3.3.2 Noise and de-stripping in image data.....	26
3.3.3 Atmospheric correction .....	26
3.3.4 Multi Date Cloud Masking and Gap Filling.....	28
3.3.5 Topographic data and DEM .....	29
3.4 Socio-economic data .....	29
3.5 Maps and Field data .....	29
<b>Chapter 4: Methodology of data analysis .....</b>	<b>31</b>
4.1. Variability of vegetation distribution and change in space and time .....	31
4.2. Methods of geostatistical analysis .....	31
4.2.1. Autocorrelation .....	31
4.2.2. Spatial autocorrelation .....	31
4.2.3. Kriging with an external drift.....	32
4.2.4. Convolution Spatial Filtering .....	32
4.2.5. Correlation coefficient.....	33
4.2.6. Multiple correlation coefficients .....	33
4.2.7. Simple linear regression model .....	33
4.2.8. Multiple linear regression model .....	34
4.2.9. Quantifying relationship between variables by analyzing spatial relationship .....	34
4.2.10. Geographically weighted regression (GWR) .....	35
4.3. Evaluation of vegetation cover's changes in relation to the driving forces.....	36
4.3.1. Post classification comparison .....	36

4.3.2.	Unsupervised Classification .....	37
4.3.3.	Supervised Classification.....	38
4.3.4.	Training stage and ground truth data.....	39
4.3.5.	Selection of Change Detection Algorithms .....	40
4.3.6.	Change detection methods and requirements .....	41
4.3.7.	Estimation of the vegetation activity trends.....	42
4.3.8.	Vegetation index differencing .....	43
4.3.9.	Vegetation covers change and its driving forces.....	44
4.3.10.	Recognition of rainfall and anthropogenic signals in the vegetation time-series .....	45
4.3.11.	Analysis of regression residuals for identification of areas experiencing anthropogenic impact .....	46
<b>Chapter 5: Results, part 1 – Analysis of climatic conditions and NDVI .....</b>		<b>47</b>
5.1.	Network of climate stations in the study region .....	47
5.2.	Statistical Analysis of Rainfall Data.....	47
5.2.1.	The inter-seasonal variability of rainfall.....	47
5.2.2.	Rainfalls variabilities and seasonal trends .....	50
5.2.3.	Within season trends of rainfall .....	53
5.3.	Variability of vegetation distribution.....	53
5.3.1.	Average characteristics of NDVI .....	53
5.3.2.	Inter annual variations difference vegetation index (NDVI).....	54
5.3.3.	Within season variations in NDVI .....	56
5.4.	Dynamics of vegetation activity and rainfall relationships .....	59
5.4.1.	Temporal behaviour of rainfall and vegetation within the growing season .....	59
5.4.2.	Temporal behaviour of rainfall and vegetation between the growing season.....	60
5.5.	Modelling spatial patterns in rainfall parameters.....	64
5.6.	Spatial distribution of (NDVI) and Rainfall in the study area .....	66
5.7.	Conclusion .....	67
<b>Chapter 6: Results, part 2 – Analysis of Vegetation Cover and Vegetation Change.....</b>		<b>69</b>
6.1.	Classification of vegetation and description of the mapped Classes.....	69
6.2.	Classification accuracy assessment .....	77
6.3.	Analysis of vegetation cover: .....	82
6.4.	Trend of vegetation change derived from classification .....	83
6.5.	Detailed analysis of vegetation dynamic in the ecological zones .....	85
6.6.	Direction of vegetation changes .....	88
<b>Chapter 7: Detection of climate and human-induced vegetation change.....</b>		<b>91</b>
7.1.	Effects of Human Activities in the island .....	91
7.2.	Conclusion .....	96
<b>Chapter General Discussion.....</b>		<b>97</b>

## Introduction

### Problem description

Climate change is a global phenomenon that challenges both sustainable livelihoods and economic while adaptation is predominately site distinctive (Kangalawe and Lyimo, 2013). However, it's effects have been recently recognized as a major force producing warmer conditions together with decreases of rainfall and increases of drought durations in many semiarid regions and therefore, its impact on vegetation types and distribution will be highly significant (Barlow et al., 2015). High quality information on the distribution, diversity and condition of native vegetation is an essential prerequisite for vegetation monitoring, mapping and an important tool for the natural resources management and land use planning to ensure better conservation approaches of the ecosystems. Vegetation is a key component of an ecosystem, however the use of advanced remote sensing technology has enabled researchers to quantify and qualify the amount and health of vegetation.

As reported by Myers et al. (2000) who were engaged in biodiversity 'hot spots' assessment, in fact "almost all tropical islands fall into one or another hot spot". This is because their high species endemism combined with proportionally extensive habitat loss and decline are becoming more common in vegetation, induced, among other factors by climate change (Wang et al., 2008b). Monitoring and mapping vegetation through remotely sensed images has been in development for decades. Rapid advancement of remote sensing technology has increased the quantity and the quality of spatial information and expands the horizon of our choices of imagery sources (Xie et al., 2008). However, the effects of atmospheric still restrain researchers to obtain an accurate relation of satellites spectral signals to the vegetation growth (Huang et al., 2009b).

Socotra Island due to its long geographical isolation however, (Pichi-Sermolli, 1957, Popov, 1957) stated that, nearly 30% of the plant species found on Socotra are believed to be endemic to the island. Until the 20<sup>th</sup> century, there was a scanty or rather heterogeneity and almost very little information and literature existed about the vegetation on the island.

This isolation for at least 18 million years (Lisa M. Banfield et al., 2011) broke down in 1990 with the country unification in which then the island received much attention and subsequently several scientific knowledge of the local flora increased.

However, the earliest explored record was provided by Isaac B. Balfour during his botanical exploration in 1880 (Brown and Mies, 2012a). Another effort was also made by Forbes, H. O. (1899), Bent, J. T. (1897), Wettstein, R. von (1906), Shinnie, Prof. P. L. (1960), [cited in; (Boxhall, 1966)], (Engler, 1910) (Popov, 1957), (Hemming, 1966), Gwynne (1968) and Knapp (1968) [cited in; (De Sanctis et al., 2013)]. Their work as described by several authors mainly focussed on the description of the local flora and vegetation niche with no attention to the spatial and temporal vegetation distribution pattern or attempting to classify the plants.

During the last decades numerous international oriented ecology conservation projects were initiated in Socotra in order to design more meaningful conservation strategy and sustainable development of the island, which have revealed several remarkable findings. These findings however, were achieved in different approaches with diverse aims and goals; (White, 1983),

(Friis, 1992), (Mies and Zimmer, 1993); plants and communities (Miller and BAZARA, 1996); physiognomy (Mies, 1999), (Mies, 2001), (Miller and Morris, 2001), (Kurschner and Ochyra, 2004); plant inventory classification, conservation and sustainable use of the biodiversity; (Knapp, 1968); (Mies, 1999, Mies, 2001), (Miller and BAZARA, 1996). Most of these contributions remained fragmented and unsatisfactory as the evidence by (De Sanctis et al., 2013) with lack of species characterisation and unsatisfactory classification of the plants and contained mainly synthesis of general descriptions of the vegetation without analysis of their distribution. Remarkable contributions can essentially be found in (Kilian and Hein, 2006), (Král and Pavliš, 2006), (De Sanctis et al., 2013) and (Attorre et al., 2011).

Potential vegetation change in Socotra has long been significantly recognized (Myers et al., 2000), (Brown and Mies, 2012a). Many of these species are currently threatened with extinction according to an assessment carried out by (Miller and Morris, 2004b) based on the IUCN classification system and criteria (Commission, 2001), (IUCN, 2010), (Král and Pavliš, 2006), (Kilian and Hein, 2006) and (Brown and Mies, 2012a).

Remote sensing data also have great importance in the studies from (Král and Pavliš, 2006) land cover map, (De Sanctis et al., 2013) classification and distribution patterns of plant communities, (Malatesta et al., 2013) vegetation mapping and (Attorre et al., 2014). Analysing the relationship between land units and plant communities' recourse to them, however, either remained discrete or amalgamating, hence there is no reliable data on the composition and temporal distribution. Owing to those different approaches it is clear that the classifications and divisions of the vegetation are still hardly comparable to each other and all attempts have remained fragmentary and unsatisfactory. However, the comment by (Král and Pavliš, 2006) about the gap between the high level of knowledge achieved and the relevant mapping still applies today and created a severe problem to develop a conservation strategy for the island. Nevertheless, there is virtually nothing in their literature on these past conditions and processes as well as how they change spatially and temporally and in need of urgent attention (Paulay, 1994).

After 1990, the island experienced rapid changes in development and constructions (e.g. new airport, harbour, and asphalt network roads) together with the massive expansion of population from the mainland. Those, however, created a pressure on the natural resources, vegetation and land use along with the effect of climate change, which increased the pressures on plant species and resource exploitation even more. Unfortunately, many of plant species are now confined to very small areas and thus are extremely vulnerable to habitat loss, overgrazing, and urban expansion (Miller and Morris, 1988).

Understanding of local ecological communities however, requires further understanding of broad spatial and long temporal scales, the "regional-historical viewpoint" (Ricklefs, 1987). Nevertheless, (Santos et al., 2014) argued that, multi temporal analysis of accurate and timely vegetation data is a critical issue to understand its conditions in the past and the potential future on a climate change context and is essential to assess its development and for best understanding and monitoring the land use practices. So as to design more meaningful conservation strategy, comprehensive information on changes and distribution with time, is required (Hiers et al., 2012, Wiens and Hobbs, 2015). The present work aimed to provide such information.

Despite the fact that all earlier and present researches and exploration activities on Socotra have brought a wealth of information to document different aspects of the island's vegetation and environment, a detailed characterization of the spatial and temporal distribution of the flora and vegetation types has to be made.

### **Objectives and aims of the study**

The overall objective of this research will attempt to assess and examine the trends of vegetation changes since 1972 to 2010 with the Landsat high resolution imagery and to examine the related driving factors such as climate change, grazing pressure, and underlying spatial variability of the landscape.

This is to answer the overall question: Is there a trend in biomass, cover and species composition on Socotra Island over the last 40 years? If so, is that trend associated with the rainfall patterns? What are the drivers behind the vegetation change? Then how can we define changes in patterns or changes in this landscape?

**Objective 1:** To assess the long term trends in vegetation cover and analyse its spatial distribution using long-term time series of satellite data.

**Question 1.1** What is the trend and variability in vegetation cover in space and time? And what is the magnitude of total vegetation (NDVI) change per pixel over the island's rangeland?

**Hypothesis** The trend in vegetation cover on the island is varying and complex from place to place due to many variables.

**Methodology** - Analyse the phenology of island vegetation using Landsat satellite data selecting key areas that depend on the different physiographic units (landform, soil, hydrology) and eco-zones, then analyse vegetation cover per type of unit.  
- Analyse the climatic data (in growing periods) for each meteorological station and analyse NDVI trends with NDVI residuals and rainfall.

**Question 1.2** Can the trend be explained by rainfall patterns, are there also some changes over time not related only to climate change?

**Hypothesis** The trend in the NDVI is not only related to rainfall and the relation between rainfall and biomass is changing over time.

**Methodology** Statistical relationships between rainfall, biomass and NDVI values will be integrated over the growing season.

**Question 1.3** What is the magnitude of the impact of the rainfall variability and human induced degradation on the vegetation pattern?

**Hypothesis** Human activities do more negatively impact the vegetation pattern than rainfall variabilities.

**Methodology** - Investigate the NDVI vs. rainfall relationship and examine the trend over time.  
- Calculate the deviations of vegetation response to rainfall for each pixel during the growing season for selected years.

**Objective 2:** Examine the dynamic changes in vegetation patterns for the period of 1972 to 2010.

**Question 2.1** What are the main vegetation types to be distinguished?

**Hypothesis** Unique remote sensing techniques can be used to categorise vegetation types.

**Methodology** - Satellite image, interpretation and classification.

- Ground truthing and field verification.

- Ancillary data analysing, manipulating and interpretation.

**Question 2.2** What is the magnitude of vegetation patterns change per each land unit? And what are the size and shape of these patterns?

**Hypothesis** The size and shape of vegetation patterns are not regularly distributed in space and time.

**Methodology** - Change detection technique.

- Field study, onsite measurements, sampling...etc.

**Objective 3:** Examine spatial heterogeneity in plant patchiness to understand the effects of landscape heterogeneity on vegetation across the study area.

**Question 3** Can the variation in rainfall explain the ongoing vegetation degradation?

**Hypothesis** Change in rainfall cannot completely explain on-going land degradation.

**Methodology** Analyse the temporal trend in rainfall and efficiency computed as the ratio between biomass and rainfall and also NDVI and rainfall. We then will analyse the trend of rainfall against the trend in vegetation cover.

### **Thesis Organization**

The research questions under **Q1** deal with the trend and variability in vegetation cover in space and time, and the magnitude of total vegetation (NDVI) change per pixel over the Island's rangeland, and how the trend can be explained by rainfall patterns (as driving factor) over time, while the question **Q2** deals with the magnitude of vegetation patterns change per each land unit or eco-zone, and with the size and shape of these patterns and human impact and its discrimination from the climate impact. Question **3** deals with the problem how the extent of slope and rainfall redistribution determine the vegetation pattern in the landscape, and what the relation between landscape heterogeneity and the rainfall distribution is.

An introduction to drylands, their dynamics and problems of their investigation follows in Chapter **1**. This section also deals with remote sensing approaches for investigating vegetation-climate relationship. Chapter **2** provides an introduction to the study region. In Chapter **3** is the general framework and description of data used and pre-processing methods for the following subsequent sections are introduced. In Chapter **4** the statistical techniques and vegetation analysis methods and an overview of the model classification scheme are explained. In this chapter we also introduce the concept of discrimination between the rainfall and human impact as the main driving forces of vegetation change in the study area. Generally, Chapters **1-4** form the basis for the analysis of the data while the results follows in chapters **5-7**. Chapter **5** as part 1 of the result is focused on the analysis of climatic conditions and NDVI in the study area. This is to highlight and analyze the spatial and temporal locality variation within seasons and the inter-seasonal dynamics (**Answer Q1 & Q3.1**). Chapter **6** covers part 2 of the results, which reports the vegetation cover classification and vegetation type change (**Answer Q2**). Chapter **7** deals with the detection of climate and human induced vegetation change (**Answer Q1.3 & Q3**). Chapter **8** as the last one provides a general discussion of the derived results with an outlook on the further development of vegetation monitoring as well as the potentialities of the investigated approaches and the further prospect which can be achieved by extended work.



## Chapter 1: Theoretical background

### 1.1. Characterization of ecosystems dynamics in semiarid regions

The importance of biological diversity and biodiversity conservation was definitely recognized at the Earth Summit in Rio de Janeiro in 1992 and more than 130 nations signed a Convention on Climate Change and a Convention on Biodiversity. Changes in forest and vegetation cover are particularly severe in most of the arid and semi-arid regions and have significant global impacts on such debatable issues as vegetation degradation, biodiversity deterioration and climate change (Skole and Tucker, 1993, Southworth et al., 2004, Chen, 2002). The hazards of drought and desiccation heavily influenced the ecosystem dynamics of these regions (Olsson et al., 2005). Due to the adverse impacts of vegetation deterioration and land degradation on agronomic productivity, the ecology and the environment, and their effect on food security and the quality of human life, they remain an important global issue and will remain high on the international agenda in the 21<sup>st</sup> century. Several studies have shown that in semiarid areas land degradation has had major effects on plant cover and biomass (Vinton and Burke, 1995, Wainwright et al., 2002, Oba et al., 2003, Trodd and Dougill, 1998).

The United Nations Convention to Combat Desertification (UNCCD, 1994) defines the desertification in arid and semiarid areas as land degradation resulting from various factors, involving climate variations and human activities. The definition also considers the degradation as a “reduce or loss of the economical or biological productivity and complexity of agricultural land, or range, pasture, forest and woodlands resulting from combination processes of land uses including processes arising from human activities and habitation patterns” (UNDP/UNEP, 1994). Semiarid areas due to (UNDP/UNEP, 1994) occupy approximately 17% of the global land mass. Examples from the United States (Brown, 2003) and (Van Auken, 2000); from Australia (Krull et al., 2005); from Patagonia (Aguiar et al., 1996) and from China (Cheng et al., 2007), argued that the change in the vegetation pattern such as invasion of grasslands in many semiarid areas by shrubs is a major form of land degradation. The strength of the tropical monsoon influences the vegetation distribution, both air temperature and rainfall variation can accompany vegetation change (Wang and Eltahir, 2000a, Wang and Eltahir, 2000b). Moreover, the extreme climatic events, extended droughts or large annual rainfall fluctuations associated with the global warming and the anthropogenic pressures collectively can also play a critical role in shaping the ecosystems (Holmgren et al., 2006), reduce the ability to regenerate vegetation cover in such ecosystems (Paul Reich, 2001) and might lead to self-organizing and patchiness on landscape (Aguiar and Sala, 1999). An extremely harsh climate and variable land use, such as decreasing rainfall combined with grazing, might suddenly shift the ecosystem towards degradation and desert conditions (Rietkerk et al., 2004, Scheffer and Carpenter, 2003); catastrophic shifts (Skidmore and Prins, 2002, Baudena and Provenzale, 2008); sudden transition from a patchy perennial vegetation state to a state of bare soil (Scheffer et al., 2001) resulting in land degradation and severe runoff (see Stafford and Reynolds, [cited in; (Roder et al., 2008)]).

Arid and semiarid ecosystem dynamics is usually influenced by hazards of drought and desiccation (Propastin, 2007) and both temperature and rainfall play key roles in regulating plant biological processes. Thus, the vegetation cover is more heterogeneous and is highly

sensitive to climate fluctuations. The vegetation species in these areas present different adaptive mechanisms against the fluctuation of summer and winter temperature (Zunzunegui et al., 2005). Nevertheless, it is not clear what might be the response of these species to climate change and particularly to the temperature increase and rainfall decrease forecasted (IPCC, 2001, Palutitkof, 2002 [cited in; (Giordano, 2007)]). Few studies have investigated the effects of climate change on the forests and shrub-lands of semi-arid areas (Barbero et al., 1990), (Lázaro et al., 2001), (Hulme, 2005), (Rotenberg and Yakir, 2010, Martin, 2006). In most cases, it can be concluded that the dynamics of productivity and species composition in the semiarid areas are believed to be generally controlled by external factors such as climatic variables, human activities, depletion of above ground biomass by herbivores and fire. The internal regulatory mechanism of the ecosystem is mostly weaker than the external mechanism. The ecosystem dynamics are essentially event-triggered with unsteady climate because of its high variability (Sullivan and Rohde, 2002, Herrmann and Hutchinson, 2005).

### **1.2. Vegetation changes and their explanatory factors based on remote sensing investigations**

The spatial complexity and heterogeneity of the vegetation as well as limited access to the data source reduce the reliability of traditional ecology approaches to produce accurate results of monitoring. Taking advantages of the future imagery and its analysis methods is recently much recommended as most suitable method for vegetation studies in such areas.

Multi temporal series of satellite data supply a wealth of information for monitoring environmental and vegetation pattern/changes (e.g. (Nemani et al., 2003, Turner et al., 2005), from regional to global scale. Therefore, use of series covering a timespan of more than thirty years might thus constitute a significant window of observation and has been firmly established (De Beurs and Henebry, 2005), only a limited number of these detection methods have been developed (Verbesselt et al., 2010). In particular, they can be used to gain insight into the complex mechanisms controlling the response of vegetation to climate variability. Moreover, remote sensing data offers unique opportunities to monitor changes in the vegetation cover. It provides the large spectral information, spatial and temporal scale necessary, even objective data (Bijker, 1997, Foody, 2003). Satellite-based Normalized Difference Vegetation Index (NDVI) data has successfully served as vegetative indicator in many studies. It was also a powerful tool in facilitating the advances of environmental monitoring strategies in the last two decades, particularly to understand the ecosystem variations and ecosystem changes as well as their causal relationships.

Temporal and spatial correlations between NDVI and climatic factors are investigated in many research works. It showed well correlations both spatially and temporally with the rainfall in the semiarid regions (Richard and Pocard, 1998, Chen et al., 2004, Weiss et al., 2004). In Sudanese savanna, (Nicholson et al., 1990b) found a strong linear relationship between NDVI and rainfall variation on mean annual rainfall ranging 200–1200 mm for the western Sahel. Temporal series of satellite derived NDVI have been used by several scientists. (Xiao et al., 2005, Li et al., 2004, Tucker et al., 2001, Piao et al., 2003, Lunetta et al., 2006, Li et al., 2013, Shen et al., 2014) and also (Sarkar and Kafatos, 2004), (Zhang et al., 2004), (Volcani et al., 2005), (Stöckli and Vidale, 2004) and (Suzuki et al., 2006), among others argued changes in NDVI to reflect changes in biological activities. (Tourre et al., 2008) found relations between NDVI trends over

South America and climate change since 1981. Whilst for example, (Anyamba and Tucker, 2005) expanded the analysis of NDVI data on Sahelian vegetation dynamics as a proxy for the response of land surface to rainfall variability for the period 1982-2003, and detected drought and 'wetter' conditions that were in agreement with the recent region-wide trends in rainfall. However, there are some basic difficulties reported in using remotely sensed data to study vegetation change (Murwira and Skidmore, 2005, Petersen and Stringham, 2008, Phua et al., 2008, Chehbouni et al., 2008, Zheng et al., 2008, Han et al., 2007) and many others). One of these involves extracting vegetation richness from measures of radiance, which is rarely measured in the field. The other leading methods, Vegetation Indices (VIs) and Spectral Mixture Analysis (SMA), attempt to quantify vegetation abundance in comparable units to field measures. Despite several studies derived vegetation cover using various methods on extracting and modelling data, not many of those studies built on such time series image processing data. (Roder et al., 2008) used a discrimination between evergreen, deciduous and mixed plantings to estimate aboveground biomass globally as an innovative mission to reduce uncertainties about net effects of deforestation (Le Bris et al., 2013) and forest regrowth on atmospheric CO<sub>2</sub> concentrations (Hese et al., 2005a). However, the relationships between bare soil and soil's colour and their effects on the NDVI are still more complex (Huete and Tucker, 1991, Major et al., 1990, Todd et al., 1998, Mutanga and Skidmore, 2004). Nevertheless, the correlation between NDVI and above ground biomass is well established. It has been reported by Nicholson et al. (1998) that NDVI is well correlated with parameters such as leaf area index (Darvishzadeh et al., 2008, Jensen et al., 2008, Tan et al., 2005), green leaf, biomass, vegetation cover, and also the NDVI/R ratio is regarded as a useful proxy for rain use efficiency (Davenport and Nicholson, 1993, Hountondji et al., 2006, Nicholson et al., 1990a). Moreover, trends in the NDVI/R ratio can be interpreted as a measure of possible vegetation degradation or revival (Hountondji et al., 2006). Majority of studies have focused on spectral indices to link properties of rangeland vegetation with remote sensing based assessments (Graetz et al., 1988, Todd et al., 1998, Moleele et al., 2001, Roder et al., 2007, Noomen et al., 2008, Cho et al., 2007, Joshi et al., 2006, Ferwerda et al., 2005). Others have successfully combined remote sensing based assessments of grazing patterns with grazing models for trend analysis and somehow pattern forecasting (Pickup, 1998, Pickup and Chewings, 1988, Mutanga et al., 2004). Several studies and techniques demonstrated the effectiveness of using satellite derived data in producing vegetation cover, land use/land cover maps as well as detecting the landscape change over time (Skidmore et al., 1997, Abou El-Magd and Tanton, 2003, Cardille and Foley, 2003, Skidmore and Prins, 2002, Lobo et al., 2004, Musaoglu et al., 2005, Garcia-Haro et al., 2005, Schmidt et al., 2004, Nangendo et al., 2007) and assessed the agreement and mapping uncertainties in existing global 1 km datasets land cover mapping (Herold et al., 2008). However, estimation of overgrazing risk in semiarid areas remains difficult (Diouf and Lambin, 2001, Hountondji et al., 2006, Ruelland et al., 2008, Leenders et al., 2005) and a number of issues such as spatial variability due to fuel-wood cutting, topography, soil types and different socio-economic triggers and land use activities which influence vegetation growth and distribution need to be considered and have to be addressed before an optimal result can be achieved. Nevertheless, due to the complexity and the heterogeneity of semiarid areas environments however, there is still a lack of methodologies adapted to its fragmented

rangelands and biodiversity setting (Western et al., 2004, Shoshany, 2000, Ruelland et al., 2008, Squires and Sidahmed, 1997).

Attempting to understand ecosystem dynamics by the earlier researches have largely been carried out within the disparate disciplines of ecology, which has led to substantial limitations (Muller, 2007, Bracken and Croke, 2007, Turnbull et al., 2008a). However, the current understanding of semiarid vegetation trend and ecological interactions across multiple space and time scales may be developed by exploring degradation within the cusp-catastrophe framework (Vanbreemen, 1993, Shoshany et al., 1995, Turnbull et al., 2008b). This is requiring that biotic and abiotic elements of the ecosystem to be understood in terms of both their structure and function, with respect to the connectivity between these elements in spatial and temporal terms.

Scientific literature, however, reveals several existing change detection techniques. Myneni et al. (2001) used seasonally integrated measures data to determine biomass with high spatial resolution at the continental scale using NDVI. Coppin et al. (2004), minimized seasonality variation by focussing on the growing season. Eriksson et al. (2003) correlated Synthetic Aperture Radar (SAR) data to biomass, (McCallum et al., 2010) compared four global FAPAR datasets, (Wagner et al., 2003) combined ERS tandem interferometric coherence and JERS backscatter. Hese et al. (2005b) mapped global biomass with respect to carbon cycle, (Bontemps et al., 2008) and (Fensholt et al., 2009) summarized temporally time series data, while (Healey et al., 2005), used normalizing reflectance values per land cover type. The comprehensive review of methods and the results of change detection by Coppin et al. (2004) and (Martínez and Gilabert, 2009) showed, however, that most existing methods focus on short image time series.

There is whole literature about the plant-soil relations for ecosystem functioning and self-organization, but I think it will be very difficult to prove in light of spatial variability of the environment. Therefore, we will not take that into account as a driving mechanism. We will point out the potentiality of studying vegetation pattern for monitoring the impacts of climate variability and human activities on this fragile area bordering hot arid region. We need to acquire a greater understanding of the interacting processes that maintain resilience and the factors that are currently limit the distribution of vegetation species. Particularly physiological and environmental factors and sophisticated predictive model may improve our understanding of vegetation and climate interactions in this area. We also will examine the distribution of the vegetation patterns depending on the duration of the wet season even with fixed total annual rainfall showing how seasonality affects the vegetation patterns.

Socotra Island is the largest Yemeni island, located in the Indian Ocean. Due to the high level of plant endemism, Socotra is placed among the most important islands in the world and among global biodiversity hotspots (Scholte et al., 2011, Malatesta et al., 2013). The island is strongly affected by the Indian Ocean Monsoon (Escadafal et al.) (Fig. 1) which is one of the major weather systems of the earth, affecting one of the most densely populated areas of the world (Fuchs and Buerkert, 2008, Burns). Rainfall seems to be the most important factor affecting life and the ecology in the island. Nevertheless, from experience in the study area, changes in the technology, tourism industry, new investments and development of infrastructure, rather than rural population increases, seem to play also major roles on breakdown of traditional land use

and land management practices creating the erratic plants patterns and leading to deteriorate the vegetation cover and then increased degradation in the landscape (Hobbs et al., 1995).

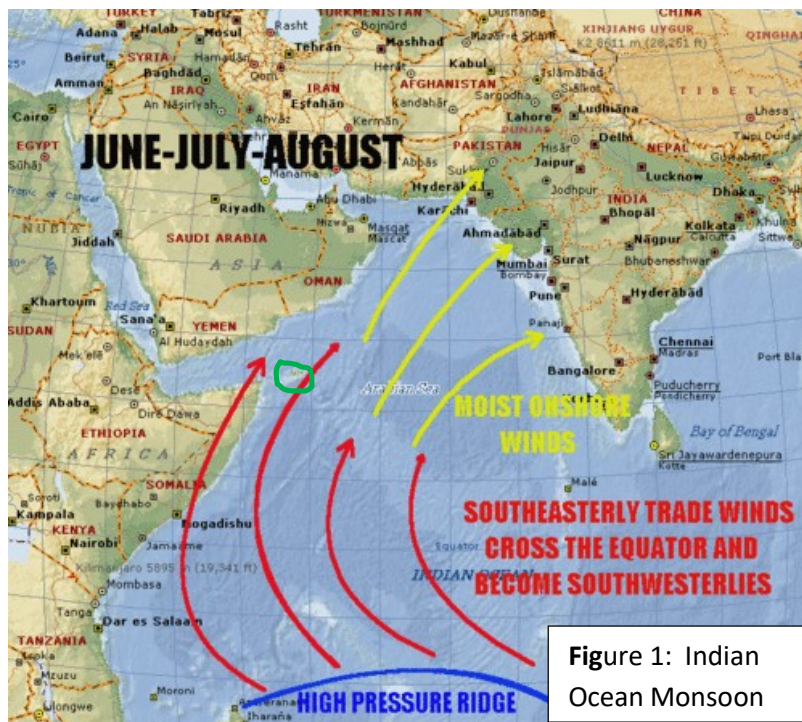


Figure 1: Indian Ocean Monsoon

Nowadays, several authors have recognised that traditional land use management practices have currently changed with urbanization enforcement (Pietsch, 2007). A new road network increased accessibility around the island and more people moved (internal migration) to Hadibu, the capital of island. Such trends also create patches of new settlements. The present building boom on the island is placing great pressure on timber and all

trees. The understanding of the interactions between human activities related causes, land use and vegetation in their spatial and temporal distribution (Gregorio and Jansen, 1997) is fundamental to understand and predict changes in that landscape. Unfortunately in many instances vegetation cover and range management are not a priority of governments (FOWECA, 2004). This situation increased the marginalization of the resource and dependent communities. The importance of this research is laid on its innovative way of defining the catastrophic destabilization over landscape. It will be more oriented towards specific management, future conservation strategies and policy issues, such as the requirements of endemic and threatened species; the impact of grazing on endemic plants and on rangeland requirements; the impact of invasive species and to help understanding the rule of runoff, on plant distribution on the landscape.

Meanwhile, the vegetation cover in the study area has been deteriorated since the 1970s due to the rainfall scarcity and the excessive human activities mainly, including overexploitation of vegetation and overgrazing and consequently resulting in great overall in ecosystems changes. However, there has been much debate whether the extinction, annihilation and lack of regeneration of *dragon blood* and *frankincense* trees result from the goats and overgrazing or from climate (Mies, 2001), (Adolt and Pavlis, 2004), (Miller and Morris, 2004a), (Attorre et al., 2007), (Scholte et al., 2008), (Habrova et al., 2009) and (Scholte et al., 2013). This challenge has been recently raised and threatened the safe existence and sustainable development bringing the great attention to the environment deterioration problems. The overgrazing we are mentioning here includes that, these activities occur often in the form of clearing lands of woody vegetation for fuel, construction and charcoal trading.

In order to characterize the complexities of land degradation and vegetation deterioration in the study area, we need to detect the role of different land use and grazing practices in

impacting vegetation cover, biomass, patterns and species compositions and then define the trend change spatially and temporally in the heterogeneous landscape (Fig. 2).

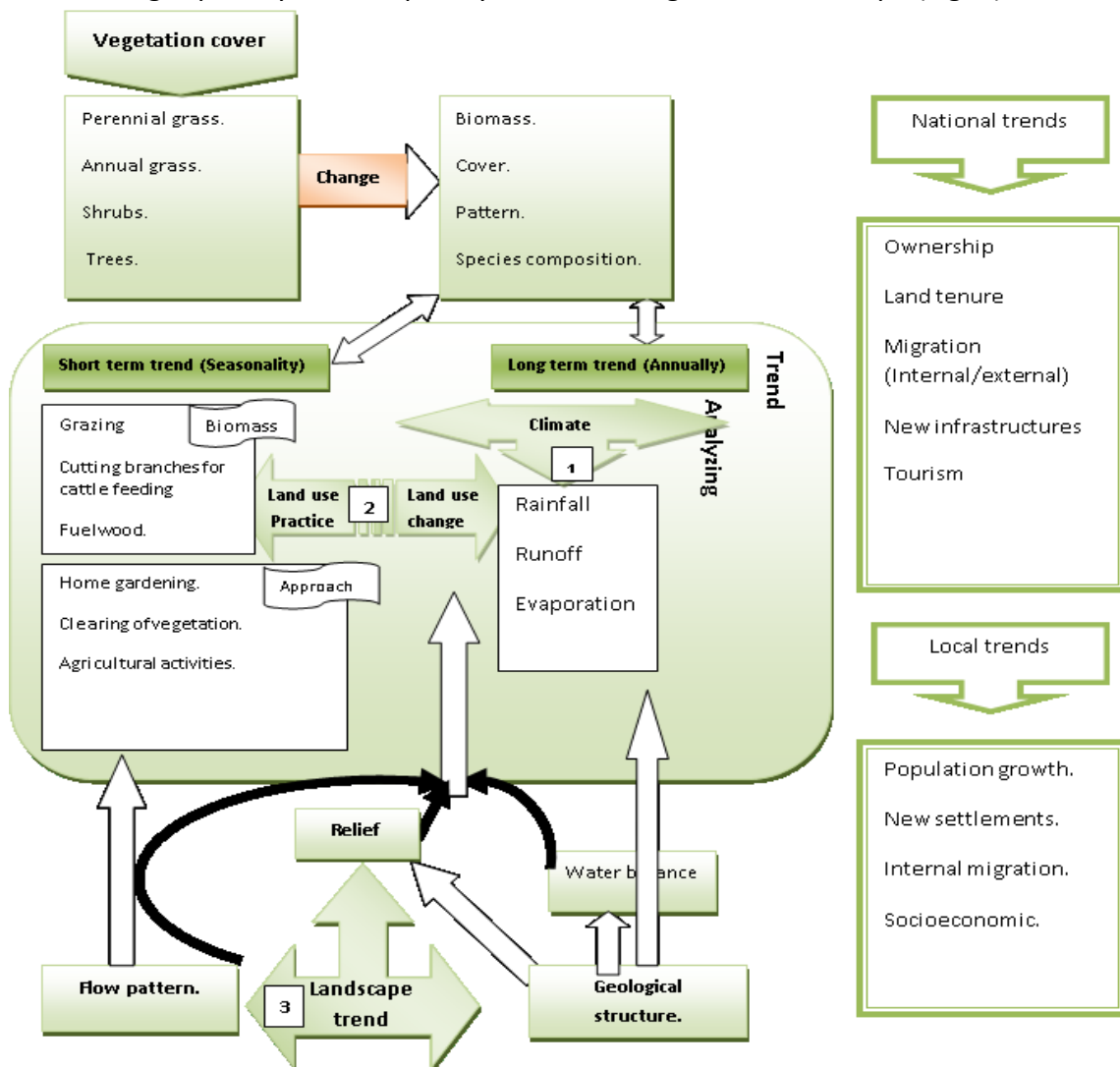


Figure 2: Schematic flow diagram how different land use and grazing practices impact vegetation cover and create a trend in a heterogeneous landscape

Some individual patterns of species and trees in the study area are seen to follow the drainage lines and seem to be affected by grazing but there are also individual trees. Some of these patterns are in dynamic changes, to follow the geological depression and are on one hand side related to flow patterns of water and others to species behaviour and grazing. So it is not quite easy to come to a decision whether these changes result mainly from degradation. In such a landscape it could be valuable to come up with indicators and good recipes or methods to determine change. In order to develop the strategies of retrieving the vegetation and preserving the island, the deterioration process of vegetation must be documented clearly. In this study, multi temporal and multi sensor Landsat MSS, TM and ETM+ images data derived series of Normalized Difference Vegetation Index (NDVI) for the period 1972 - 2010 were used quantitatively to examine the dynamic vegetation changes and their inter-seasonal variability. The integrated NDVI during the growing period (GP) data are compared with rainfall (R) data in the island from 1972 to 2010. Trend analysis is then applied on the obtained time series of this indicator in order to identify areas suffering from desertification.

## Chapter 2: Study area and geographical location

Socotra is the largest Yemeni island, situated in the Arabian Sea around 400 km south of the Arabian Peninsula. It lies between the latitudes  $12^{\circ} 8' - 12^{\circ} 42'$  north of the equator and the longitudes  $53^{\circ} 19' - 54^{\circ} 33'$  east of Greenwich (Fig. 3), with an area of  $3607 \text{ km}^2$  approximately 120 km long by 35 km wide. It is comprised of a basement complex of Precambrian igneous and metamorphic rocks, overlaid by younger limestone and sandstone sedimentary rocks (Cumberlidge and Wranik, 2002). Generally, three main stratigraphic geological units dominate Socotra Island. Paleocene-Eocene plateaus extend in the middle altitudes all over the island and overlay the Proterozoic-Paleozoic granitic basement. The latter can be found in Haggeher massif and in Qalansiyah and Ras Shúab in the westernmost part on the island. It is also reported that the highest part of the Haggeher massif was never submerged since the Cretaceous (Fournier et al., 2007), moreover, marine fossils can be found on limestone plateaus up to 800 m a.s.l. Mesozoic outcrops is the second geological feature rising along the main wadis and steep edges of Paleocene-Eocene plateaus (Fournier et al., 2007). Third, the lowest parts of the island consist either of Quaternary Formations and or might be interpreted according to same reference as Oligocene-Miocene or Lower Cretaceous strata.



Figure 3: Basic structure of Socotra Island (topography, main roads; top) and its location in the Arabian Sea (left, encircled)

The population is considerably under potential expansion. It has been estimated with 11.220 according to (Brown, 1966), 30.000 according to (Wranik, 1996), and 80.000 according to (Al Sagheir and Porter, 1996) and according to the latest CSO census survey even up to 120.000 (Organisation, 2007). People living in the island subsist mainly on fishing, the cultivation of date

palms and pastoralism for their livelihood. The island has a semiarid tropical climate (Pietsch and Kühn, 2009) with average annual rainfall of 120 - 400 mm. This quantity fluctuates to a great extent from one year to another and there is little seasonal change in temperature with the mean daily temperature ranges of about 25<sup>o</sup>-28°C.

### **2.1 Physiographical characterisation and ecological zonation**

Due to the purpose of their studies many authors have contrarily categorised the physiography features of the island. Dividing the island landscape into variously sized ecological units might be important and have significance both for resources development and environment conservation (Bailey, 1983). Such units can be used as a base for estimating ecosystem productivity and the probable responses to management practices, thus reflecting the influence and reaction between the climate, vegetation and soils and, to a lesser degree, the fauna. Such approaches depend on prior knowledge of functional relationships between site parameters, ecosystem and the specific form of biological production.

Because of the complex topography and the large climate range throughout the island, and for the purpose of investigating the vegetation distribution with relation to their latitude location and climate-ecological interaction, we used the results of all previous authors' works as a guidance to divided the entire area into six ecological subregions (Figure 4).

- **The central mountains:** Igneous Haggher is the most important and the largest mountain located at the eastern part of the island, overlooking the island with capital Hadiboo. It extends north easterly to south westerly at a distance of 25 km with their jagged granite highest peak Daksam with 1630 m. Haggher mountains rise from 750 to 1500 m on a granitic substratum (BEYDOUN and BIGHAN, 1969) covered by Cretaceous and Tertiary limestones
- **Hillslopes:** A semi-arid upper zone, surrounding the central mountains to the east, west and south, covering most of steep slopes averaging 450-750m in altitude interspersed with hills and small plains. They drop away at the edges in steep cliffs and are eroded on the surface into karst topography.
- **High plateau:** Arid limestone zone plateau. A transition zone between the alluvial substratum and the upper limestone area ranging 250 – 450 m above sea levels with the surrounding limestone areas dating to the mid-Tertiary.
- **Low plateau:** Dissected limestone plateau, it occupies most of the internal areas of the island, ranging from 110 to 250 m and dissected from north to south by several ephemeral wadis.
- **Wadis (valleys):** Several streams run into the island with running water which sometimes incised deep canyons into the slopes of the Haggher massive in the south-west direction. The most important are Tatrat and Azroo valleys, which are intersecting the island from north to south. They often have only irregular runoff that occurs during the rainfall and it might last for few months per year, whereas the rest time of the year, their beds fall dry or lead only a few amount of water. In addition, several springs are also running along the year from the Haggher Mountain.
- **Coastal plains:** The arid coastal plains are mainly located on an alluvial substratum, intersected plains. Situated in the north and south of the island, while the drift in the



east and west parts of the island extended to the coast. The southern coastal plain, which is 4 - 7 km in width, stretches over approximately 60 km along the southern coast. It is terminated northwards by a precipitous escarpment averaging about 110 m in elevation. Southwards it descends in terraces, the marine sediments of which meet a strip of dunes at the shoreline and continue at a shallow gradient over at least 15 km out into sea. A much more irregular coastal plain occurs in the north, backed by the deep slopes of the plateau edge. This plain is less barren than the southern plain and is interrupted to the east by a number of headlands which break it up into several small enclosed fertile areas to the north of the Haggher range, characterized by shrubland and grassland communities.

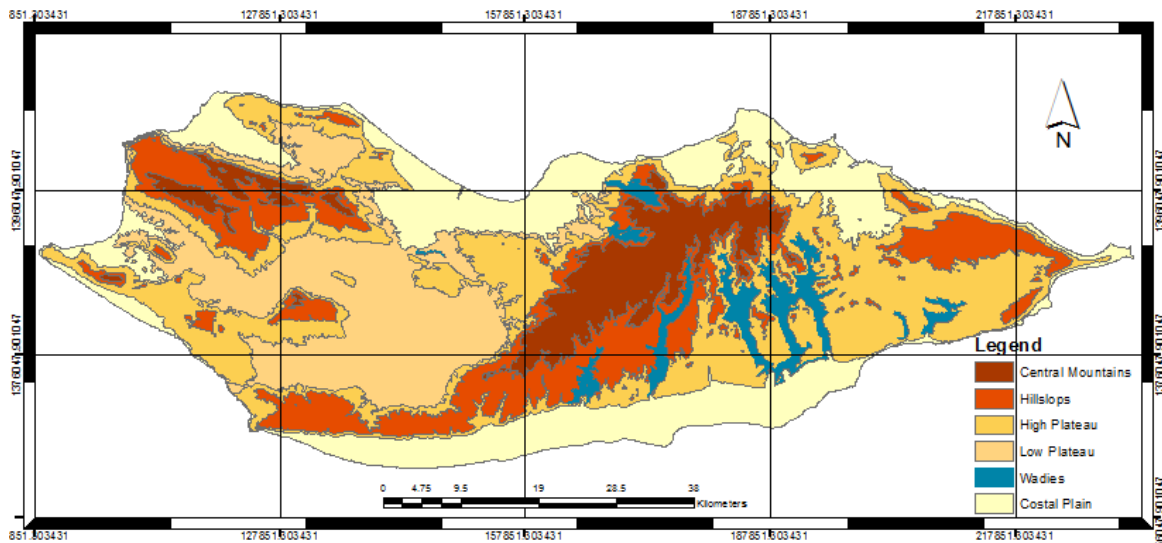


Figure 4: The six major ecological zones of Socotra.

Due to its discrete and isolated nature, the island has a diversified sparse vegetation and uniqueness of diverse endemic plant species with local adaptations and radiations (Lisa M. Banfield et al., 2011) dominated by *Halophytes*, *Croton socotranus*, *Jatropha*, *Euphorbia* and *succulent shrubs, bottle trees, frankincense trees, and dragon's blood trees* (Mies, 2001); (Le Houerou, 2003); (Miller and Morris, 2004a); (Attorre et al., 2007).

Furthermore, there are several distinctive vegetation formations on Socotra, particularly with respect to their physiognomy and structure. The (IUCN, 2008) has reported that 37% of Socotra's 825 plant species, 90% of its 30 reptile species and 95% of its land snail species are not found anywhere else in the world. The site is also well-known with 192 land and sea birds species, 44 of which breed on the island, while 85 are regular migrants (UNESCO, 2008), including a number of threatened species. The marine life is also very diverse, with 730 species of coastal fish, 253 species of reef building corals and 300 species of crab, lobster and shrimp (source: <http://whc.unesco.org/en/list/>).

However, (Sindaco et al., 2012) mentioned that the island is one of the most remote and most biodiversity rich and distinct islands in the world. In 2008, it has designated by the UNESCO as a World Heritage Natural site. Despite the richness in fauna and flora with a high level of endemism, only little is known about its biodiversity and the biogeographical distribution of most of the islands' species (Sindaco et al., 2012).

## 2.2 Climatic characteristics

The island is sited in the arid tropical zone where generally evapotranspiration greatly exceeds the rainfall and is subjected to intense summer monsoon activity (Fig. 5) which has created a seasonal period of isolation. According to (Bruggeman, 1997) Socotra is located in the Zone 14 of Agro-climatic zones of Yemen where potential evapotranspiration varies between 3.5 mm/day during the cool period and 6.5-7.5 mm/day during the months June to August (Fig. 6). The average total amount of evapotranspiration per year is about 1750 mm/year.

Long-term detailed climatic data is lacking ((Scholte and De Geest, 2010), with only scarce information covering a few years. Average air temperatures range from 23.5 °C in the coolest to 35.0 °C in the hottest months of the year. During summer, temperatures can exceed 40 °C at noon with relative humidity more than 70% (Bruggeman, 1997), and fall no lower than 25 °C at night on the coastal plain and in the lower parts of the interior of the island. There are two annual rainy monsoon seasons, which are related to the two main annual wind directions (Haake et al., 1993). From August to October, the South West monsoon brings occasional heavy rains (Rathjens et al., 1956), (Villwock, 1991) and (Mies BA, 1996). Additional intense down-pours causing flash flooding of coastal wadis occur from November to January, while the smaller rainy season takes places in April and May, driven by the winter half year's NE trade winds.

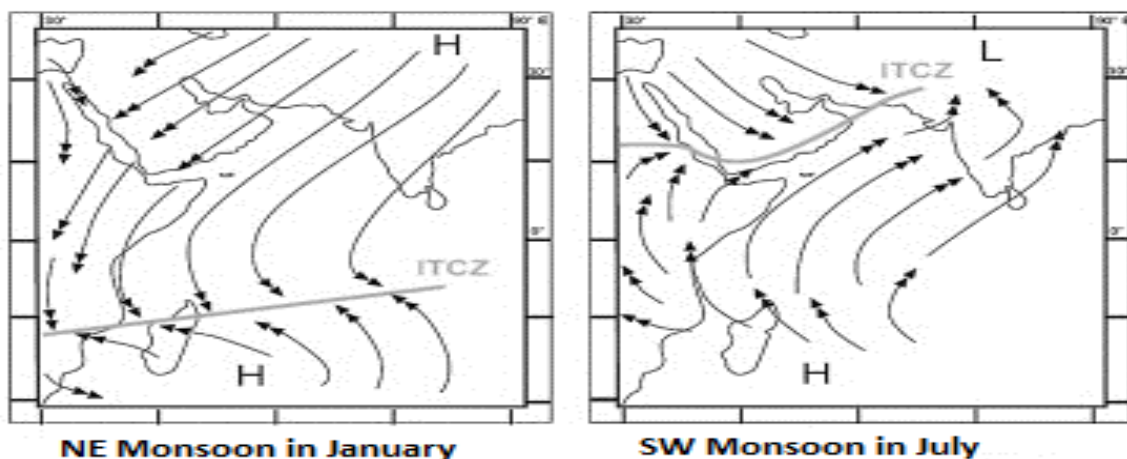


Figure 5: Stream pattern of winter monsoon (Scholte et al.) and summer monsoon (right) in the western Indian Ocean (Adapted after (Fleitmann et al., 2004).

Rainfall in Socotra is unpredictable in time and space and greatly affected by the Indian monsoon strength and diminish (Fleitmann et al., 2007, Fleitmann et al., 2004). Some measurements of rainfall, temperature and wind were started earlier in the last 19th century (Kerr, 2004) and (Popov, 1957). About 11 automated weather stations with some other rainfall gauges were installed during last decades by Socotra Conservation and Development Programme (SCDP). There is still an irregularity in collection of data and only a limited data is available.

Climate change on Socotra due to (Attorre et al., 2007) has been projected to cause considerable aridification on the island and is expected to put further pressure on it's ecological system. A review of local climate knowledge and data collected (Scholte and De Geest, 2010) showed considerable variation in the mean annual rainfall among those stations and also illustrated the gaps of sequence climate data knowledge. It is generally revealed that the winter

rain (October to December) is higher than the summer rain (April to May) with the maximum rainfall reached in December, whereas generally no rain is available during July and August (Scholte and De Geest, 2010, Mies, 1995).

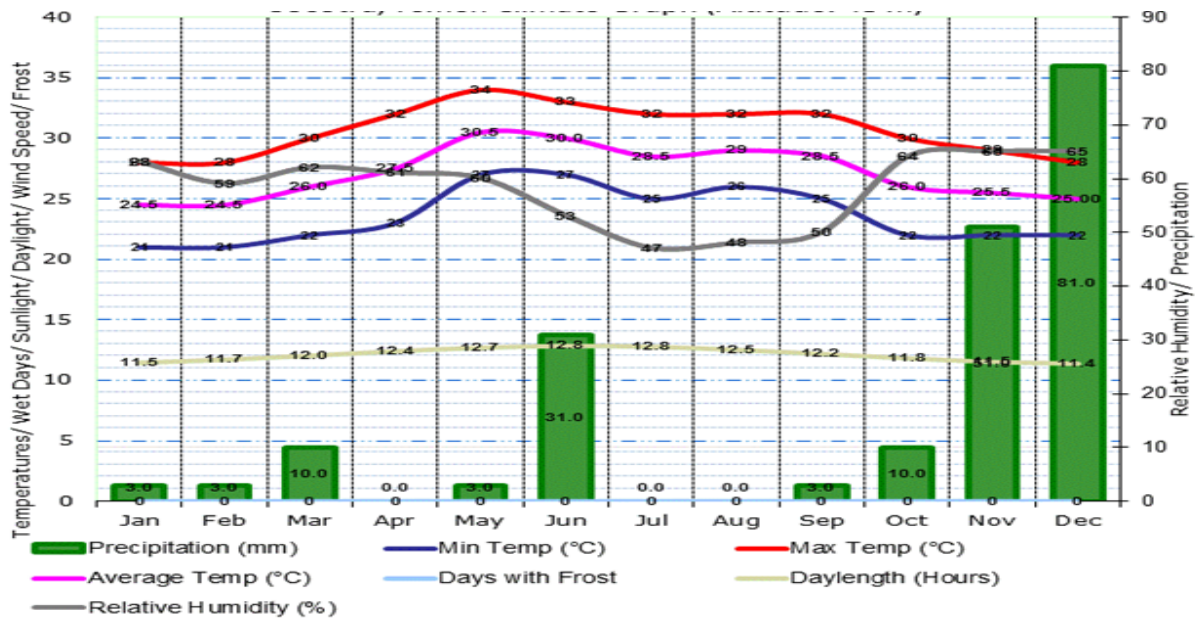


Figure 6: Annual pattern of climatic variables of Socotra (After Chen and Chen 2013) source: (Scholte and De Geest, 2010)

### 2.3 Soils Characteristics

Large parts of the island are comprised of a basement complex of Precambrian igneous and metamorphic rocks, overlaid by Tertiary limestone and sandstone sedimentary rocks (Cumberlidge and Wranik, 2002). The soil parent material due to the recent survey by (Board, 2003) consists of limestone plateaus and basins, granite basement, wadis and alluvial plains. The north-eastern part is dominated by crystalline rock, including granites which make up the Haggher Massif formed by pre-Cambrian and Palaeozoic (Birse et al., 1997), the easternmost parts predominate of carbonate with thicknesses from the Triassic and Jurassic era Bott et al., (1994) and Samuel et al.,(1997) [cited in: (Birse et al., 1997)]. These fragments indicate strong chemical weathering, preceding erosion, and redistribution.

No soil data of Socotra island existed so far, except for a basic work in three areas in the northern part carried out by Pietsch during 2008 and 2009 to determine the development of most distributed soils (Pietsch and Kühn, 2009). The soil in Socotra is similar to those in the semiarid region soils which possess unique characterization distinguishing them from other in humid regions. It is commonly poor in organic matter, high alkalinity in reaction, richer in iron and generally rich in bases-especially in soluble salts with high concentration of calcium carbonate. The later can be accumulated in the form of individual nodules or of a continuous crust in the soil profile. Soil profile has commonly a weak or moderate structure development with coarse texture and is somehow covered by surface stones or gravel (Dregne, 2011). The main factors affecting the soil formation in these areas are climate, vegetation and biological activity ((Verheye, 2006).

In the World Reference Base Taxonomy, these soils generally belong to the order of Aridisols. However, results of soil investigations on Socotra by (Pietsch and Morris, 2010) and our random representative sampling, showed that the island is poor in soil resources with heavy texture range from clay to silty clay loam in the intermountain plains and the wadies respectively with shallow or even strongly calcified (crusting by calcification). Cambisols and Calcisols are the most common soil classification orders with Haplic, Petrocalcic or Hypercalcic horizons in the lower part of the soils such as in Homhil basin and Ayhaft (Pietsch and Lucke, 2008). Furthermore, due to the same study, Calcium carbonate is found at a depth of up to 30 cm in 52% of the layered soils (Table 1). The coarse fragment content lies between 0 and 78% with many surface stones, where Calcisols are often present silt, comprise 40–80% and between 30% and 60% clay (Pietsch and Kühn, 2009)see Fig. 7 profile picture).

#### Wadi Ayhaft 1 (cmolckg–1)

Depth cm	Sand %	Silt %	Clay %	Texture	OM%	CaCo3 %	CEC (cmol/kg)	pH
0-38	7.4	27.4	65.2	Clay	1.12	5.1	33.7	7.9
38-80	15.2	73.8	11.0	Silty Clay Loam	0.34	81.1	10.3	8.8
80-125	15	75	10	Silty Clay Loam	0.21	77.5	6.0	8.8

#### Homhil 9

Depth cm	Sand %	Silt %	Clay %	Texture	OM	CaCo3 %	CEC (cmol/kg)	pH
0-5	19	46.7	33.4	Silty Clay Loam	0.95	3.2	21.6	8.5
5-25	24.4	28.8	46.8	Clay	0.83	17.9	20.5	8.6
25-75+	24	29.3	46.6	Clay	0.5	27.5	13.4	8.6

Table 1. Soil contents on two sites and classification.



Depth (cm)	Soil profile description
0-40	Red (2.5YR4/6) moist, slightly humus, moderately calcareous, heavy clay, sub-angular blocky structure, diffuse iron, 1mm Fe-Mn Concentrations, bioturbation. Substrate <i>red cover clay on slope without detritus</i> , undulating abrupt boundary.
40-80	Yellow (10 YR7/6) moist, slightly or sparsely humus, extremely calcareous, silty loam, coherent structure, patches of secondary carbonate concentrations, bioturbation. Substrate <i>carbonate coherent cover loam and slope with much detritus</i> , unclear diffused boundary.
80-125	Radish yellow (5YR6/8) and slightly yellow (2.5Y8/2) moist, sparsely humus, extremely calcareous, silty loam, massive, coherent patches of secondary carbonates, single carbonate concentration. Substrate <i>carbonate cover loam with slope detritus</i> , inclined clear boundary.
>125	Parent material (mostly limestone)

Figure 7: Haplic Cambisol (Clayic, Calcaric, Rhodic) above Hypercalcic Cambic Calcisol (Thaptocambic,Sodic) [Vertic Haplocalcids]. ( After (Pietsch and Kühn, 2009).

## 2.4 Vegetation

Due to its endemic biodiversity, Socotra is currently being described as the “Galapagos of the Indian Ocean” (Elie, 2014). It has been ranked as a fourth place among the ten richest of the

world's oceanic islands that are distinguished by the richness of their biodiversity. The island has reported as a unique in its flora and therefore, a home to diverse terrestrial plant and animal life with a high number of species and endemism found nowhere else on the earth (Alexander and Miller, 1995). This high species level of endemism as also reported by (Miller and Morris, 2004b) inventory, hosts 825 species of vascular plants, of which 308 (37%) are endemic ((Miller and BAZARA, 1996). Out of the eighteen plant genera endemic to the Arabian Peninsula, ten genera are restricted to the Socotra archipelago (Miller and Morris, 2004b). The figures for botanical diversity confirm the Socotra Archipelago's global status as one of world's most botanically important island groups, comparing favourably in floristic richness and endemism with such famous islands as Mauritius, the Galapagos and the Canary islands (Rössler, 2006). The essential statistics for the Flora of the Socotra Archipelago are summarised in table 2 below.

Species	No.
Flowering plants and ferns species	850
Flowering plants and ferns genera	389
Flowering plant families	99
Endemic taxa	293
Endemic genera	12

Table 2. Plant richness in Socotra (After (Rössler, 2006)

The island received much attention from collectors during the late 90's and in the beginning of the 2000's. The Government developed major strategies such as the Socotra Archipelago Master Plan and the Biodiversity, Ecotourism, Women and Environment strategies. Parallel to this, the public awareness and concern have grown, supported by the increased NGO activity and the media involvement in environmental issues.

The existing literature on Socotra has revealed valuable information (Table 3) on the vegetation and it can be widely categorised associated among the four main topographical zones. The majority of woody species forming natural forest in the island are woodland and shrub communities which rank among the endemic species. Among important and valuable of them are arborescent dragon's blood trees (*Dracaena cinnabari*) which is mostly located on the high altitude plateau and mountain areas and is a source of gum resin, frankincense trees (*Boswellia ameero*, *B. elongata*, *B. dioscorides*, *B. popoviana*, *B. nana*, *B. socotrana*), myrrh trees (*Commiphora socotrana*, *C. ornifolia*, *C. parvifolia*, *C. planifrons*), arborescent spurges (*Euphorbia arbuscula*, *E. socotrana*), the rare endemic shrub *Dirachma socotrana* and the wild pomegranate species (*Punica protopunica*). Typical of Socotra are remarkable succulent woody species, particularly the endemic cucumber tree (*Dendrosicyos socotrana*), the only woody species from the family of *Cucurbitaceae*, desert rose (*Adenium obesum ssp. sokotranum*) and endemic *Dorstenia gigas* from the family of *Moraceae* rarely growing on shady rocks. Also fauna of Socotra is rich in species and little investigated yet (RAP-CMO, 2004) and (MWE-EPA, 2004). The vegetation societies are mainly stressed by water shortages and have developed adaptations to cope with this phenomenon ).

Land form	Geology	Associated Species
<b>Mountains</b>	Limestone Granit	<i>Dracaena cinnabari</i> , <i>Buxus hildebrandtii</i> , <i>Croton sp.</i> and <i>Rhus sp.</i> , <i>Tamarix sp.</i> , <i>Ormocarpum caeruleum</i> , <i>Mussoenda capsulifera</i> , <i>Jasminum grandiflorum</i> , <i>Porana obtuse</i> , <i>B. elongata</i> , <i>B. pedicellatus</i> , <i>B. ameero</i> , <i>Euclea divinorum</i> and <i>Hypericum scopulorum</i> .
<b>Plateaus</b>		<i>Croton socotranus</i> , <i>Dracaena cinnabari</i> , <i>Buxus hildebrandtii</i> , <i>Heliotropium nigricans</i> , <i>Corchorus erodiodes</i> , <i>Trichocalyx obovatus</i> , <i>Rhus thyrsoiflora</i> , <i>Aloe perry</i> , and <i>Pulicaria stephanocarpa</i> .
<b>Coastal Plain</b>	Sand, Alluvial	<i>Limonium axillare</i> - <i>Atriplex griffithii</i> , <i>Croton socotranus</i> - <i>Cissus subaphylla</i> , <i>Aizon canatiensis</i> , <i>Salsola sp.</i> , <i>Salvadora persica</i> , <i>Indigofera nephrocarpoides</i> , <i>Panicum rigidum</i> , <i>Acacia edgeworthii</i> , <i>Tamarix nilotica</i> , <i>Limonium socoranum</i> , <i>robecchii</i> , <i>Justicia rigida</i> , <i>Jatropha unicostata</i> , <i>Pulicaria stephanocarpa</i> , <i>Dendrosicypos socotrana</i> , <i>Limonium axillare</i> - <i>Atriplex griffithii</i> , <i>Croton socotranus</i> - <i>Cissus subaphylla</i> , <i>Aizon canatiensis</i> , <i>Salsola sp.</i> , <i>Salvadora persica</i> , <i>Indigofera nephrocarpoides</i> , <i>Panicum rigidum</i> , <i>Acacia edgeworthii</i> , <i>Tamarix nilotica</i> , <i>Limonium socoranum</i> , <i>robecchii</i> , <i>Justicia rigida</i> , <i>Jatropha unicostata</i> , <i>Pulicaria stephanocarpa</i> , <i>Dendrosicypos socotrana</i> , and <i>Adenium obesum subsp. sokotranum</i> .
<b>Wadies</b>		<i>Croton socotranus</i> , <i>Cissus subaphylla</i> , <i>Jatropha unicostata</i> , <i>Pulicaria stephanocarpa</i> , <i>Dendrosicypos socotrana</i> , and <i>Adenium obesum subsp. sokotranum</i> .

Table 3. Dominant species corresponding to the geological features and land form type.

## 2.5 Land use

Land use is not consistent throughout the islands. Socotra as stated by (Morris, 2002) must be viewed as a mosaic of different traditions, conventions and priorities. Thus what is found and is a practice to be true for one area will not necessarily be found to be so for another. The rich diversity of flora and fauna is mirrored by an equally rich diversity of human behavior and custom. Thus what is regarded as suitable human food, for example or what is seen as a useful medicinal or veterinary practice, what an appropriate response to drought, what takes priority over something else even what is seen as good browse for livestock can be expected to differ from area to area. Traditional land management practices have played major roles on the survival of flora and vegetation during the last decades (Scholte et al., 2008). Socotranis people live in the island and subsist mainly on fishing, the cultivation of date palms and pastoralism for their livelihood. Milk and date palms are the most important food on the island and therefore, goats, sheep and cattle, are the main source of economic production for the people in rural areas (but not coastal areas, (Scholte et al., 2008)). Newly many spread home gardens introduced for family need vegetables and fruit. All the livestock species in the island are well adapted over many centuries to the peculiarities and rigours of the Socotra terrain and climate (Morris, 2002). However, major developments in land use have taken place with the starting of the SCDP 1997. There was an increase in inventories of the terrestrial and marine environments and land use (Mies, 2001, Morris, 2002, Wranik, 2003, KRUPP, 2004, Miller and Morris, 2004a). After 1990, the land use system of the study area experienced a change similar to collapse. The collective and state farm ownerships were abolished. The people, having been discharged by herding, left their settlements and moved into the nearest cities hoping to find a job (Fig. 8). Numerous settlements were fully abandoned and nowadays stay uninhabited.

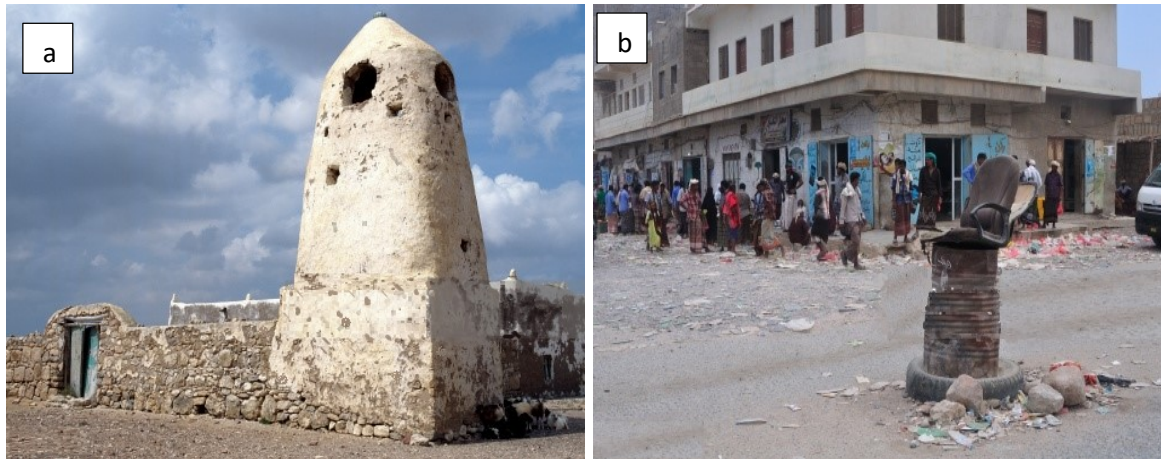


Figure 8: Trace of the radical changes in land use in the island, (a) abandoned rural areas, (b) new urbanization system.

### **Change in land use practices**

Over the last few decades, the island experienced a great trend for people to settle in towns and villages. The increased arrival of great numbers of people from the mainland with division of land between the tribes has increased land value and resulted in an increase in land ownership conflicts. This has caused more pressure on some areas (Morris, 2002) and less movement of livestock. The expanding roads network has triggered a new type of movement and livestock widely undertaken by cars. Although, little is known of its impact, but it is likely that the more accessible areas experienced an increased grazing pressure (Morris, 2002). Land use management has also greatly changed and the pace of this change is accelerating and many of the traditions procedures and skills have either already been lost or are undergoing change (Miller and Morris, 2004a). However, Socotra's pastoralism and care of domesticated livestock regarding herd care and mobility history is reflected in the inherited learned knowledge and land tenure system. This has been highly influenced with the increasingly newly permanent land uses, such as tourism and agriculture, urbanization and land rights being claimed and are often a source of land use conflict (Scholte et al., 2011).

During the decades of Socialism, the common areas were considered public property that everyone could use but no one cared for. Since the collapse of the Soviet Union followed by the country unification on 22nd May 1990 people have gained the possibility to own their properties. As the next step after the privatization of land and housing, the management of land is now being transferred from the public sector to the private sector. This has encouraged the new market-oriented housing, tourist and urbanization system which is being built on the legacy of the land and grazing areas and which has a great impact on the current situation.

### **Changes in land ownership and land use**

The island tends to have high population density with intensive land uses in which the need for importing products arises, associated with high rates of introduced species for food, wood and medicines, or as ornamentals. However, increased population pressure on land enhances the importance of private tenure and decreases the importance of community rights.

As results of the political transition in the early 1990s, there was a radical transformation in the conditions of proprietorship and the establishment of private property as the dominant form

of property. Many conflict problems arose out of those and are the economic and social demands; on the one hand, the unavoidable new change in the structure of land ownership, and on the other hand, the compensation for the damage caused to private property by the previous regime. The access grazing to the large areas of rangelands is generally held collectively. This does not mean that access is uncontrolled, only that rangeland use is regulated at the level of a collective rather than at the level of individual landowners. Use of the rangeland involves system rules obeyed by the community of users whereas non-members are excluded. On Socotra, there are in place traditional rules to enforce transhumant movements and rotation of grazing. When grazing and browse is exhausted in one area, tradition demands access to the rangeland of other communities. At such times, group leaders negotiate rights for their members to use the pastures of another group, on the understanding that the agreement will work in reverse when conditions demand.

The danger of such agreements is that in a widespread drought, all pasture will be grazed out. Socotra pastoralists move their animals between the upland and lowland grazing according to season, weather, available food, browse and water.

#### **Changes in rangeland management practices**

- Preventing grazing practices after rains ("Nabituh" or "Qabih" practices) allowing the grass and plants to recommence is almost neglected.
- A decreasing number of sheep with slightly increase in the number of the goats has been noticed (this probably will create more pressure on the goats grazing areas).
- Fencing and grazing practices (i.e. "Alzaraib"), which prevent enclosed pasture in the mountainous areas, was declined or rather abandoned.
- Sheep and goats nowadays are left to roam freely, instead of herded to an overnight compound.



## **Chapter 3: Data used and data pre-processing**

### **3.1 Data collection**

Different methods and data collection techniques were used in this study to collect quantitative and qualitative data from both primary and secondary sources. A series of high spatial resolution satellite data from 1972 to 2010 including Landsat products Multi Multispectral Scanner (MSS), Thematic Mapper (TM), Enhanced Thematic Mapper Plus (ETM+), a finer and highest resolution ASTER Digital Elevation Model (1 arc-second or approximately 30 m) grid are the main sources were accessed through the global facility of the NASA Landsat program. All other data used will be described in the chapter.

We reviewed both published and unpublished maps, reports and different literatures from various sources to gather the secondary data. These reviews resulting in a valuable data have been used to support various aspects related to the study. The primary data sources were images from satellite data freely available through the web as well as rainfall data from different stations. Valuable additional information came from ground truth data and physical observation conducted through two prolonged visits to the island during varied weather seasons in transition, summer monsoon 2009 and winter monsoon 2012.

Secondary information came from existing reports and databases as well as from focus group discussions and interviews at target villages. This was aimed at capturing the diversity of livelihood activities, land use and grazing practicing that reflect adaptive capacity and extent of community vulnerability to rainfall changes and related grazing, land use and vegetation growth. This data collected were used to establish the perceptions of rainfall fluctuations changes and its influence on greenness of the island, livestock, existing adaptive capacities and extent of vulnerability of local communities to these changes.

Both primary and secondary data were collected in order to address the objectives of this study (Fig. 9). The summaries of the narrations are used in the discussion in subsequent sections.

### **3.2 Rainfall data and pre-processing**

Different sources were used for the climate. We used the main and old meteorological station at the Mouri Airport as a reference data, then the data from Yemen Civil Aviation and Meteorology Authority (CAMA) along with meteorological stations in the island. We selected all available rainfall data for 11 recent stations (2000–2006) and the old station (Mouri) for the period (1972–2010) and also the gridded monthly rainfall data from the Global Rainfall Climatology Center (GPCC) and Intergovernmental Panel on Climate Change (IPCC). We also reviewed oral local knowledge, passed on through generations (Morris, 2002) for a long-term understanding of the Socotra climate. All available data were merged onto one file, which has been checked and quality controlled.

#### **Preparation of gridded climate maps**

Due to scarcity and discontinuity of meteorological data for the island we used 0.5° rainfall data from the gridded monthly rainfall Reanalysis v4 product (<https://reanalyses.org/>) of the Global Rainfall and Climatology Center (GPCC) (Schneider et al., 2014) to be compared with the available data for analysing rainfall trends in the island. To verify the accuracy of the GPCC data in our study area, we compared available rainfall station data from Mouri station with GPCC

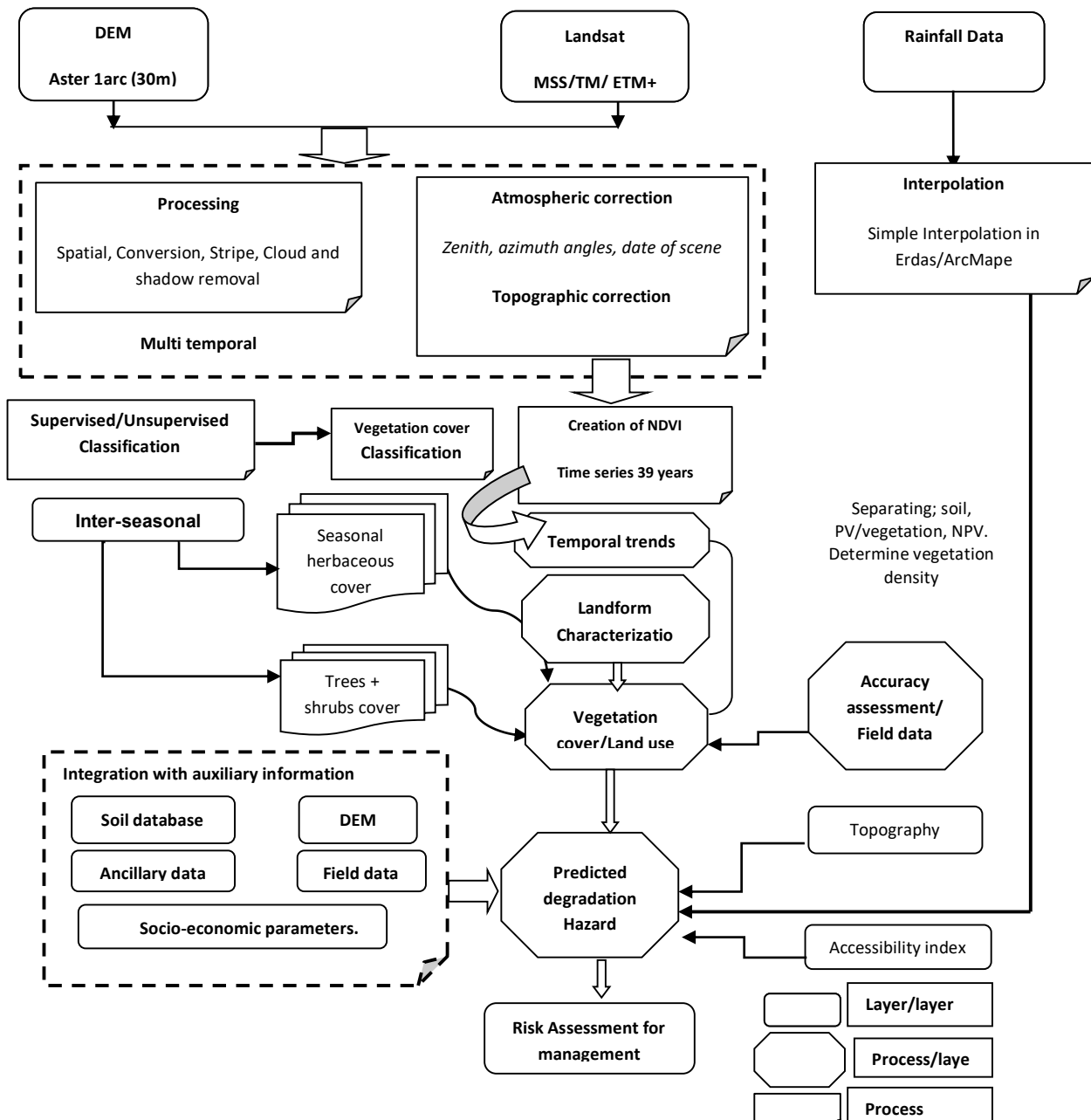


Figure 9: Schematic overview of image processing of satellite data and subsequent analysis to create maps of rainfall, NDVI and vegetation to detect temporal changes and possible degradation.

data from for the same period. Preparation of gridded rainfall maps was made by interpolation of these records based on longitude/latitude and the altitude of the weather stations. Use of a secondary variable, elevation, for modelling gridded maps was important because there is a strong influence of relief on the spatial patterns of climate parameters in the study area. The magnitude of elevation ranges from the sea level to 1500 m. The general increase in rainfall with elevation is well known (Foody and Atkinson, 2002). Several studies have compared different algorithms for deriving predictions of rainfall from point data in conjunction with secondary data (Hevesi et al., 1992b), (Hevesi et al., 1992a), (Gómez-Hernández et al., 2001), (Lloyd, 2002). These algorithms included such techniques as inverse distance weighting (IDW), simple kriging with locally varying means (SKlm), ordinary co-located cokriging (COK) and kriging with an external drift (KED). All these techniques exploit relationships between primary

and secondary variables by regionalizing climate data from point data and enable to increase the prediction accuracy essentially. In this study, all raster maps of rainfall for the study area were constructed using the interpolation method known as kriging with an external drift (KED). A brief description of the KED technique will be given in Chapter 4.

Data obtained from the rainfall multi sources were used to attain the long-term average monthly and annual rainfall at each station. Therefore, we averaged these gauges data for the purposes of the spatial analysis and to be compared with Mouri and give an average value for the island. Data from Mouri were used in the analysis from 1972 to 2010, whereas data from all gauges were used for the period 2005 to 2010. Rainfall data were aggregated into a monthly format to produce a 24 month-long series and then compiled into seasonal wet period (October to March) to examine the differences in rainfall distribution along with the vegetation greenness (NDVI).

Two types of exhaustive secondary information, elevation and distance to the regional rainfall maximum, were used for rainfall interpolation. The elevation was extracted from a DEM with a grid size of 10 m. The distance was computed as the linear distance from the location of the regional rainfall maximum to each respective gauge. Then the location of the regional rainfall maximum was selected as the gauge with total rainfall over each of the aggregation periods. Finally, we used the same grid cells depicted in the DEM to determine distance from the regional rainfall maximum.

### **Interpolation Methods**

After quality control these data were suitable for input into a computer interpolation and mapping technique. The geostatistical analysis extension module of ArcGIS 10.2 (<http://www.esri.com/software/arcgis/arcgis-for-desktop>) was used. A brief description of the rainfall interpolation methods used to estimate rainfall depth at unsampled locations will be subsequently described. These include spatial correlation, different regression types, Thiessen polygon, Kriging, IDW, linear regression, OK, and SKIm. More detailed descriptions of these methods, can be founded in (Goovaerts, 1997, Goovaerts, 2011). Finally, a total of 12 rainfall point data were spatially analyzed to generate rainfall spatial variability maps.

### **3.3 Satellite data**

A crucial decision the analyst must make when undertaking change analysis using multispectral satellite images is image selection. Over the almost 40-year life span, approximately, 73 images were selected for analysis and detecting the vegetation change for Socotra. We followed several steps in choosing the images to analyze. Firstly, since our interest is in changing of the vegetation cover, so we have considered the temporal frequency of human activities on vegetation cover. Trees cutting, overgrazing, development in the area and preservation activities have to be spectrally identified. Development and preservation activities might begin at a particular time point and then will most likely remain throughout the Landsat time series. Overgrazing and trees cutting in this region, however, will result in an initial pattern of disturbance might be followed by regrowth and possible cutting again from time to time throughout the 40 years. (Schweik and Green, 1999) consider, given that the Landsat system has been operational for more than 40 years, that maximizing the temporal extent of the image time series can more appropriately sample the overgrazing and trees cutting activity. In this

regards approximately 15 Landsat MSS, 30 Landsat TM and 28 Landsat ETM images during the growing season were selected from the archives (<http://eros.usgs.gov/doi-remote-sensing-activities/2015/Home>) for the period 1972 to late 2010). Second, we considered the impact of seasonal effects on spectral response. We selected the late summer and early winter as an appropriate scene for the study of vegetation resources when trees and canopies are fully green. Moreover, the gaps where cutting or overgrazing exposes some bare soil is more apparent when a tree canopy is in full leaf (Miller et al., 1996) cover than in fall or spring scenes. There is also a contrast between herbaceous growth and forests in late summer when dry conditions promote herbaceous senescence. For these reasons, we selected only images acquired between October and March. We also insured that the images were selected as nearly time as possible with the season and time of year coincident with the favorable atmosphere and high biomass in order to minimize the influence of sun's synchronous orbit and diurnal variability in the satellite images. Third, we considered the year to year climatic variability in the images. Despite the irregular rainfall and the dense presence of clouds, it became apparent that our selected images were dramatically aligned with the rainfall in the area under the hypothesis that the difference might have happened due to a higher than normal rainfall during other year. It is important, then, to select images that have had similar rainfall and temperature patterns during the months or even the year prior to image acquisition. Finally, the cost drives image selection. For this study, we used the free online geo-registered time series of Landsat MSS, TM and ETM+ images made available at no cost through EROS DATA CENTER-USGS, through the website.

### **Satellite imagery review**

Remote sensing imagery, including the Landsat products Multi Multispectral Scanner (MSS), Thematic Mapper (TM), Enhanced Thematic Mapper Plus (ETM+), and Operational Land Imager (OLI), have ideal sampling characteristics for monitoring diverse land cover and vegetation types at a regional in historic level (Cohen and Goward, 2004, Cohen et al., 2010, Miller and Rogan, 2007). The 30 m spatial resolution of Landsat sensors allows for spatial detail to be captured at a scale appropriate for monitoring vegetation structure and composition (Willis, 2015). General changes in land cover classes are also detectable through Landsat, such as conversion between water resources and agricultural land (<http://eros.usgs.gov/doi-remote-sensing-activities/2015/Home>, Urban, Marcel et al 2014 and Hese 2012). The two sensors of Landsat Data Continuity Mission (LDCM/Landsat 8), the OLI sensor and the Thermal Infra-Red Sensor (TIRS), well known provide seasonal coverage of the global landmass at a spatial resolution of 30 meters (visible, NIR, MidIR); 100 meters (thermal); and 15 meters (panchromatic) to be used for current monitoring purposes since its launch in February 11, 2013. Change detection of ecosystems became repeatedly monitored by Landsat imagery. Associated methods are rapidly evolving due to free access to data, increased automated algorithms, and detailed information becoming available over large geographical swaths (Cohen et al., 2010).

Many techniques have been proposed for change detection in medium resolution radar or multispectral data. However, the availability of very high resolution data (even formally under 1m) acquired by many space borne sensors such as QuickBird in the US Fish and Wildlife Service Desert National Wildlife Refuge, Earth Observing Mission 1 (EO-1), IKONOS/Geoeye, Advanced

Land Observing Satellite (ALOS), Advanced Space borne Thermal Emission and Reflection Radiometer (ASTER) and Advanced Land Imager (ALI) (Wiens et al., 2009) resulted in a new set of possible applications, by a high geometrical precision. Nevertheless, this increase in the resolution induces new constraints that are more complex to mitigate the new born geometrical considerations and radiometrical considerations.

We have chosen Landsat which provide a high resolution and an adequate range of spectral bands. It is highly acquired in most of natural resource studies since many other sensors do not offer freely available data. Table 4 shows different satellite sensors ensuring varying scales of vegetation that can be studied. Landsat is useful for vegetation communities, whereas SPOT or QuickBird may be used for species or specific vegetation change monitoring. Or high resolution aerial imagery along with QuickBird can be used to monitor changes in sensitive ecosystems such as aquatic habitat (<http://eros.usgs.gov/doi-remote-sensing-activities/2015/Home>).

### Data acquisition

Several optical space borne sensors with different temporal and spatial resolutions allow regular monitoring of the different temporal properties of ecosystem dynamics as they provide multi-temporal measurements of the land surface. In this context, sensors that provide data on an inter-seasonal time scale are particularly useful as they can be used to monitor the seasonal temporal trajectory driven by plant phenologies sometimes. These sensors are varied based on their temporal and spatial characteristics for describing the ecosystem phenomenon.

The entire image base of Landsat imagery has recently been released to the public, and this family of satellites would seem to hold promise for long-term low cost studies of vegetation cover. Images were accessed through the global facility of the NASA Landsat program (<http://landsat.usgs.gov/> and <http://glovis.usgs.gov/>). It was not possible to obtain Landsat images of the study area for the similar time of each decade because of cloud cover (see e.g. Figure 10) and the limited availability of the images release by NASA. The choice of Landsat sensors was made because of the need for either a sufficient spatial resolution allowing to distinguish the main different vegetation species in the study area and to have a sufficiently long image time series.

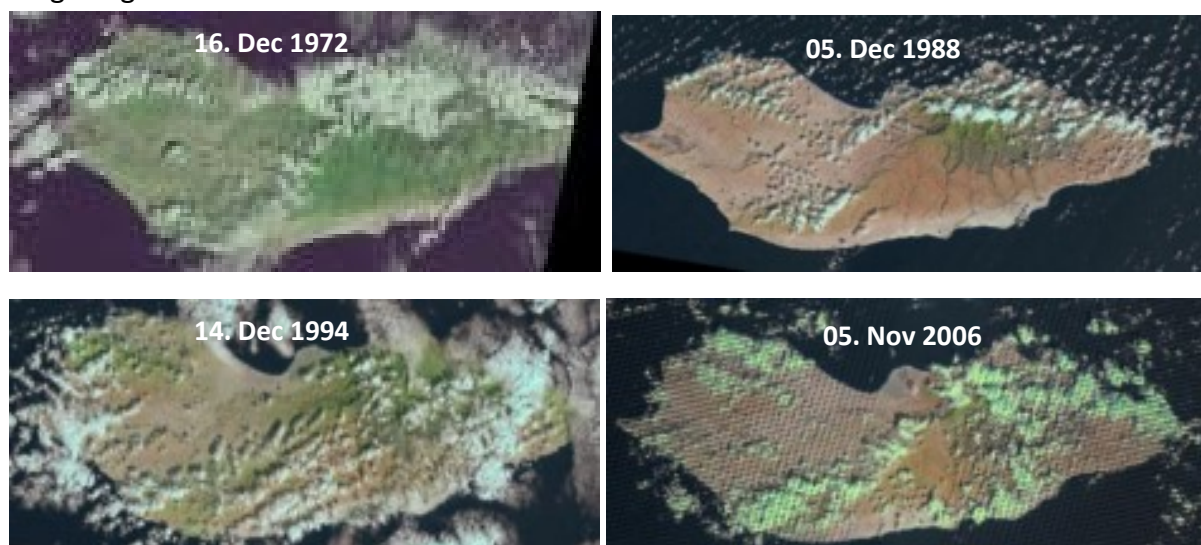


Figure 10: Examples for cloud cover of Socotra Island though the last 40 years (see Appendix 1)

A series of this high spatial resolution satellite data from 1972 to 2010 was acquired (Table 5), all referring to the late winter/early spring period and thus relating to the seasonal peak of vegetation development period in the area under study.

Table 4. Example of a 2014 cost-benefit analysis for choosing appropriate satellite imagery (after (Willis, 2015)).

Satellite	Background information	Spatial resolution	Nominal revisit time	2014 Base cost for images (per km <sup>2</sup> )	2014 Base cost for images (per km <sup>2</sup> )	Spectral resolution	Applications
<b>MODIS</b>	NASA product on Terra and Aqua satellite, launched 1999	250 m (bands 1–2), 500 m (bands 3–7), 1000 m (bands 8–36)	1–2 days	Free	n/a	36 Bands available at different resolutions	Phenology
<b>Landsat TM/ETM+/OLI</b>	NASA product since 1972	30 m	16 days	Free	n/a	7 Bands on Landsat 5, 8 bands on Landsat 7	Land use/land cover change
<b>IKONOS</b>	First high resolution color imaging satellite since 1999, owned by DigitalGlobe	0.80 m pan <sup>a</sup> , 2.4 m multi <sup>b</sup>	3–5 days	\$10 (minimum order 25 km <sup>2</sup> )	\$20 (minimum order 100 km <sup>2</sup> )	Pan <sup>a</sup> , multi <sup>b</sup> (4-band), natural color (3-band), color IR <sup>c</sup> (4-band) pan-sharpened, or pan <sup>a</sup> + multi <sup>b</sup>	Data validation
<b>GeoEye-1</b>	Highest resolution commercial color imagery satellite since 2008, owned by DigitalGlobe	0.46 m pan <sup>a</sup> , 1.84 m multi <sup>b</sup>	<3 days	\$13–29 (minimum order 272 km <sup>2</sup> )	\$22–38 (minimum order 100 km <sup>2</sup> )	Pan <sup>a</sup> or multi <sup>b</sup> (4-or 8-band)	Data validation
<b>Quickbird</b>	Owned by DigitalGlobe, launched 2001	0.61 m pan <sup>a</sup> , 2.4 m multi <sup>b</sup>	1–3.5 days	\$13–29 (minimum order 272 km <sup>2</sup> )	\$22–38 (minimum order 100 km <sup>2</sup> )	Pan <sup>a</sup> or multi <sup>b</sup> (4-or 8-band)	Data validation
<b>SPOT 1-7</b>	Launched in 1986, owned by Spot Image, France	2014 1.5 m pan <sup>a</sup> , 6 m multi <sup>b</sup> ; 2002–2014 2.5–5 m pan <sup>a</sup> , 10 m multi <sup>b</sup> 1986–2002 10 m pan <sup>a</sup> , 20 m multi <sup>b</sup>	1–3 days	\$32 (minimum order 60 km <sup>2</sup> )	\$24–72 (minimum order \$3600)	Pan <sup>a</sup> or multi <sup>b</sup> (4-band)	Data validation
<b>ASTER</b>	NASA product on Terra satellite, launched 1999	15 m visible near IR <sup>c</sup> , 30 m shortwave IR <sup>c</sup> , 90 m thermal IR <sup>c</sup>	16 days	\$1.50/imagery\$0.75/DE M <sup>d</sup>	n/a	15 bands	Supplementary data source, DEM <sup>d</sup>

A Pan – panchromatic includes one greyscale band of combined red, green, and blue of visible electromagnetic spectrum.

B Multi – multispectral covers multiple bands along the electromagnetic spectrum.

C IR – Infrared.

D DEM – Digital Elevation Model.

Among available scenes in the USGS data archive only few datasets had relatively low cloud contamination for the selected study area, i.e. the Landsat 4 (MSS) for 1972-1973, the Landsat 5 (TM) for 1985-1986 and 2 (TM) for 1994-1995 and finally 7 Landsat (ETM+) scenes with the 1T level of pre-processing for 2009-2010 (Table 5&6). These data sets are located on the satellite path 171 and row 51 for the Landsat 1-4 and the path 159 and row 51 for the Landsat 5 and 7. The satellite images were acquired during early October until late March of the consecutive year, respectively. It is generally a dry season in Socotra between June and September and therefore no significant spectral differences in the images are expected due to seasonal differences.

Satellite	Sensor	Band No.	Spectral Range	Scene Size	Pixel Res.
<b>Landsat MSS</b>	MSS multi-spectral	1,2,3,4	0.5 - 1.1 $\mu\text{m}$	Appr. 170 X 185 km	60 meter
<b>Landsat TM5</b>	TM multi-spectral	1,2,3,4,5,7	0.45 - 2.35 $\mu\text{m}$		30 meter
	TM thermal	6	10.40 - 12.50 $\mu\text{m}$		120* meter
<b>Landsat7 ETM+</b>	ETM+ multispectral	1,2,3,4,5,7	0.450 - 2.35 $\mu\text{m}$		30 meter
	ETM+ thermal	6.1, 6.2	10.40 - 12.50 $\mu\text{m}$		60* meter
<b>Landsat 8 (OLI)</b>	Panchromatic	8	0.52 - 0.90 $\mu\text{m}$		15 meter
	Multispectral	1,2,3,4,5,6,7,9	0.43 – 1.38		30 meter
	Panchromatic	8	0.50 – 0.68		15 meter
	Thermal	10,11	10.60 – 12.51		100*

Table 5: Spectral characteristics and spatial resolution of the image data used.

Data type	Path	Row	Acquisition date	Cloud Percent (%)	Spatial resolution
<b>Landsat MSS</b>	171	51	<b>1972 10 05</b>	5%	79 m
	171	51	1972 12 16	18%	79 m
	171	51	1972 11 10	5%	79 m
	171	51	1973 01 03	30%	79 m
	171	51	1973 02 26	1%	79 m
<b>Landsat TM 4 &amp; 5</b>	159	51	<b>1984 12 02</b>	20%	30 m
	159	51	1985 01 19	25%	30 m
	159	51	1985 03 08	3%	30 m
	159	51	1994-10-11	10%	30 m
	159	51	<b>1994-11-28</b>	40%	30 m
	159	51	1995-01-15	5%	120* m
	159	51	1995-02-16	7%	30 m
	159	51	1995-03-04	2%	
<b>Landsat 7 ETM+</b>	159	51	2005-10-01	1.5%	30 m
	159	51	2005-11-02	1%	30 m
	159	51	2005-11-18	10%	30 m
	159	51	<b>2005-12-20</b>	5%	30 m
	159	51	2006-03-10	5%	30 m
	159	51	2006-03-26	0%	30 m
	159	51	2009-10-12	10%	30 m
	159	51	<b>2009-10-28</b>	2%	30 m
	159	51	2010-03-21	2%	30 m

Table 6. Scheduled images used for the study area. (\*) Bands are acquired at this resolution, but products are resampled to 30 meter pixels.

### 3.4 Data pre-processing

Pre-processing of satellite images prior to image classification and change detection is essential. First of all, we tried to eliminate or to reduce the errors of satellite images. However, this stage required a long sequence of time-consuming procedures and the use of numerous techniques. It takes into account measurable reflectance of the atmosphere, aerosol scattering and absorption and the earth's surface to avoid the volatility of the atmosphere, which might introduce variation between the reflectance values or digital numbers (DN's) of satellite images acquired at different times. However, image pre-processing is necessary to correct any distortion inherent in the images due to the characteristics of imaging system or sensor conditions. It commonly comprises a series of operations, including atmospheric correction or normalization, image registration, geometric correction, radiometric correction and masking (e.g., for clouds, water, irrelevant features). When pre-processing is completed, then images can be enhanced to improve their visual appearance of the objects on the image and help in extracting useful information that assists image interpretation. Commonly used image enhancement techniques include image reduction, image magnification, transect extraction, contrast adjustments, band ratioing, spatial filtering, Fourier transformations, texture transformation and statistical numerical methods (e.g. regression variable substitution, arithmetic combination, mathematical convolution operation, high-pass filtering, principal component analysis, canonical variable substitution, wavelets transforms and component substitution), fuzzy logic and multivariate statistical analysis. Images from different Landsat sensors containing distinctive features in reflecting vegetation cover and land surfaces were used in our study (Fig. 11). During image-to-image registration, nearest neighbour resampling algorithm was used to resample the images in order to avoid the change of digital numbers and also to maintain the same pixel size of 30 m by 30 m for all images. Sun angle and elevation as well as the gain and offset for each band were obtained from the image data file. Geometrically corrections and atmospherically calibrations and many several subsequent processes were used to develop clear textural images for vegetation indices and farther image classification analysis. Many of those processes will be described later.

The data processing was carried out using the following software packages: Erdas Imagine 2014, Geomatica 5, ENVI 5, ArcMap 10.1, Geospatial Modelling Environment and PANCROM ver. 5.97.56. All images were resampled to 30 m pixel size for all bands using the nearest neighbor method. Subsequently, they have been geo-referenced and projected to the Universal Transverse Mercator (UTM) coordinate system, Datum WGS 1984, zone 40 North. To ensure that time series images are directly comparable to one another, the relatively cloud free 2004-26-05 Landsat TM was selected as a reference image for the geo-reference. The images were subsequently clipped to the final study area then radiometric enhancement was applied. This step takes into account a set of techniques that are applied including corrections related to the sensitivity of the sensors, sun angle and earth surface as well as the atmospheric scattering and absorption. Thus however, involves haze and noise reduction, destripe data, histogram matching and topographic normalization. Furthermore, geometric rectification was achieved using polynomial model based on 100,000 scale British topographic maps and twenty ground control points (GCPs). Finally, images were corrected to remove the effects of atmospheric scattering (Teillet and Fedosejevs, 1995, Richter and Schläpfer, 2016). We also performed



additional georeferencing verification by overlaying a very accurate GPS new recorded roads network over each image and visually confirmed the georeferencing of each image. Other ancillary data, such as topography information, soils data, census tract, roads and networks, statistics and meteorological records, were also combined with remotely sensed data to improve classification performance (Jupp et al., 1994, Congalton and Green, 2008, Belgiu and Drăguț, 2016, Gao et al., 2016). Consequently, thematic vector layers provided by the local UNOPS/EPA Office (e.g. fishing villages, geology layer, land cover map etc.) were also incorporated in the rule based pre-processing. As discussed before, GIS techniques then will play an important role in the effective use of ancillary data in improving vegetation cover classification performance. For data compatibility and avoiding data conflict analyses, all the data were standardized and resampled to 30 m of resolution.

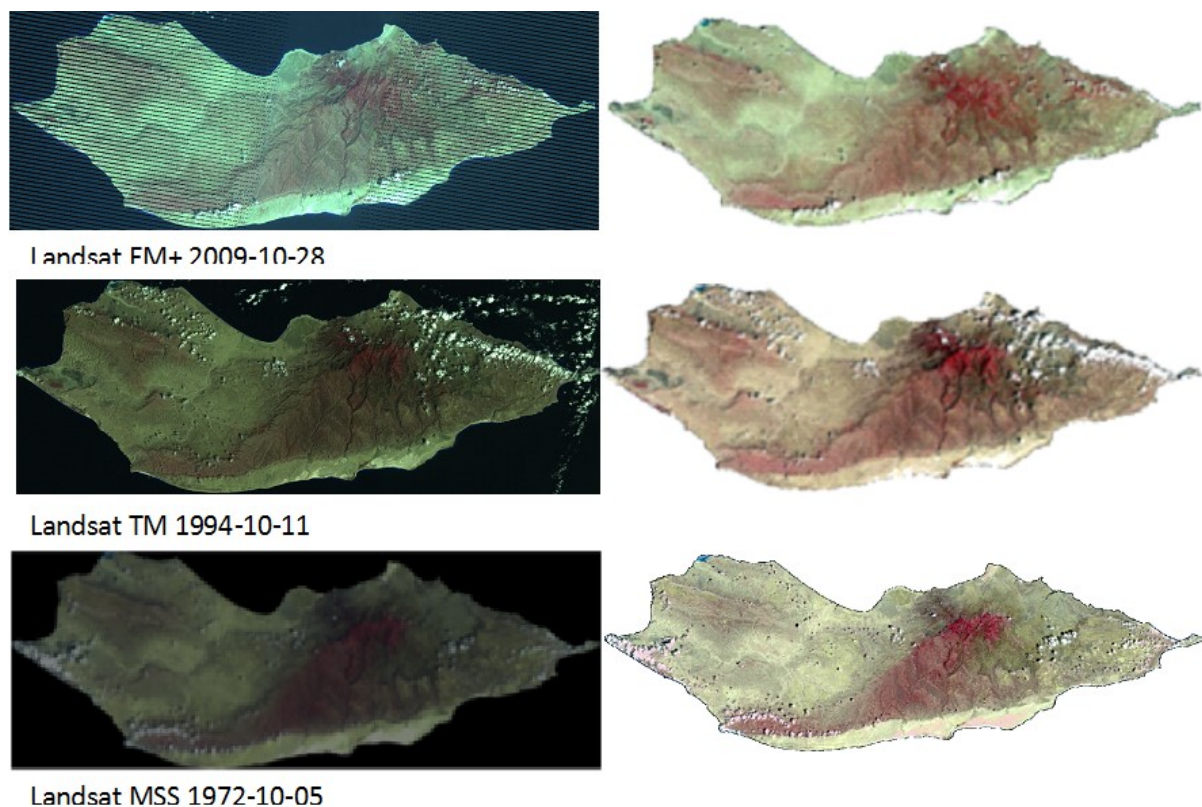


Figure 11: Three different Landsat images left side before and right side after pre-processing.

### 3.4.1 Geometric corrections

Although the new generation of sensors show improved data acquisition and image quality, some inherent distortions affecting the signal coming from the Earth surface and collected by satellites still remain and require correction before performing reliable analysis. Typical corrections include geometric and radiometric distortions (Toutin, 2004). Image geometric characteristics are set by the orbit, spacecraft attitude (roll, pitch, yaw), scanner properties and earth rotation and shape.

As a first step, 20 GCPs were used to georeference and register the entire Landsat data sets to the Universal Transverse Mercator (UTM) projection System (zone number 40N; reference datum WGS84). The first order polynomial transformation model which is also known as quadratic polynomials and nearest neighbour method for resampling were used for

rectification of the images. The Root Mean Square (RMS) of GCPs in x and y directions for TM and ETM scenes was 0.32 and 0.270 pixels, and 0.51 pixels for MSS respectively which is less than one pixel (30m). All these GPS data were taken among the island using the asphalt road junctions, and the natural distinct as land-shapes, seacoast, buildings and wadis.

#### **3.4.2 Noise and de-stripping in image data**

Inherent noise in the images is still present in any downloadable data set and, therefore, these images need to be smoothed before being used for NDVI time series. Such noise is mainly due to remnant cloud cover, snow, water, or shadow. Such sources of errors tend to decrease the NDVI values. Unfortunately, it was hardly to obtain Landsat images of the study area for the exact time of each decade because of the cloud cover density. Furthermore, a malfunctioning of Scan Line Corrector-off acquisition mode in the Landsat TM system from May 31<sup>st</sup> of 2003 (see [http://landsat.usgs.gov/slc\\_off.html](http://landsat.usgs.gov/slc_off.html), for references) created more difficulty in which we got to deal more synchronously though the cloudy satellite data.

#### **3.4.3 Atmospheric correction**

Topographic effects are well known problems that influence spectral reflectance and temporal data used for monitoring vegetation changes and land cover classification in the mountainous and steep terrain. It is critically influenced by the shadow due to the sun position and might cause variations in surface reflectance values for the same cover (Richter et al., 2009, Richter and Schläpfer, 2011). Therefore, in correcting surface reflectance, it is essential to remove the effects of the attenuation from highly variable aerosols, different sun illumination conditions due to topographic effects, scattering by the atmosphere and to put multitemporal data on the same radiometric scale, (Li et al., 2016c). Relatively considerable effort has been expended on quantitative atmospheric correction of remotely sensed imagery and different techniques have been developed. These efforts dealt with invariant-object, histogram matching, dark object, and contrast reduction. (Kaufman and Tanre, 1992, Carlson and Ripley, 1997, Miura et al., 1998, Teillet and Fedosejevs, 1995, Gao et al., 2009, Franch et al., 2013, Fuyi et al., 2013, Richter, 1996, Song et al., 2001, Potter, 1984), (Lee et al., 2016, Mao et al., 2016, Okin and Gu, 2015). Huang et al. (2009b) categorized those techniques into two categories: theoretical approaches using an atmospheric model and empirical approaches with ground data, whereas (Balthazar et al., 2012) categorised them into three groups based on their degree of complexity and data required (i.e. simple empirical methods, such as band ratioing, semi-empirical approaches, such as the Cosine correction and the physically based approaches), while (Thompson et al., 2016) used Bayesian inference for the atmospheric correction.

While seriously efforts have been devoted to refine the topographic correction methods, however, still according to many authors there is no generally and standard accepted universally applicable model. Consequently, ATCOR3 semi-empirical algorithm atmospheric correction developed by Dr. Rudolf Richter from the DLR institute is reported as a well performance procedure over a wide-ranging of satellite sensors in diverse terrains. It has been widely used for eliminating topographic and atmospheric content from the images data as well as correcting the radiometric variability might cause by haze and been implemented in many

GIS software such as ERDAS Imagine and PCI Geomatics (Richter et al., 2009, Hantson and Chuvieco, 2011, Balthazar et al., 2012)

In this study atmospheric correction and haze normalization were performed individually per each image using same procedure described in semi empirical ATCOR3 algorithm procedure developed by Richter et al., (2009) and (Richter and Schläpfer, 2014). However, it is an algorithm that computes the ground reflectance for each pixel in each spectral band. Despite the broad range of ATCOR3's database which consists of standard values for different pressure altitude, air temperature, visibility, humidity, ground elevations, solar zenith angles as well as solar azimuth and acquisition date/time, nevertheless some of these parameters such as solar zenith need to be adjusted. A new calibrated file (\*.cal) was created for each image with modified  $c_0$  and  $c_1$  values based on gain and bias values calculated using max and min radiance for each spectral band obtained from the imagery metadata. These files were then used to calibrate the radiance in the based ATCOR approach (after Richter et al., 2009):

$$L = c_0 + c_1 * DN \text{ Units } (mW / cm^2 sr \mu m),$$

where  $c_0$  and  $c_1$  are the radiometric calibration coefficients (offset and slope) to convert the digital number (DN) into corresponding at sensor radiance  $L$ .

$$Bias = L_{min} - \left( \frac{L_{max} - L_{min}}{Q_{max} - Q_{min}} \right) * Q_{min}$$

$$Gain = \left( \frac{L_{max} - L_{min}}{Q_{max} - Q_{min}} \right), \text{ then } c_0 = 0.1 * Bias \text{ and } c_1 = 0.1 * Gain \text{ for the unit conversion.}$$

For the other parameters, we tried out various atmospheric conditions until attaining satisfactory results. Thus *rural* worked quite well as an aerosol type as well as the *midlate\_winter\_rural* for the humidity. Solar zenith was calculated as;

$$\text{Solar zenith} = 90 \text{ degrees} - \text{solar\_elevation (in degrees)}.$$

However, for the Empirical Bidirectional Reflectance Distribution Function (BRDF) we followed the recommended rules for the incident angle in mountainous terrain (see (Richter et al., 2009, Richter and Schläpfer, 2011),(Balthazar et al., 2012) and Richter et al., 2009). An approximation of the BRDF threshold angle of  $\beta_t$  was estimated as;

$$\beta_t = \theta_s + 20^\circ \text{ if } \theta_s <$$

$$\beta_t = \theta_s + 15^\circ \text{ if } 45^\circ < \theta_s <$$

$$\beta_t = \theta_s + 10^\circ \text{ if } \theta_s > \theta_s, \text{ where } \theta_s \text{ is solar zenith angle, } g \text{ is the lower boundary threshold.}$$

Factor  $g$  is a lower bound to prevent a too strong reduction. It's value is varied between 0.1 and 1.0 by increment of 0.1 (Vincent Balthazar et al 2012), the default value is 0.25 (Richter and Schläpfer 2011). The high value of  $g$  leads to a rise of bright pixels in the shaded areas while choosing a low value lets dark pixels remaining in low illuminated zones. Therefore, the user is

highly encouraged by several authors to use trial and error in order to obtain adequate results for his specific dataset.

Finally, low pass filter for adjacent correction and linear contrast stretch were applied to each image to ensure adequate contrast.

#### **3.4.4 Multi Date Cloud Masking and Gap Filling**

Clouds and their shadows are a compounded problem inherent with Landsat satellite imagery. However, considerable research efforts have been devoted and several threads of discussion on eliminating its effects and therefore, various techniques have been developed to remove cloudy pixels (Helmer and Ruefenacht, 2005, Ackerman et al., 1998, Lin et al., 2013, Song and Civco, 2002, Martinuzzi et al., 2007). We followed both techniques from (Song and Civco, 2002) and (Martinuzzi et al., 2007) which are simple and straightforward to create masks for identifying clouds and cloud shadows by the use of the benefit of both the clouds highly reflective in the short wavelength band 1 and the cold in band 6, meaning they will appear darker in the thermal band. Different ERDAS model maker algorithms were designed to discern the remains semi-transparent clouds at the cloud edges and such as Cirrus cloud and their projected shadows. We also used the brightness value in Landsat band 4 (near infrared) to verify detection of cloud shadows.

The gap-filling techniques have emerged to mend the masked images and the stripe lines in Landsat 7 due to the significant data loss in each SLC-off scene with the use of the multi-date image compositing techniques. A combined data from two images which have had similar rainfall and temperature patterns during the same month or even a similar month in the year prior or subsequent to image acquisition, was used, under the assumption that the land covers changed insignificantly over a short period of time (Lin et al., 2013). Some other effects such as radiance and color shade due to lighting and atmospheric effects were also somewhat corrected by ERDAS and PANCROMA.

Six-band algorithm in the PANCROMA was used based on the method of (Martinuzzi et al., 2007). Each band of the reference and adjust image was subset into actual extent for effectively eliminating the area beyond the extent of the study area. For the gap filling procedure to perform correctly, the software demands that each pair of matching bands from the two images have identical corner coordinates and row and column sizes. Each of the red, blue, green, and NIR pairs was resized to same numbers of columns and rows, respectively. This method considers both the pixel values in the adjust image and the reference image, and then estimates appropriate new values based on an interpolation of the raster's cells. So gaps were filled in each image individually by selecting matching bands from the reference and adjust images and running the algorithm. Cloud altitude, sun azimuth, and sun elevation were used to calculate the expected clouds and cloud shadows. However, the digital number (DNs) thresholds of the cloud areas were manually determined by inspecting the band 1 and the band 6 and interrogating it using the cursor. The algorithm selected all pixels with DN's below the band 1 user-defined threshold and above the band 6 threshold and classified each pixel as either cloud or non-cloud. The cloud pixels were set equal to zero and the non-cloud pixels are left alone. The result is a band file with the cloud areas blacked out. The Noise (Dust & Scratches) filters were subsequently used to eliminate the remaining ETM+ scratches.

The result was an image with clouds masked and gaps filled in the adjusted image as shown in Fig. 12.

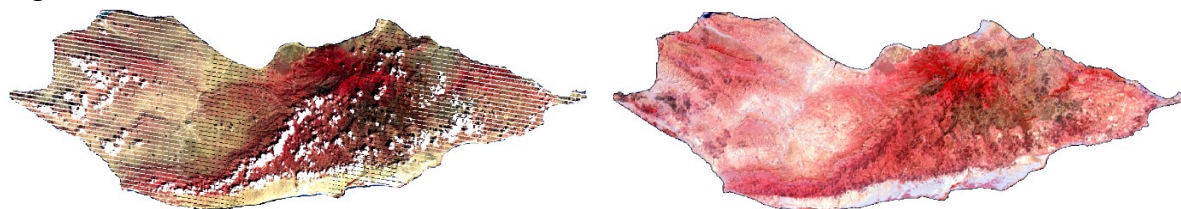


Figure 12: Illumination of clouds with clouds shadows and SLC-off image gaps (Scholte et al.) and adjusted image (right). (Full images see appendix 2)

### 3.4.5 Topographic data and DEM

A new freely available global digital elevation model data set derived from ASTER GDEM satellite system METI/NASA (<http://gdex.cr.usgs.gov/gdex/>) which is characterized by a finer and highest resolution (1 arc-second or approximately 30 m) grid (Balthazar et al., 2012) and best available coverage to date (Hirt et al., 2010) was used in this study. The terrain model was indispensable for pre-processing of satellite data and the supplementary statistical analysis in the main part of the study. Therefore, a topographic normalization of NDVI scenes was carried out to remove these effects. Second, by analyzing spatial relationships between vegetation patterns, climatic factors and relief, the terrain model played an important role appearing in regression equations as an independent constant.

The topographic maps were useful for geometrical correction and rectification of the satellite data, especially that of fine resolution. The vegetation maps were used for identification of areas covered by various vegetation types and validation of the results of modelling land cover change.

### 3.5 Socio-economic data

The population of Socotra is a mixture of many different ethnic groups and developed its own culture and tradition, such as the spoken language, which is distinct from that of the mainland Yemen. They also developed a unique environmental conscience, which is heavily threatened by the pressures of the modern way of life. Socotrani people were originated on the island with its peculiar pastoral culture. They live in tribes (called "bedu") leaded by Sheikhs and have common land ownership so far (Habrová, 2004). In actual fact they know virtually the name of all species for local trees and shrubs and are able to differentiate them by their local Socotran language.

### 3.6 Maps and Field data

Two types of topographic and thematic maps were used in our research work. We used.

- Analogue maps of topography (scale 1,100,000) from 1982
- An analogue vegetation map (scale 1,500,000) from 1995 covering the whole study region
- A digital map of land cover derived from Landsat 7 ETM image (Path/Row 159/051) acquired on 29 April 2001 by (KRÁL, K. & PAVLIŠ, J. 2006).
- A Digital Elevation Model (DEM) derived from ASTER GDEM satellite system METI/NASA (1 arc-second or approximately 30m grid).

- Thematic vector layers provided by the local SCDP/EPA office (e.g., geology map, vegetation type maps, location of villages, etc.) were incorporated in the rule-based post-classification sorting (Knowledge Base classification).
- A set of 20 Ground Control Points (GCPs) acquired by GPS during the ground truth was used for geometric corrections. More than 450 reference points located by GPS were gathered during the field investigation in November 2009.
- Numerous relevant data and figures from SCDP/EPA such as local vegetation database, locally collected GPS data by Bucek and Pavlis in 2002; Pavlis and Habrova 2005; Dr. Miller and Dr. Dana Pietsch, during their field survey between 1999 and 2008, were used mainly as a training data for mapping of altitudinal vegetation zones and partly for land-cover mapping.
- A set of 250 GPS digital photographs were also taken during the fieldwork 2009 to be used for similar purposes especially in areas with lack of other terrain data.
- More than 600 of field data points have been collected during the fieldwork during April 2012 in order to be used for further analysis, validation and modelling of satellite data. The main dataset contains surveys of vegetation distribution (dominant species) and soil types. Contemporary land use (land use type, crops composition/change etc.) have been checked directly in the field. Data for historical dynamics of land use have been derived by interviews with farmers or from statistical reports of local authorities. In order to estimate density of vegetation cover, photos of vegetation cover have been made at every test site (100 m\*100 m). Common indicators for degradation processes have been noted and evaluated where any degradation of vegetation cover was observed.

## Chapter 4: Methodology of data analysis

In this chapter, we briefly describe the main processes and various techniques or rules from which we used specific methods to interoperate our data and highlight the major steps.

### 4.1. Variability of vegetation distribution and change in space and time

An analysis of spatial and temporal variability in vegetation cover was based on the use of elementary methods and variables of descriptive statistics. These methods, described in every statistical textbook, have been widely used as extensions in different GIS and remote sensing software. Here we still have to briefly mention them: Linear time-trends were calculated by regressing a variable (for example, NDVI or Rainfall) as a function of time over the study period, using least-squares estimation. The time-trend calculations included determination of both the regression slope coefficient and increase or decrease of the variable during the study period. The time-trends were determined for area-averaged classes of all variables and, in order to exhibit spatial trends for each grid cell.

### 4.2. Methods of geostatistical analysis

#### 4.2.1. Autocorrelation

Autocorrelation is one of the main tools in geostatistical analysis. It involves correlating a timely sequence of data with itself, statistically known as random process between values at different times (Majid et al., 2016). In other words, the two sets of values to be correlated are achieved by pairing each value  $X_t$  with  $X_{t+r}$ , where  $t$  gives the time or position in the space and  $r$  is an integer value of displacement known as the lag. The correlation coefficient between the samples and a displaced copy of itself is known as the autocorrelation coefficient,  $r_r$ . It can be calculated at successive lags and the resulting series of  $r_r$  values revealing useful information on the structure of the data (Propastin, 2007). These are plotted on an  $r_r$  versus  $t$  graph called an autocorrelogram (Swan and Sandilands, 1995, Griffith, 2013). Where  $t$  is zero, pairs of  $X$  values are identical and the coefficient of autocorrelation clearly equals 1. As  $t$  increases, the similarity between the pairs of values is likely to decrease. At a certain value of  $t$ , we reach a point at which the  $r_r$  ceases to decrease this is the range value. Points with distance exceeds the range value are independent (Wang, Haicheng, Qiuming Cheng, 2015).

#### 4.2.2. Spatial autocorrelation

Spatial autocorrelation actually measures the similarity between samples for a given variable as a function of spatial distance (Sokal & Oden, 1978a,b; Griffith, 1987; Legendre, 1993; Rossi & Quénéhervé, 1998, cited in: (Diniz-Filho et al., 2016). The spatial autocorrelogram describes the degree and form of spatial dependence, which is the similarity between values separated by a given distance. Positive autocorrelation means that geographically nearby variables values tend to be alike on a map (Plutzer et al., 2016). In contrast, with negative spatial autocorrelation geographically nearby values of a variable tend to be dissimilar on a map. Most ecological data tend to be moderately positive spatially auto-correlated because of the way phenomena are geographically organized (Griffith and Chun, 2014). The coefficient of autocorrelation can be calculated on different ways. Moran's  $I$  coefficient is one of the most commonly used coefficient in univariate autocorrelation analysis and is given as;

$$I = \left( \frac{n}{S_0} \right) \left[ \frac{\sum_{i=1}^n \sum_{j=1}^n w_{ij} (X_i - \bar{X})(X_j - \bar{X})}{\sum_{i=1}^n (X_i - \bar{X})^2} \right],$$

where  $n$  is the number of samples,  $S_0$  is the sum of the  $w_{ij}$ s,  $X_i$  and  $X_j$  are the data values in quadrants  $i$  and  $j$ ,  $\bar{X}$  is the average of  $X$  and  $w_{ij}$  is an element of the spatial weights matrix  $W$ .

Under the null hypothesis of no spatial autocorrelation,  $I$  has an expected value near zero, the positive and negative values, indicating positive and negative autocorrelation, respectively. When this positive autocorrelation occurs, it means that Moran's  $I$  is close +1 and this means the values are clustered together.

#### 4.2.3. Kriging with an external drift

Kriging with an external drift (KED) is a geostatistical method used for predicting values and regionalization of point data in space and incorporates the local trend within the neighborhoods. It takes into account one or more external influences on data distribution (Liu et al., 2016). Generally, KED is used for deriving prediction of point data in conjunction with secondary data. A benefit of using KED for regionalization of climate data is the possibility of incorporation of relief and topography variables into a kriging system as external drift function. For further details see (Wackernagel, 1998). The KED predictions are a function of (1) the form of the variogram model, (2) the neighboring primary data (rainfall data), and (3) the modelled relationship between the primary variable and the secondary variable (elevation) locally. The local mean of the primary variable is derived using the secondary information and ordinary kriging (OK) (Jin et al., 2016). The KED prediction is given by the following equation

$$\hat{Z}_{KED(x_0)} = \sum_{a=1}^n \lambda_a^{KED} Z(x_a)$$

The weights are determined through the KED system of linear equation

$$\left\{ \begin{array}{l} \sum_{\beta=1}^n \lambda_{\beta}^{KED} \gamma(x_a - x_{\beta}) + \psi_0^{KED}(x) + \psi_0^{KED}(x) y(x_a) - \gamma(x_a - x_0) \\ \sum_{\beta=1}^n \lambda_{\beta}^{KED}(x) - 1 \\ \sum_{\beta=1}^n \lambda_{\beta}^{KED}(x) y(x_{\beta}) - y(x), \end{array} \right.$$

where  $y$  and  $x$  are the secondary (i.e. elevation) data.

In practice, kriging with an external drift was performed as follows: (i) deriving the underlying (trend-free) predictions for primary data by ordinary kriging; (ii) estimating external drift coefficients at all locations as well as at the nodes of the estimation grid through modelling the relationship between primary and secondary variable; (Xiao et al.) pertaining the obtained coefficients for external drift to the trend-free predictions (Pereira, Maria João, et al. 2016).

#### 4.2.4. Convolution Spatial Filtering

This is a mathematical process on two functions to produce a modified version of the original one. In image processing is an important technique principally to identify different objects and their associations to make an assessment about a phenomenon or process. This spatial



enhancement is a mathematical processing of image pixel data to emphasize spatial relationships (Raja et al., 2016). It modifies pixel values based on the Digital Numbers (DN) values of the surrounding pixels (Dong et al., 2014). Filtering is known as a process meant to enhance certain features or to remove unwanted signal or disturbance (noise) or to remove the effect due to sensor. Convolution explains the relationship between the input image, the kernel or window and the output image in linear spatial filtering.

$$V = \left[ \frac{\sum_{i=1}^q \left( \sum_{j=1}^q f_{ij} d_{ij} \right)}{F} \right],$$

where;

$f_{ij}$  = the coefficient of a convolution kernel position  $i, j$ ,  $d_{ij}$  is the data value of the pixel that correspond to  $f_{ij}$ ,  $Q$  is the dimension of kernel, (if  $q = 3$ , the kernel  $3 \times 3$ ),  $F$  is either sum of the coefficient of kernel, or 1 and  $V$  is the output pixel value (Jensen 1996; Schowengerdt, 1983 cited in: (Sahu, 2007)

#### 4.2.5. Correlation coefficient

In a bivariate distribution where two variables are involved, we were interested to find out if any relationship exists between the variables under study. The existence of any relationship can be proved by calculation of correlation for the couple of variables. If the change of these variables is in the same direction, the correlation is said to be positive. If the variables deviate in the opposite direction, the correlation is negative. A measure of correlation strength reflects correlation the coefficient which may be given as;

$$r(x, y) = \frac{\text{Cov}(x, y)}{\sigma_x \sigma_y} = \frac{\sum (x_i - \bar{x})(y_i - \bar{y})}{\sqrt{\sum (x_i - \bar{x})^2 (y_i - \bar{y})^2}},$$

#### 4.2.6. Multiple correlation coefficients

Multiple correlations are believed to represent the combined effect of several explanatory variables on a response variable. In this study, multiple correlations enable us to estimate the collective influence of environmental factors on NDVI. The used equation for the calculation of multiple correlation coefficients from the derived simple correlation coefficients is given as;

$$R_{xyz} = \sqrt{\frac{r_{xy}^2 + r_{yz}^2 - 2r_{xy}r_{xz}r_{yz}}{1 - r_{yz}^2}},$$

where  $R_{zxy}$  is the multiple correlation coefficient;  $r_{xy}$ ,  $r_{yz}$  and  $r_{xz}$  are simple pairwise correlation coefficients between variables  $x$ ,  $y$  and  $z$  (e.g. NDVI, rainfall, slope, aspect and elevation).

#### 4.2.7. Simple linear regression model

The simple linear model between  $y$  and  $x$ , mostly fitted by Ordinary Least Squares methods (OLS), is;

$$y_t = a + bx_t + \varepsilon,$$

where  $a$  is the intercept,  $b$  represents the slope coefficient for independent variable  $x$ , and  $\varepsilon_t$  is a random error at time  $t$ . The two variables to be related in this model are the dependent variable  $y$  (the NDVI), and the independent variable  $x$  (such as rainfall, temperature, evapotranspiration etc.). We actually applied this predictable regression model to study the relationships between vegetation distribution and environmental parameters, on the hypothesis that at each point of the study area this model will definitely represent and quantify that relationship.

#### 4.2.8. Multiple linear regression model

A multiple linear regression analysis was performed using the response variable, NDVI, and both of the climatic variables. For every year we fitted a multiple linear regression model describing the NDVI value for each pixel in its dependence from the climatic predictors. The full linear model equation is expressed as

$$y = \alpha + \beta_1 X_1 + \beta_2 X_2 + \varepsilon,$$

where  $a$  is the intercept,  $\beta_1$  and  $\beta_2$  are the slope coefficient for the independent variables  $X_1$  and  $X_2$  while  $\varepsilon$  is a random error.

The model parameters were tested sequentially first, the term for rainfall  $\beta_1$  next, the term  $\beta_2$  for elevation and then the intercept  $\alpha$ , and then these parameters were averaged when they were not significantly different as well as the model was refitted, using the averaged parameters.

#### 4.2.9. Quantifying relationship between variables by analyzing spatial relationship

Statistical regressions and correlations have been the most common techniques used to quantify the relationship between a response variable (mostly NDVI) and explanatory variables in studies on monitoring vegetation change. The authors tended to use conventional (OLS) regression as the basic approach for definition of relationships between NDVI and other environment and biophysical variables. However, these conventional statistical methods, especially by quantifying spatial relationships at regional or global scales, are usually not adequate for spatially extended data. In ArcGIS the OLS tool basically will automatically scan for problems associated between the variables under study and automatically checks for redundancy as well as computes standard error values. This approach assumes the constancy of this relationship at every point of the analysis space, i.e. uniformity over space. Unfortunately, in many cases this relationship is not stable in space and appears to vary over space (Foody, 2003), (Ji and Peters, 2004). In such circumstances, the parameters of the global regression model derived by applying conventional OLS regression may not represent local conditions within the study area which might have high variance of relief conditions. Moving window local regression techniques (MWR) and geographically weighted regression (GWR) might overcome this problem and calculate the model parameters varying in space. These techniques are believed to provide a more appropriate and accurate basis in our case for descriptive and predictive proposals and are quite common in geography ((Stewart Fotheringham et al., 1996); (BOSTAN, 2013); (Propastin, 2007); (Zhou and Leung, 2010). Several authors such as (Propastin, 2007), (Foody, 2003)); (Castillo-Santiago et al., 2013); (Imran et al., 2015); (Li et al., 2016b) confirmed that, there are only a very limited studies in the field of

remote sensing in which local regression techniques for analyzing of spatial relationships between NDVI and other biophysical variables have been applied.

#### Moving window regression

Several statistical analysis processes are used for estimating the relationships among variables. They include moving window regression (MWR) and other techniques for analyzing and modeling the relationship for instance between NDVI values and its predicting variables for each point (Propastin, 2007). By moving a window (MWR) of specific size over the study region, both regression and parameters for each pixel are quantified separately from the other points. The size of the moving window can be identified depending on the size of the study region and can be varied from one area to another. All data that lie within the selected window will be estimated and calibrated. This process is repeated for all regression points. Additionally, the process will continue and the local estimated results can be viewed and mapped for each locations of regression points (Fotheringham et al., 2003).

This relationship between the variables within MWR can be expressed as:

$$y = \alpha(\theta) + \beta(\theta)X + \varepsilon,$$

where  $\theta$  indicates that the parameters are to be estimated at a location.

#### 4.2.10. Geographically weighted regression (GWR)

Geographically weighted regression is known as a local form of linear regression often used to model spatially varying relationships. Therefore, it works similarly to the moving window regression except that it always uses a fixed bandwidth and inverse distance weighted kernel. Then each point data will weight by its distance from the regression point. In the local regression, the point closer to the regression is weighted higher than the points further away. In GWR all observations are weighted in accordance with its distance to location  $i$  so that the weighting of an observation varies with  $i$ . The matrix form of parameter estimation for  $i$  is expressed (after (Hutabarat et al., 2013) as;

$$\hat{\beta}(u_i, v_i) = \left( Z^T W(u_i, v_i) Z - (n-p) \sum_{uu} \right)^{-1} Z^T W(u_i, v_i) Y,$$

where  $u_i$  and  $v_i$  are state the point of coordinates (latitude, longitude) in location  $i$ ,  $\hat{\beta}$  is the parameter to be estimated and  $W(u_i, v_i)$  is the weighing matrix whose diagonal elements representing the geographical weighting associated with each measurements site were made for location of  $i$ . Various methods can be used to calculate the weighting function. For fixed kernel size, the weight of each point might be estimated by applying Gaussian function,

$$W_{ij} = \exp\left[-1/2(d_{ij}/b)^2\right],$$

where  $d_{ij}$  is known as the distance between regression point  $i$  and data point  $j$ , and  $b$  is referred as a band width. Further extended description of geographic weighted regression and its treatments can be found in (Fotheringham et al., 2003, Foody, 2003).

### 4.3. Evaluation of vegetation cover's changes in relation to the driving forces

#### 4.3.1. Post classification comparison

Considerable literature, previously specified, is concerned with image classification. (Lu and Weng, 2007) provided a comprehensive valuable review of classification approaches and techniques. The classification results required high accuracy data sets for identifying detailed land use, land cover and vegetation with detecting the changes over time. For many purposes, satellite data that were collected from the earth's surface, that represents a continuous variation signal needed to be categorized. All similar spectral signature pixels were grouped together in a process called image classification. In this technique we intended to categorize and group all pixels in a digital image to represent one of several land cover features or vegetation types and producing thematic maps with different classes types present in an image. Digital image processing and remote sensing classification is a multi-step process (Fig. 13) and the complex procedure requires consideration of many factors (Lu and Weng, 2007). Generally, it involves three main image classification techniques;

- Supervised classification.
- Unsupervised classification.
- Object-based analysis.

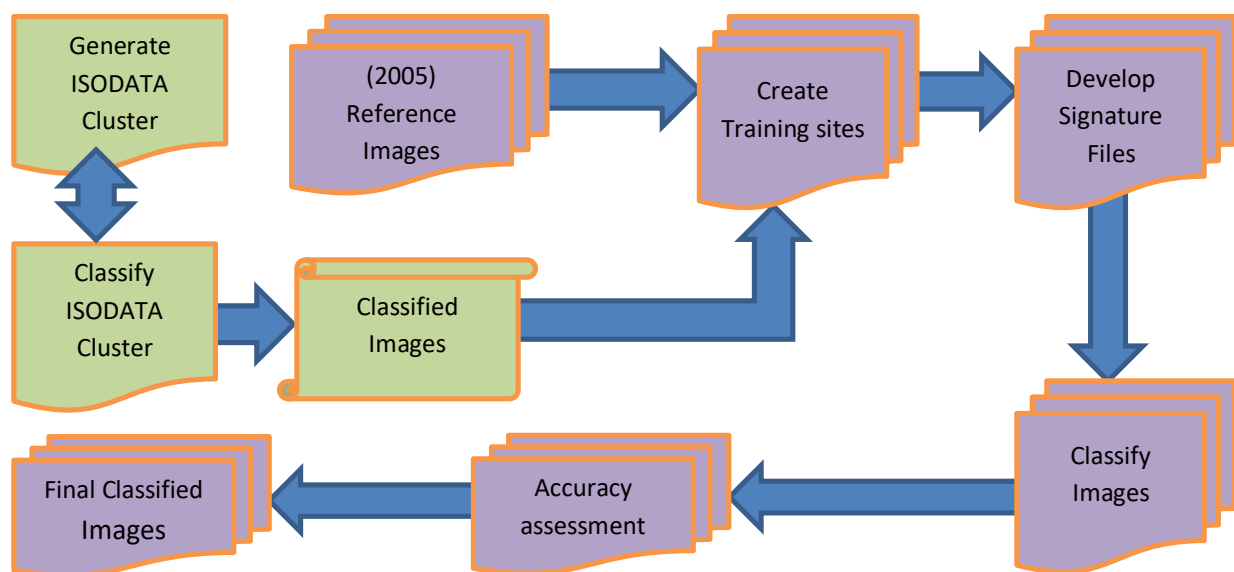


Figure 13. Schematic overview of the model classification scheme

However, supervised and unsupervised are well-known as the two most common image classification approach. We used automated supervised (Maximum likelihood) and unsupervised (Isodata) classification techniques on the combination of Landsat MSS 4,3,2,1 and bands 1, 2, 3, 4, 5, 7 of TM/ETM among of Landsat MSS/TMETM+ images described previously in Table 5. We selected then one image per decade which has low cloud cover, namely the images from 16.12.1972, 02.12.1984, 28.11.1994 and 20.12.2005, for image classification and detection of the changes in vegetation cover in the island. The near infrared wavebands (band 7 on Landsat MSS and band 4 on the Landsat Thematic Mapper TM)/Landsat Enhanced Thematic Mapper Plus ETM+) facilitated an advanced land classification analysis based on differences in spectral reflectance of different vegetation cover types. It is therefore that the

vegetation pigments absorption, specific plant's foliar reflectance and the foliar moisture wavelength ranges represent the basis of vegetation class analyses (Mancino et al., 2014). Moreover, availability of different spatial and temporal scales of vegetation cover data facilitates our ability to understand vegetation and ecosystem dynamics by use of several change detection techniques (Cohen and Fiorella, 1998, Coppin et al., 2004, Martínez and Gilabert, 2009).

For this study we chose the relatively cloud free 2005-12-20 as a reference image for spectral signature training sites. We tested two alternative techniques, each one based on a different approach of signature extraction and image classification technique (Malatesta et al., 2013). These are Isodata with a minimum distance and the post-classification comparison. The effectiveness of these two methods was compared. Initially, pretreatments and post processing were applied to reduce the variations between the images.

#### 4.3.2. Unsupervised Classification

All pre-processed image bands except the thermal and the panchromatic were stacked together. The three bands data Near Infrared (NIR), Red (R) and Green (G) composite image for the selected images was classified using ERDAS IMAGINE's ISODATA Algorithm technique (MacQueen, 1967) in order to group of the different vegetation types into their categories (classes). ISODATA is found best for image clusters and approximation to the natural structure of the data, rather than trying to impose an assumed structure on the data (Mahi et al., 2015),

$$V = \sum_{i=1}^k \sum_{x_j \in S_i} |x_j - \mu_i|^2,$$

where  $k$  is the number of clusters  $S_i$ ,  $i = 1, 2, \dots, k$ , and  $\mu_i$  is mean point of all the points  $x_j \in S_i$ .

The ISODATA is a clustering technique forming clusters and limiting the maximum number of groups by using the minimum spectral distance formula. According to (Ball and Hall, 1965) it is an iterative procedure for the sorting of a set of multi-dimensional (multi-variable) patterns into subsets of patterns. (Batista, 2011) explained that "an average pattern is used to represent each subset of patterns and the iterative process changes the composition of these subsets and creating new average patterns" (Fig. 14). These new average patterns define new subsets each of which has reduced variation about the average pattern. The process also combines average patterns that are so similar that their separation fails to provide a significant amount of additional information about the structure of the patterns. Therefore, final image classification then require knowledge of each scene in order to verify what each class might represent in the real world.

However, the unsupervised (Isodata) classification was initially applied to separately classify each image into 20 similar categories. We found the separability between these 20 classes was poor. So, with these trial and error iterative technique we were able to distinguish several terrestrial categories of vegetation by merging together small classes and producing eventually nine vegetation groups (classes). Finally, using Maximum Likelihood (ML) classifier of the supervised classification as a decision role to label each pixel was applied. Simple accuracy assessment was carried out to compare the final vegetation cover map with the reference field data. Consequentially, the confusion matrix was generated and the basic accuracy measures

such as producer's and user's accuracy as well as overall accuracy (Congalton and Green, 2008) were computed. In order to detect the change from a certain class to another we compared the four classified images of 1972-12-16, 1984 12 02, 1994-11-28 and finally 2005-12-20 in a pixel by pixel manner.

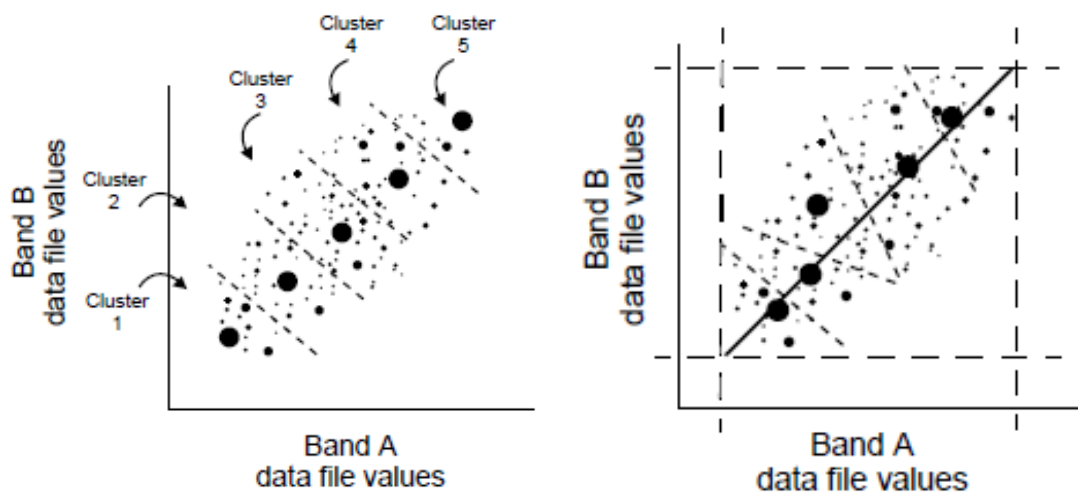


Figure 14. First and second iteration of the ISODATA algorithm always give results similar to those in the figure.

#### 4.3.3. Supervised Classification

In this study we applied the common supervised maximum likelihood method and minimum-distance classification with the digital image processing software, ERDAS 2011, for our interpretation based on the satellite imagery.

Initially, the most recent relatively cloud free image 2005-12-20 Landsat ETM+ was selected as a referenced classified image. This image is sequentially classified by both unsupervised and supervised maximum likelihood methods based on the spectral signature defined as training sites and the ground truth data. Nine vegetation categories were identified (see chapter 6).

Supervised maximum likelihood classifiers retraining technique for an unsupervised cluster has been presented that constitutes a useful support for remote sensing monitoring systems based on multitemporal images (Banerjee et al., 2015)

The main idea of the proposed technique is to initiate the supervised classifier through unsupervised clustering procedure. This approach, described by (Bruzzone and Prieto, 2001), “allows the generation of accurate vegetation cover maps of a specific study area from images for which a reliable ground truth (hence a suitable training set) is not available”. However, after the cluster iteratively refined the maximum likelihood of supervised classifier makes decisions using the cluster statistics (Vibhute et al., 2016). For assigning spectral clusters into labeled classes, we used the same set of reference (training) signatures that were used for testing supervised classifiers. Thus, a total of 114 reference signatures represent 20 major vegetation cover categories in the study area to create classification results by the supervised maximum likelihood classifier (Loog, 2016). Consequently, more than 600 reference signatures were used to refine our classes into 9 major vegetation categories and provided to the maximum likelihood and minimum-distance (Euclidean distance) classifiers for testing and assessing the accuracies.

#### 4.3.4. Training stage and ground truth data

The image classification process was carried out using supervised classification. A post classification comparison was then conducted to reveal the most recent changes in vegetation cover in the study area. As post classification judgment is sensitive to the accuracy of the input classifications (Singh, 1989) and the sampling design is considered to be one of the most important processes in the collection of ground truth data (Biging et al., 1999). Therefore, we used a broad classification scheme to ensure highly accurate individual classifications. These broad classes also might reduce the effects of variations of soil conditions and sparsity of the vegetation, which might have caused problems if a more detailed classification scheme had been used to detect change. The quality and the quantity of these inputs training samples are essential to generate an accurate classified image. These inputs existed in the form of training sites, which were homogenous polygons digitized within the boundary of several different feature classes. For the aims of our study, the placement of these polygons was based primarily on the spectral reflectance of pixels as seen in different wavelength band combinations after the segmentation resulted from unsupervised classification with aid of the area experience knowledge. In addition, the previous 22 classified land cover types by (Král and Pavliš, 2006) were compared with the 28 classes initiated and mapped by (Malatesta et al., 2013) using RapidEye image with 5m pixel resolution and used to help identifying what each feature was in reality. The zonation of vegetation communities and distribution patterns efforts by (De Sanctis et al., 2013) along with the relationship between land use and the plant communities of Socotra Island by Attorre et al. (2014) revealed useful information to differentiate between some pixels of similar reflectance and comparing vegetation distribution and land cover. More than 450 reference points and approximately 250 digital photographs with it's GPS data were also taken during the fieldwork 2009 to be used for similar purposes especially in areas with lack of other terrain data. Furthermore, during the fieldwork 2012 more than 650 of field data points have been collected in order to be used for further validation analysis and modelling the data. After a very limited manual amending applying our field knowledge, we used only the density areas of 100m\*100m (almost 3 pixels) that consist of more than 70% of each class in the classifier approach.

An example of the training sites digitized for each feature class is shown in Fig. 15. The training process was then repeated for each year's image under the strong expectations hypothesis there are no apparently sudden decline in the whole vegetation but instead was able to sustain itself and it has remained until today. This evidence of various studies suggested that the most dominant tree species in the island with respect to their physiognomy and structure are rather prehistoric appearance (Balfour, 1888). For instance, the age of dragon tree (*Dracaena*) due to Humboldt (1814) (cited in; (Adolt and Pavlis, 2004) is still generally unknown and estimated by several thousand years. However, it has been suggested by (Bystroem, 1960) and later by (Symon, 1974) and (Magdefrau, 1975) a probable average age of not more than 700 years. Nevertheless, no authentic study on ageing of natural populations of most tree species has been published (Adolt and Pavlis, 2004). The training sites digitized for each image were kept relatively consistent in regards to polygon sizing and placement. It is worth to be mentioned that several features considered to be similar were clumped together into the same class.

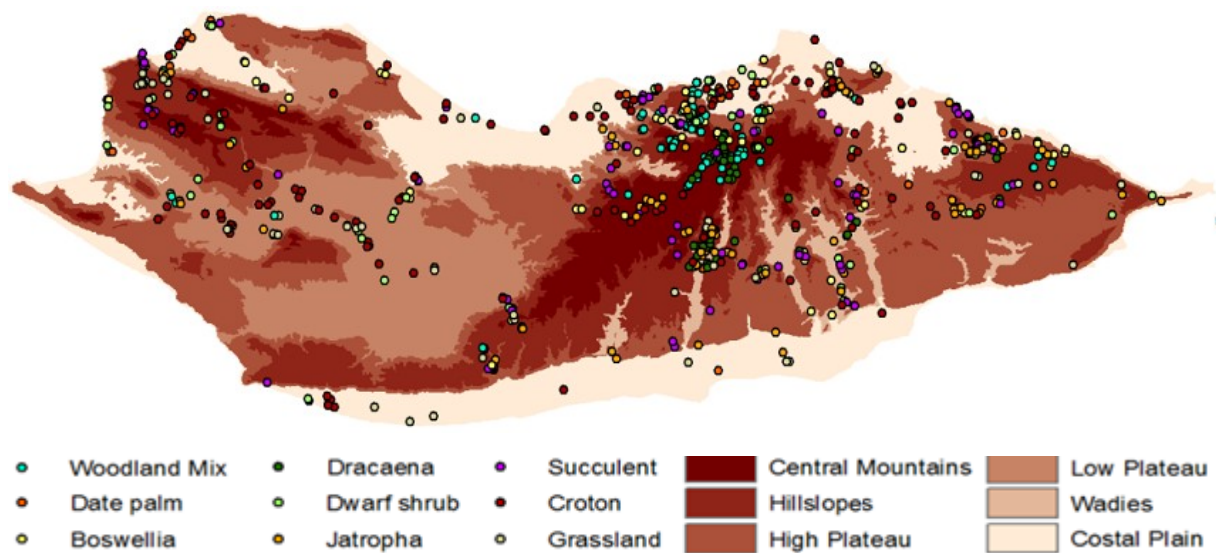


Figure 15: Training sites per ecological zones (For sites and related data see Appendix 3)

#### 4.3.5. Selection of Change Detection Algorithms

Earlier literature ((Lu and Weng, 2007, Ghimire et al., 2010) has been specifically addressed some concerns with image classification and change detection techniques. These revealed comprehensive reviews of classification approaches and techniques. Moreover, our ability to systematically study the great changes might be restricting and more difficult when historical time series images are either partially or totally obscured by abundant cloud cover during the year. Additionally to the difficulties caused by cloud cover, Landsat 7 experienced a permanent failure since May 2003 that has influenced all images captured by its sensor by more than 20% black stripes with null data. Meanwhile, data from other free satellites of the MODIS family are too coarse to reliably detect land cover or vegetation changes in this area, and radar data, while extremely useful in peering through clouds, is costly. Some parameters of the response function were estimated from alternative same month data and they are applied to the data to remove the scan stripe noise.

However, due to our consciousness for implementing a change detection in our study, we were also aware of the major concerns described by (Petit and Lambin, 2001) which involved

- Image pre-processing and topographic correction
- Change trajectories of vegetation cover types
- Spatial distribution of changed types
- Selection of suitable techniques algorithms to implement change detection analyses
- Accuracy assessment
- Knowledge and familiarity of the study area.

These classification techniques are based on a comparison to measure detailed change. Among those, we applied the most common methodology adopted in the change detection studies which can involve both the pixel and the object: post classification, image differencing with knowledge and familiarity of the study area and image ratioing. The later can only provide change/no-change information, whereas other techniques, such as post classification comparison, are known as a more vulnerable techniques and can provide a complete matrix of change directions by determining the changes from a certain class to another throughout the study period. The outputs of this stage were positive change/negative change/non-change



images, which classify overall changes and identify the total areas of these changes. Excel and SPSS were then used for further statistical analysis.

#### 4.3.6. Change detection methods and requirements

Change detection has widely been used to investigate changes in land use, and disturbance of vegetation cover. It has been defined earlier by (Singh, 1989) as “the process of identifying differences in the state of an object or phenomenon by observing it at different times”, while (Hussain et al., 2013) argued that vegetation change information is essential because of its practical use in various environmental issues. According to (Huang et al., 2009a) the effective change detection should be carried out over a time period of at least 10 years. However, (Lu et al., 2004) discuss the difficulties in selecting the most suitable method or algorithm for change detection while it comprised a complex data and affected by various elements including spectral, spatial, temporal constraints as well as radiometric resolution, atmospheric conditions and soil type (Li et al., 2016c) and (Jensen, 2005). Nevertheless, these techniques of change detection are in rapid increase and mostly using automated approaches in detecting the changes within discrete time periods across a large amount of image data (Kibret et al., 2016, Yu et al., 2016) and (Hansen et al., 2014). Enormous researcher's efforts have resulted in developing various change detection methods such as traditional pixel-based (Xiao et al., 2016, Zhang et al., 2016, Hussain et al., 2013, Mas, 1999) and the more recently, object-based (Yu et al., 2016, Mather and Tso, 2016) methods. Once classes are randomly selected and field verified, the accuracy assessment would then run, which validates the classification in a confusion matrix format regarding to the ground truth data.

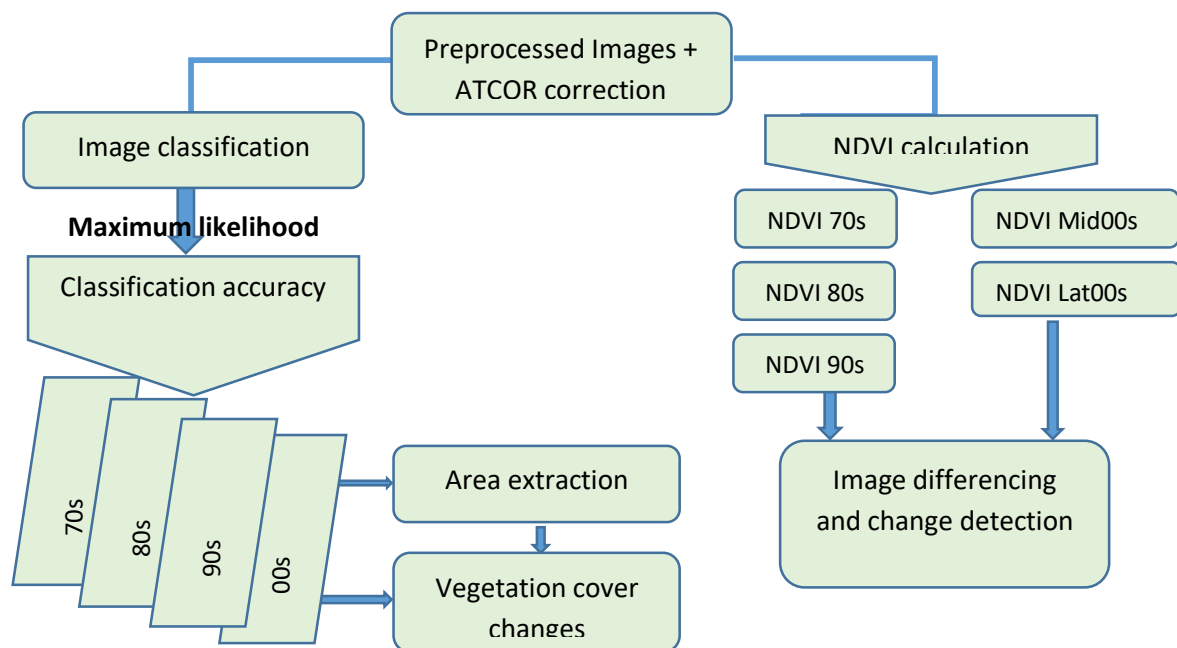


Figure 16. Schematic overview of change detection and subsequent processes.

The overall accuracy is expressed as a percentage value, and owing to (Fitzpatrick-Lins, 1980, Willis, 2015) and this value typically regarded acceptable for land management purposes if it is above 85%. The accuracy percentage and numerical pixel value are reported for each

vegetation class along with the number of misclassified pixels. Fig. 16 briefly describe an overview of change detecting approach used with the subsequent process.

Accuracy assessment and evaluation of classification results are important processes in the classification methods (Lu and Weng, 2007, Gong et al., 2016, Vibhute et al., 2016). Various qualitative and quantitative processes can be implemented, ranging from evaluation based on expert knowledge to accuracy assessment based on sampling strategies. Many literatures have provided insight in meanings and calculation methods for these elements, earlier by (Congalton et al., 1983), (Smits et al., 1999) and (Foody, 2003) and in some other new studies, such as (Congalton and Green, 2008, Padilla et al., 2015, Fetene et al., 2016, Khorram et al., 2016). The error matrix based accuracy assessment method is the most common and useful method for the evaluation of change detection results (Foody, 2008) and (Roff et al., 2016). In this process it is presumed that the differences between image classification results and the reference data in many cases are due to the classification error (Morisette and Khorram, 2000), (Khorram, 1999). The Cohen's kappa coefficient was used to evaluate classification results and to measure the agreement between the observed accuracy with an expected accuracy (Žliobaitė et al., 2015, Jiang et al., 2016) after (Landis and Koch, 1977a):

$$\hat{K} = \frac{P_o - P_c}{1 - P_c},$$

where  $P_o$  is probability of observed agreement, and  $P_c$  is probability of agreement by chance. So it measures the overall statistical agreement of an error matrix, which considers the non-diagonal elements into account. Kappa analysis is acknowledged by many researchers as a powerful method for analyzing a single error matrix and then comparing the differences between various error matrices (Congalton and Green, 2008), (Smits et al., 1999) and (Mubea et al., 2016).

Geostatistical and spatial analysis ArcGIS 9.3/10.1 software as well as EXCEL and SPSS statistical functions were applied to compile the classification results and visualizing data showing the trends of the different vegetation cover with the areas proportions from 1972 to 2005. The average proportions were also calculated per each ecological zone.

#### **4.3.7. Estimation of the vegetation activity trends**

By analyzing a time series of yearly fluctuating data, it is possible to reveal and quantify variations data over the observation time period (Reed et al., 2007) and (Stosic et al., 2016). Consequently, this data series can be modelled by a trend line indicating the variation between certain limits, possibly a negative or a positive trend or constancy. For each direction of change, therefore, it is possible to associate a hypothesis with these trends according to the known elements of the data dynamics concerned (Reed et al., 2007).

In our study, both vegetation cover and NDVI time series (mean and max NDVI in growing period) indicators represent an integrated measure of vegetation activity. Trends with significant positive or negative slope values are respectively associated with vegetation areas under progressive or regressive vegetation dynamics, whereas non-significant trend represent bare rocks or vegetation areas under stable dynamics.

Image algebra technique has been used for detect change including image differencing, regression analysis and vegetation index differencing. In this technique however, two precisely

registered classified images were used to produce a residual image to represent changes. The difference then can be measured directly from the pixel values of the extracted/resulted images. The resulted image can be illustrated as:

$$Diff(x, y) = m_1(x, y) - m_2(x, y),$$

where  $m_1$  and  $m_2$  are images from time  $t_1$  and  $t_2$ ,  $(x, y)$  are the coordinates of each pixel and  $Diff$  is the difference image. Pixels with no change in values are distributed around the mean (Lu et al., 2005), while pixels with change are distributed in the tails of the distribution curve (Singh, 1989). As the change can occur in both directions and it is therefore up to the analyst to decide which image has to be subtract from which ((Gao, 2009)) thus for our vegetation change study we subtracted 80s NDVI image values from the 70s images, 90s from 80s and so on. The resulting images were threshold based on 15% changes (within  $\pm 15\%$  difference "constancy" was assumed) and the areas with more than 15% increase or decrease in NDVI values were defined as "changed". Finally, with the aim of investigation changes in NDVI values, we used density slicing method mentioned by (Nath, 2014, Markos and Youssuf, Kaszta et al., 2016, Islam et al., 2016) to categorize the resultant NDVI change images into 11 ranges by using the Natural Breaks method (Jenks, 1977 cited in; (Rey et al., 2016) fixing the thresholds categories from very low ( $> 0$ ) to very high NDVI values ( $> 0.8$ ).

#### 4.3.8. Vegetation index differencing

The Normalized Difference Vegetation Index, NDVI, is one of the oldest spectral Vegetation Indices (VIs) and most widely used. It is a ratio-based index designed to evaluate the spectral contribution of green vegetation to multispectral observations. These indices enhance the spectral differences due to strong vegetation absorbing the red and strongly reflecting the near infrared band. They are basically well known as a ratio or a linear combination of two or multiple spectral bands for the change detection. The Normalized Difference Vegetation Index (NDVI) was computed as a ratio of the difference between near infrared (NIR) and red (R) reflectance for each image to the sum of both as follows:

$$NDVI_{TM\&ETM+} = \frac{TM4 - TM3}{TM4 + TM3} ,$$

$$NDVI_{MSS} = \frac{MSS7 - MSS5}{MSS7 + MSS5} ,$$

where TM4 and TM3 are the NIR and R spectral bands for Landsat TM and ETM+ and MSS7 and MSS5 are the corresponding spectral bands from Landsat MSS. NIR and R are the near-infrared and red light respectively, that reflected by the vegetation and been captured by the satellite sensor. The NDVI is well known as a measure of photosynthetic activity, due to absorption of the red light by plant chlorophyll in the leaves and reflection of near infrared light. Therefore, the formula is based on the fact that chlorophyll absorbs R wave length whereas the mesophyll leaf structure scatters NIR waves. Thus, NDVI values range from -1 to +1, where negative values or close to zero of NDVI correspond to the absence of vegetation or water and generally correspond to barren areas of rock, sand, or sparse shrubs, whereas shrub and grassland might be represented with low positive values and high values indicate very dense vegetation and forests (F. Attorre et al., 2014) (see:

<http://earthobservatory.nasa.gov/Features/MeasuringVegetation/>).

Estimating the above ground biomass during the growing period by the mean of using the reflectance from the red and near infrared bands of remotely sensed data acquired from satellite sensors to compute the vegetation indices such as the normalized difference vegetation index (NDVI) became a widely and well-known technique (Chen et al., 2009, Wang et al., 2016) , , and others). Moreover, integrating NDVI has proved to be a good measure of above ground biomass production (net primary production) in Sahara and semi-arid areas (Rasmussen, 1998) and (Begue et al., 2011). Nevertheless, reaching a saturation level is an associated problem only with high density biomass calculated from these sensors. It responds to changes in amount of chlorophyll content and biomass (Liang et al., 2005). We used the concept of Multi-temporal image differencing (MTID) algorithm and integrated NDVI between 70s, 80s, 90s and 00s images under a shifted basis for NDVI of 2005. The change intensities will also to be rendered by summation of the absolute NDVI differences between subsequent years. The positive value implies a dominant change trend towards improved vegetation conditions, while the negative value represents deterioration tendencies in the vegetation cover. However, use of MTID approach in this study can provide helpful information for analysing the actual meaning of a pixel-by-pixel correlation analysis during the approximately forty year's composite NDVI data, as well as to reveal the relationships between rainfall factor and vegetation coverage changes.

#### **4.3.9. Vegetation covers change and its driving forces**

Several studies concerning discrimination between climate and human induced change in vegetation cover have shown a strong relationship between inter-seasonal changes in vegetation activity and rainfall or temperature. Climate is well known as a substantial factor influencing the NDVI through amount of annual rainfall or duration of the wet season in the semiarid areas. This influential however, has to be identified and quantified in the study area with the respect to the statistically significant relationship between NDVI and rainfall in which it might help in discrimination between these two major factors driving vegetation change. Some examples of dealing with climatic signal and discrimination between human-induced and climate-induced degradation have been presented in the recent literature (Gang et al., 2014, Liu et al., 2012, Koutsodendris et al., 2015, Madin et al., 2016) and (Li et al., 2016a). Assessment of human activities in the island (e.g., livestock grazing, wood and grass collections and garden farming) will be documented with respect to the distinguished vegetation types. Using secondary data on the livestock trend and vegetation cover changes, in the western and eastern parts of the island particularly at the Hadibo, Alqalansyah towns and central mountains, the currently existing grazing practices, livestock and urban development expansion activities will be assessed in relation to their effects on the natural vegetation (Fetene et al., 2016). Small group discussions were conducted with relevant stakeholders of the all administrators, the SCDP group leaders and people's region. Each discussion was related to the resource use by the communities. All results were also checked with the information provided by the SCDP management team and with the documented previous studies in the island. We will implement a simple framework system module based on the methodology proposed by (Propastin, 2007) to discriminate between climate and human driving forces in vegetation change. This concept is explained on a basic example framework (Fig. 17. In panel 16a and b the upward and

downward trends in NDVI and rainfall are synchronous and, obviously, can here be understood that the increase/decrease in vegetation cover is mainly driven by increasing or decreasing rainfall amounts excluding the impact of humans (even though it somehow may exist). In Fig. 17c the positive trends in NDVI with the decrease of rainfall would be understood as a case when vegetation cover is recovering due to diminishing of conservation and plant protection activities. Increasing of rainfall without causing an improvement of vegetation cover as in panel 16d is interpreted as a human-induced degradation of the vegetation cover.

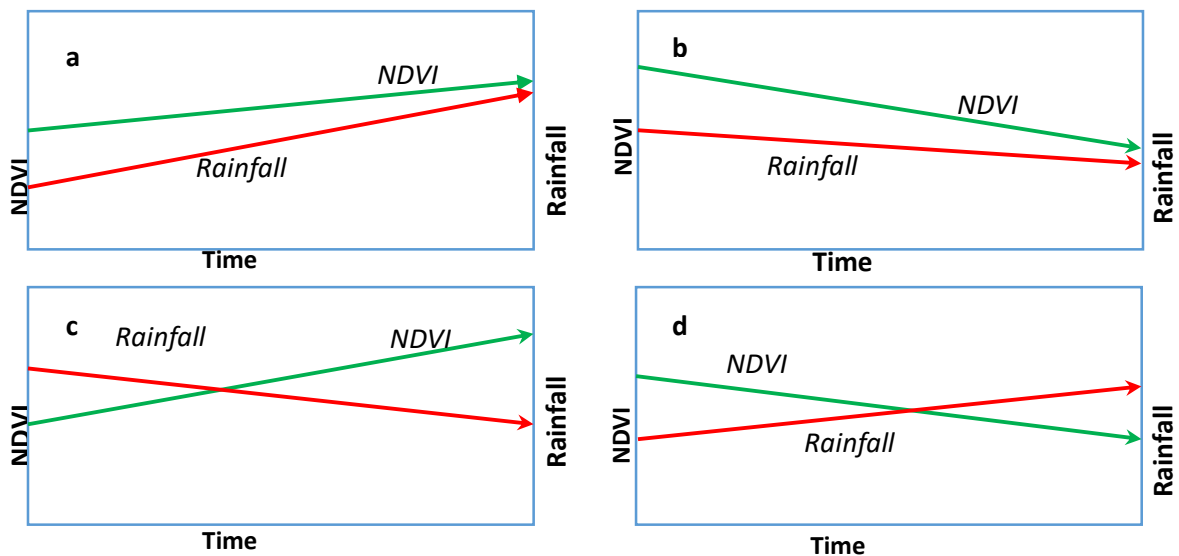


Figure 17. Model illustrates the relation the vegetation (NDVI, in green) and the driving forces (rainfall, in red, or human-induced). (a) improving vegetation cover with increase in rainfall, (b) vegetation degradation due to lower rainfall, (c) recovering in the vegetation cover in spite of decreasing rainfall, (d) degradation in vegetation cover under increasing rainfall caused by human impact.

#### 4.3.10. Recognition of rainfall and anthropogenic signals in the vegetation time-series

This system would be satisfactory work in areas where relationship between trends in vegetation and trends in climate factors are statistically significant and strong enough. In order to detect these areas, trends in vegetation cover were computed and compared with trends in climatic predictors in each ecological zone. This task was solved in three steps. **First**, areas with statistically significant trends in vegetation activity over the study period were identified and extracted. **Second**, correlation and regression analysis with inter-seasonal time series of rainfall and altitude have been carried out for every pixel in the extracted areas. **Third**, synchrony or asynchrony between trends in vegetation conditions and trends in climate and latitude factors were analyzed and determined by comparing the trend direction of vegetation activity and correlation coefficient with these factors.

For example, if a trend in vegetation cover is positive and this area reveals statistically significant positive correlation with rainfall, it is considered to indicate a climate (rainfall) driven change in vegetation cover (Fig. 17a). If a trend in vegetation cover is positive but the area reveals negative correlation with rainfall, it is considered to indicate an improvement of vegetation cover due to a decrease of human impact (Fig. 17c). The same approach was applied to identify climate-induced and human-induced degradation of vegetation cover (Fig.17b and

d). Furthermore, identification of the climate signals in the inter-seasonal dynamics of vegetation activity can be then used as a base methodology for discrimination between climate and human influence on vegetation cover.

#### 4.3.11. Analysis of regression residuals for identification of areas experiencing anthropogenic impact

Analysis of residuals from regressions between NDVI and rainfall was undertaken in order to detect those areas which might not fit with scenarios as in Fig. 17). Such proposed models are based implicitly upon the assumption that the relationship between rainfall and NDVI under study area is linear (Nicholson et al., 1990a). This is because the idealistic conditions in these scenarios are not always to be found in the reality. It is expected that not all trends will exhibit asynchrony or synchrony with values of equal magnitude. Special cases of this problem are shown in Fig. 18). The trends in these panels are synchronous but exhibit different magnitudes. It means that in (Fig 18a) vegetation response to rainfall is getting worse. An opposite case is shown in panel 18b, here vegetation cover demonstrates increasing response to rainfall.

For every pixel and for each year a given value of NDVI, a value of rainfall predicted by the regression was obtained, this value was considered to reveal the time trend in climatic component. The observed NDVI may show deviations from the regression line. It can be understood that positive deviation indicates well response of vegetation to rainfall while negative deviations indicate worse response. Deviations in  $NDVI_{obs}$  from  $NDVI_{pred}$  expressed in the regression residuals were computed at pixel-by-pixel basis for each decade. Then we calculated temporal trend of regression residuals for each pixel over the study period. Then it can be understood that any trend through time presented in the residuals will indicate changes in NDVI response not due to climatic variables. A negative trend would imply reduced response of vegetation cover to climate. This reduction can be caused either by a decrease of vegetation cover forming patchy shape distributions or by a change in plant species composition and structure. According to this suggestion, the area would be experiencing human induced degradation if negative trend is statistically significant. A positive trend would indicate improving in vegetation cover.

Concerning the panels shown, Fig. 18a, shows a positive trend in residuals and, on the contrary, panel (b) displays a negative trend in residuals.

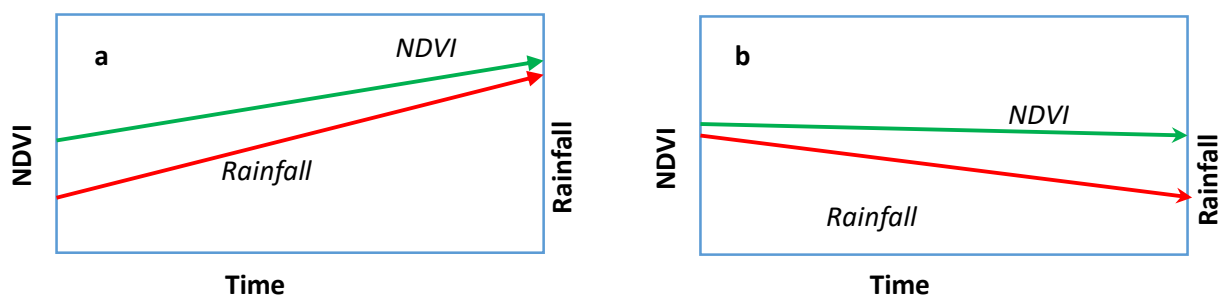


Figure 18. Other cases of trends interpretation: (a) both trends are positive but the trend in vegetation reveals a much lower magnitude, which should indicate a slight process of degradation in spite of good climate conditions; (b) opposite case presenting a slight rehabilitation of vegetation cover in spite of rainfall decrease.

## Chapter 5: Results, part 1 – Analysis of climatic conditions and NDVI

### 5.1. Network of climate stations in the study region

The main meteorological station in Socotra is administrated by the Civil Aviation and Meteorology Authority (Camargo et al.). It was established at the end of 19th century by the British military and with this time are associated first climate records from the region. A very rapid growth of 11 stations network is associated with the period of Socotra Conservation and Development Program (SCDP) 1997 until 2009. Many of these meteorological stations were abolished and abandoned because of diminishing financial support by the country government. In the remaining stations, climate observations have revealed many deficiencies in measurements and reporting. At some meteorological stations, climate observations have been carried out not by skilled specialists but by occasional people without any special education and experience which are employed for a low salary. There has been some improvement of the implementation of the climate network within the last years but the entire situation remains insufficient. For this study, climate stations in the study area were mainly used with respect to other authors and international sources. We used 0.5° rainfall data from the gridded monthly rainfall reanalysis of (GPCC). To verify the accuracy of these data in our study area, we compared available rainfall data from Mouri station from 1972 to 2010 with GPCC data from for the same period. We found a very high correspondence between the two datasets for the available time period with high positive correlation coefficient ( $r = +0.72$ ). Nevertheless, since these are the only data available until 2000 we statistically correlated them with the overall data of the 11 stations. As it has been discussed earlier, the monsoon months of October to December provide almost three-quarters of total rainfall. In this case we calculated the annual rainfall in year  $t$  starting from October  $t$  to the end of September in the next year  $t+1$ . The general characteristics of the stations are listed in Table 8 and the spatial distribution is shown in Fig. 19. The network seems to exhibit insufficient density of the climate stations, particularly in the southern part of the island. Mean distance between the climate stations equals to approximately 15 km while distance from the station Bidholah in the south to the nearest station in the north is about 20 km. This density might appear insufficient due to the complex topography. But we must take into account that the southern portion of the island is occupied by a more or less straight stripe plain with an elevation of 0 - 80m over 6 km x 70 km. Here, we do not have to expect any significant local variances in climate conditions like in the middle or the northern parts of the study area.

Figure 19: Meteorological stations in the study area and their total annual rainfall (in mm, coded in size of green circles).

### 5.2. Statistical Analysis of Rainfall Data

#### 5.2.1. The inter-seasonal variability of rainfall

Arid and semi-arid climates are characterized by a high variability of climate parameters from one year to another, particularly extremely high rainfall variability. This causes high variability of ecosystem conditions and is the main driver for the difficulties of vegetation and animal's survival.

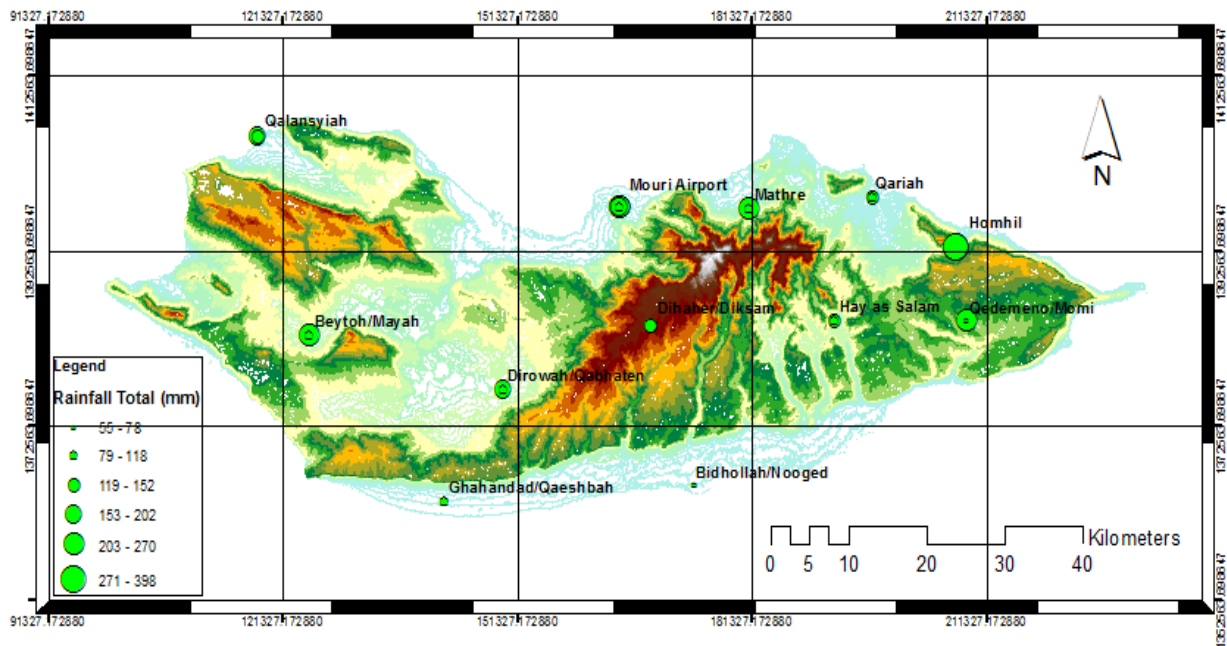


Figure 19: Meteorological stations in the study area and their total annual rainfall (in mm, coded in size of green circles).

The variability of rainfall may be illustrated with the aid of standard deviation and coefficient of variation (CV) for each climate station in Table 7. Throughout the study region, the variability in rainfall generally decreases from the north towards the south (Fig. 19), growing period reaches in some case up to more than 50% of annual rainfall. This might support that variability in rainfall plays a major role in ecosystem dynamic in the study region. The highest CV for growing season rainfall is in the mountainous areas (QAR and DIK) with values around 172% and the lowest in the coastal low land (HAD) with 64%. Our results also coincide with the theory by (Habrova et al., 2007) relating the key issue of extreme variability of the climate caused by both monsoon effect and the topography of the island, see Fig. 20 with a scatterplot of CV vs. elevation. They also concluded consequently that one may find a completely different distribution of rainfalls and shifted vegetation seasons within two sites distant just few kilometres.

The variability of rainfall for separate seasons is higher than that for the entire growing season. The highest variation is associated with the climate stations in Homhil, Dihaher/Diksam, Qalansyah, Mathre and Ghahandad/Qaeshbah (Fig. 21), whereas the lowest variation is found with Bidhollah/Nooged, Hay as Salam and Qedemeno/Momi. On the other hand, Mouri Airport station showed highest amount of rainfall but with slightly low inter-seasonal variability. Although at the stations of Dirowah, Dihaher, Ghahandad and Bidollah winter rainfall dominated, the monthly differences were less pronounced. Additionally, highest values of CV were observed in Dihaher/Diksam.



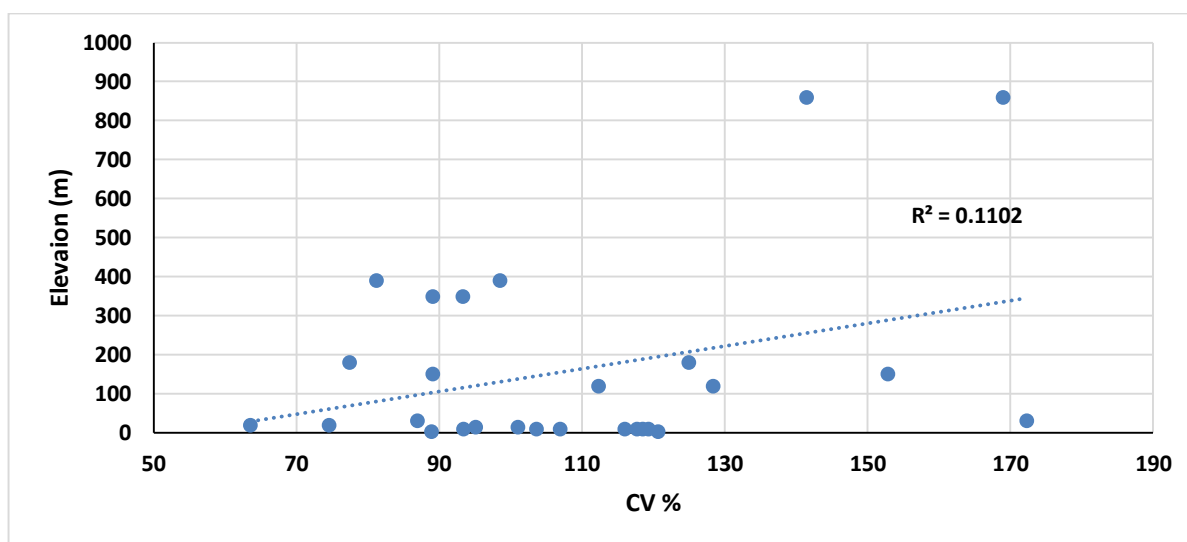


Figure 20. Coefficient of variation in rainfall versus elevation (m) as computed for the weather stations in the study area.

Name	ID	Alt. (m)	Year	Tot. Ann.	Tot. GP	%GP	SD.GP	CV %
Qalansyah	QAL	3	2005	273	134	49	20	89
		3	2009	125	102	81	49	121
Beytoh/Mayah	MAY	150	2005	260	93	36	14	89
		150	2009	209	97	46	50	153
Mathre	HAD	20	2005	279	100	36	11	64
		20	2009	189	83	44	10	75
Mouri Airport	MOU	10	1972	275	229	83	45	118
		10	1984	252	221	88	44	119
		10	1994	299	270	90	53	119
		10	2005	264	112	42	22	116
		10	2009	130	102	78	18	107
Dihaher/Diksam	DIK	860	2005	328	140	43	33	142
		860	2009	151	75	50	21	169
Dirowah/Qabhaten	QEB	120	2005	192	118	61	22	112
		120	2009	139	58	42	12	128
Ghahandad/Qaeshbah	QAE	15	2005	171	115	67	19	101
		15	2009	105	70	67	11	95
Bidhollah/Nooged	NOO	10	2005	116	55	48	9	93
		10	2009	117	54	46	9	104
Qariah	QAR	30	2005	308	118	38	34	172
		30	2009	105	89	84	13	87
Homhil	HOM	350	2005	246	84	34	13	93
		350	2009	184	168	92	25	89
Hay as Salam	CEN	180	2005	180	95	53	12	77
		180	2009	205	39	19	8	125
Qedemeno/Momi	MOM	390	2005	148	59	40	10	98
		390	2009	127	84	66	35	81

Table 7. Total annual rainfall (Tot. Ann.), rainfall during growing period (October-March; Tot. GP) as well as corresponding standard deviation (SD) and coefficient of variation (CV in %) for selected years for the 12 individual climate stations in the study area.

This station is situated on the southern edge of the central mountain with an altitude of 860 m. It exhibited highest variability between seasons and for the entire growing season. As we discussed earlier, winter is the season with the highest variation of rainfall. Therefore, with comparison to other seasons and to the growing season, Mathre being the most northern station exhibited the lowest CV of rainfall whereas Bidhollah/Nooged being the most southern station exhibited a very low CV in the southern part of the island.

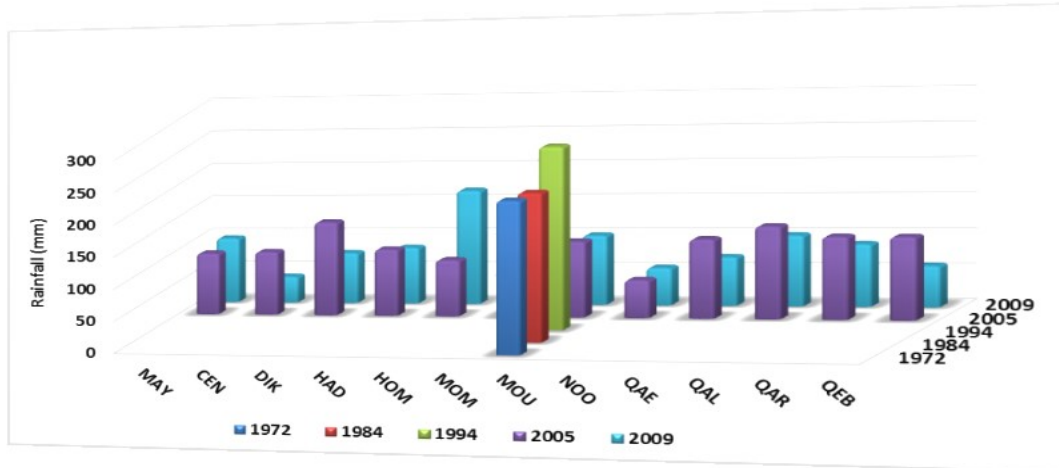


Figure 21: Variation associated with the rainfall during the wet season for different climate stations.

### 5.2.2. Rainfalls variabilities and seasonal trends

Although time series of rainfall averaged over the study region for the period 1972-2010 include drought years and to some extent also present extremely dry conditions, there is clear evidence of a negative trend in the amount of rainfall. From late September to earlier March, winter monsoon winds blow from NE direction bringing the largest annual rainfall in November. This event affects the entire island, although the northern regions might be more influenced due to orographic rainfall. Fig.22 shows the rainfall peaks around November and December, but sometimes starting at the beginning of October. Generally, the wet period lasts till early February but heavy rain events might also occur in May or early September (and reaching incredible amounts, e.g. 211 mm in September 27<sup>th</sup> 2004 (Habrova et al., 2007)).

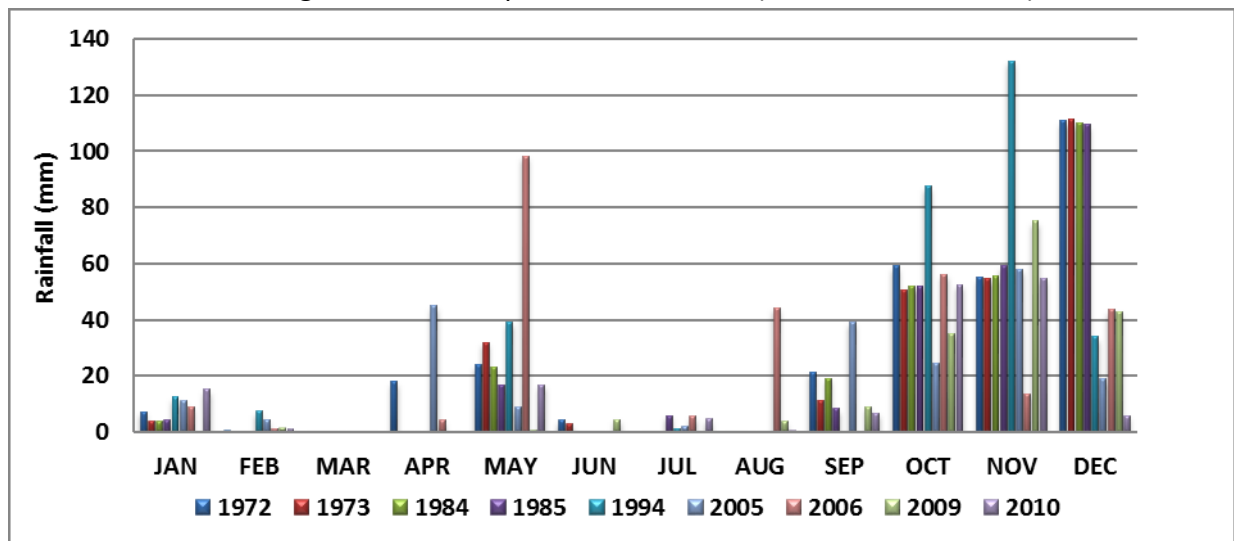


Figure 22: Observed pattern of monthly rainfall during the study period 1972 to 2010 indicating the wet season from October to January and a short rainfall peak in May.

The rainfall registered at Homhil with exceptional annual values suggested errors in registration. Excluding Homhil, the total annual rainfall registered on Socotra during 1972 and 2010 was 275 and 130 mm at only Mouri station. Of these approximately 229 mm and 102 mm fall during the growing period of the same years respectively. We also found that the average annual rainfall at the 11 new stations was 189 mm for the period 2005 to 2010, while the average total amount using both Mouri and the new stations records was 199 mm.

Altogether, the rainfall amount decreased during the last decades. Comparing the rainy seasons from 1972 to 2010 at Mouri (Fig. 23) we noticed that they occurred during the same periods but with variations in total amount and duration. There was slightly higher amount in rainfall during growing season between 1994, but later it dropped down substantially (Fig. 23). Waiting for the monsoon is an annual ritual of the villagers in the island. If the early summer months passed without rain followed by failing winter monsoon, this would have huge consequences. As evidence from informal interviews that we held during the fieldwork amongst the Socotra's old survival people and SCDP community liaison officers as a complementary source of climatic information, we noted that several summer rains completely failed, such as in 1972, 1976, 1981, 1984, 1993, 1999 and 2009. As well as several severe winter drought episodes also occurred during 1978 - 1979 and 1980 - 1981 and in some years rains were very light, causing death to lot of cattle, goats and sheep and dropping down to 40% (Scholte et al., 2008). In one hand, as can be seen from Fig. 23, the island exhibited dry conditions with rainfall below the long time-mean, on the other hand it might face severe winter floods after failing summer rainfall such as 1999. This is for socotranis more disastrous than these droughts (Morris, 2002).

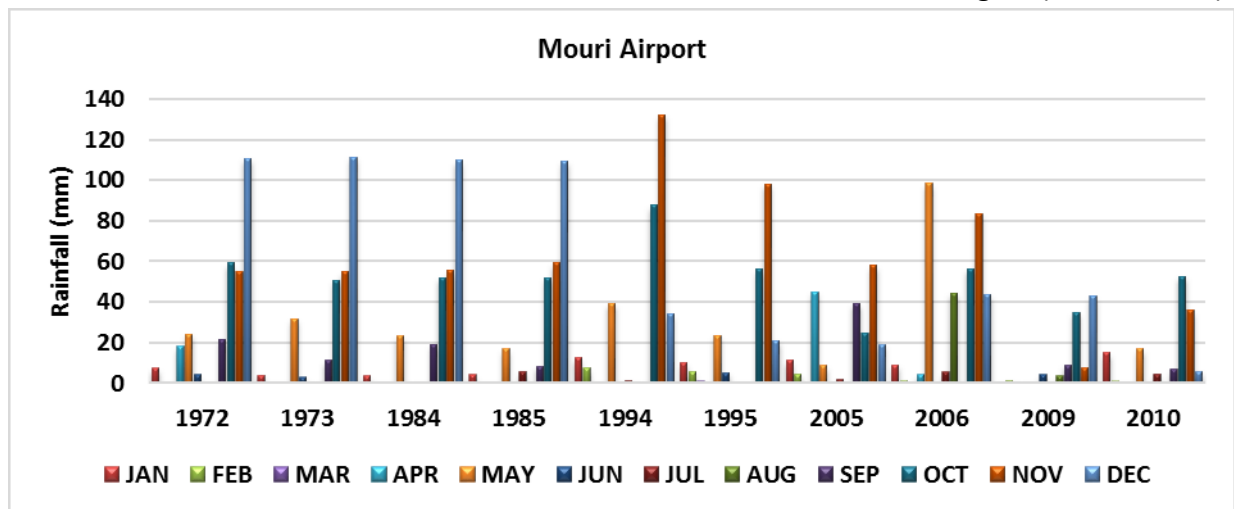


Figure 23: Monthly rainfall amounts (mm) at Mouri station for the period 1972 to 2010.

The trends in rainfall over the period 2005-2010 for individual climate stations are shown in Fig. 24. The magnitudes of trends varied by climate station and season to be analyzed. Unfortunately, most trend values (in a linear regression) for most stations exhibited only low coefficient of determination  $R^2$  and were not statistically significant. The reason is the relatively short period of 5 years comprised for the time series analysis. Thus, only three climate stations exhibited significant positive trends in growing season rainfall in this late 2000 period. However, all examined stations with an exception of MOM exhibited significant negative trends in winter rainfall. As for seasonal trends of rainfall, HOM, CEN, HAD and MAY located mostly in northern part, facing the winter and the summer monsoon, demonstrated significant upward changes of

seasonal rainfall, whereas downward trends occurred in QAL DIK, QAE, NOO and QAR while MOM exhibited slightly significant upward trends across the seasons. The trend magnitudes varied only a little by climate stations but the results indicate a strong general tendency for winter rain. On the contrary, the trends observed from Mouri old station for the total annual rainfall and the growing seasons throughout study period have demonstrated statistical significance downwards winter trends with overall decrease values. (Fig. 24).

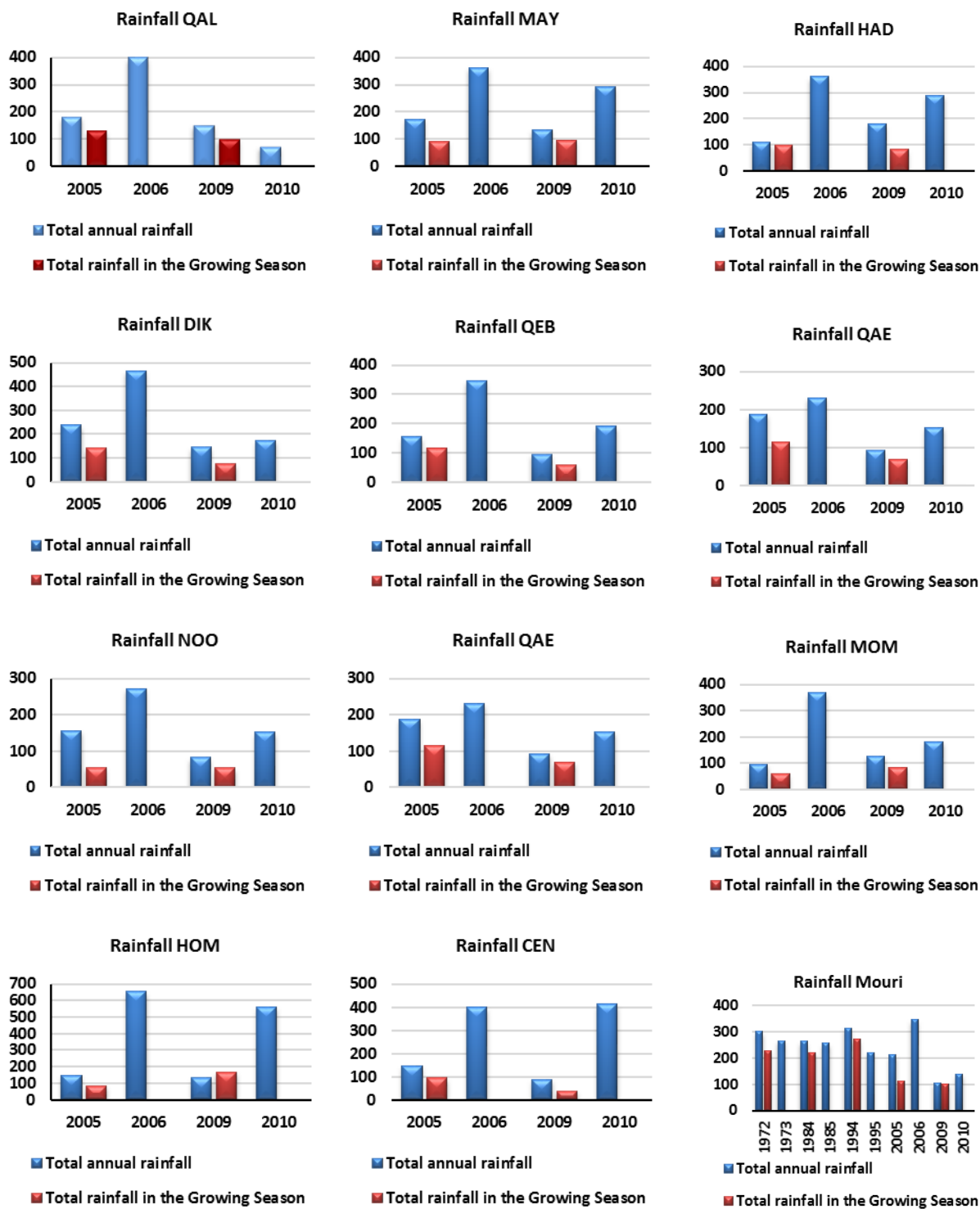


Figure 24: Total annual rainfall and rainfall in the growing season (in mm) for the 11 rainfall stations in 2005 - 2010 and for Mouri old station from 1972 - 2010, showing the trend direction.

### 5.2.3. Within season trends of rainfall

In the previous section variations of the rainy season over the decades were examined. The high variability within the monsoon has generally been observed. As the relationships between vegetation growth and rainfall is essentially controlled by the amount and duration of rainfall events (Cissé et al., 2016) the total and the cumulated rainfall within the season were calculated over the period 1972–2010. However, within season temporal variations in rainfall resulted from the monsoon variability, evident decreases in rainfall are observed within season each decade during the growing period. There is thus good temporal trend agreement between rainfall for the data collected from Mouri and the recently established stations. They show similar rainfall characteristics behaviours. Fig. 25 depicts the major rainfall variations within the season.

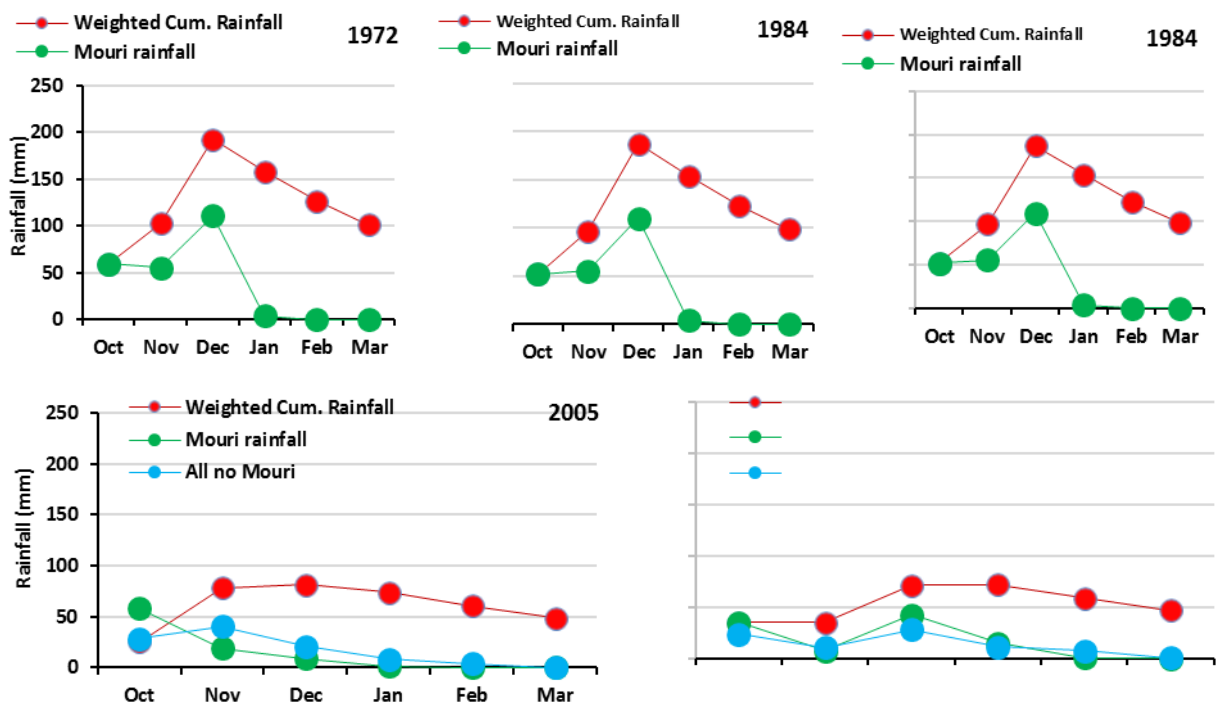


Figure 25: Typical shape of monthly rainfall during the growing period (Oct – Mar) over the study span 1972-2010.

### 5.3. Variability of vegetation distribution

#### 5.3.1. Average characteristics of NDVI

The NDVI calculated from atmospherically corrected Landsat MSS, TM and ETM+ data were used as the variable explaining the vegetation cover. The spectral reflectance and ratios of the NIR and the red wavelength bands were correlated to field-measured vegetation coverages. As a cursory examination of pseudo color image of NDVI the bare land and rocks have a broadly low reflectance in the NIR and giving NDVI close to Zero while the presence of vegetation gives NDVI values little higher than zero. Average seasonal rainfall generally decreased from south to north. In the south of the study region, the rainfall achieves 55-70 mm at Nooged and Ghahandad/Qaeshbah, whereas the northern area is about 102 to 270 mm at Mouri during the wet season. Consequently, the 40-years average of NDVI ranges from less than 0.05 in the southern area of the study region to more than 0.8 in the plains zone. These values are stated

as typical values for dominant xerophytic formations by (Polyakova, 2016). Values lower than 0.05 in the southern area indicate areas with very few to non-photosynthetic activity. These are rare-vegetated desert grassland or rocky areas. Rare little forested islands in the plains show NDVI values over than 0.5. They are placed at altitudes of more than 700 m and manifest a presence of vertical zonation in the study region.

Figure 26, shows that the high reflectance of vegetation in 1972 image, with an increase in NDVI values while the vegetation reflectance in low in 2005. The highest average NDVI values for the growing season cover mostly the central mountains and the hillslopes zones. Those areas as we can see in the next chapter generally categorized by Miller (1990) and Liston (1996) as mostly dense vegetation, followed by the semi-dense montane mosaic woodland in the high plateaus and submontane open shrublands. Lowest reflectance values are shown at north-western and south-western part and some areas of low plateau zone in the study area.

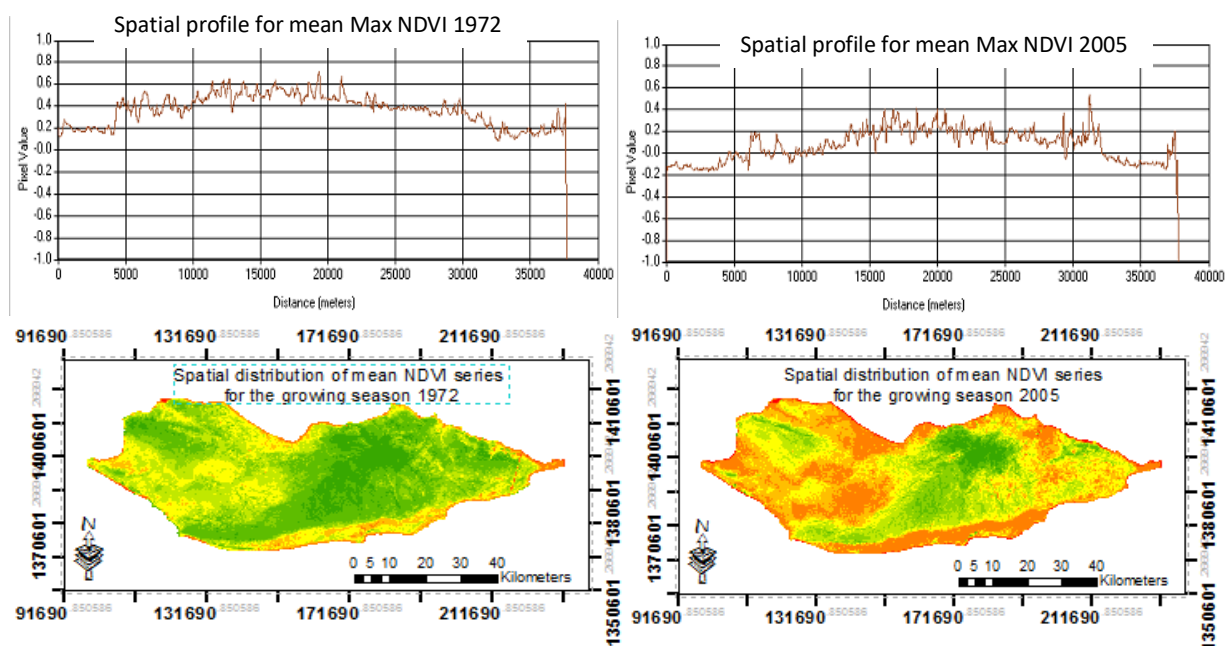


Figure 26: Spatial distribution of mean Max. NDVI and North-South spatial profiles in 1972 and 2005.

### Island Greenness change

Figure 26 illustrates perfectly the change over the entire island during the period 1972 to 2005 (see appendix 4 for more information and full extent images). The NDVI cross section curve rises up to 0.8 and declines again with the physio-eco zones, which present clearly the spatial distribution of the vegetation pattern from the north to the south coastal areas passing through the hillslope and the central zones. It shows also that the areas indicated as bare, rock, desert and very open grassland have increased gradually from 1972 to 2005. Dense vegetation and mosaic woodland clearly were reduced with some areas indicating shifting sand dunes. More NDVI changes during and between the growing seasons and further vegetation aspects will be consecutively discussed.

#### 5.3.2. Inter annual variations difference vegetation index (NDVI)

The NDVI time series for all vegetation community in the island displays a typical inter-seasonal variability from 1972 to 2010 throughout the growing season. For instance, all plains and coastal desert grassland exhibit NDVI time series decreasing in 1984, 1994, and 2010, but little

to no increase in the remaining years. On the contrary, the central mountains and hillslope zones in somehow succeeded to preserve their situation with a little decrease (Fig. 27). Due to irregularity of the rainfall in the area accumulation of wet seasons in 1972, 1984 and 1994 created a highest peak during January and February with NDVI of 0.4, 0.2 and 0.3, respectively (Fig. 28). The NDVI decreased in 2005 due to the failure of rainfall during the winter time and mostly the greenness and NVDI values depended on the summer rainfall and the fog existent in this period. It showed a reasonably high NDVI peak in November and December. Different decades showed reasonable vegetation distribution and closely correspond to our finding in the vegetation cover maps for the same time. The area also showed ordinal consistency, with short grass regions having highest NDVI, grass/shrub regions second highest and shrubby desert regions lowest, in agreement with values in other studies performed in the island. The variability in the mean and maximum per pixel in time series NDVI values 1970-2010 is shown in Table 10. (For the seasonal variation Max and Mean NDVI images see appendix 5)

Period	MIN	MAX/Pixel	MEAN/Pixel	SD	MIN	MAX/Pixel	MEAN/Pixel	SD
70s	-1	0.72	0.59	0.12	-0.66	1	0.32	0.14
80s	-1	0.91	0.63	0.1	-1	1	0.20	0.13
90s	-1	0.99	0.85	0.13	-1	1	0.34	0.18
Mid 00s	-1	0.99	0.99	0.12	-1	1	0.36	0.17
Lat 00s	-1	0.68	-0.68	0.11	-1	1	0.04	0.14

Table 10. Inter-decadal variability in the mean (left columns) and maximum (right) values of NDVI per pixel in 1970-2010.

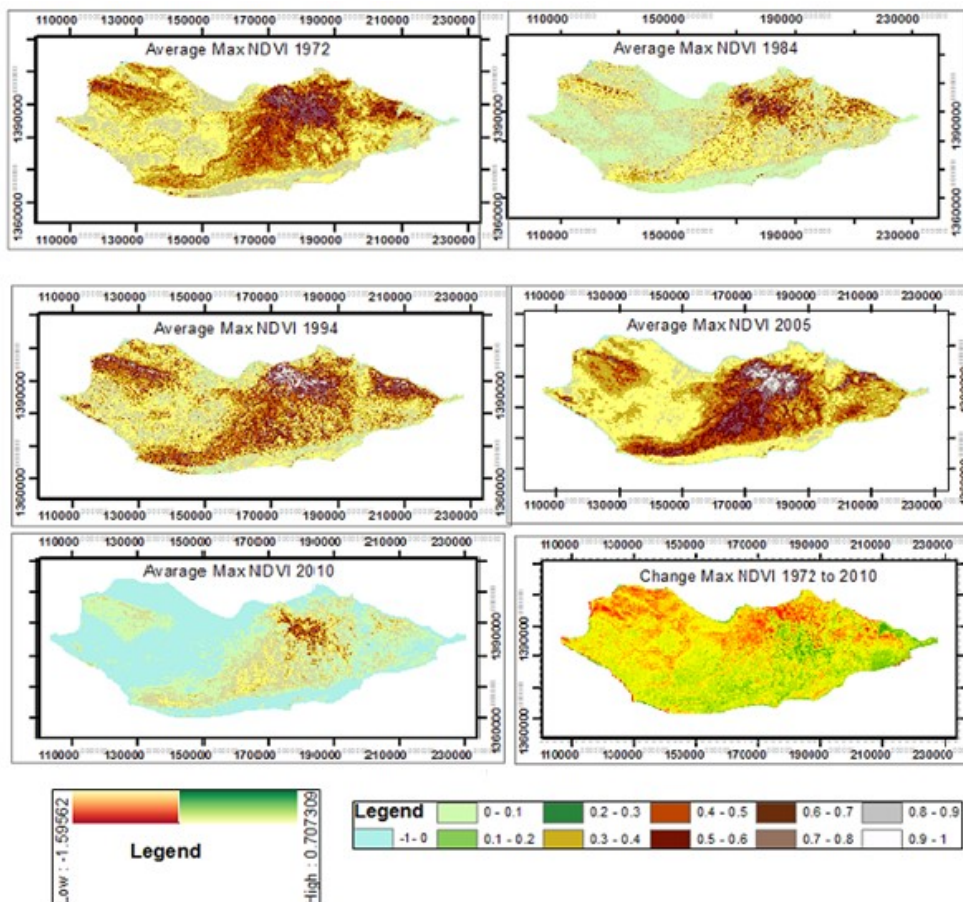


Figure 27: Maps of time-integrated NDVI from 1972 to 2010 (mean maximum within seasons)

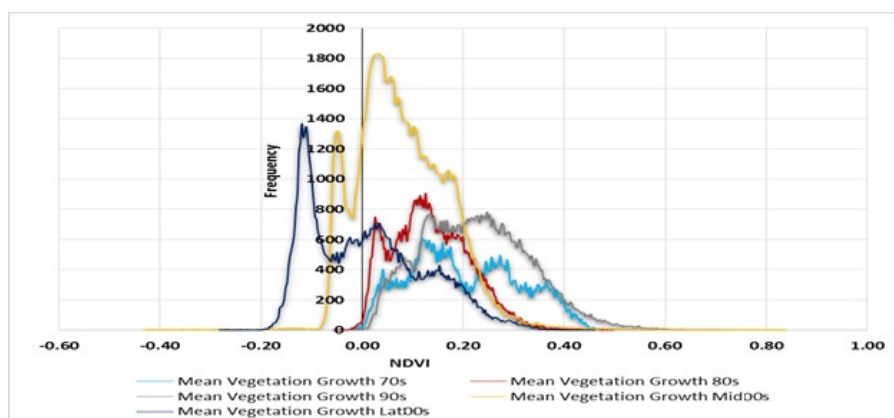


Figure 28. NDVI spectra for selected years 1970 – 2010

According to the high correlations between NDVI values and biomass density, we used a simple NDVI threshold approach to categorise the study region into areas with different vegetation coverage rank. We categorized NDVI values into different ranges with the aim of providing anonymity to biomass distribution over the study area. Dependent on our data we made our breaks value into discrete classes as 0, 0.1, 0.2, 0.3, and so on by making sure this breaks are the same in every image. Using geostatistical and spatial analysis as well as employing pixel value in excel the variation area percentage of NDVI series accounting for the island were computed from 70s to 00s and illustrated in figure 29.

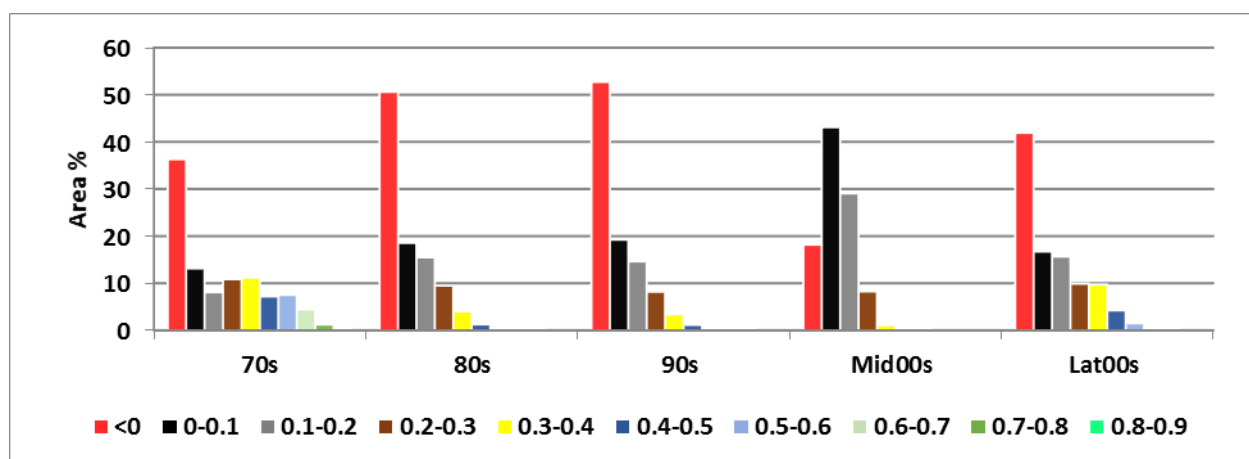


Figure 29: Histograms of spatial NDVI values distribution across the island from 1972 to 2009

The histogram shows contentious growing of no and very sparse vegetated areas (NDVI values below 0.1) while the dense vegetation (> 0.5) decreased and disappeared during the 90s and 00s.

### 5.3.3. Within season variations in NDVI

Hence, correlation is calculated for many different combinations of rainfall and NDVI, allowing us to identify its distinct optimum correlation (i.e. growing season). We also tried to generate time series of rainfall accumulated over two consecutive years and to calculate correlation between them and time series of NDVI. In the north and south of the island upwards trends spread broadly from the west border to the east. Especially high increases in NDVI were associated with areas covered with dense vegetation in the mountainous regions in the middle to north as well as the low and high plateau zones.

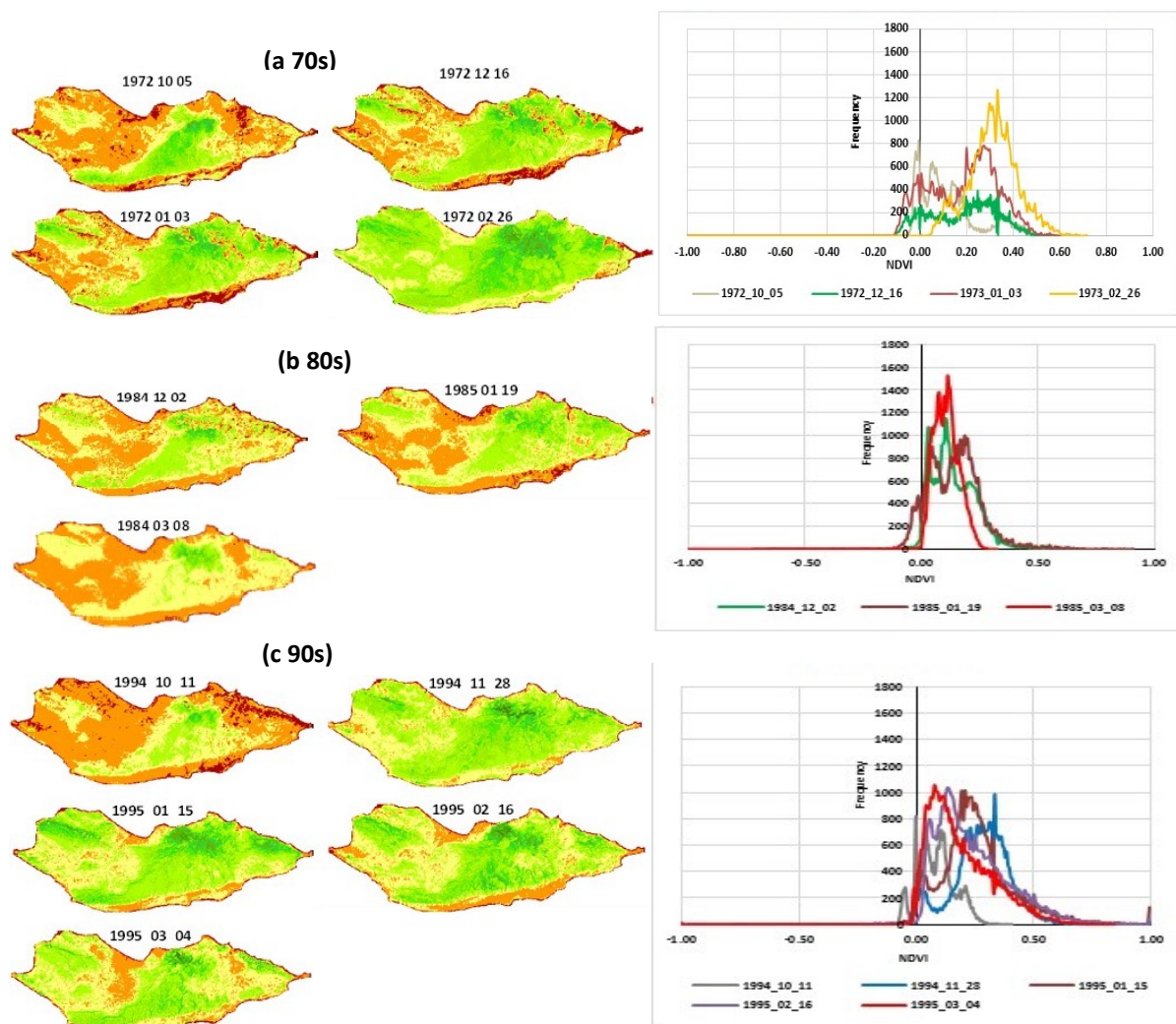


The results of this study showed that approximately 76% of all pixels exhibited significant positive correlation ( $r > 0.24$ ) between within season monthly time series of NDVI and rainfall (Table 11).

Growing Season	Oct. 2005	Nov. 2005	Dec. 2005	Feb. 2006	Mar. 2006
<b>Correlation R</b>	0.24	0.15	0.18	0.11	0.11

Table 11. Pearson correlation coefficient between within season monthly time series of NDVI and rainfall.

All vegetation types have a low NDVI values at the beginning of the growing season, in September. Generally, all vegetation types display increases in NDVI from late October into February, followed by gradual decreases in late March and permanent declines in July-August (Fig. 30, a, b, c & d). Although this increase in NDVI often happen during the second half of the growing season, it can be varying from year to year. In 1972 and 1984, for instance, the NDVI peaks in January and February with extend to March while in 1994 and 2005 the peak occurs in early November. Minimum NDVI values during the growing season occur at the beginning and end of the growing season or immediately before the of the southwest wind (June-August) start, while maximum values occur during the winter monsoon season in all examined decades except in 1972 when the maximum occurs in March. (See appendix 6 for the whole image size)



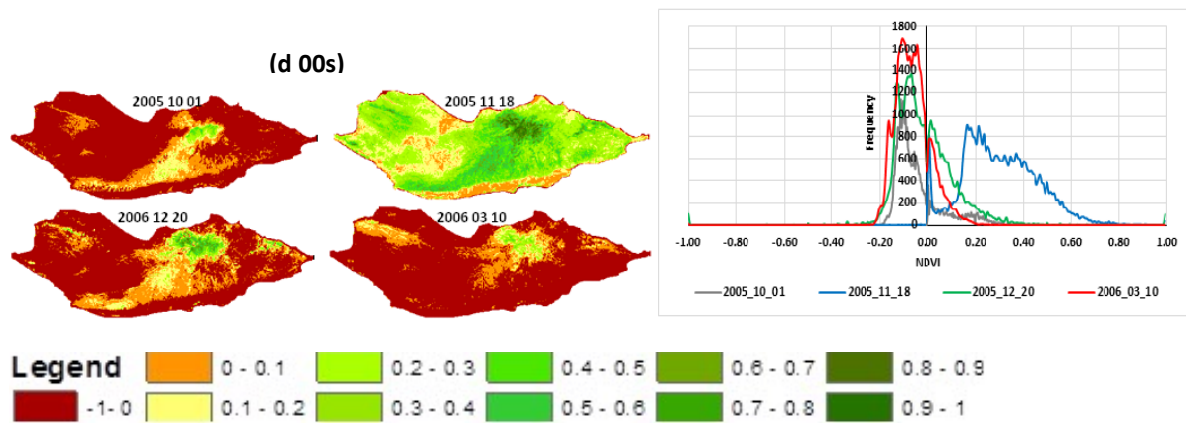


Figure 30: Within-season NDVI variation (a) for 70s, (b) 80s, (c) 90s and (d) 00s, respectively, with spatial maps on the left and histograms on the right. Highest NDVI values are associated with mid to late growing period, which varies between decades depending on the time of rainfall.

### Conclusion

The NDVI time series data derived from Landsat images is a useful technique to monitor the vegetation changes in the study area. The growing season NDVI images show the abrupt transition that occurs surrounding the central mountains from the coastal plains and low plateaus in the south and the north of the island. The detailed pattern around the central mountain and hillslope zones is related mainly to variations in topography, but the overall zone location affects is clearly determined by the general monsoon circulation. Some unexpected high NDVI values can be seen within seasons due to the unanticipated rainfall events. Generally, the average NDVI time series of the vegetation types show uniform behavior through the growing season. Despite similar values of NDVI during the growing period, the sand dunes, shrubland, the scattered trees and grassland exhibit lower NDVI values. In December, the NDVI values of all three vegetation types become again almost analogous. Grassland and small shrubs vegetation begin it's development earlier after the first rainfall, causing sometimes early rise in the NDVI by end of September and the beginning of October, then the dense vegetation which seems to be affected by cumulative rainfall rather than the timely rains. During the growing period months, a rapid increase of NDVI values then follows. Usually, the NDVI associated with the dense vegetation turns over the zero in January. The shrub vegetation of higher plateaus, hillslopes culmination started in a minimum in late December or at the beginning of January. These zones reach the maximum value between end of December and mid-January, depending on the rainfall regime of the associated year. After that, the values gradually decrease and reaching their minimum at the end of August. As well as the dense vegetation regions, then its NDVI values remain high until mid-February, afterwards decreasing slowly until the end of the growing season. The 40-year average seasonal cycle of NDVI provides a clear distinction between the major vegetation behaviors. The best favorable distinction time between the vegetation can be obtaining within the late winter months, from December to February. During this time, the vegetation types in the island display quite different and clearly distinguishable attributes of their canopy cover such as percent coverage, and biomass, in

which those attributes directly affect and reflect in clear differences in long time series NDVI. The highest differentiation between NDVI values of the separate vegetation types is observed in the mid Januarys when they exhibit their maxima in dense.

#### **5.4. Dynamics of vegetation activity and rainfall relationships**

##### **5.4.1. Temporal behaviour of rainfall and vegetation within the growing season**

NDVI time series are usually non-stationary (Pinzon and Tucker, 2014), i.e., they present different frequency components, such as seasonal and within seasonal variations, long-term as well as short-term rainfall fluctuations (Guo et al., 2015). Such series according to (Brown and de Beurs, 2008) are characterized by seasonality trends patterns and localized abrupt changes resulting from diverse disturbance events. The high temporal resolution of satellite offers the opportunity to define time profiles definition (Borak et al., 2000) and characterize the vegetation dynamics on the basis of varied temporal scales essentially related to the aforementioned patterns. The direct correlation of rainfall anomalies with NDVI anomalies over the 1972–2010 time series shows a slight delay (by approx. two weeks). Figure 31 illustrates the within-season cycles of NDVI and rainfall averaged over the entire island for five selected periods. NDVI values (1972-2010) increased rapidly during winter (early October-mid-March), with a highest peaked starting from December, and decreased by mid-March. As it has been discussed in the previous chapter, the total rainfall during the growing season at individual stations showed considerable variation. The overall monthly rainfall shows generally two peaks (Fig. 22), increasing from early April to early June, after that a clear gap follows, showing then an increase from late September until the next large peak in early January. During the wet season the maximum rainfall was reached in November and December, with an average of 180 to 200 mm or approximately 60% of the mean annual rainfall. Minimum of rainfall occurs in July and August. The wet growing season is commenced approximately from October to early March with a high peaking started in late December to late January. The growth of vegetation begins after the first short growing seasons of May and then gradually decreases during July-August, approximately value has reach down to zero. Both variations of rainfall and NDVI have the nearly similar trends, but NDVI curve is delayed in response to rainfall in some years.

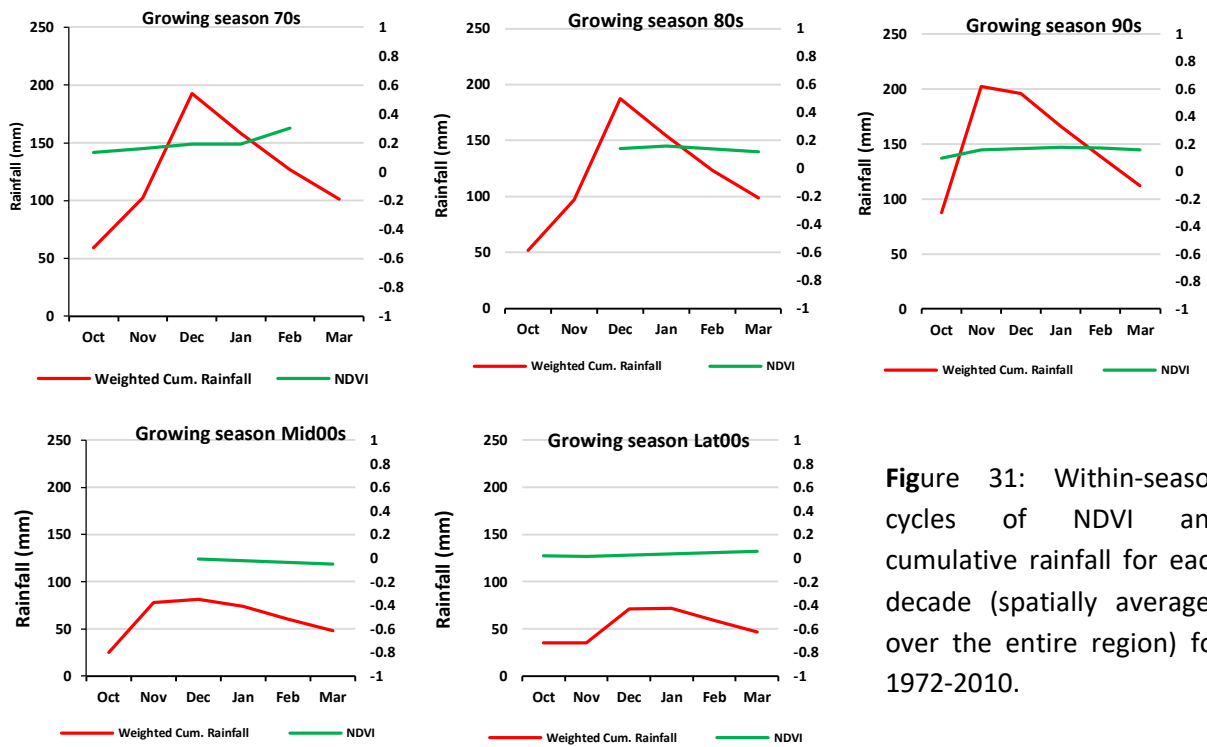


**Figure 31:** Within-season cycles of NDVI and cumulative rainfall for each decade (spatially averaged over the entire region) for 1972-2010.

Figure 31, also provides a visual comparison of rainfall and NDVI averaged over the growing season and the entire study period. Even by the visual comparison one can support a significant association between spatial patterns of NDVI and rainfall. Calculations of correlation coefficient proved this assumption. In the following section we will show the calculated global spatial correlation between both variables for every year for the period 70s to 00s. Our calculations resulted that weighted cumulative rainfall-NDVI correlations (Fig. 31) were between 0.96 and 0.42. High correlations indicated a strong association between rainfall and NDVI averaged over growing season, with also some significant inter-seasonal variation in the magnitude of the correlation coefficients.

#### 5.4.2. Temporal behaviour of rainfall and vegetation between the growing season

Figure 32 (a) and (b) show the mean total growing season evolution of rainfall for every pixel in the study region for the period 2005 and 2009 whereas (c) and (d) exhibit the NDVI within-season cycle for the same period respectively. It shows stronger correspondence with patterns in rainfall amounts. These illustrations presenting Hovmoller diagrams provide a general overview of the dynamic of the rainfall. Nevertheless, the temporal pattern in rainfall varies in space. During the wet seasons the southern part of the island have a peak of rainfall with average of 111 to 130 mm near the center and then a rainfall lack gradually toward the east and west, whereas it reaches more than 150 mm in the north and central part. The 300 to over 600 m high limestone cliffs at the northern and southern parts with elevated hillslopes and plateaus around the Haggeher Mountains cause orographic uplifts. Comparing both rainy seasons from 2005 to 2009, we notice a highly temporal variation between the two seasons in which it might reflect the variability and failure of rainfall in the area. The rains in south part of island are more common during SW monsoon during May and June and then at the beginning of October, when heavy rains in Northern part may also occur and is highly influenced by a rain

shadow with no or less rainfall than in northern part. Moreover, this might prove the impact of locality and latitude by (Habrova et al., 2007).

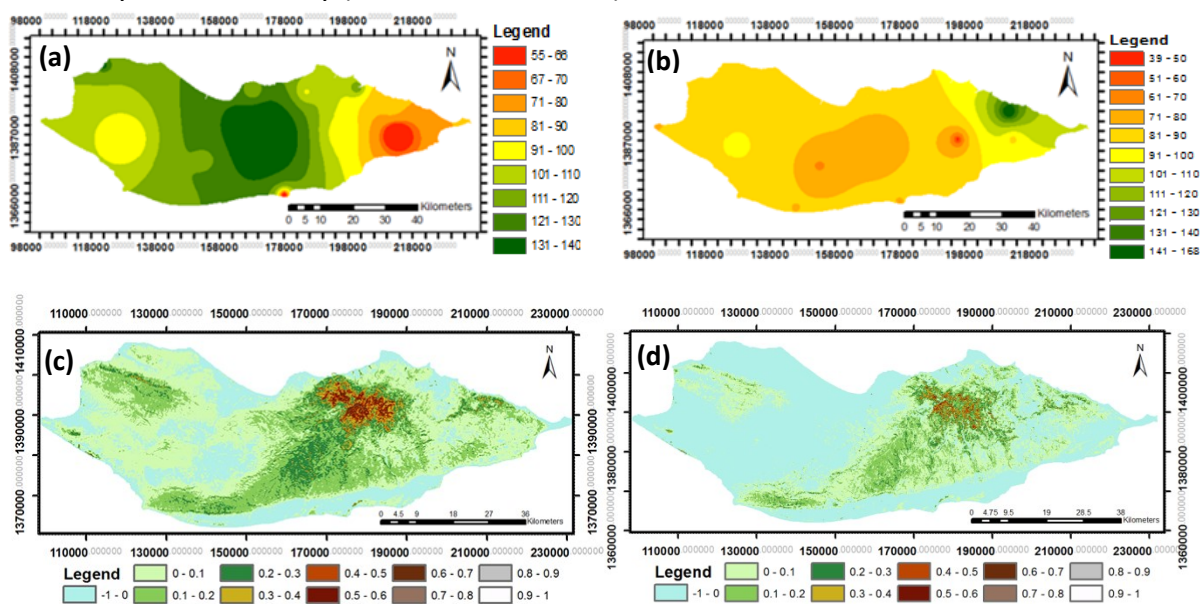


Figure 32: Inter-seasonal dynamics of rainfall for (a) 2005 and (b) 2009 during the growing season interpolated using KED compared with the temporal behavior of (c, d) spatially averaged NDVI within the same time growing season, respectively.

It might be meaningful to introduce some kind of **“weighted” cumulative rainfall**, indicating that rain is absorbed by the soil, but partially evaporated through solar radiation. A simple caricature of this dynamics is covered by the following equation:

$$WCR_t = WCR_{t-1} + R_t - 0.2 * WCR_{t-1} = R_t + 0.8 * WCR_{t-1} ,$$

where  $WCR_t$  is weighted cumulative rainfall and  $R_t$  is the actual rainfall in month  $t$ .

While cumulative rainfall ( $CR_t = R_1 + R_2 + \dots + R_t$ ) is always increasing in  $t$ ,  $WCR_t$  will decrease once the loss  $0.2 * WCR_{t-1}$  exceed the new income  $R_t$ . By systematic variation we found that a factor of 0.8, i.e. 80% remaining to the next month, gave highest positive correlation with NDVI.

Fig. 33, shows the corresponding scatter plot between NDVI values and weighted cumulative rainfall grouped and a logarithmic fit between them. The high correlation coefficient of  $r = 0,81$  It clearly shows that nearly 73% of all variations in log NDVI can be explained by variations in rainfall. This conceives a high dependence of vegetation growth on rainfall but also still a certain amount of NDVI variance remains unexplained. Another problem is that a spatial average over the entire study region gives a good general impression of the relationship between vegetation activity and rainfall but it response of individual vegetation types and vegetation communities to the climatic factor to be investigated and discussed in the following sections. To investigate this response, we performed correlation analysis disaggregating the territory into ecological areas occupied by different vegetation types. Since the relation between Mouri rainfall data and the other newly rainfall stations data are highly variable between the months we cannot estimate the rainfall before 2000s. Our only chance is to use Mouri station as a representative for the overall rainfall in the Island at least for the growing periods October – March. Therefore, we can presume a conceptual model hypothesizing that, the highly rainfall amount will not exceed the value of 1 in NDVI.

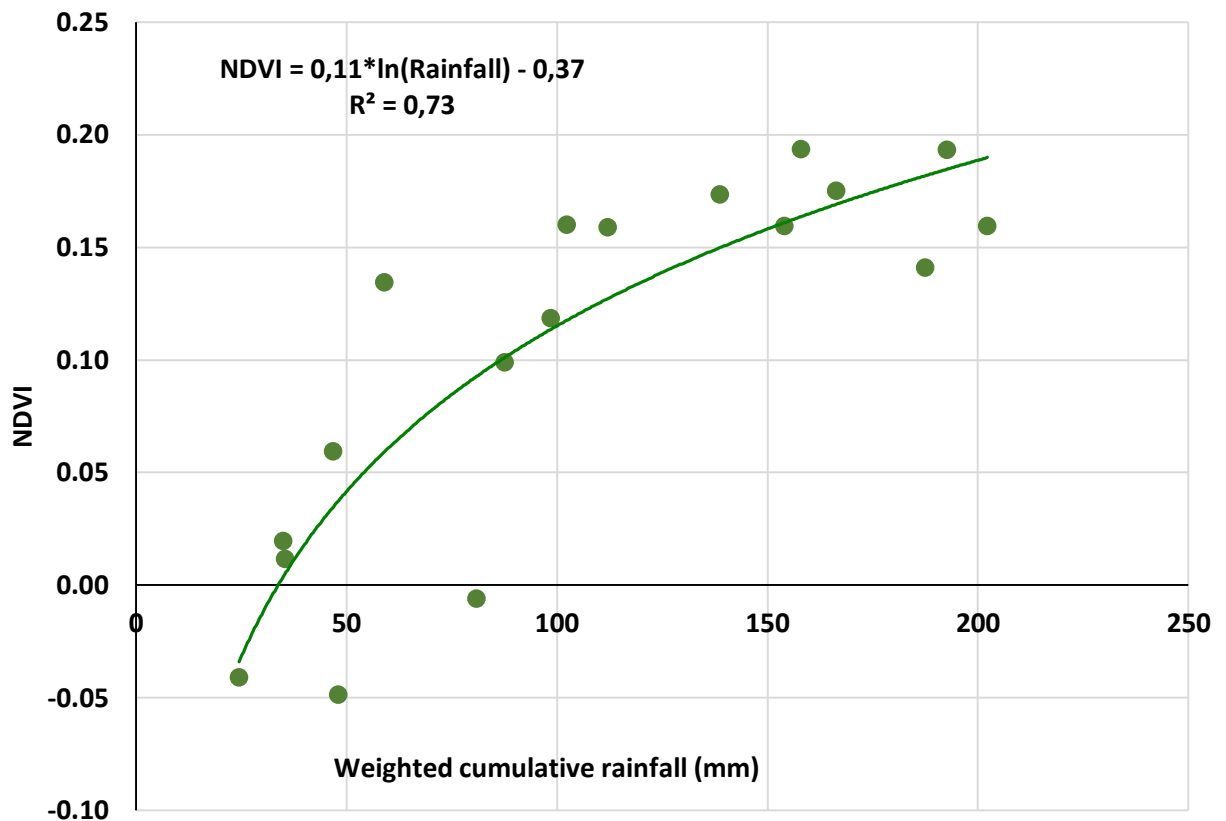


Figure 33: Scatterplot of mean NDVI values and weighted cumulative monthly rainfall for the time periods 1976-2005) and fit of a nonlinear (logarithmic) regression.

These results confirm earlier findings by (Miller and Morris, 2004a, Nicholson et al., 1990a, Scholte and De Geest, 2010) that vegetation greenness in semiarid environments is more strongly related to soil moisture content and a function of rainfall accumulated over a period of time than to instantaneous rainfall. Reasons for a large discrepancy might be due to a large difference in moisture and temperature conditions over the territory of the study area and differential responses of vegetation cover to climate conditions such as responsiveness to rainfall or limitations from high temperatures. In this section we abandoned a description of existing influence of climatic predictors on vegetation development during the phenological cycle. This influence is very versatile and complicated; it reveals differently during various time-periods of phenological cycle. We carried out a detailed investigation of relationships between NDVI and ecoclimatic parameters during the growing season and devoted separate section to the results description. Temporal responses of vegetation cover to rainfall within the growing season will be examined in detail in the following sections.

At the seasonal scale, the vegetation growth seems to be highly dependent on the rainfall amount and its distribution during the rainy season. In the previous section, the mean effect of variations within the rainy season over the decade was examined. Examine year-to-year or inter-seasonal variations might help well understanding the impact of rainfall anomalies within the season on the vegetation phenology and its influence on vegetation growth. **Figure 33**, showed considerable year-to-year variation in rainfall and NDVI during the study period.

Therefore, correlation coefficients between the cumulated rainfall and the maximum NDVI between the growing seasons exposing variability in response of vegetation to rainfall were significantly higher. There was a notable association between the strength of NDVI / rainfall relationship in according year.

Along with the variation of the rainfall, the variability in seasonal maximum and the mean greenness of NDVI data was computed to determine the area of potentially higher and lower within-growing period variability in vegetation production, and it might be very useful to estimate the vegetation drought events.

The time-integrated NDVI for each growing season was also found somehow to be closely correlated with rainfall (Fig 34). However, also (Herrmann et al., 2005) and (Barbosa et al., 2015) contended that NDVI is highly sensitive to the presence, condition, and density of vegetation and is highly correlated with absorbed photosynthetically active radiation (PAR) and vegetation primary production. (Forkel et al., 2013) argued that inter-seasonal variability would influence the accuracy of NDVI trend change detection. So we applied a wide range of trend estimation methods involves regression and spatially geostatistical analyses (Fig 34).

Changes in seasonal timing such as the start and end of season, duration of growing season, and maximum productivity can in turn have an impact on a large number of species that are dependent on natural cycles of vegetation. For all these reasons, trends in the relationship between the annual NDVI and rainfall may be diverse depending on internal heterogeneity of the eco-climatic region (Brandt et al., 2014).

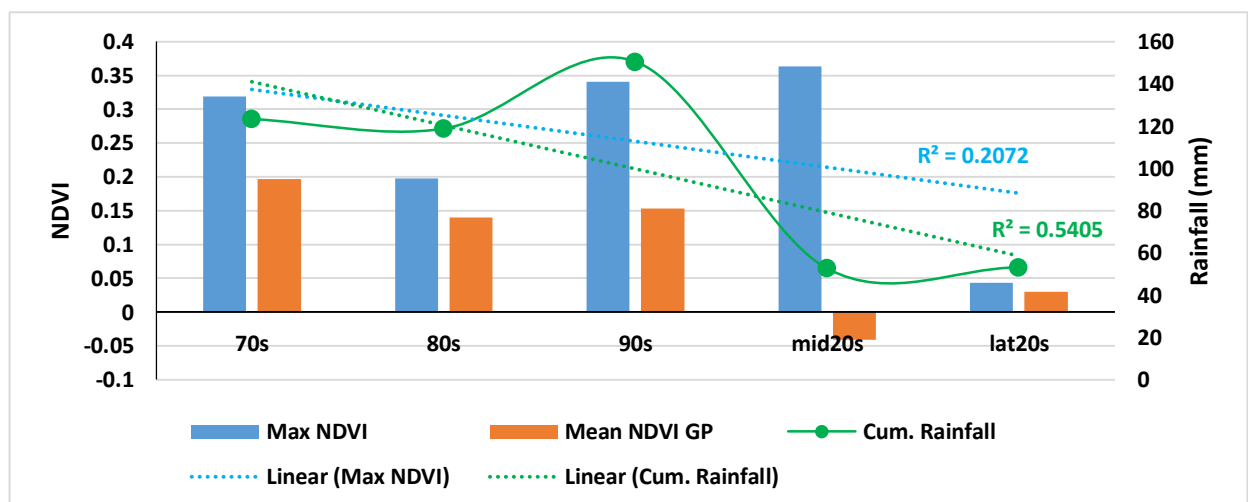


Figure 34: Seasonal average of the mean, max and cumulative rainfall (mm) are shown for the period from 1972 to 2010. The linear regression line (dash lines) shown with regression equations and  $R$  squared.

Within seasonal rainfall distribution as we described previously in Fig. 31, showed some irregular groups in the growing season. The cumulative sums of deviations detected three periods, November/December 1994, December/January 1984 and October / November 2005, which had average rainfalls of 190, 170 and 60mm, respectively, whereas the island experienced drought periods during 2005 and 2009. Seasonal series also reflected the irregularity in rainfall intensity and timing, and showed a slightly decreasing trend until approximately end of 90s, and a considerable decrease after that year (Fig. 35). The slightly

decreasing trend might be detected in the first half of the seasonal series and is caused mainly by spring and summer rainfalls.

Monthly rainfall distribution during the wet season has been discussed early in this study and found considerably variable during the last 40 years studied. It showed a maximum in October - November and a minimum in July - August and having both very high and very low values (Fig. 22). For example, 132 mm was registered in November 1994 (42% of that year's total annual rainfall), 43mm in December 2009 (7%) and 111 mm in December 1973 (21%). With regard to low values, it is very common that rainfall delayed during the wet season and some cases totally failure.

For the island as a whole the analysis of spatially averaged NDVI versus rainfall in the wet season showed, that the Pearson correlation between synchronous data of growing season NDVI and rainfall was statistically significant,  $r^2 = 0.71$  (Fig. 35), however the values for each decade were different. At the level of individual decade, correlations with the total rainfall were also strong with value of 0.94, 0.43, 0.42 and 0.64, for decades, 70s, 80s, 90s and 00s, respectively.

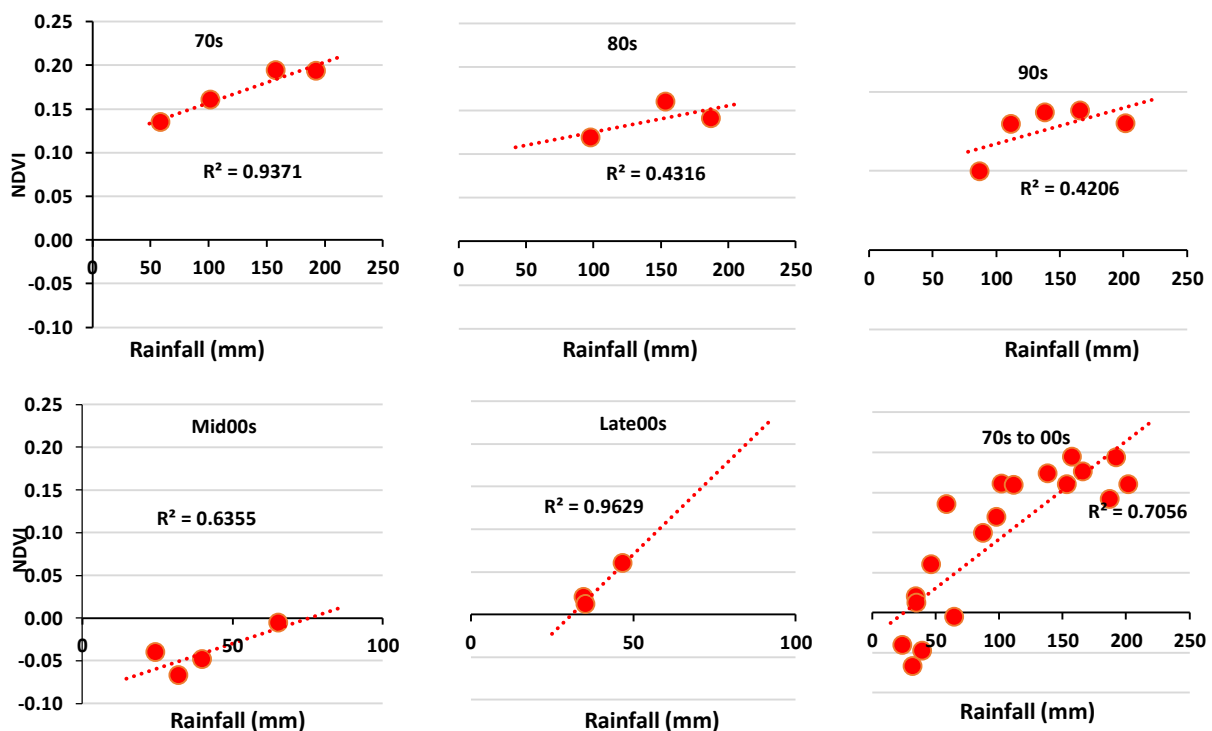


Figure 35: Correlation coefficients between NDVI and average cumulative rainfall for separate growing season, 70s, 80s, 90s, and 00s (and all together) with linear regression curves displayed.

### 5.5. Modelling spatial patterns in rainfall parameters

In this study, the spatial distribution of rainfall variables was incorporated in ArcMap by preparing gridded maps using geostatistical analysis model. Therefore, several mapping techniques for the interpolation of rainfall were used such as kriging/cokriging, spline-surface fitting, Inverse Distance Weighting (IDW), and the multivariate geostatistical method kriging with external drift (KED).

The results obtained using Inverse Distance Weighting (IDW) are presented in Fig. 36. They can be characterized as a near gradual up-step in rainfall when going northwards. This map does not take into account any external influence on climate patterns. It is less smooth (Fig. 37 than



the corresponding map produced by kriging with external drift (KED), of Fig. 38 and 39, which show clearly the form of the terrain, particularly in the mid and northern parts of the study area.

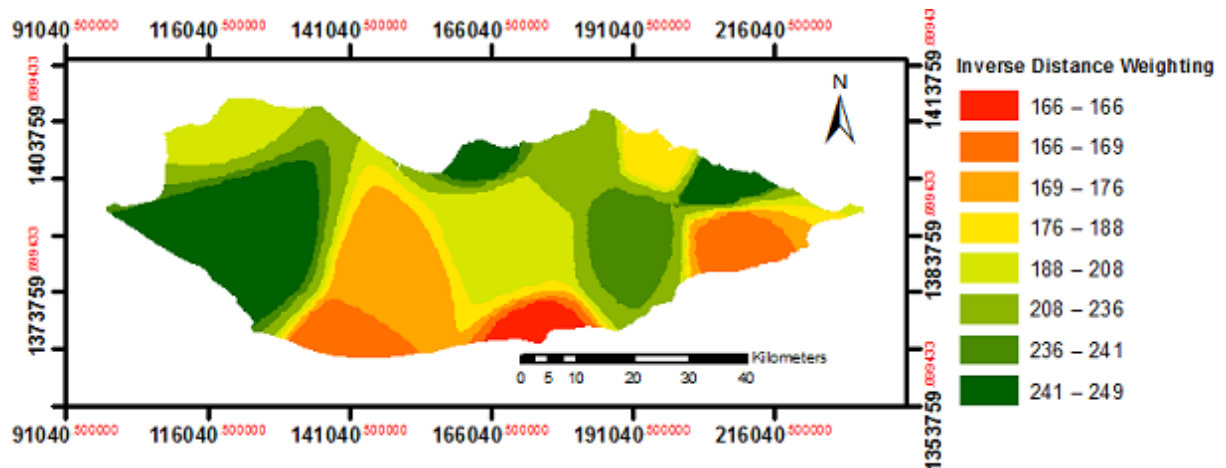


Figure: 36 Spatial distribution of the total amount of rainfall over the growing season derived using IDW method.

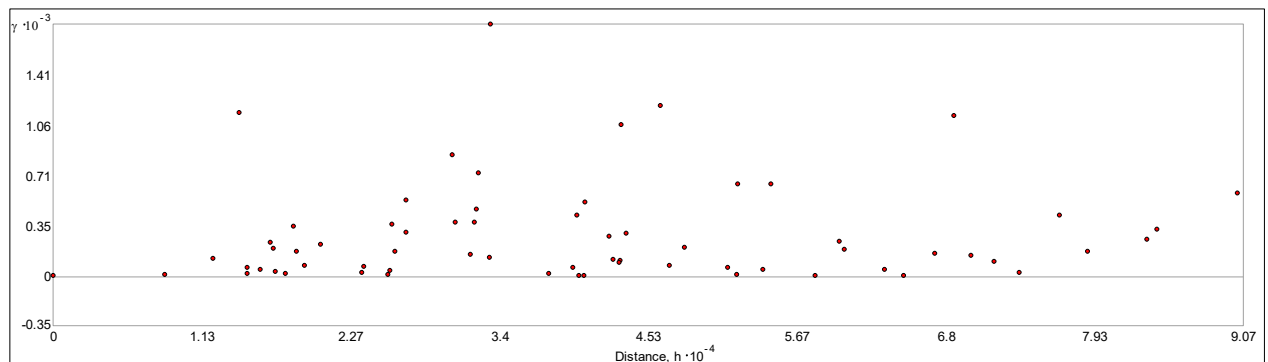


Figure 37: Performance of seasonal total rainfall with IDW interpolation.

Despite the impact of various semivariogram techniques on the rainfall's interpolation performance was low and the spatial pattern in average rainfall was varied over the event time, an overall averaged semivariogram interpretation was sufficient.

Figure 38, based on KED, shows that the average annual rainfall increases markedly in the south east and from north to south in the western island, with clearly shows the impact of the central mountains, introducing different rain shadows with mean annual rain from below 100 mm at both sides of the mountainous area to over 239 mm inside the mountainous area. The average rainfall in the growing season generally increased from south to north and decreases in the eastern part except the heights plateau of Homhil. There are noticeable anomalies in the patterns caused by influence of relief on the climate, since elevation in the study region ranges from the sea level to over 1450 m.

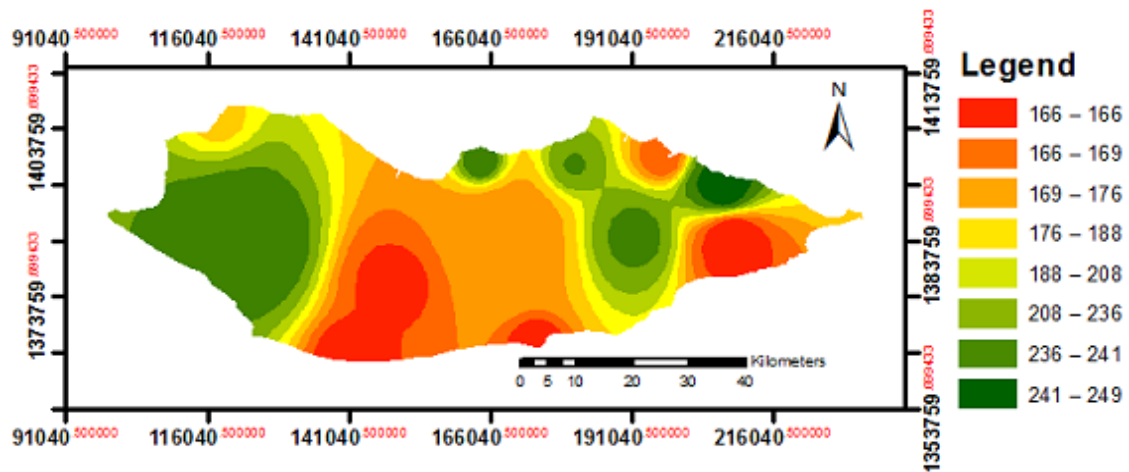


Figure: 38 Spatial distribution of the total amount of rainfall over the growing season derived using KED method (with elevation and wind direction as external drift).

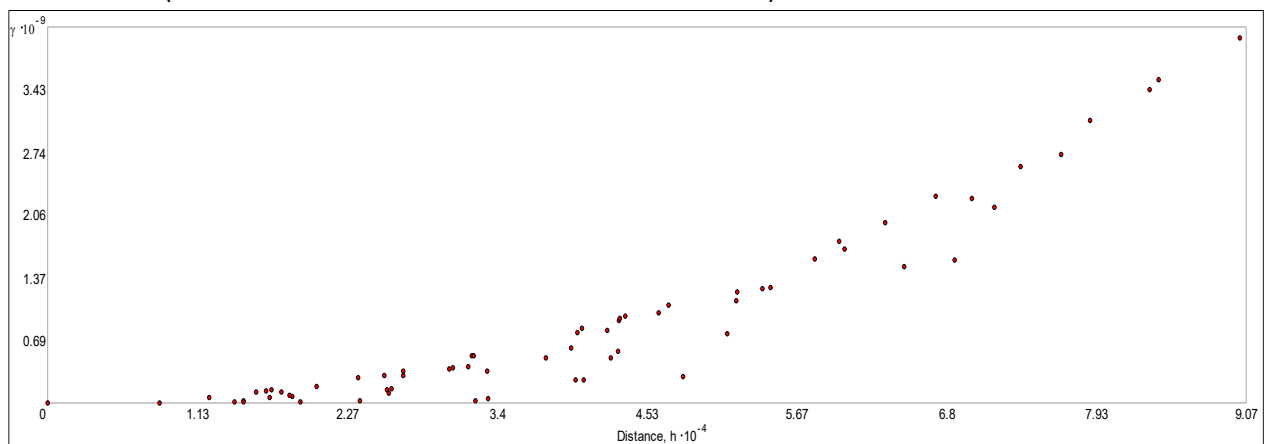


Figure 39: Performance of average seasonal total rainfall with KED semivariogram interpolation, using additional topography information and monsoon wind direction.

In order to assess the accuracy of the data preparation, we compared the data obtained from the interpolated stations with the rainfall cumulative data from the old Mouri station data. Average error was less than 3% for KED and about 8 % for Inverse Distance Weighting (IDW). It means that the approach of kriging with external drift worked more effectively. The root mean squared error (Nidumolu et al.) was also used as a guide to the accuracy of the prediction. For KED, the RMSE for 12 climate stations was less than for IDW.

### 5.6. Spatial distribution of (NDVI) and Rainfall in the study area

Rain is usually the major source for soil moisture, which is critical to plant survival and productivity. The amount and timing of rainfall was reported as a major factors influence the NDVI of native vegetation (Schultz and Halpert, 1995). Numerous studies have also shown presence of a time-lag between a rainfall event and the vegetation response to it, e.g. (Pu et al., 2008, Martiny et al., 2006, Paruelo and Lauenroth, 1998, Yang et al., 1998, Yuan et al., 2015, Tsai and Yang, Hocking and Kelly, 2016, Fan et al., 2016, Cissé et al., 2016). Fig. 31 illustrated that, there is a time-lag of estimated by 2-3 weeks between rainfall and NDVI time-series averaged over the whole study area. Thus, long-living trees seem to exhibit a higher impact in long-term NDVI time series as compared to shrubs. In this regard, the trend analysis of the NDVI time series reported to be more suitable for monitoring long-term vegetation changes. Along

with its values assessing the trend over long periods, it also can be useful in assisting the within seasonal changes of vegetation dynamics and reveals meaningful information on the response of vegetation to climate driving, such as drought events (Martínez and Gilabert, 2009). For each year covered by the data set, a maximum and mean value composite NDVI image was generated and the total seasonal rainfall calculated. The relationship between the derived NDVI (dependent variable) and total rainfall (independent variable) was then generated for each season using geographically weighted regression analysis. This procedure allowed to assess and to evaluates the spatial and temporal relationship between NDVI and rainfall over the region. There are two factors obviously influencing the spatial patterns of vegetation and climatic variables in the study area; the south-north monsoon direction and altitude gradient. Generally, the spatial variance of NDVI and rainfall variables are strongly predicted by the south-north monsoon factor, but the relief conditions slightly deform this rule and make the spatial patterns more difficult. Vegetation and rainfall variable display similar spatial patterns. Total rainfall during the growing season varied and increased markedly from south to north; from about 54 mm in Nooged (Noo) south coastal area to over 270 mm in Mouri, 401 mm in the Homhil and 353 mm in Diksam (central mountainous zone) areas (Fig. 40).

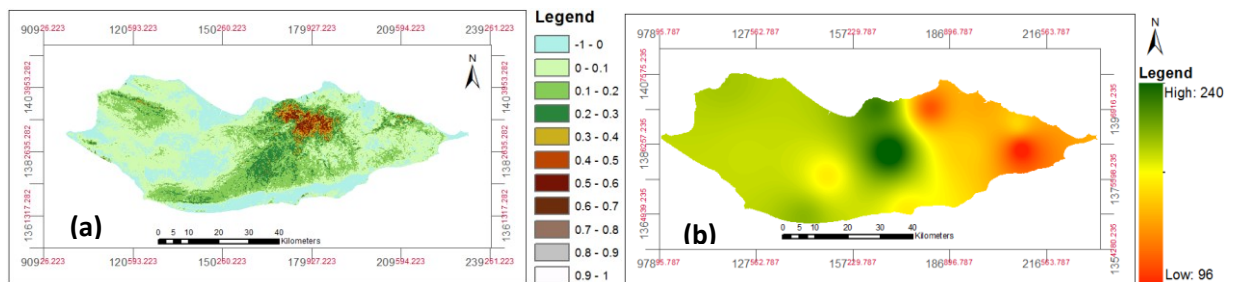


Figure 40: (a) Mean growing season NDVI calculated from the average Landsat for the period 2005-2010. (b) Regionalized predicted rainfall amount throughout the growing season using KED.

## 5.7. Conclusion

The aim of this part of thesis is to test the temporal trend analysis in rainfall values as an important climate parameter influencing the vegetation variability in the island.

In this chapter Landsat satellite data were used to evaluate the impact of within-season and inter-seasonal dynamics of vegetation activity and their relationship to rainfall variability on the natural vegetation growth of Socotra Island. The island was subdivided into six eco-zones, mainly homogeneous in terms of vegetation and topography type and related climate aspects. These zones were sufficiently large to allow the use of rainfall, NDVI satellite products, but small enough to properly depict the spatial heterogeneity of the rainfall and vegetation cover.

Firstly, well-known winter monsoon rainfall was compared over nearly a 40-year period at the scale of the homogeneous zones. Despite differences in the cumulated rainfall amounts, rainfall and NDVI were strongly corresponding and well correlated over the whole region. The inter-seasonal variations were found to correlate with the variations in vegetation phenology. This chapter shows how the combined analysis of rainfall data and satellite generated NDVI data can help to better understand the vegetation/rainfall relationships and to assess spatiotemporal variability in vegetation growth. The significant correlations obtained indicate that NDVI is a good index of the quality of the monsoon season and its (positive/negative)

effects and that NDVI data can be used to monitor these indicators. The next step would thus be the developing of a statistical prediction tool, which then could be used to predict the vegetation biomass during each growing season. Topography and physiographic relief features as well as the monsoon behaves played a major role in changing the duration of growing period and seasonal timing such as the start and end of season, which in turn can have an impact on a large number of natural vegetation species. For all these reasons, we found that trends in the relationship between the annual NDVI and rainfall were distinctly depending on the internal heterogeneity of each eco-region. For clearer understanding of the inter-seasonal variability of Socotra's climate and especially in relation to the expected climate change and the variability between NDVI and rainfall, it could only be better established, endorsed with (Scholte et al., 2011), by continued data collection through an enlarged meteorological station network that covers Socotra's ecological zones. To extend this study, the methodology should be incorporated into process based vegetation growth models in order to evaluate the impacts of rainy season onset, cumulated rainfall and dry event on the vegetation production biomass and grazing practices.

## Chapter 6: Results, part 2 – Analysis of Vegetation Cover and Vegetation Change

This part of the thesis attempts to detect change of vegetation in the island during the last 40 years with distinguishing the main terrestrial vegetation cover into characteristic classes.

### 6.1. Classification of vegetation and description of the mapped Classes

It is the first detailed research examining the potentiality of imagery time series to detect and categorising the change in the vegetation cover in Socotra island using archive Landsat images MSS, TM and ETM+ sensors, covering four periods of time around 1972, 1984, 1994 and 2005. However, it was extremely difficult to obtain multi-date data of the same time of the year because cloud cover is common (see chapter 3).

To improve the classification performance and assigning classes, the variation in sun elevation differences and azimuth (Singh, 1989) was reduced by selecting images data belonging to the same time of the year (i.e. December) except end of November for 1994. Moreover, we implemented an atmospheric/topographic correction algorithm for our image data using ATCOR 3. This processing is very important to allow an optimal comparison of classifications in a time series as it stated by (Baraldi and Humber, 2015).

With respect to the finding by (Carleer and Wolff, 2004) vegetation types among the study area present indistinct spectral features of multispectral imagery both between and within each type. This heterogeneity in vegetation spectra can be understood according to (Yu et al., 2006) and (Ehlers et al., 2016) as a result of an irregular shade or shadow accompanying vegetation physiognomy and floristic characteristics in the pixel values in high resolution images. Moreover, the rough distribution of vegetation type also created difficulties in the selection of training sample size for each class and for classification. Facing all those problems, we proposed to use a simple system of classification techniques (i.e. Image Segmentation and Euclidean Distance of unsupervised classification) that correspond to the spatial and spectral resolution of the available images as well as the heterogeneity of the acquisition dates and final scale of analysis to individually classify each image into 20 categories (classes). We found that the separability between these 20 classes was rather poor. So, these classes were reclassified and merged together to produce eventually 9 broad categories of vegetation cover classes on the basis of both physiognomic and floristic criteria.

Finally, a supervised classification with Maximum Likelihood (ML) classifier as a decision role to label each pixel as the class it most closely resembles was applied. This approach involves reviews of huge ancillary datasets bearing in mind the previous classification attempting in the area and expert knowledge, as well as the comprehensive field survey in the years 2009 and 2012.

Characterization of these nine vegetation classes found was done by typical species comprise or typical physiognomy. We named these classes as presented in Table 13.

Considering the large mapping area and the complex vegetation types (classes) in this study area, we expect that these new maps give sufficient information of the vegetation dynamic on the local level.

Class	Class Name	Code
1	Mix woodland	WM
2	Date Palms	Dp
3	<i>Boswellia</i>	Bo
4	<i>Dracaena</i>	Dr
5	Dwarf Shrubs	DS
6	<i>Jatropha</i>	Ja
7	Succulent Shrubs	Ss
8	<i>Croton</i>	Cr
9	Grassland	Gr

Table 13. Major vegetation covers categories.

Before we present the classification error and detected temporal changes, a short description of each class will be given.

**Mixed woodland (Class 1)** occurs mainly on steep escarpments in the central mountains, hill slopes and deep ravines and wadies. It comprises several vegetation types that cannot be individually separated, including all deciduous woodland types, mixed of *Commiphora* woodland, *Boswellia elongata*, *Boswellia ameero*, *Sterculia africana*, *Dracaena cinnabari* woodland, *Leucas* and *Ficus* (Fig 41). The composition can be highly variable from place to another. This class appears in specific areas with closed canopy of trees that are higher than 4-5 m.

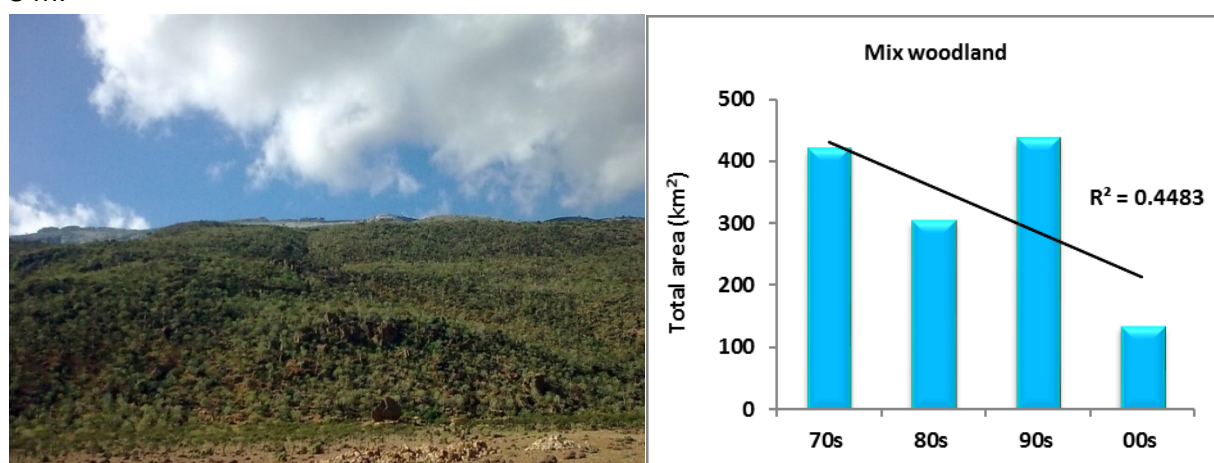


Figure 41: Spatial distribution of Mixed woodland on Socotra and the trend over last 40 years (upper right).

**Date palms, *Phoenix dactylifera*, (Class 2):** Date palms plantations are one of the main economic activities and provide an important part of the Socotran diet on which the population on the island relies upon. It has been introduced to the island centuries ago, no data are currently available on when these species entered exactly (Morris 2002). It is an important traditional cultivation plant and the number of date palm gardens has enormously increased since the 1990s when the distribution of land-ownership was reorganized (Morris 2002). Nowadays, date gardens exist along most wadies on the east, north and middle part of the island, while also an extensive plantation was carried out on the southern areas where the soil is inadequate for the growth of the plant. However, it has been recently documented that date palms plantations have been suffering from unidentified pest which is negatively affecting fruit yield. These plants are quite sensitive to saline soil and being widely spread along the wadies, where water-table is high, and commonly on the dune areas close to the sea (Fig. 42).

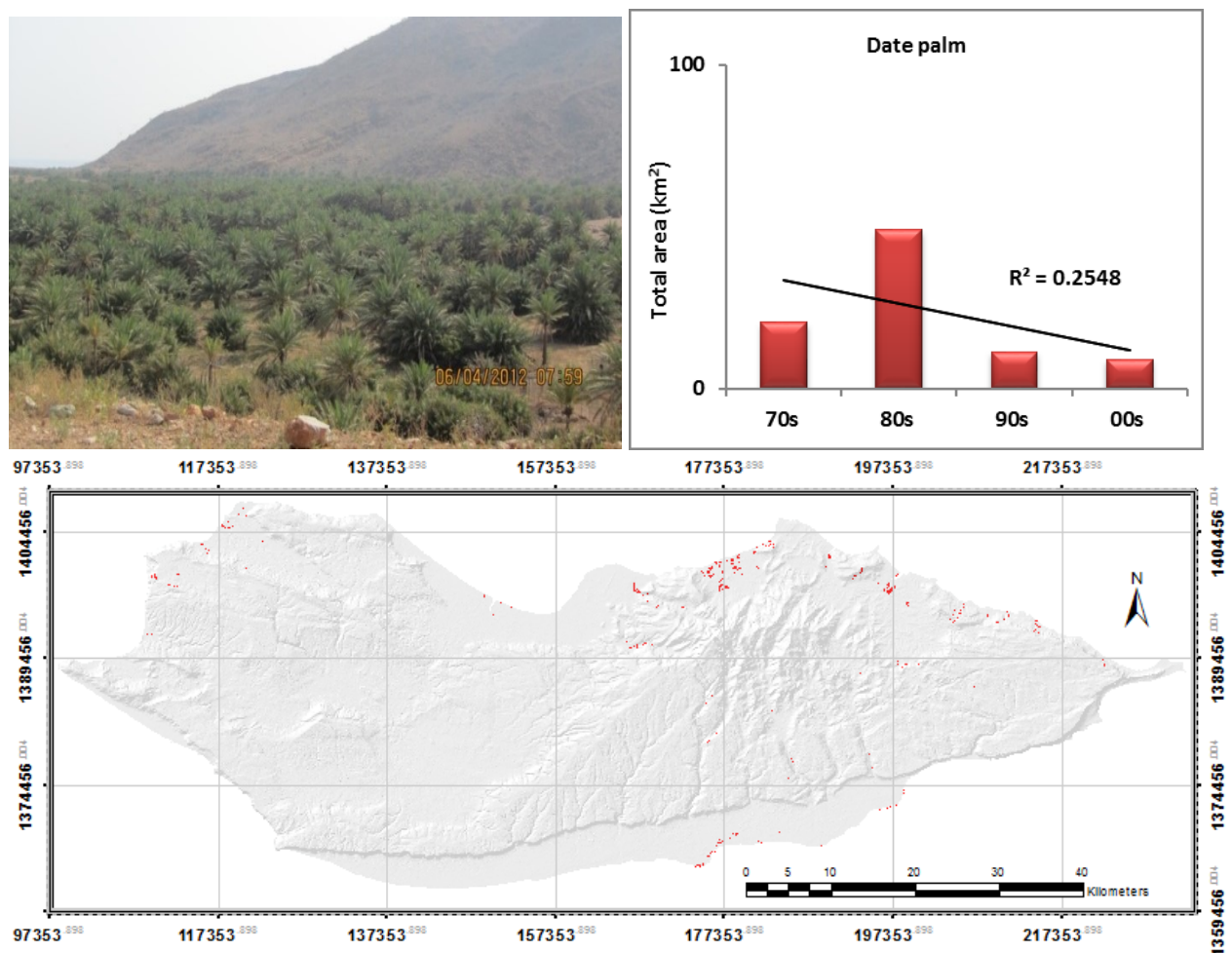


Figure 42: Date palms plantations.

**Boswellia (Class 3),** including *Boswellia ameero* and *Boswellia elongata* woodland. This class is dominant within several eco-zones. It shows a close coverage of trees and a dense shrub and herbaceous layer (Figure 43). It grows on stony limestone soils and is sometimes categorized as a forest with a dense shrub layer and scattered trees, including species such as *Acridocarpus socotranus*, *Rhus thyrsoiflora*, *Ruellia insignis*, *Gnidia socotrana*, *Maerua angolensis* and *Anisotes diversifolius*. *Boswellia elongata* is among the seven endemic frankincense species of Socotra.

Attorre et al. (2011) stated that is difficult to judge whether it is a natural woodland formation that has been degraded by overgrazing or is a remnant of former plantations for gum production. It definitely produces the most valuable incense for human use.

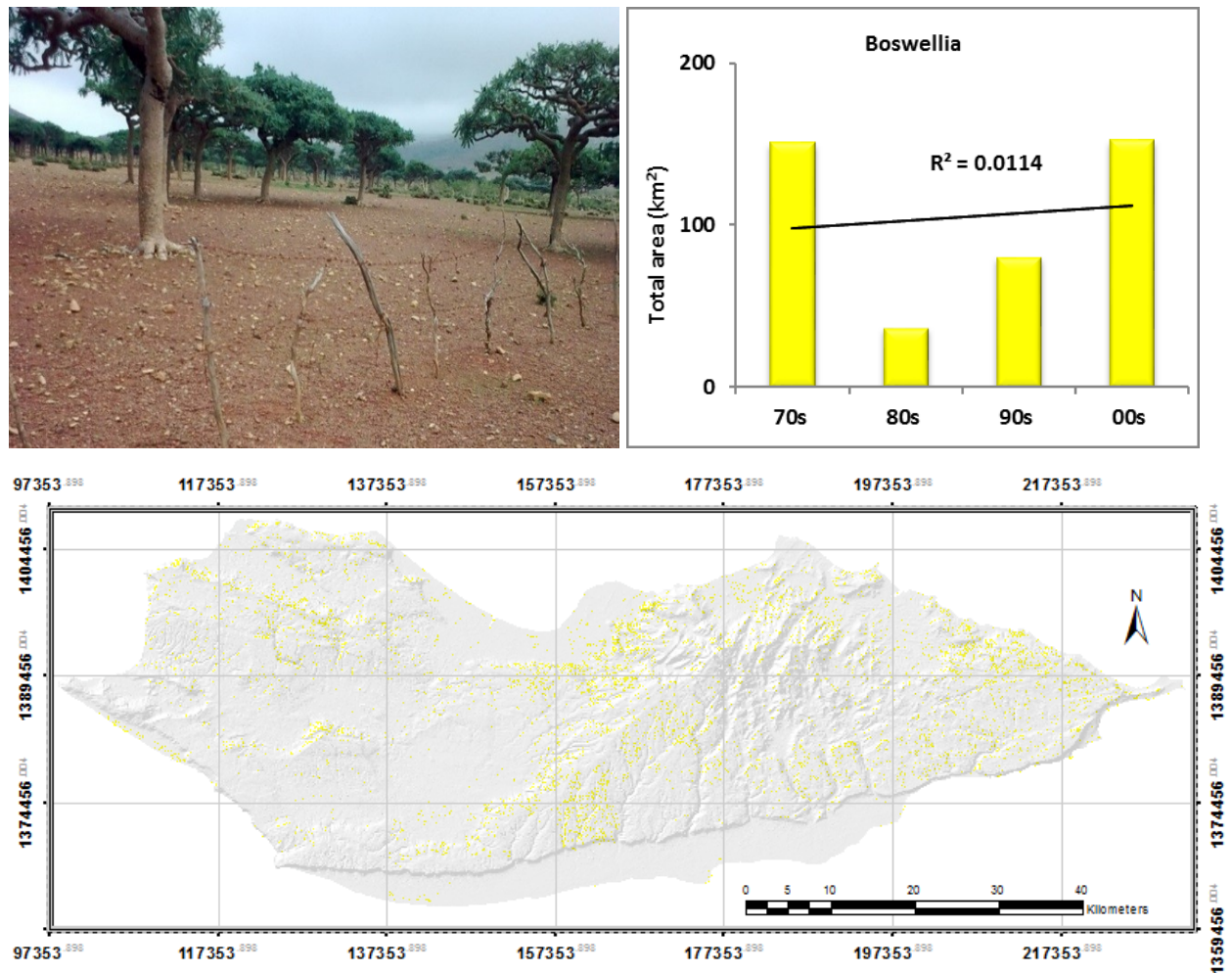


Figure 43: Spatial distribution and temporal trend in *Boswellia* trees.

**Dracaena**, *Dracaena cinnabari* (Class 4) is a typical vegetation type of Socotra that is characterized by the evergreen endemic tree *Dracaena cinnabari* which is widely distributed in the central mountains and normally associated with some other vegetation on limestone on stony or rocky soils (Fig. 44). However, it has a rather open canopy, but it is also found as a forest in many areas in the central mountains reaching sufficient density in Firmihin. *Dracaena cinnabari* is unique and as one of Socotra's flagship species extremely important.

(Beyhl and Mies, 1996) believe that this vegetation type shares its typical growth with another 15 related species which have evolved under a high level of atmospheric humidity in arid environments, such as Socotra. It should be remarked that regions with a similar climate, such as the Canary Islands, Cape Verde Islands, some countries around the Mediterranean and Oman, were all part of the *Laurasian* subtropical forest about 200 million years ago.



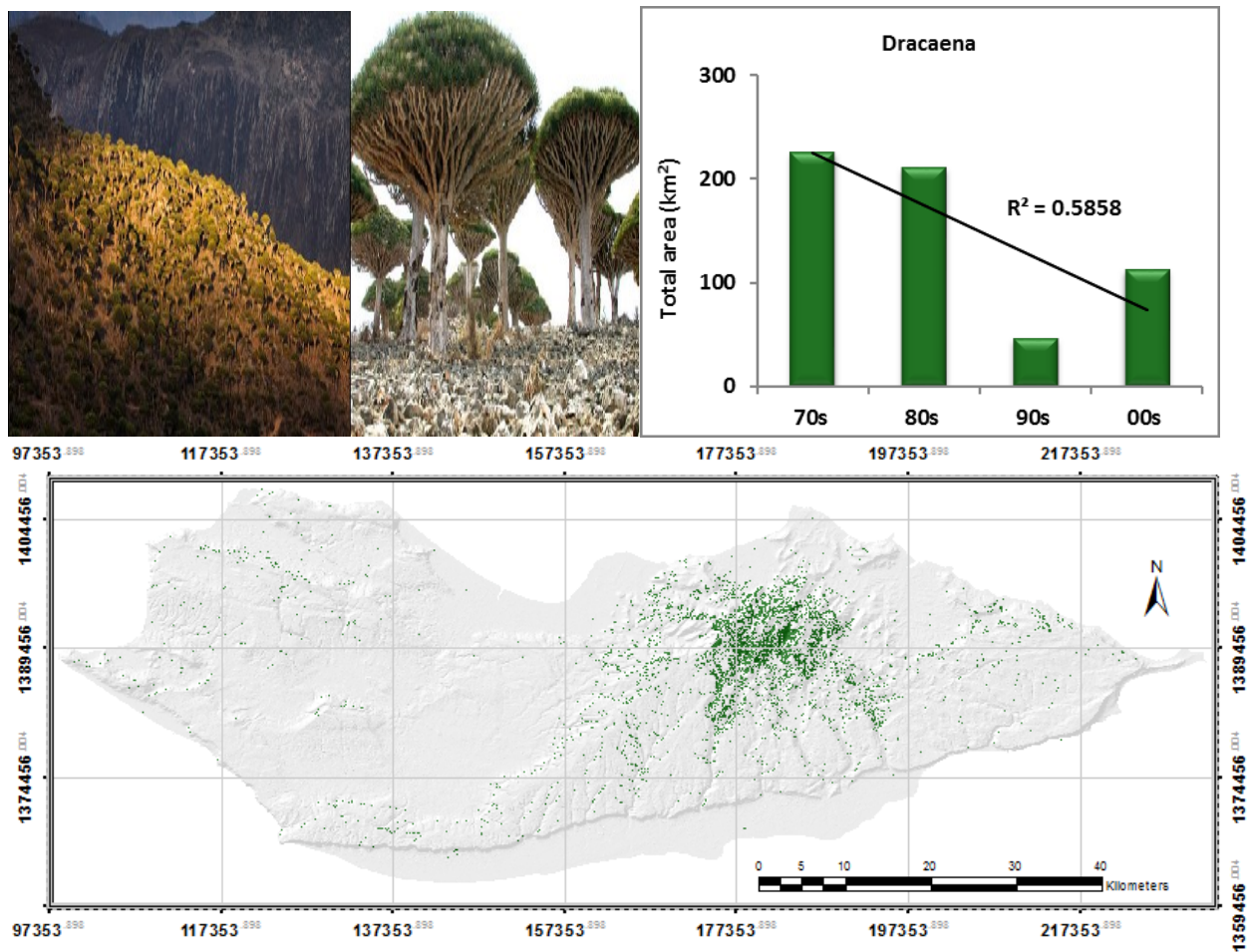
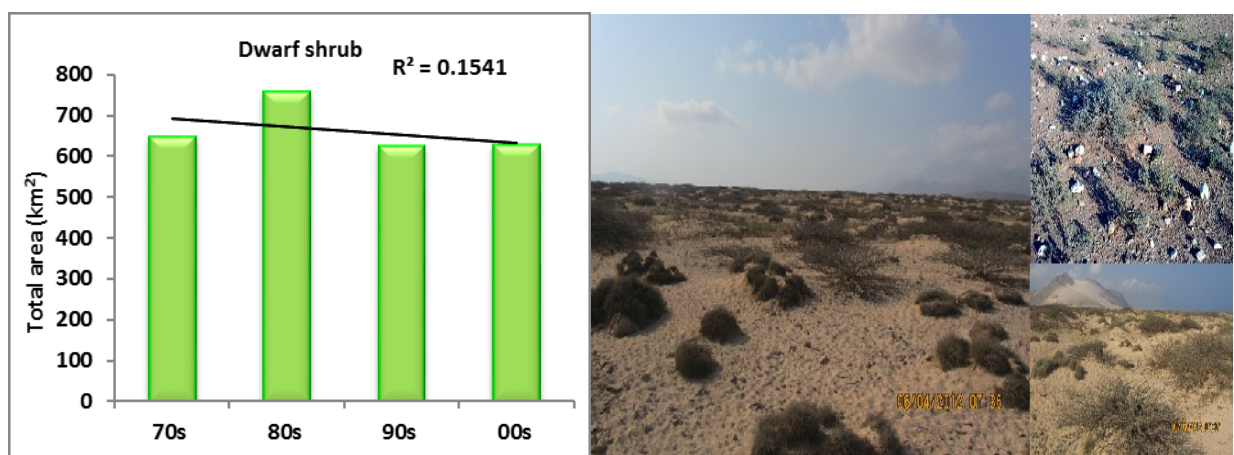


Figure 44: Spatial distribution and temporal trend in *Dracaena* trees.

**Dwarf shrublands (Class 5)** merges all sparse dwarf shrubs of low plateaus and coastal plains with height usually not exceeding 1 m (Fig. 45). They are either naturally shaped by climate conditions and soil type or influenced by wood collection and heavy overgrazing which is often arise by degrading low *Croton* or *Jatropha* shrubland or trees (Miller and BAZARA, 1996).



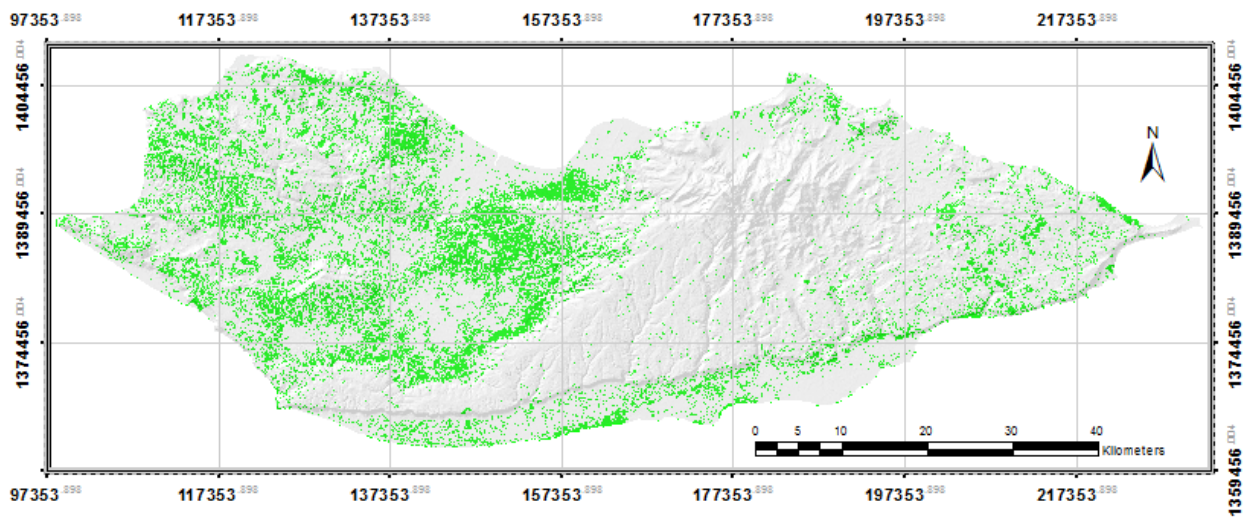


Figure 45: Occurrence and dynamics of dwarf shrublands.

**Jatropha**, *Jatropha unicastata* (Class 6), is a dominant vegetation type on Socotra, occupying steep hillslopes and slopes of central mountains as well as foothills of most of the limestone plateaus and coastal plains (Figure 46). Differences in height usually range from 2 m to 5 m. Sites are characterized by a higher percentage of bare rocks. This vegetation type, as noticed by (Malatesta et al., 2013) replaces *Croton* shrubs on the escarpments of hillslopes associating the edge of the basalt plain with the limestone high plateau.

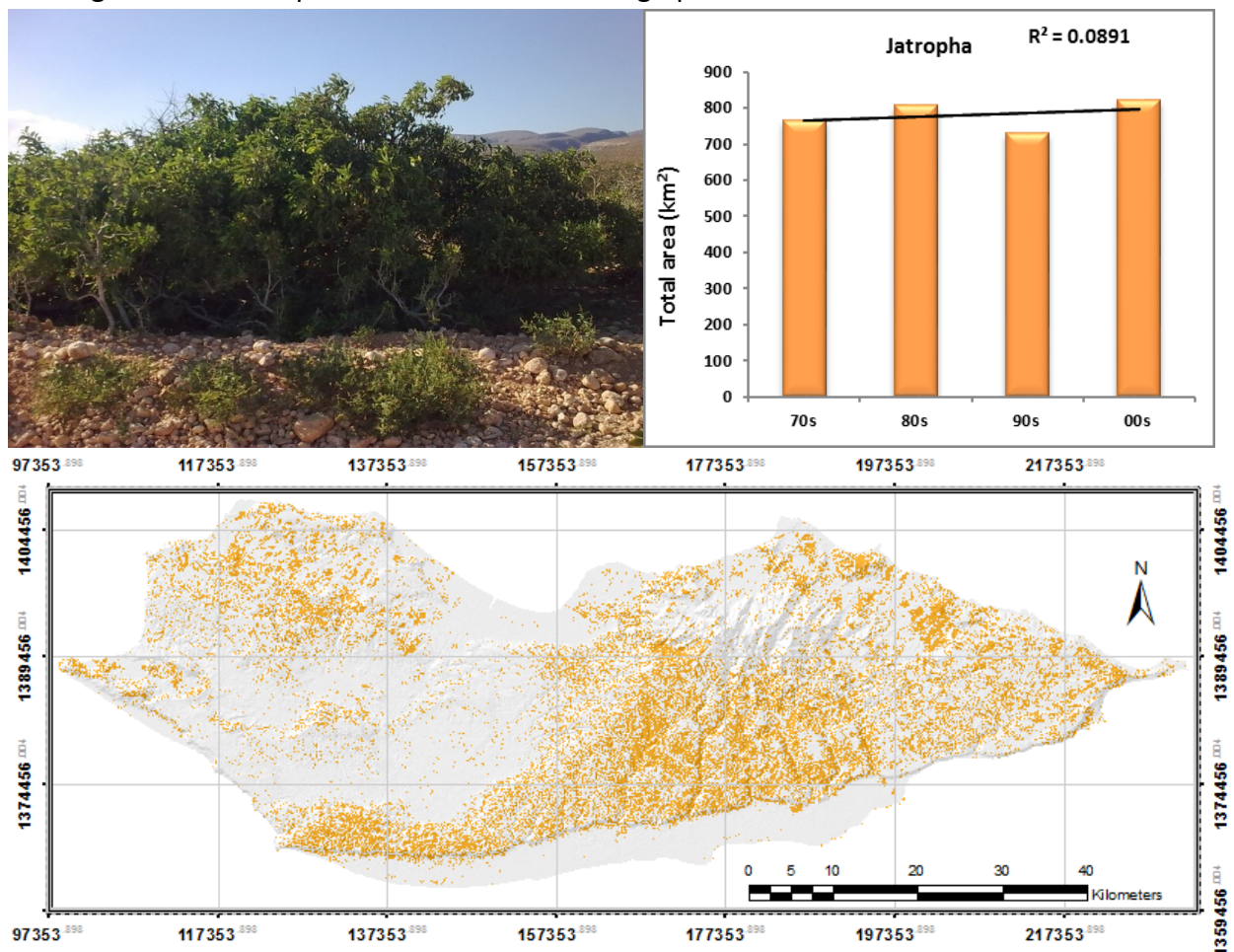
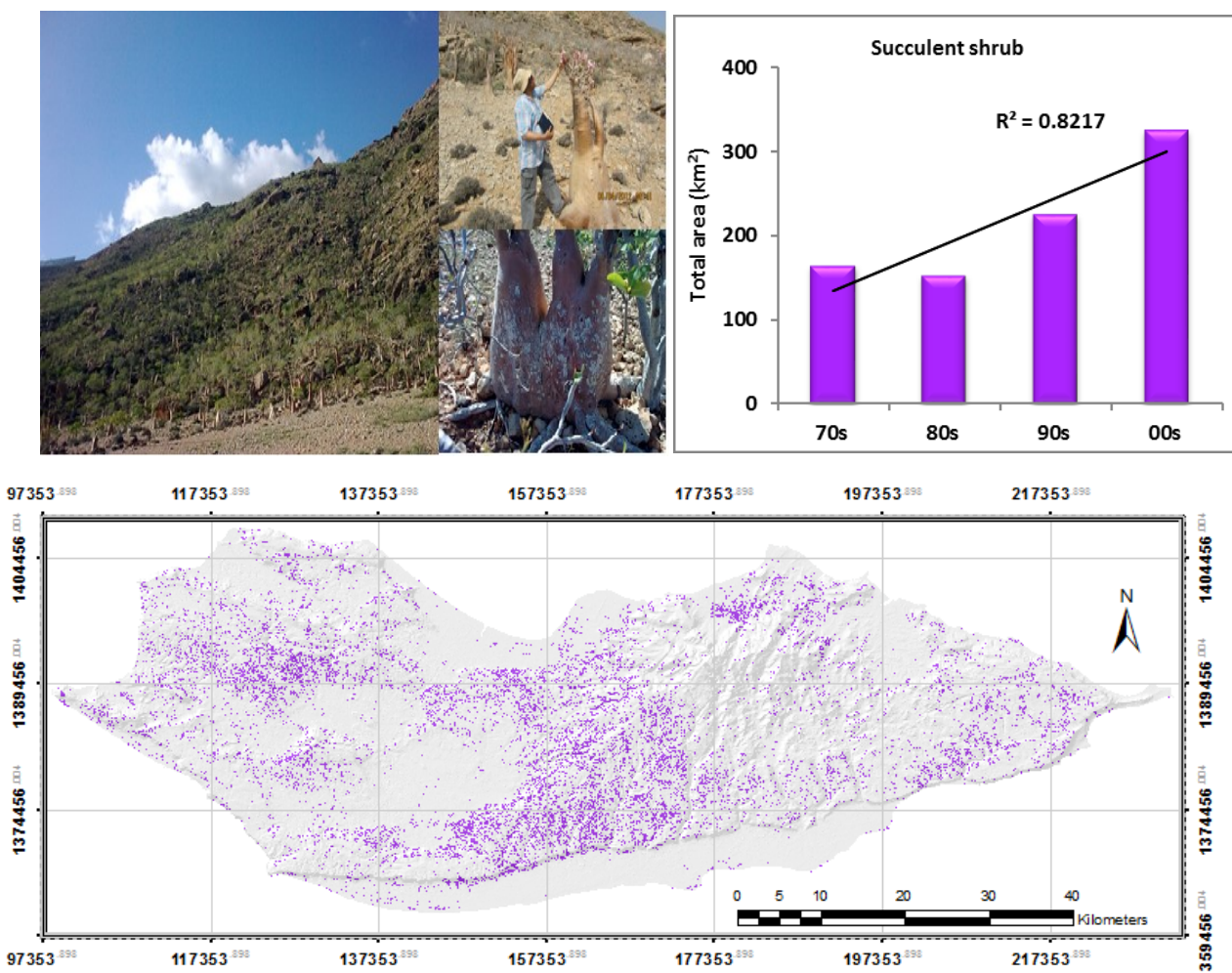


Figure 46: Spatial distribution and temporal trend in *Jatropha* shrubs

**Succulent shrublands (Class 7)** is a community and predominated by scattered succulent shrubs species (Fig. 47). It is also comprises several perennial herbaceous plants, such as *Zygophyllum simplex*, hemicryptophytes, and the Poaceae. Due to the harsh and very limiting environmental conditions, the spatial sequence of these communities are very similar to those identified along coasts of the Arabian peninsula (Kurschner and Ochyra, 2004) as interior salt marshes with marina vegetation *Arthrocnemum macrostachyum*, *Limonium sokotranum* and *Urochondra setulosa* communities. They are reported by (Miller and Morris, 2004a) as heavily grazed communities due to their palatability by small livestock and camels and are considered as an important rangeland providing a healthy amount of salt. This plants as descried by (De Sanctis et al., 2013) are naturally found dynamically linked and at different levels disturbing other vegetation types, such as *Croton* and dwarf shrubland, *Dracaena* and *Boswellia*, and associated with some grasslands.



**Figure 47:** Distribution and dynamics of succulent shrubs.

Moreover, it has been noticed that *Euphorbia arbuscula* and *Dendrosicyos socotrana* can be found scattered mainly with *Boswellia socotrana*, *Commiphora ornifolia* and *Dracaena*, in agreement with other studies' findings. This class comprises all drought resistant thick, fleshy and swollen stems plants in which the leaves stem or roots have become more than usually fleshy by storing water in their tissue (Wiersema and Leon, 2016). It may include several morphologically adapted plants from Apocynaceae, Moringaceae, Asparagaceae, Alismatales,

Aloaceae, Asteraceae, Malvaceae, Asclepiadoideae, such as *Adenium obesum*, *Caralluma socotrana*, *Kalanchoe farinacea*, *K. rotundifolia*, *Dendrosicyos socotrana*, *Euphorbia arbuscular*, endemic species of *Echidnopsis*, *Aloe perryi*, *Duvaliandra dioscorides* and *Socotrella dolichocnema*. It extends over the island from central mountains down to the coastal zones on steep hill slopes, passing through steep and rolling hill sides as well as in deep wadis.

**Croton shrublands**, *Croton socotranus* (Class 8), is one of the common vegetation types in the island (Miller and Morris, 2004a) It is widespread over most of the ecological zones from the low altitudes in the coastal plains to the top central mountains, especially in the dry limestone plateaus and rolling hills alluvial stony soils (Fig. 48). It can be found associated with other plant associations such as *Dactyloctenium robecchii* grasslands and *Aristida adscensionis*, *Tephrosia apollinea* and *Pulicaria stephanocarpa* dwarf shrubland as well as some scattered trees, mainly *Commiphora ornifolia*, *Boswellia socotrana*, *Euphorbia arbuscula* and *Dendrosicyos socotrana*. *Croton socotranus* community is one of the most studied plant communities on Socotra and has been early noted by (Popov, 1957) as a unique one. He described it as ‘Croton short grass community’, while (Pichi-Sermolli, 1955) defined it as ‘subdesert shrub and grass’. (White, 1983) depicted it as ‘Somali-Masai semi-desert grassland and shrubland’, (Kral and Pavliš, 2006) classified it as ‘Low Croton shrubs’ and finally De Sanctis et al., (2013) as ‘*Croton socotranus* shrubland’.

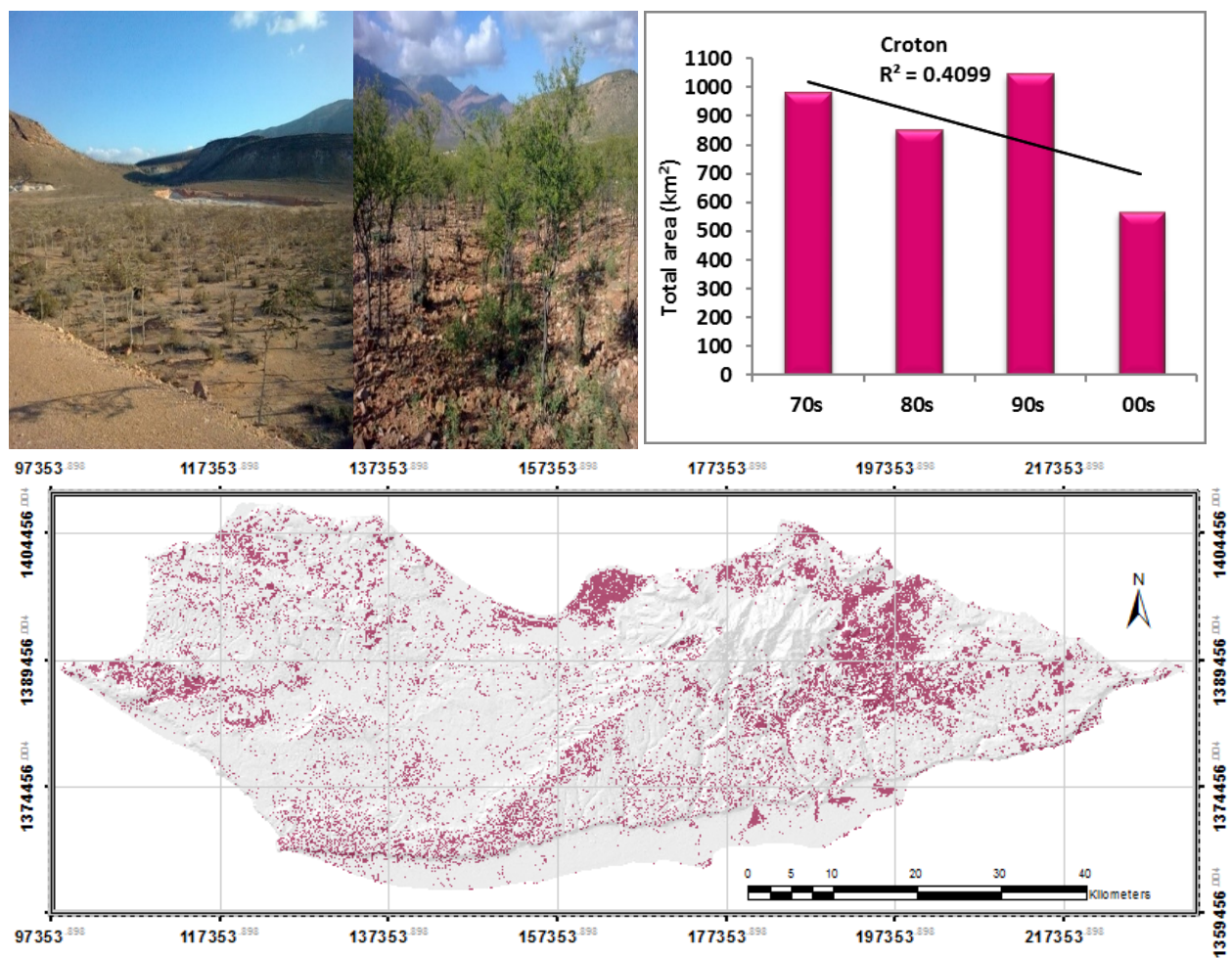


Figure 48: Spatial distribution and temporal dynamics of *Croton* shrublands.

**Grassland (Class 9)** is often combined with rock outcrops, sparse vegetation and/or some open shrub woodlands. It is found mainly on low to moderately dissect undulated plateaus, usually without shrubs or with low numbers of small dwarf shrubs, often present on rocks and stones. It is confined to gentle slopes of the central mountains, high and low plateaus as well as the coastal plain (Fig. 49). Rock outcrops and sand dunes area are usually used for grazing, so they were incorporated into this grassland class. Grasslands in all ecological zones are facing serious threats from urbanization and ongoing spread of invasive plant species as well as from conflicts with non-overgrazing policy. This class covers several types of grassland communities, identified by (De Sanctis et al., 2013) as *Indigofera pseudointricata*, *Aristida adscensionis*–*Tephrosia apollinea*, *Dactyloctenium robecchii*, *Panicum atosanguineum*, *Heteropogon contortus* *Eragrostis papposa*–*Arthraxon micans* grassland as well as *Juncus socotranus* marshland.

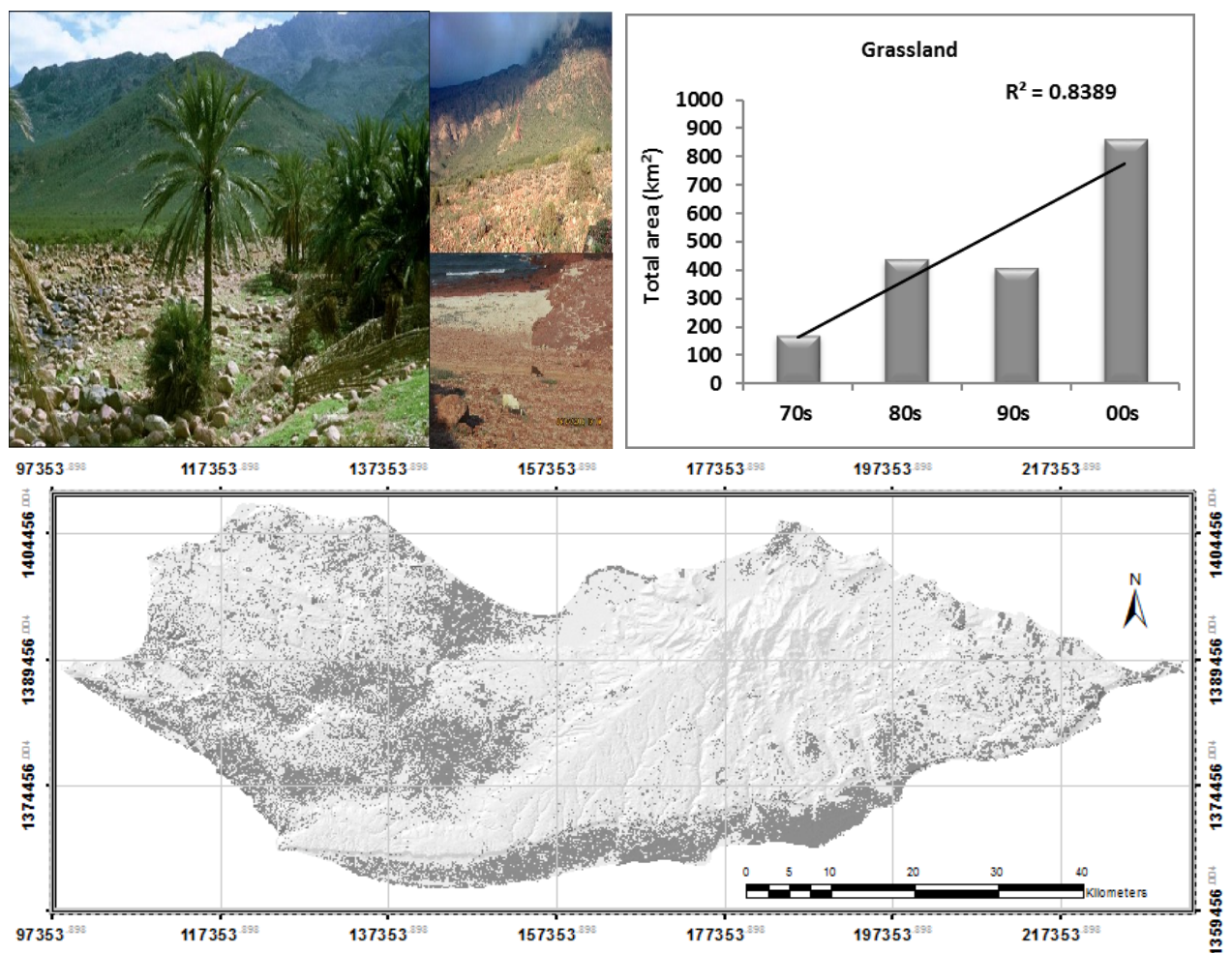


Figure 49: Spatial occurrence and temporal change in grassland.

## 6.2. Classification accuracy assessment

As we have discussed in chapter 4, the accuracy of the classification is sensitive and highly dependent on to the sampling design and the ground truth data collection as well as the post classification process. The high heterogeneity of between pixels' value in our study area might result of the interaction of climatic (e.g. drought) and disturbance factors (such as grazing) with complex topographical and geomorphological patterns, which produce different communities

and vegetation mosaic types. Our extrapolated vegetation cover maps are not argued to be without errors and therefore, some facts have to be considered: Despite cloud masking, refined gap filling and topographic and atmospheric corrections, vegetation in the central mountains and very deep undulating hillslopes zones which are dominated by perennials might behave differently as compared to the vegetation in the eastern and southern relatively flatted areas in the island. Similar vegetation type may receive different amount of annual rainfall across the island, partially due to the two monsoon periods mentioned in chapter 5. Moreover, the growing season phenology (which we defined from October to early March) can differ in starting date and might fail in some years in which the plant growth is inhibited with low density of leaves, causing decreased biomass accordingly. Moreover, sampling errors and processing uncertainties are usual errors associated to satellite data processing due to gaps in temporal data and difficult adaptation to satellite data period.

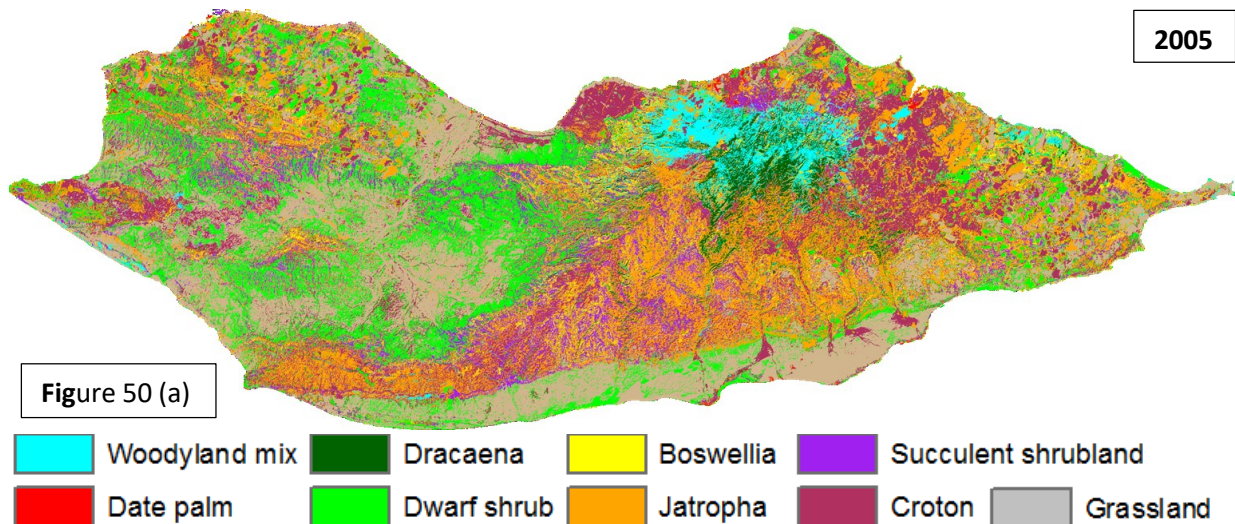
Thus, we used a broad classification scheme to ensure highly accurate individual classifications. These broad classes also might reduce the effects of variations of soil conditions and sparsity of the vegetation, which might have caused problems if we had been aimed a detailed classification scheme to detect the changes. In addition, a simple accuracy assessment was carried out comparing our final vegetation cover classes with other findings results and with our intensive field training references evaluation. We used the knowledge derived in 2005 by (Kral and Pavliš, 2006) on classified land cover in which he illustrated results of 22 terrestrial land cover mapping classes with sufficient spatial and thematic accuracy (overall accuracy estimated about 80%). We also compared the twenty-eight classes which were mapped by (De Sanctis et al., 2013), with an accuracy of 87%, using RapidEye image with 5 m pixel resolution and applying Gaussian mixture distribution model with sequential maximum a posteriori (SMAP) classification. Those studies were also useful to differentiate between some pixels of similar reflectance. Under the stronger evidence for the hypothesis described in chapter (4) assuming there are no apparently sudden decline in the whole vegetation along with assumption that vegetation species are normally in equilibrium with climate the training process then repeated for each year's image. The training process with more than 600 reference field locations was used to refine our classes and was repeated for each year's image. Moreover, the digitized training sites for each image were kept relatively consistent in regards to polygon sizing and placement and, therefore, all features considered to be similar were clumped together into the same class.

A comparison between the four classified images of 1972 Dec 16, 1984 Dec 2, 1994 Nov 28 and finally 2005 Dec 20 was performed in a pixel by pixel manner to detect the change from a certain class to another.

Our results produce maps with moderately high classification accuracy. The common practice confusion matrix was computed to assess the basic accuracy measures such as producer's and user's accuracy as well as overall accuracy (Congalton and Green, 2008, Biging et al., 1999, Vibhute et al., 2016).

In study area, the main sources of error were confusion between low density mixed woodland, grassland, succulent shrubs, *Jatropha* and *Croton*, as well as confusion between low and high density *Dracaena* and *Boswellia* lands. The confusion matrix of vegetation cover types using field observations showed that the overall accuracy of our classification was 90 %, 77%, 70%

and 73% for the classified images of the years 2005 (00s), 1994 (90s), 1984 (80s) and 1972 (70s), respectively, with an overall Kappa statistic of 0.89, 0.73, 0.65 and 0.68, respectively. User's and producer's accuracies of particular classes are listed in Table 14a-d, Figures 50a-d show the corresponding distribution on the island. User's accuracies for the 00s decade ranged from 80% for *Jatropha* to 100% for date palms and producer's accuracies ranged from 81% for dwarf shrubs to 100% for date palms.



		2005										Reference Data	
Classification Data	Classes	Mw	Dp	Bo	Dr	DS	Ja	Ss	Cr	Gr	Total	User's Accuracy %	
	Mw	107	0	3	2	0	1	2	0	0	115	93	
	Dp	0	24	0	0	0	0	0	0	0	24	100	
	Bo	0	0	85	0	1	0	5	0	0	91	93	
	Dr	0	0	0	56	0	0	0	0	0	56	100	
	DS	0	0	0	0	39	0	1	0	3	43	91	
	Ja	2	0	2	3	1	66	4	4	1	83	80	
	Ss	0	0	0	0	2	4	67	4	0	77	87	
	Cr	2	0	4	0	3	7	0	112	0	128	89	
	Gr	0	0	1	0	2	1	2	0	52	58	90	
<b>Total</b>	111	24	95	61	48	79	81	120	56	675	-		
<b>Producer's Accuracy</b>		96	100	90	92	81	84	83	93	93	-	90	

Table 14a. Confusion error matrix for the classification of the Landsat TM 2005 image using a stratified random sample of points over the study area, showing users and producers accuracy. (**Mw** = mixed woodland, **Dp** = date palms, **Bo** = Boswellia, **Dr** = Dracaena, **Ds** = dwarf shrubland, **Ja** = Jatropha, **Ss** = succulent shrubland, **Cr** = Croton, **Gr** = grassland)

The overall Classification Accuracy is 91%, the corresponding overall Kappa Statistics is 0.886, which demonstrates the excellent quality of classification (according to (Landis and Koch, 1977b, Helmer et al., 2008) as well as (Gwet, 2002, De Klerk et al., Bencherif et al.).

With the aim of evaluating the correctness of the classification mapping results for the particular classes by means of the following mentioned accuracies indicators for each class in

the four decades, we can find some indispensable misclassifications. These misclassifications mostly evolve particularly between spectrally similar classes, e.g. some of dwarf shrublands was often mistaken as grassland. This can be understood since people still use natural materials and dry wood in building their houses and fences which in fact might be spectrally identical with surroundings.

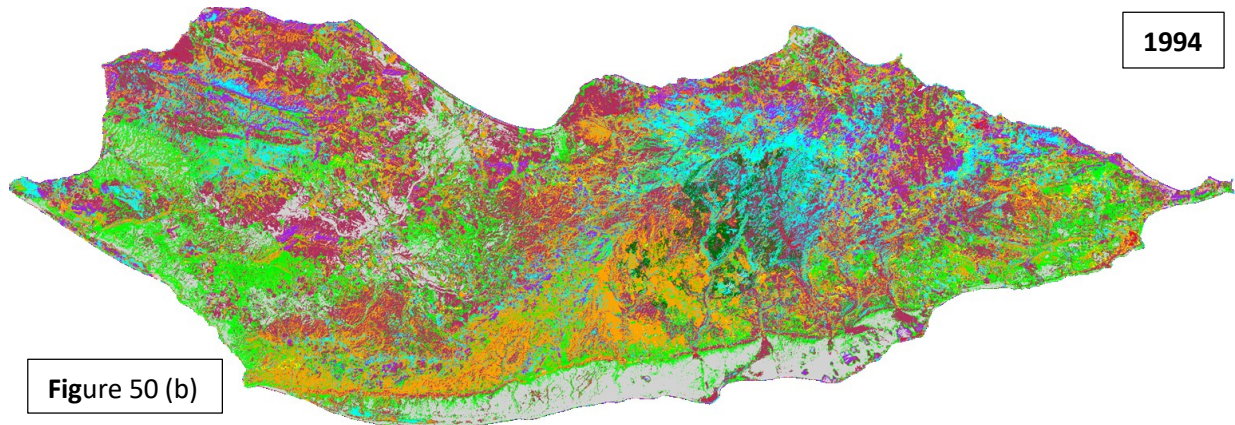


Figure 50 (b)

1994		Reference Data									Total	User's Accuracy %
Classes	Mw	Dp	Bo	Dr	DS	Ja	Ss	Cr	Gr			
Classification Data	Mw	103	1	0	6	0	1	8	5	1	125	82
	Dp	0	18	0	0	0	0	0	0	0	18	100
	Bo	0	0	78	0	0	0	1	0	0	79	99
	Dr	1	0	0	49	0	2	2	0	2	56	88
	DS	0	1	1	0	39	1	3	0	7	52	75
	Ja	4	2	2	2	3	65	8	9	14	109	60
	Ss	0	1	13	0	0	1	40	0	3	58	69
	Cr	3	1	1	4	6	9	19	106	9	158	67
	Gr	0	0	0	0	0	0	0	0	20	20	100
<b>Total</b>	111	24	95	61	48	79	81	120	56	<b>675</b>	-	
<b>Producer's % Accuracy</b>	<b>93</b>	<b>75</b>	<b>82</b>	<b>80</b>	<b>81</b>	<b>82</b>	<b>49</b>	<b>88</b>	<b>36</b>	-	<b>77</b>	

Table 14b. Confusion matrix for the classification of Landsat TM 1994 image (for details see Table 14a).

The overall Classification Accuracy is 77%, the corresponding overall Kappa Statistics is 0.731, which is still very good.

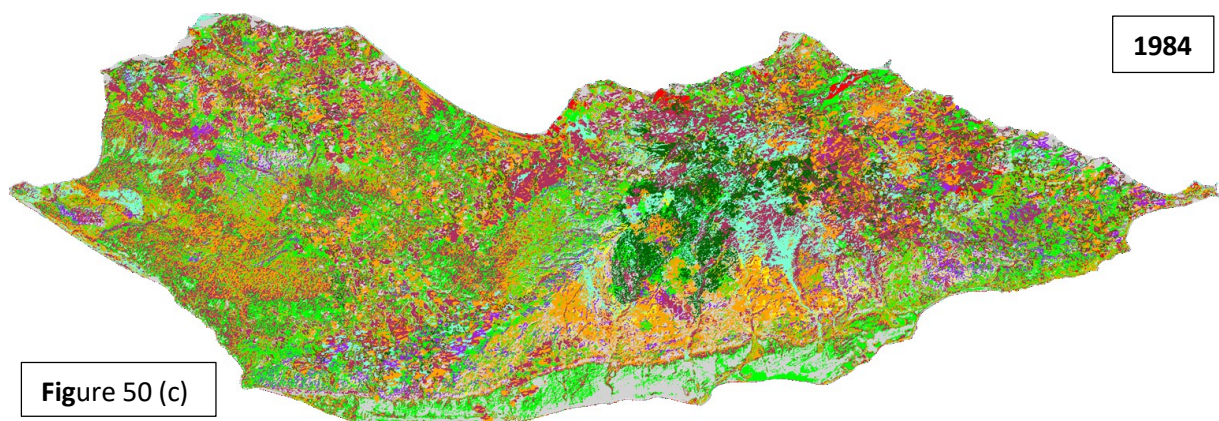


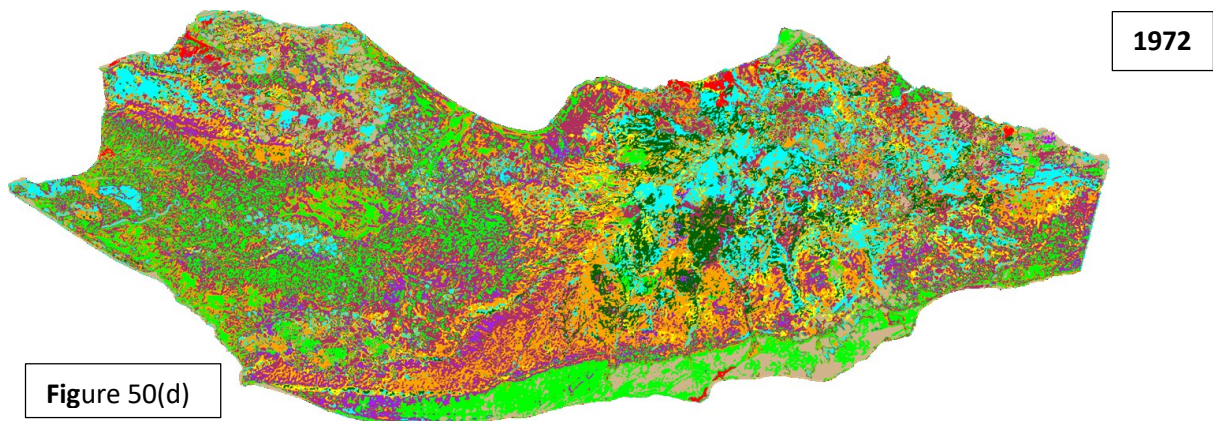
Figure 50 (c)



1984		Reference Data										
Classification Data	Classes	Mw	Dp	Bo	Dr	DS	Ja	Ss	Cr	Gr	Total	User's Accuracy %
	Mw	87	2	11	4	3	9	7	9	2	134	65
	Dp	0	16	1	0	0	0	0	0	0	17	94
	Bo	0	0	56	0	0	1	0	0	0	57	98
	Dr	5	0	7	57	1	1	5	4	1	81	70
	DS	0	1	0	0	31	6	4	3	6	51	61
	Ja	4	2	8	0	4	56	9	16	3	102	55
	Ss	2	0	4	0	0	0	47	0	2	55	86
	Cr	13	2	8	0	9	6	7	88	8	141	62
	Gr	0	1	0	0	0	0	2	0	34	37	92
<b>Total</b>	111	24	95	61	48	79	81	120	56	675	-	
<b>Producer's Accuracy (%)</b>	78	67	59	93	65	71	58	73	61	-	70	

Table 14c. Confusion matrix for the classification of Landsat TM 1984 image (for details see Table 14a).

The overall Classification Accuracy is 70%, the corresponding overall Kappa Statistics is 0.654, which is good.



1972		Reference Data										
Classification Data	Class	Mw	Dp	Bo	Dr	DS	Ja	Ss	Cr	Gr	Total	User's Accuracy %
	Mw	86	0	1	3	2	1	8	6	8	115	75
	Dp	0	20	0	0	0	0	0	0	0	20	100
	Bo	1	0	88	0	0	1	2	0	4	96	92
	Dr	11	0	0	54	0	3	9	7	4	88	61
	DS	0	0	0	0	37	0	7	0	2	46	80
	Ja	8	2	2	2	5	72	11	4	11	117	62
	Ss	0	0	3	0	1	0	20	3	0	27	74
	Cr	5	2	1	2	3	2	24	100	14	153	65
	Gr	0	0	0	0	0	0	0	0	13	13	100
<b>Total</b>	111	24	95	61	48	79	81	120	56	675	-	
<b>Producer's Accuracy (%)</b>	78	88	93	89	77	91	25	84	23	-	73	

Table 14d. Confusion matrix for the classification of Landsat TM 1972 image (for details see Table 14a).

Figure 50 a-d: Terrestrial vegetation cover maps for the period 1972 – 2005 derived from image classification. (a) December 2005 (b) November 1994. (c) December 1984. (d). December 1972.

The overall classification accuracy for 1972 is 73%, the corresponding overall Kappa Statistics is 0.684, which proves that the classification is good. The Kappa statistics for comparison of given vegetation classes between two maps clearly indicated some differences as well as many similarities between maps. Therefore, with reference to the findings by (Landis and Koch, 1977b, Helmer et al., 2008), Kappa coefficient measures of agreement between 0.6 and 0.8 are considered “substantial”, while kappa values above 0.8 are called “almost perfect”. The approach in this study of detailed mapping of vegetation cover was in overall successful for mapping the nine (Bryant et al.) classes in the island as described above. The results from overall accuracy of the error matrices indicate relatively good agreement between the classifications results and the field observations. However, certain components obtained higher scores than others. *Jatropha* and *Croton* which are represented the major component both in the truth data and in the classification between 1972 and 2005 were particularly well classified with a producer’s accuracy over 70% and user’s accuracy of over 60%. On the other hand, confusions remained with respect to dwarf shrubs and grassland particularly with sparse vegetated areas. As far as grasslands is concerned, the degree of producer’s accuracy was unsatisfactory from 23% to 93%, depending on the period, representing a deficit error mainly with respect to most class types. Although better, the producer’s user’s accuracy and for succulent shrubs was still around average (around 25–87%), representing a deficit or excess error mainly with respect to *Dracaena* and *Boswellia* classes. Those confusions underline the difficulties involved in accurately discriminating areas, in which we decided that more than a 70% threshold must be included to properly categorize the class types. For instance, sparse vegetation in the sample could in reality represent a gradient from bare soils to fairly dense vegetation cover (herbaceous species, built-up area, wetland, etc.) depending on the season in which the image was acquired. Without recourse to seasonal multi-date monitoring, more precise discrimination appears to be difficult at this scale. Grouping the two classes (bare soils and very sparse vegetation) into one enabled us to increase the overall accuracy scores for the three periods concerned.

### **6.3. Analysis of vegetation cover:**

The pixel values for each classified image were introduced into Microsoft Excel 2013 and SPSS in which it was used to handle all the statistical functions such as converting areas into square kilometre (km<sup>2</sup>) using the formula below as well as calculating the percentage values and plotting the graphs and histograms for analysis and interpretations:

$$(number\ of\ pixels\ in\ a\ given\ class) * 900 / 1000000,$$

where 900 is the area of each pixel in square meters, and 1000000 is the converting number into km<sup>2</sup>.

Some vegetation cover types, including the dwarf shrubs, *Dracaena* and *Croton* ecosystems, have declined steadily, while changes in other vegetation cover types have been slowed during certain times or were even temporarily reversed, such as in the case of the *Boswellia* and *Jatropha* areas. Grassland comprises bare areas expanded particularly in the plateaus and coastal zones among the western and southern parts of the island, and has more than doubled

since the 70s with a particular strong increase after 90s (Fig. 51). Among others habitat conversions were observed from mixed woodland to shrublands and from shrublands and dwarf shrubs to bush/shrublands colonized by encroaching plants. The area of *Dracaena* has substantially decreased from 70s to 00s while succulent shrubs and grassland areas increased. Dwarf shrubs and *Jatropha* areas remained relatively intact between 1972 and 2005, with some encroachment by succulent species and grassland along the coastal zone, hillslopes and the plateaus. However, the periods between 80s and 90s saw a massive decline in the *Dracaena* and *Boswellia* areas where it reduced by 22% of its 80s extent (Table 15).

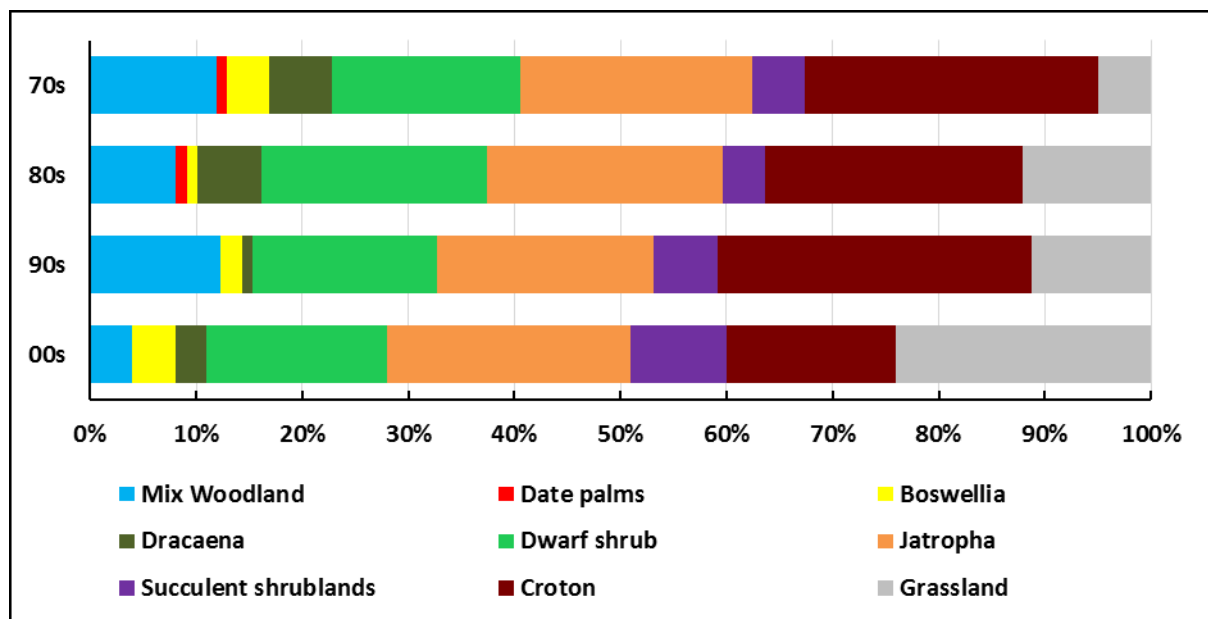


Figure 51: Visualization of the magnitude of vegetation change between the four decades from the 70s (top bar) to the 00s.

Veg. Cover	70s (km <sup>2</sup> )	% of veg. 70s	80s (km <sup>2</sup> )	% of veg. 80s	90s (km <sup>2</sup> )	% of veg. 90s	00s (km <sup>2</sup> )	% of veg. 00s	Ave %
Mixed woodland	419	12	303	8	436	12	132	4	9
Date palms	21	1	49	1	11	0	9	0	1
<i>Boswellia</i>	151	4	37	1	80	2	152	4	3
<i>Dracaena</i>	226	6	211	6	47	1	113	3	4
Dwarf shrub	646	18	757	21	624	17	627	17	18
<i>Jatropha</i>	765	22	807	22	731	20	820	23	22
Succulent shrublands	165	5	153	4	226	6	326	9	6
<i>Croton</i>	981	28	851	24	1045	29	563	16	24
Grassland	175	5	439	12	407	11	849	24	13

Table 15. Absolute area and proportions of vegetation cover for each of the nine classes for the four decades from 70s to 00s.

#### 6.4. Trend of vegetation change derived from classification

The classified maps dated to the 70s, 80s, 90s and 00s were compared to each other using the logical operations to detect the change from a certain class to another resulting in the classified change reference map as previously shown in (Fig. 51 and Table 16). A comparison between

the four classified images representing four subsequent decades was performed in a pixel by pixel manner. The overall trend in vegetation change for the study period was determined based on the series of the integrated classification images in the growing seasons by fitting simple linear regression estimation (dependent variable Area occupied by vegetation classes; independent variable decades time). Since a rough estimate of the size and direction of change was sought, we assumed for simplicity an equidistant spacing in time (70s, 80s,90s, 00s). Percent of change for time periods was estimated. Once the final thematic is determined, the pixel values for each image are input into Excel and SPSS for further statistical analysis and determine the trend among the decade's images.

**Estimation of changes since the 1970s**

Analysis of vegetation cover changes since the 1970s revealed diverse changes. Therefore, we used the following formula to calculate the percent of relative changes;

$$\text{Percent Change} = \frac{\text{Final value} - \text{initial value}}{\text{initial value}} * 100$$

If the result is negative, then this is a percentage decrease (of Table 16).

As far as the whole island is concerned, the expanse of urban areas, bare land and grassland areas with incipient of sparse vegetation and bare soils (class 9) more than doubled between 1973 and 1984 and continued expanding, until it reached more than 800 km<sup>2</sup> (+395%) in 2005 (Tab. 16). This is mainly due to recession of other vegetation types, such as woodland areas and *Croton* shrubs with expansion of built-up areas, the new development constructions as well as the fluctuation of rainfall and drought periods. Succulent shrubs showed a massive increase between 1984 and 2005 with almost (+97%). However, many species of this class have medicinal importance and are consumed by medical plants trading. On the contrary, *Croton* shrubs have decreased between 1972 and 2005 by 43%, whereas woodland areas appear to have decreased by 68% during the same period. *Boswellia* seems to have progressed regularly between the three periods. Nevertheless, it experienced a large decrease in the 70s and revived during the period 80s and 90s to reach nearly the 70s level again by 2005.

Vegetation Cover	70s to 80s	80s to 90s	90s to 00s	70s to 00s	R <sup>2</sup>
Mixed woodland	-28	44	-70	-68	0.45
Date palms	141	-77	-20	-56	0.25
Boswellia	-76	118	90	1	0.01
Dracaena	-7	-78	143	-50	0.59
Dwarf shrub	17	-18	0.41	-3	0.15
Jatropha	6	-10	12	8	0.07
Succulent shrub	-7	48	44	97	0.82
Croton	-13	23	-46	-43	0.52
Grassland	151	-7	109	386	0.84

Table 16. Absolut percent changes in vegetation areas between decades for the nine vegetation types. Decreased values are in brown colour and increased are in green.

The proportion of *Jatropha* remained nearly constant over time. The rate of the changes appears to have been more rapid between 90s and 00s, even if we consider that between 80s and 90s some changes had opposite directions.

### 6.5. Detailed analysis of vegetation dynamic in the ecological zones

Figure 52 shows local changes for the six typical ecological zones along the bioclimatic gradient in Socotra (see chapter 2). The central mountains area is known as steady limo Granite Mountains configuration (middle in the map) classified as montane mosaic of evergreen woodland to dense vegetation and, consist dwarf shrubs dominated by *Dracaena*, *Boswellia*, mixed woodland and *Croton* showed an overall 8.5% change between 1972 and 2005 in which an average of 24% decreased and 16% increase. The Wadies (valleys) showed slight variations in mix woodland, *Jatropha* and *Croton* with smoothly increase bare areas and sparse open vegetation surfaces, whereas dwarf and succulent shrubs areas increased, especially after 1994. High plateau exhibit typical karst features with some large areas of bare pavements, shallow soils, gullies and cliffs. It underwent to huge proportional increases in grasslands (class 9) and succulent shrubs (class7) while dwarf shrublands, *Jatropha* and *Croton* have steadily gradual changes, with an extension of the anthropic zones grow around the villages. Mixed woodland showed however; in one hand flexible increase during 70s, 80s and 90s, and in the other hand abruptly decreased in the 00s in the Low plateau with a growth of the anthropic zone grows around the villages and new houses, the consequence of this extension is the increase of the bare soils, sparse vegetation, grassland and dwarf shrublands classes. The Hillslopes showed slight variations in *Jatropha* shrubs with increase in the succulent shrubs and grassland after 90s, whereas the *Boswellia* and *Dracaena* was subjected to smoothly reviving increased after 90s. However, bare areas and sparse open vegetation and grasslands surfaces also increased with a corresponding decrease of Dwarf and *Croton* shrubs areas. Along the coastal plains, various distinctive formation and sharply ecosystems zone can be distinguished comprise of adapted perennial saline habitat predominated by succulents and dwarf shrubs, and therefore, capable of growing in sandy and saline soils. Likewise, (Ghazanfar and Fisher, 2013, De Sanctis et al., 2013) argued that, this sort of arrange zonation and species composition of these formations might depends on several factors, such as, soil type and texture, fertility components, availability of water holding capacity in the soil, latitude and the sea level tidal effects and also the distance from the shore. Proportion of vegetation cover in each eco-zone during the period 1972 – 2005 observed from the satellite interpretation presented in (Fig. 53). The vegetation in this zone are characterized as a dynamic interactive associated with *Croton* shrubland, dwarf shrubland and grasslands, according to the level of disturbance. Scattered *Boswellia* and Mixed woodland can be also found. The woodland, date palms, dwarf shrubs and *Jatropha* in this zone decreased with increase of bare areas and grasslands. As can be seen in the more or less vegetation in this zone experienced overall decreased specially after 90s with exceptional to grassland.

This bears witness that, the harsh and very limiting environmental conditions, with more intensive pressure on the vegetation from the centre to the north to south and around of the village, mainly for urban development, new agriculture and grazing practices, and farming systems socioeconomic practicing.

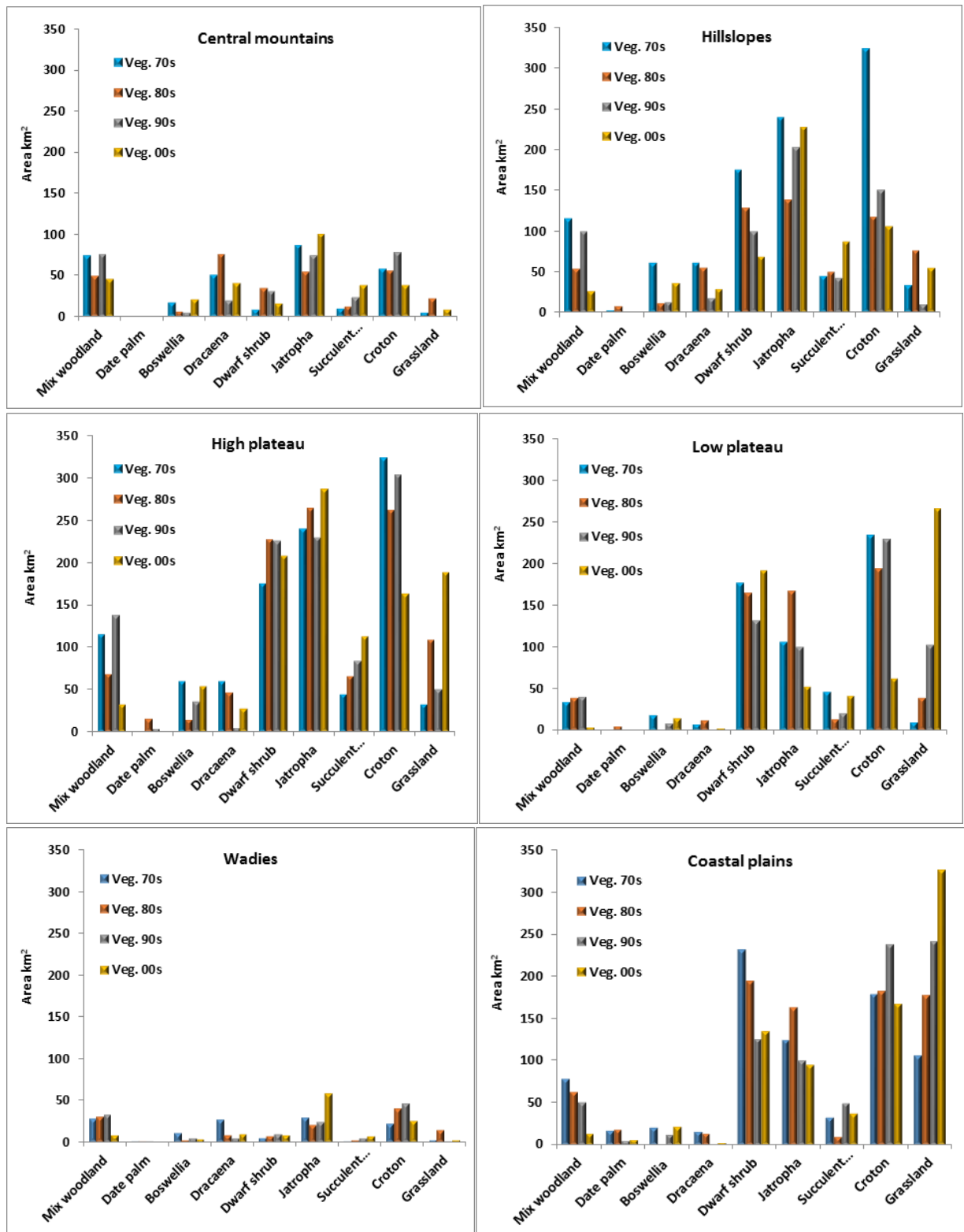


Figure 52: Dynamic of vegetation changed during study period in each ecological zone.

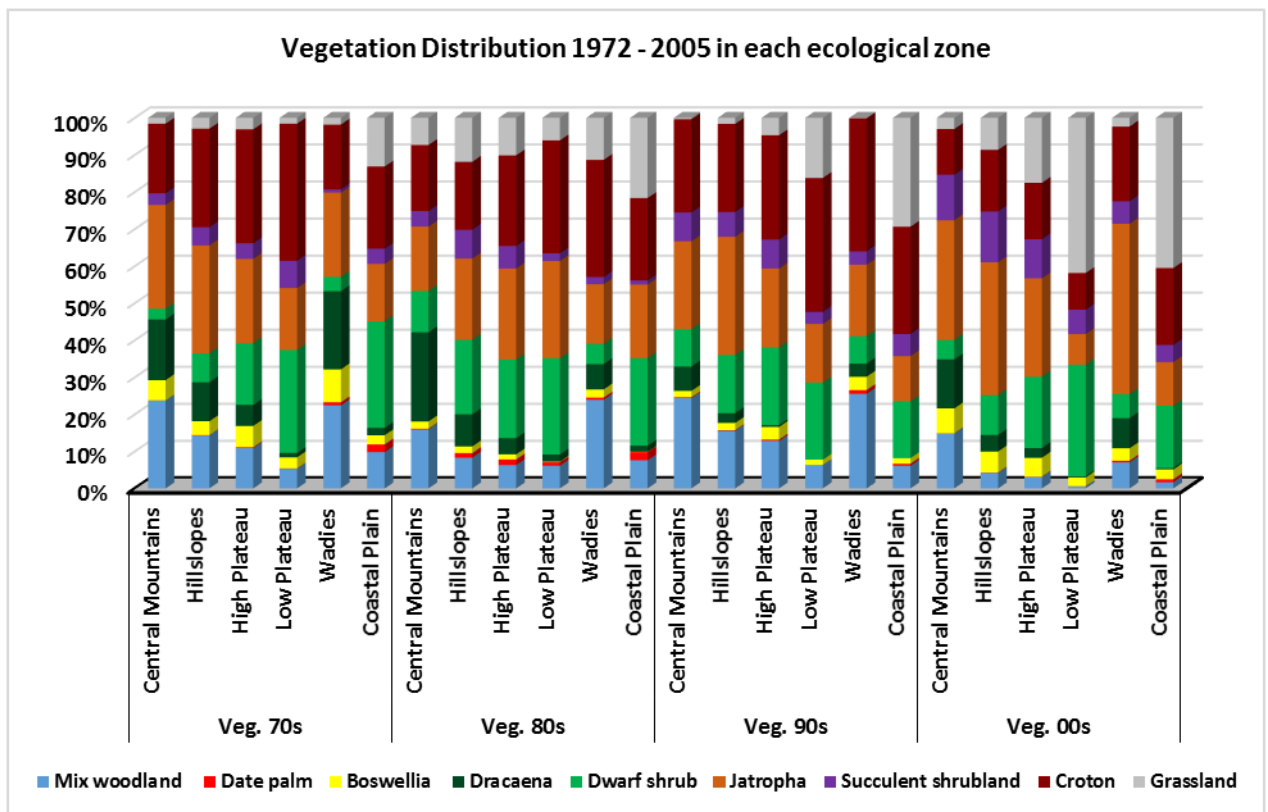


Figure 53: Proportion of vegetation cover in each eco-zone during the period 1972 – 2005 observation from the satellite interpretation.

Vegetation cover in the arid regions are characterised by many authors as rainfall drift growth and therefore have strongly seasonal changes. As it has been discussed in the previous chapters, the climate in the region follows a typical rainfall pattern, with the rainy season generally starting in early November and ending late February, despite large annual vibrations. Therefore, the period from November to March is usually the best growing season for green plants in the island in which we obtained the greater average rates of vegetation cover in TM images during these times. While during the dry season (generally from end of May to October), the most of the island plants gradually go into dormancy, due to a lack of water. Figure 54 looking at the same data above but is articulating different message in which indicates the proportion of changes in each eco-zone of vegetation from 1972 to 2005 was vary. Most of the vegetation was markedly shown decrease in the coastal and low plateau zones. However, other vegetation cover is varied per eco-zone While the mix wood was the most vegetation class shows range of decrease from (-34%) in the central zone to almost (-80%) at the coastal areas.

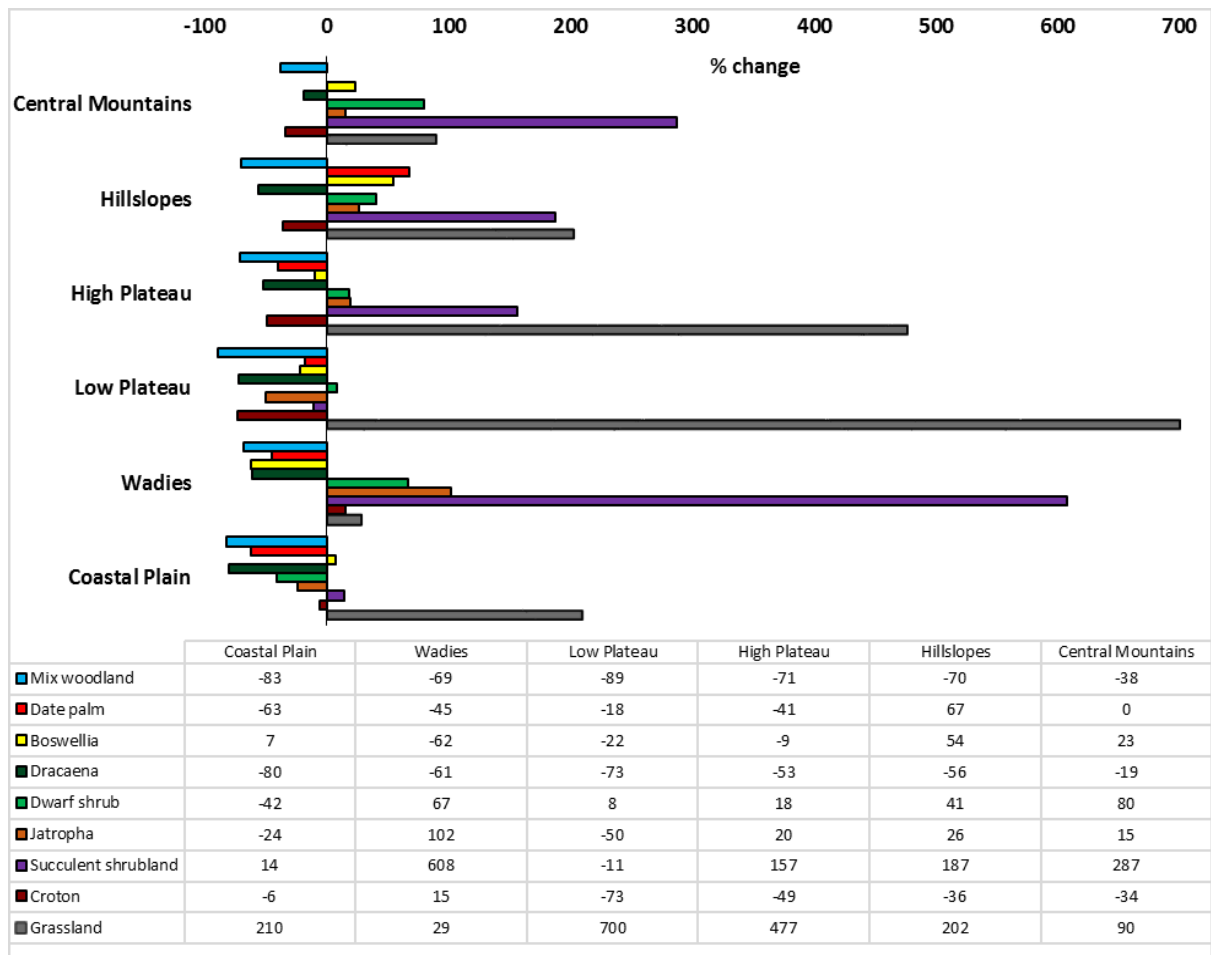


Figure 54: change percentage in each eco-zone of vegetation between 70s and 00s.

### 6.6. Direction of vegetation changes

Monitoring the extent of undergoing changes in each vegetation class with the intention to investigate which pixels have changed from certain class to another or any other transition class been reported by many authors (Alberti, 2005, Townshend et al., 1992 and Mithal et al., 2013) as a critical due to its strong need for accurate, timely, and regularly updated extent and dynamics.

Remote sensing classifier with the training samples are able to assign a vegetation cover class from a finite set of classes to every pixel, based on its observed spectral values (the feature space). Thus, every pixel is assigned a sequence of vegetation class labels corresponding to the time period of image collection. In this context, we explored the use of temporal sequences of class labelled for improving vegetation cover classification and identify trend direction within each class. However, to avoid misleading results, which might occur in pixels contain two or more vegetation cover class in our analysis we identify pixels that belong to class from sequences of only more than 70% vegetation class labels. However, it is important to note that our approach identify mixed pixels and does not provide the exact proportion of pure classes in the pixel. Given temporal classification results, 70s, 80s, 90s, and 00s, one can create a change map for any pair of time steps (T1; T2). In particular, we can show however, the type of improvement in both changes of negatives and positives prospective in the previous section. We used cross-tabulation in Arc map for detecting change as a pixel by pixel comparison



between two layers representing the same data for a study area at different decade's times. Table 17 shows the multi temporal detecting changes in each vegetation type between the years 1972 and 2005 as representative of these time decades.

Classes	Mw	Dp	Bo	Dr	Ds	Ja	Ss	Cr	Gr
Mw	14	1	1	14	14	22	3	25	5
Dp	9	6	0	5	15	24	1	23	16
Bo	10	1	2	8	16	25	5	22	10
Dr	15	1	2	23	7	19	2	25	5
Ds	3	1	0	2	28	29	3	21	14
Ja	6	1	1	6	18	29	6	23	10
Ss	3	1	0	3	28	29	5	23	7
Cr	5	1	0	4	22	32	6	23	6
Gr	4	1	0	3	22	15	2	16	38

**a**

Classes	Mw	Dp	Bo	Dr	Ds	Ja	Ss	Cr	Gr
Mw	15	0	3	13	10	33	8	11	6
Dp	11	2	4	5	9	34	6	22	7
Bo	5	0	4	4	10	40	10	19	9
Dr	5	0	3	19	1	49	9	13	1
Ds	1	0	2	2	21	22	12	12	28
Ja	2	0	4	2	12	40	15	16	10
Ss	5	1	9	4	11	33	12	16	10
Cr	2	0	1	2	22	25	7	22	20
Gr	0	0	0	0	14	3	1	4	79

**c**

Classes	Mw	Dp	Bo	Dr	Ds	Ja	Ss	Cr	Gr
Mw	19	1	2	5	9	22	8	31	3
Dp	8	1	3	0	15	24	12	33	4
Bo	14	0	2	4	9	35	4	32	0
Dr	19	0	3	11	10	25	8	24	1
Ds	6	0	2	0	20	23	6	27	16
Ja	7	0	2	1	20	25	6	33	6
Ss	8	0	2	0	20	44	9	16	1
Cr	11	0	2	1	18	22	8	29	9
Gr	6	0	2	1	13	23	6	19	30

**b**

Classes	Mw	Dp	Bo	Dr	Ds	Ja	Ss	Cr	Gr
Mw	8	0	4	8	10	38	8	16	7
Dp	6	12	4	2	10	18	8	31	9
Bo	2	0	4	3	13	45	11	17	5
Dr	11	0	3	12	4	51	6	10	1
Ds	1	0	1	1	22	12	7	12	44
Ja	2	0	3	3	13	33	14	16	16
Ss	1	0	1	1	19	22	11	14	30
Cr	2	0	2	2	19	24	11	18	22
Gr	1	0	2	1	18	15	4	9	48

**d**

Table 17. Multi-temporal context-based classification, identify pixels that changed from certain class to another (between time t1 and t2). The column represents the percentage areas for the period t2 and the rows represent the percentage areas in t1. (a) is 70s to 80s, (b) is %80s to 90s %, (c) is 90s to 00s and (d) is the overall from 70s to 00s.

Those matrixes illustrate the progressive decrease in the vegetation class types and replacement with new or previously less dominant vegetation cover types. The diagonal axis represents areas that have no changed during study period. However, the overall similarities agreement (Total diagonal/Total area) was vary range from 23% to 30% in which reflect the magnitude of change almost 80% to 70%. This can be figure out as some vegetation types have grown by replacing others. On the other hand, it can be also understood as we observed during the fieldwork a domination of some species due to deterioration of others. Results shows the mixed woodland, *Dracaena* and *Boswellia* areas were largely superseded by *Jatropha*, dwarf and succulent shrubs and open shrublands particularly after 90s. Some cultivated land expanded particularly date palms in the Wadies (Valleys), the western and southern parts of the island, and has in 80s more than doubled since the 70s. In addition to expansion of the succulent shrubs, woody species have become dominant in many of the grass and shrub lands, likely as a result of over grazing by domestic animals. The most dramatic reduction in vegetation cover was seen in *Croton* which declined from previously about 981km<sup>2</sup> in 1972 to about 563km<sup>2</sup> in the 2005 (Table 15).

## Conclusion

The magnitude of changes detecting reported in this section using image classification techniques is consistent with the greening trend in NDVI in the early sections. Our classification results indicate an average of the vegetation areas in the island have prospective both negatively and positively significantly changes during the growing season between 1972 and 2005. All vegetated pixels exhibited statistically significant positive trends were approximately (20%) and exhibited relatively strong correlation more than ( $r=0.4$ ) in growing season. Areas with negative trends in growing season were also calculated and measured. The percentage of these areas was (-24%). The classification results showed the area of *Dracaena* has substantial decreased from 70s to 00s while Succulent shrubs areas increased. Dwarf shrubs and *Jatropha* areas remained relatively intact between 1972 and 2005, with some encroachment by succulent species and grassland along the coastal zone, hillslopes and the plateaus. However, the periods between 80s and 90s saw a massive decline in the *Dracaena* and *Boswellia* areas where it reduced by 22 % of its 80s extent. Therefore, this percentage of area with trends in growing season was varied significantly according to vegetation cover type and the time period. It is particularly high for grassland and succulent shrubs in which above 90% of all pixels with the positive trend in growing season exhibited strong correlation ( $r^2 > 0.80$ ) between 70s and 00s. Mixed woodland experienced a dramatically decreased in their areas from 12 %, 8 %, 12, % and 4 % during 70s, 80s, 90s and 00s respectively, while grassland showed an increase by 5%, 12%, 11, and 24% for the same periods. However, succulent shrublands and grasslands were observed as the most expanded vegetation classes through all ecological zones. These classes were grown more than its double size particularly in the low and high plateaus. Apart from these classes change detection results show the coastal plain and low plateau were the most underwent areas with more than (-40%) averaged reduced followed by the high plateau with (-27%) whereas the central mountains and hillslopes zones were the least areas affected by change with only averaged (4%). Among all, *Boswellia*, mixed woodland and date palms were the most affected whereas, *Jatropha*, succulent shrubs and grassland were the most increased during the period 70s to 00s. Despite the harsh climate condition, the peripheral location of the islands and the strong traditional land use management practiced employed by the indigenous population, have both served played a significant role in the past to protect the vegetation and biodiversity of the Island.

## **Chapter 7: Detection of climate and human-induced vegetation change**

Vegetation cover is one of the major components of an ecosystem and very sensitive to changes of environmental factors. In our case, the main external influences are rainfall variability and human impact which are usually not constant over time. Socotra Island is located in the semiarid zone, where the rainfall is reported as the dominant natural factor which limits vegetation growth, especially in the growing seasons. Additionally, temperature, solar radiation and evaporation do have influence on vegetation, but due to (Li et al., 2008, Balakrishnaiah et al., 2016) they actually do not play primary roles in arid and semiarid zones, because, contrary to rainfall, their seasonal pattern is rather predictable. Other natural factors such as soil type, topography and landform do not change much on a decadal scale and thus their impacts can be neglect at least for the purpose of this study.

Owing to remote sensing techniques it is possible to monitor vegetation status during relatively long time periods and to compare it with rainfall variability and irregularity in human influence. In order to simplify the analysis of the causes and trend of vegetation in our study, we only considered the rainfall as the major limiting factor severely affecting the vegetation and causing change during the growing periods. Evidences by (Richard and Pocard, 1998, Wang et al., 2008a, Tian et al., 2015) is that in many cases, rainfall variability was a driving force for trends in vegetation activity in the semiarid regions. Thus, modelling the vegetation dynamic with the dynamics of rainfall and human induced trend might theoretically help understanding the individual and the combined roles of both external factors on a long time scale. It has been reported in many studies that the effects climate change and anthropogenic influences are often closely interrelated and therefore, discrimination between their causes of change in vegetation is rather difficult and uncertain (Propastin et al., 2008). There are number of modern studies that tried to discriminate between these two factors. These studies have reported that time series NDVI is a successfully tool to indicate vegetation deterioration and observed land degradation (Weiss et al., 2004, Wessels et al., 2007, (Propastin et al., 2008), (Suepa et al., 2016, Qu et al., 2015, Zhou et al., 2015 and Miebach et al., 2016). utilized actual deviations from the regression between the time series of NDVI values and rainfall data in the past as an evidence for vegetation response to change. The regression curve can be understood as the climatic signal and deviations of the measured NDVI value from the value predicted by the regression are interpreted as an indication of vegetation response to climate change.

### **7.1. Effects of Human Activities in the island**

There are several studies which suspected increasing anthropogenic activity to be the major cause of vegetation deterioration in the island (Scholte et al., 2011, Malatesta et al., 2013). (Naumkin, 1993)), suggested that the South-Semitic nomadic tribes were the first inhabitants, coming to the island probably some 3000 years ago. They developed over many centuries a relatively balanced land management system, in order to secure self-sufficiency in food themselves. These traditional approach and nomadic herding patterns of use have evolved and strongly influenced the biodiversity of the island. These traditionally build-up indigenous knowledge in land use management practices employed by played a vital role in protecting against the over-exploitation of natural resources and the diminution of biodiversity during last

centuries. An obvious example of breakdown of the basic traditional rules can be perceived by cutting and removing of live trees for the present booming building on the island and consequently increasing pressure on all trees (Damme and Banfield, 2011 and Brown and Mies, 2012b), reported that the human disturbances have catastrophic impacts on the island ecosystems over short timescales. In the other words (Alexander and Miller, 1995) and (Morris, 2002) described collapsing of traditional land use practices in which have led to vegetation deterioration of the in the island since 1990s.

In consequence, the recent grazing practices, such as freely opened goat grazing practices increased livestock numbers and therefore lead to loss control on it spatially and temporally ((Morris, 2002) (Miller and Morris, 2004a). This situation is changing with practices have influenced plant communities and remarkably contributed to the current distribution and structure of plant populations all over the island, including endemic *Commiphora*, *Boswellia*, *Dendrosicyos socotranus* and *Dracaena cinnabari* (Král and Pavliš, 2006, Mies, 1993, Miller et al., 1996, Lisa M. Banfield et al., 2011). Nevertheless, (Král and Pavliš, 2006) argued that the incidence of *Croton* and *Jatropha* shrubs degradation were in one hand subjected to unfavorable dry tough winds and man-made biotopes and on the other hand those were influenced also by heavy overgrazing and wood collection. Moreover, results from (Cronk, 1992, Morris, 2002, Cheung et al., 2006 and Brown and Mies, 2012b) reveal that the island is under imminent real loss of biodiversity due to these major types of threats affecting the vegetation in the island and mentioned keys as: (1) the new infrastructure development (e.g. booming of the real estate, roads networks ... etc.), (2) overgrazing due to collapsing of traditional grazing practices and land management's rules, (3) invasion of exotic species and (4) climate changes. Those main threats are also mentioned in the IUCN report for Socotra's World Heritage Nomination (IUCN, 2008). Moreover, the island seems to be swept many times by natural disasters, the most recent was in December 2005, and at the end of 2015 by Tsunami and Chapala disasters causing damage to all natural resources in the island. However, areas facing significant demographic expansion are seen to be affected more strongly than others. Thus, the greatest impacts occurred in the vicinity of the main towns as well as the easy accessible areas along with new asphalt roads which expand the urbanization and increased human activity.

In chapter 5 we discussed the inter- and intra-seasonal relationships between NDVI and rainfall. Here we only will give concretization concerning the significant influential of rainfall and human-induced degradation in vegetation cover and examine the trends. This influential however, has been identified and quantified in the study area with the respect to the statistically relationship between NDVI and rainfall in order to help discrimination between the impact of these two major factors. The simple approach described in chapter 4 is based on the concept of synchronization between NDVI and the rainfall. Investigation results showed notable association trend over the study period 1972 – 2010 between NDVI and rainfall in each year (Fig. 55). Correlation coefficients between the (weighted) cumulated rainfall and the maximum NDVI at the scale of individual decades exhibited positive values which means generally improvement of vegetation cover in the study region driven by the higher rainfall. These investigation results are in agreement with the earlier published reports and finding results by Scholte and De Geest, 2010, Scholte and Miller et al. 2008 and (Miller and Morris,

2004a) in which they strongly linked the vegetation greenness in the island to soil moisture content and a function of rainfall accumulated over a period of time than to instantaneous rainfall. Even though some trends in rainfall factor were relatively weak and statistically not significant, they pointed into the same direction. Hence, rainfall may be considered to be the major driving force in the long-time change in vegetation cover (Fig. 55).

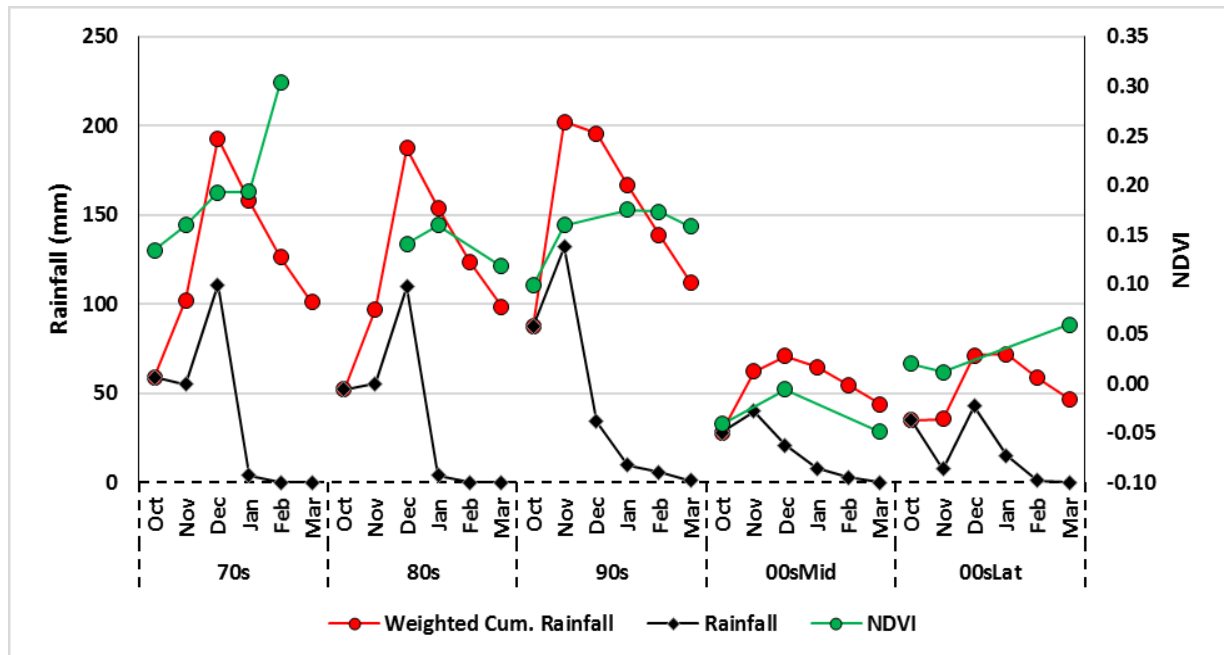
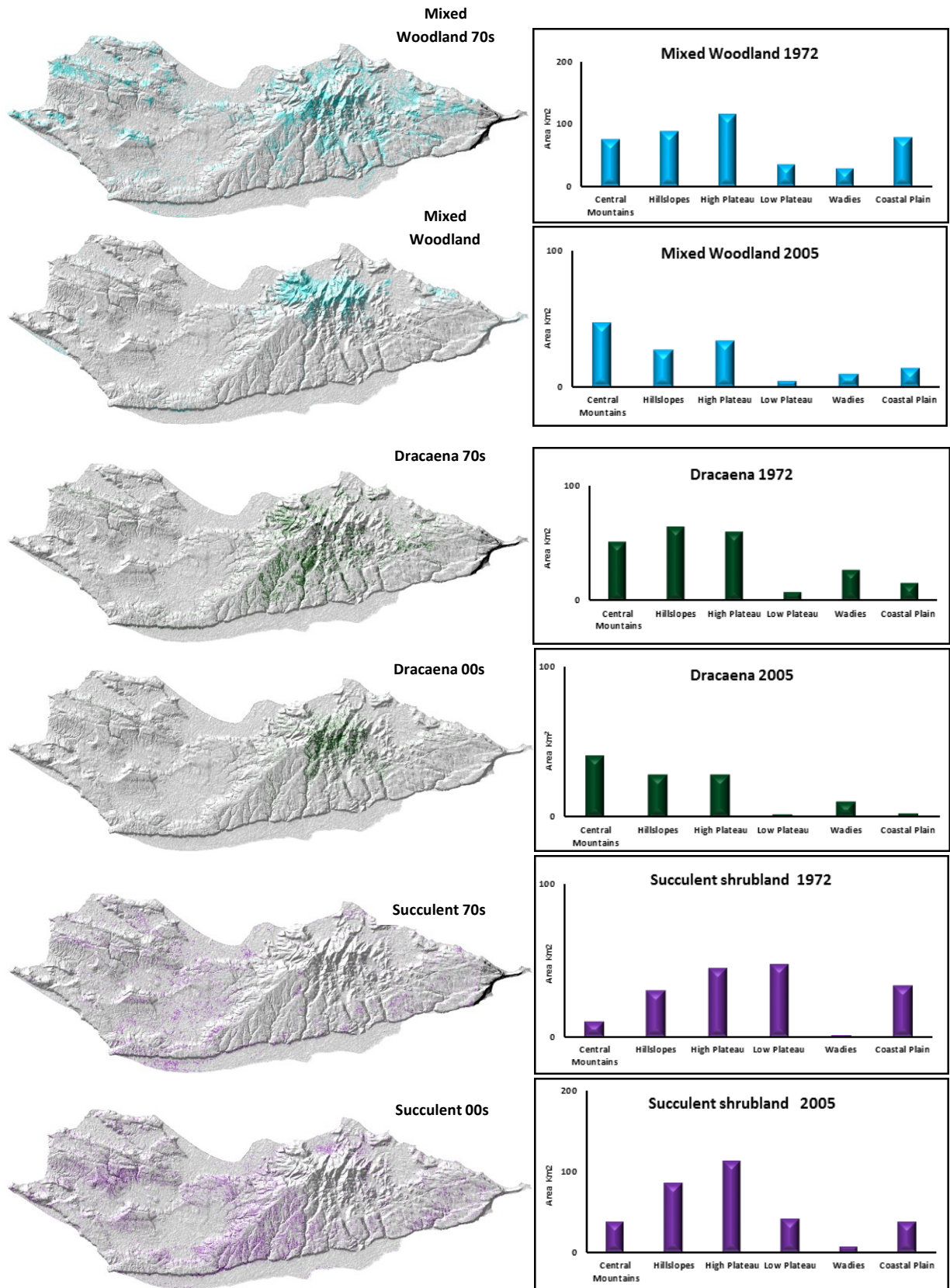


Fig. 55: The time-integrated NDVI for each growing season shows somehow to be closely correlated with rainfall and weighted cumulative rainfall.

The substantial decline of vegetation in the mid and late 2000 years is primarily a consequence of the much lower rainfall in these years and, therefore, a consequence of global climate change. However, as already shown in Fig. 33, the relation between NDVI and weighted cumulative rainfall traced over the different growing seasons is significantly different in the 2000 years if compared with 70s to 90s. This can only be interpreted as human influence in which a similar amount of rainfall provided to degraded areas allows only a lower growth of biomass. It can be seen as an indication that the situation on Socotra, although already heavily stressed by unfavourable climate change, has become even more worse through inappropriate land management and land use.

Our analysis of spatial vegetation cover during the last four decades revealed local changes of varying degrees of intensity. Results presented that mixed woodland, *Dracaena*, *Boswellia* and the date palms were the most decreased vegetation whereas, grassland, succulents and *Jatropha* shrubs were the types which mostly increased in area during the period 70s to 00s. The opposing increase in the extent of grassland and succulent shrubs is mostly concentrated in the northern plateaus and central part of the island, bearing witness to the intensification of grazing, urbanization and road networks construction, notably in the two main towns Hadebo and Alqalansiya. There was also a clear trend towards deforestation with a corresponding increase in woodland in the north and northeastern part of the island during the 90s, which has been also confirmed by colleagues at SCDP (personal communication). In agreed with (Brown and Mies, 2012b) the east and east-central part of the island, *Croton* and woodland appear to

have decreased with a corresponding increase in succulent shrublands. Elsewhere, any 'drifts' from one class to another (clearing or renewal) have tended to balance out between the periods and consequently do not always appear as clear logical tendencies. Fig. 56, below demonstrates the spatial distribution of decrease or increase for some of those mostly affected vegetation types.



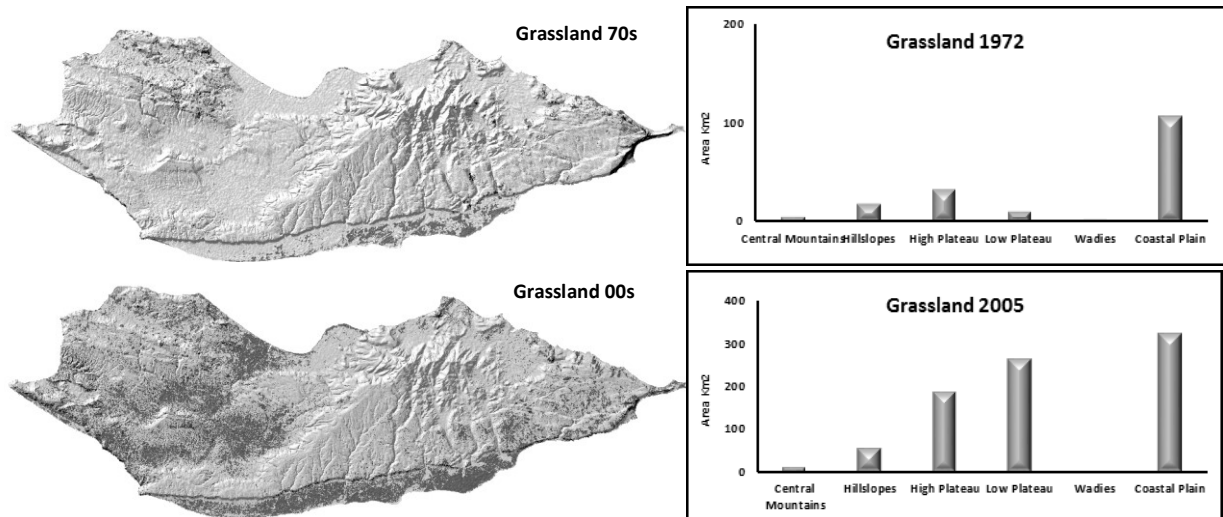


Figure 56. Obvious trends of vegetation cover (increase or decrease) and spatial distribution for the most effected vegetation classes in Socotra Island between 70s and 00s.

The figure above illustrates the progressive decrease in some vegetation class types and its replacement with new or previously less dominant vegetation cover types. Mixed woodland forest areas were largely seen replaced by succulent shrubs and open shrublands. However, some cultivated land expanded mainly date palms in the western and southern parts of the island particularly in the wadies (Valleys). In addition to expansion of the succulent shrubs, woody species have become dominant in many of the grass and shrub lands, likely as a result of over grazing by domestic animals. Some vegetation cover types, including the dwarf shrubs, *Dracaena* and *Croton* ecosystems, show steadily decline, while changes in other vegetation cover types have been slowly down during certain times or were even temporarily improved, such as in the case of the *Boswellia* and *Jatropha* areas. As we discussed in chapter 6 there are some grassland and bare areas expanded particularly in the plateaus and coastal zones among the western and southern parts of the island and have more than doubled since the 70s with a particular strong increase after 90s. On the one hand the more awareness and conservation knowledge attained by the SCDP which was established in the mid-1990s, encouraged the persisted vegetation surface rapidly to increase in the north, northwest, east and south parts of the island, but on the other hand spreading more roads with new constructed infrastructures and development after 1990 might played a major role in emergence of bare areas and reduce others vegetated areas.

Results showed significant improvement in *Dracaena*, *Boswellia* and *Jatropha* areas associated with the period from 1991 to 2005. In which it might reflects the positively affected of the new institutional changes in 1990 and the prompted the island by UNESCO as one of the most important human heritage sites and world's natural reserves and. Nonetheless, there also numerous studies reported about worsening of climate conditions over several parts of the island that are unfavorable for vegetation growth.

## 7.2. Conclusion

Our results showed that human activities are predominantly observed among three plant communities, mixed woodland, *Dracaena* and *Croton*. Moreover, as a results of livestock and human pressure, the low plateau and the coastal plain have shown the most degraded zones whereas several grassland areas were invaded by numerous unusual and undesirable plant species. As the mixed woodland is severely disturbed by human settlement, the results also showed that several *Croton* and dwarf shrubs areas were targeted by severe deforestation and. therefore, converted into small crop farms, bare land or settlement areas. In the high plateau and the hillslopes zones the fuel wood collection was observed as a routine activity by the people from Haheboo and Alqalansiya towns. During our field work numerous people were observed while collecting wood resources from those areas. Observation of human and livestock impact on environment is much more recorded in the woody mixed zone and grasslands as compared to other habitat types of the Island. Results of group discussion also confirmed that a large portion of the communities within (Hillslope and High Plateau) and the nearby areas have been directly or indirectly excessively exploited *Dracaena* and *Boswellia* resources. It has to be taken into account that these human activities, often degrading valuable plant communities, have to be seen as a deteriorating factor acting additionally to the negative influence of climate change.



## Chapter 8 General Discussion

The potential vegetation change in Socotra island has been demonstrated by means of two directions of vegetation change investigation approaches. We used the NDVI time series based on spectral information from medium resolution Landsat satellite images during the wet season to monitor the vegetation conditions between 1972 and 2010. The second approach, we used the reflectance-vegetation cover relationships using different Landsat satellite images for varying seasonal conditions. Therefore, each previous chapter (Chap. 5-7) has its own specific discussion. However, this chapter will summarize the main findings with regard to the research questions, as well as we will discuss the findings and trying to point out the limitations and obstacles facing our work and outline directions for future research. Both approaches support our hypothesis that the island experienced rapid vegetation alterations along with the effect of climate change as well as by human influence. Thus coupled changes bring a pressure on the natural resources and plant species and therefore, a trend in biomass, vegetation cover and species composition on Socotra Island over the last 40 years. Our study shows the effectiveness of using a combination multi-temporal series of medium resolution satellite data for monitoring environmental and vegetation pattern/changes along with environmental variables and rainfall in investigating changes and mapping vegetation areas in Socotra semiarid region. This powerful environmental monitoring strategy, consisting of collaborative classification approaches, helps in discriminating ecologically meaningful vegetation cover informational components as mosaics of different vegetation classes. For instance, our study was able to represent and map classes exhibiting similar greenness, among others, and differentiate classes having close spectral characteristics (such as *Dracaena* and mixed woodland).

To summarize the discussion, we examined the applicability of integrated NDVI during the growing period (GP) data compared with the variability in rainfall and the possibility of detecting biomass based NDVI changes and the trend of the vegetation cover in the island during 1972 to 2010 in chapter 5. We also quantitatively examined the dynamic vegetation changes and their inter-seasonal variability using advanced land classification analysis techniques based on differences in spectral reflectance of different vegetation cover types for the same period in chapter 6. The results showed a close agreement with some previous finding about the island, but we were able to extend substantially. We expanded our discussion on the detection of climate-induced and human-induced vegetation change, which is highlighted in chapter 7.

### **Analysis of climatic conditions and NDVI in the study area**

To be able to fulfil the goal of the research objectives and answer their questions, we started analysing climatic conditions and NDVI in the study area. This is to highlight the spatial and temporal locality variation within season and inter-seasonal dynamics and to answer Q1 & Q3, whether the fluctuation in rainfall reflects the ongoing vegetation degradation, and to detect the trend and variability in vegetation cover in space and time.

Results showed temporal variability both in the rainfalls and the vegetation cover during the period 1972-2010. However, rainfall variability found strongly depended on geographical location and elevation of the station. These results are in agreement with other published results by (Scholte and De Geest, 2010, Habrova et al., 2007). For individual stations, the

coefficient of variation in rainfall was higher than 100 in some stations. Similar to the earlier notice by (Cronk, 1985, Oldfield and Sheppard, 1997) we found the magnitude of rainfall changeability during the growing season to decrease from the north to the south. Statistical analysis of rainfall exhibited low inference of trends among different stations throughout the period 1972 - 2010. While the stations Qalansiyay (QAL), Diksam (Heuvelink et al.), Qabhaten (QEB), Qariah (QAR), Nooged (NOO), Qaeshbah (QAE) and Mouri (MOU) exhibited downward trends in growing season rainfall, four of them, Mather (HAD), Mayah (MAY), Hay as Salam (CEN) and Homhil (HOM), showed significant upward trends, (and Momi (MOM) showed almost neutral response). These results are somehow in agreement with the results obtained by (Habrova et al., 2007, Habrová, 2004, Haake et al., 1993, Brown and Mies, 2012a, Fritz and Okal, 2008, Scholte and De Geest, 2010, Morris, 2002). According to these studies, the mean long time decrease in rainfall occurred in winter.

The analysis of rainfall conditions and NDVI found a strong determination of the vegetation dynamics by the rainfall both within the growing season and on an inter-seasonal time scale. The correlation between NDVI and cumulative rainfall was for all vegetation types high. We clearly showed that nearly 73% of all variations in log NDVI can be explained by variations in rainfall. These results therefore conceive a high dependence of vegetation growth on rainfall stated by (Miller and Morris, 2004a) but still a certain amount of NDVI variance remains unexplained. However, stronger correlations were exhibited in areas dominated by grass vegetation and weaker ones in areas dominated by shrubs and trees. Our results are consistent with the observed relations between NDVI and climate parameters in other dry regions. It confirms earlier findings by (Miller and Morris, 2004a, Nicholson et al., 1990a, Scholte and De Geest, 2010) that vegetation greenness in the semi-arid environments is strongly associated to rainfall accumulated over a period of time than to instantaneous rainfall. The strength of NDVI vs. rainfall associations not only depended on vegetation type but there were variations in the response of NDVI to rainfall within each vegetation class on the per-pixel basis. Consequently, the less dense and less rained west region is more sensitive to both inter-seasonal and within seasonal variations. This might also indorse the result from (Scholte and De Geest, 2010, Brown and Mies, 2012a) who believed that areas above 700 m received half of the moisture originating from fog. Nevertheless, our results showed similar findings as by (Habrová, 2004) that winter monsoon in south part of island is influenced by a rain shadow with no or less rainfall than in northern part. These differences can be attributed to the impact of local storms being more frequent in the northwest during the winter and southeast in the summer times, being therefore greater in the upper part of the island where the vegetation is less sensitive to dry spells and showing a better adaptation to cope with negative or positive rainfall fluctuations. We were able to characterize the 40-year average seasonal cycle of NDVI and to provide a clear distinction between the major vegetation behaviors. This was the concern by some authors (Král and Pavliš, 2006 and Miller and Morris, 2004a) who mention “still completely lacking the long-term climatic observations from different parts of the island and the relationship between the NDVI and some environmental variables”. Our results confirm that the best distinction between the time profiles can be made within the late winter months, from Decembers to Februarys. During this time, the vegetation types display quite different and clear distinguishable attributes of their canopy such as leaf area, percent coverage, and

biomass. The highest discrepancy between NDVI values of the separate vegetation group types is observed in the mid Januarys when the vegetation types exhibit their NDVI maximums density.

Assessing of spatial relationships of different vegetation types resulting from supervised classification with the plant foliage biomass data calculated as an average of maximum NDVI however, showed variability in the classes density and frequency of biomass during the last four decades. Among the vegetation types, *Jatropha*, date palm and *Dracaena* had the highest NDVI values. Examining the greenness of pixels' value between decades 70s/80s and 80s/90s showed a variation of changes. Results show quite an improvement in the extent of the total green areas by approximately 328 km<sup>2</sup> (9%) and 268 km<sup>2</sup> (7%), while the lowest increase was shown during 90s/00s with 99 km<sup>2</sup> (3%).

### **Vegetation cover classification and vegetation type change**

To answer the second question (Q2), concerning the main vegetation types that can be distinguished and the magnitude of change in each different vegetation classes: We classified the vegetation cover and examined the dynamic changes and the temporal distribution of the vegetation patterns depending on the duration of the wet season for the period of 1972 to 2005. To ensure that time series images are directly comparable to one another, an accurate per-pixel registration of multi-temporal Landsat image data was attained to avoid overestimation of mismatching errors. Our image classification approach with moderately high classification accuracy was able to categorise and map eventually broad categories of vegetation cover as classes having unique spectral characteristics, which were then similar on the basis of both physiognomic and floristic criteria. However, it reveals consolidate results indicate a detailed vegetation cover map with nine (Bryant et al.) classes in the island namely Mixed woodland, Date Palms, *Boswellia*, *Dracaena*, Dwarf Shrubs, *Jatropha*, Succulent Shrubs, *Croton* and Grassland. Our accuracy results were compared in the common practice confusion matrix missioned by (Congalton and Green, 2008 and Vibhute et al., 2016) in which we have to assess the basic accuracy measures such as producer's and user's accuracy as well as overall accuracy. Therefore, this accuracy as described in chapter 6 was assessed at various stages of complexity of reference databases. It was possible to classify them applying our field knowledge with only areas that consist of more than 70% of each class type in the classifier approach, most vegetation types were then classified with overall accuracy greater than 70%. The confusion matrix showed an overall accuracy of 90 %, 77%, 70% and 73% for the classified images years 2005 (00s), 1994 (90s), 1984 (80s) and 1972 (70s), with an overall Kappa statistic of 0.89, 0.73, 0.65 and 0.68, respectively. Nevertheless, some other dominant vegetation types in the island that closely had similar phenological appearance and sharing common elevation ranges are naturally overlapping each other (Schwantes et al., 2016) and show some confusion in the common elevation range (De Sanctis et al., 2013). The disturbance and physical factors associated with the mapped units and the spatial proximity and interactions among structural types might fruitfully highlight the ecological meaning of the units defined, giving insights about their adequate management (Cingolani et al., 2003). For instance, the presence of a small amount of massive rock outcrops and grass areas in class grassland (class 9) or in succulent shrubs (class 7) might indicate incipient erosion processes and suggest that this unit is recently under excessive grazing pressure and, therefore, must be carefully managed to prevent a

complete transformation into rock pavement. Other examples are class 1 and class 4, where woodland and *Dracaena* are combined with other mixed types experiencing a recession in these former classes and expansion of *Croton* and/or *Jatropha*. These classes are extremely important for vegetation diversity ((Attorre et al., 2011) and (Lisa M. Banfield et al., 2011) which is higher than in units where only one of those structural types dominates (e.g. class 2 or class 8). These, as well as other examples show that classes defined as mosaics not only solve an important technical problem (Pietsch and Morris, 2010) but also have an emergent ecological meaning and reflex the bio-geomorphic feedbacks (Moffett et al., 2015), being therefore ideal for management purposes in markedly heterogeneous areas (Morris, 2002).

Results on investigation trends in vegetation activity convey expansion of urban, bare land and grassland areas with incipient of sparse vegetation and bare soils (class 9), which more than doubled between 1972 and 1984 and continued expanding, until it reached more than 800 km<sup>2</sup> (+395%) in 2005. These results confirmed other published reports which they mentioned trends in vegetation activity in the island, (Tucker et al., 1991, Begue et al., 2011, Brandt et al., 2014, Chen et al., 2012, da Silva Rodrigues, 2014, Forkel et al., 2013, Hanafi and Jauffret, 2008, Attorre et al., 2007, Cassola and Wranik, 1998, Pietsch and Morris, 2010, Adolt and Pavlis, 2004). Nevertheless, the percentage of vegetated areas with positive and negative trends during the growing season was substantially different according to vegetation cover type and the time period. The results indicated that an average of 20% of the vegetated areas in the island showed significant increase of greenness during the growing season between 1972 and 2005, while 24% of these areas showed a significantly decrease. However, from biogeographical point of view, low plateau and the coastal plain were the most underwent areas with more than 40% decrease in their vegetated areas followed by the high plateau with more than 17% decrease, whereas the wadies and the central plains were the least areas affected by change with percent increase of 4%.

However, our findings show *Dracaena* and Mixed woodland have substantially decreased from 70s to 00s while succulent shrubs areas markedly increased. Therefore, our findings somehow disagree with the assumption of Martin Rejžek et al., (2016) that *Dracaena* in Firmihin “have not been replaced by any species” while H. Habrová, J. Pavliš (2015) confirm that this area has been rapidly overgrown by herbaceous plants. In this regards, our study confirmed the reduction and lack of germination for *Dracaena* stated by (Adolt and Pavlis, 2004, Attorre et al., 2007, (Adolt et al., 2013 and Hubálková et al., 2015).

Dwarf shrubs and *Jatropha* were the least affected in percent of total areas with some shifting between 1972 and 2005. Moreover, *Boswellia* areas exhibits critical reduced between the period 70s and 80s with quite improvement after 90s. As the expansion of succulent shrubs widely spread after 90s, the dense mixed woodland areas were largely seen reduced. It might have been accompanied with some encroachment by succulent species and grassland along the coastal zone, hillslopes and the plateaus (Senan et al., 2012), (Brown and Mies, 2012a) and (Miller and Morris, 2004a) Date Palms and some cultivated land expanded particularly among the wadies (valleys) western and southern parts of the island, and have doubled in their areas in the 80s.

ArcMap cross-tabulation pixel by pixel was executed with the intention to investigate which class have changed from certain class to another and monitor the extent of undergoing

changes. It reveals an overall similarities agreement (Total diagonal/Total area) from 23% to 30% in which reflects the magnitude of change of more than 80% to 70%. This can be figured out as some vegetation types have grown by replacing others. On the other hand, it can be also understood, as we observed during the field work, as a domination of some species due to deterioration of others. Our results show that grassland, *Jatropha*, dwarf and succulent shrubs have spatially dominated over other classes particularly after 90s.

#### **Detection of climate and human induced vegetation change**

Results from chapter 5, 6 and 7 provide evidence to answer (Q. 1.3) that rainfall and human induced activities may play a significant role in deterioration of vegetation cover in the study area and establishing what we call a catastrophic landscape. However, we have demonstrated that, there are concentration of areas of decreasing vegetation density as measured by NDVI throughout the island. Our results showed that human activities are predominantly observed among four communities of plants, the woody land, *Dracaena*, *Croton* and *Boswellia*. Moreover, as a results of livestock and human pressure, the low plateau and the coastal plain have shown the most degraded zones whereas several grassland areas were invaded by numerous unusual and undesirable plant species (as also observed by Scholte and De Geest, (2010) As the mixed woodland is severely disturbed by human settlement, the results also showed several *Croton* and dwarf shrubs areas were target to severe deforestation through conversion into small crop farms or bare lands or settlement areas. In the high plateau and the hillslopes zones the fuel wood collection (Ritzema, 2006) was observed as a routine activity by the people from Hadeboo and Alqalansiya towns. Thus during our field work a numerous number of people were also observed while collecting wood resources from those areas. Observation of human and livestock impact on environment is much more recorded in the woody mixed zone and grasslands (Miller and Morris, 2004a) as compared to other habitat types of the Island. Results of group discussion also confirmed that a large portion of the communities within hillslope and high plateau and the nearby areas have been directly or indirectly excessively exploited *Dracaena* and *Boswellia* resources.

As we described in chapter 4 the maximum NDVI values during the growing periods for each pixel in the selected images between 1972 and 2005 were extracted and used to study the relationship between the trends in vegetation and trends in rainfall. This is in order to identify climate signal in the vegetation activity. Despite the complexity of human and environment interactions generally, results showed strong rainfall signs in the inter-seasonal dynamic of vegetation cover and proved that NDVI trend was significantly correlated with trends in rainfall.

#### **Obstacles and limitations:**

- Many obstacles and challenges were frustrating and limited the achievements of this research. Deficiency and lack of climatic data was one of the main limitations. The network seemed to exhibit insufficient density of the climate stations with lack of long term detailed climatic data (Scholte and De Geest 2010), with only scarce information covering a few years. The NDVI database has only been used to analyze whether in the whole of the study area there is a significant increase of NDVI as well as the role of climatic variables in the process.

- Lack of adequate temporal satellite data. It was not possible to obtain Landsat images of the study area for the similar time of each decade because of cloud cover and the limited availability of the images released by NASA. Furthermore, a malfunctioning of Scan Line Corrector-off acquisition mode in the Landsat TM system from May 31<sup>st</sup> of 2003 on created a serious difficulty for which reason we got to deal more synchronously though the cloudy satellite data.
- Finally, Lack of funding. This research was basically held on self-funding, except for a small and limited financial support from my country covering only a part of the research period.

### **Final Conclusion**

This study presented capability of satellite-based observation to examine the long term pixel-based change detection of vegetation from 1972 to 2010 and investigate the effects of climate changes by examining trend NDVI/Rainfall relationships over time. Moreover, coupled supervised and unsupervised classification provided satisfactory results in terms of categorizing and distinguishing different vegetation types. Nevertheless, our approach with moderately high classification accuracy was able to categorise and map eventually nine broad categories of vegetation cover. Use of NDVI time series provides applicable tool for characterizing vegetation variability and revealed inter-seasonal variation as well as motility changes in the vegetation types over the period of 1972-2005. The magnitude of this deviation observed depend on the response of the vegetation cover to the rainfall. This study also confirms findings by (Scholte and De Geest, 2010, Habrova et al., 2007) that the topography and physiographic relief features as well as the monsoon pattern play a major role in the spatial distribution of rainfall in the island.

Image classification results indicated that an average of 20% of total area in the island showed a significant increased vegetation biomass during the growing season between 1972 and 2005, while 24% of the areas showed a significant decrease. However, low plateau and the coastal plain were the most underwent areas with more than 40% decreased in their vegetated areas followed by the high plateau more than 17% loss.

Human activities are predominantly observed among the four communities of plants (the woody land, *Dracaena*, *Croton* and *Boswellia*). Moreover, as a results of livestock and human pressure, the low plateau and the coastal plain are shown the most degraded zones, whereas several grassland areas have been invaded by numerous unusual and undesirable plant species. Observation of human and livestock impact on environment is much more recorded in the mixed woody zone and grasslands as compared to other habitat types of the Island. Results of group discussion also confirmed that a large portion of the communities within (hillslope and high Plateau) and the nearby areas have been directly or indirectly excessively exploited *Dracaena* and *Boswellia* resources.

Finally, it can be concluded that, despite the harsh environmental conditions faced by the island, that the strong traditional land use management practices employed by the indigenous population knowledge, have both served and played a significant role in the past to protect the vegetation and biodiversity of the Island (Miller and Morris, 2004a) We were able to point out in detail how this vegetation, being stable over centuries, has been underwent dramatic

changes in the last 40 years or so both by climate change and by anthropogenic activities. Our results also showed which vegetation types or areas, respectively, have the highest vulnerability and need special attention and clear management.

## References

- ABOU EL-MAGD, I. & TANTON, T. W. 2003. Improvements in land use mapping for irrigated agriculture from satellite sensor data using a multi-stage maximum likelihood classification. *International Journal of Remote Sensing*, 24, 4197-4206.
- ACKERMAN, S. A., STRABALA, K. I., MENZEL, W. P., FREY, R. A., MOELLER, C. C. & GUMLEY, L. E. 1998. Discriminating clear sky from clouds with MODIS. *Journal of Geophysical Research: Atmospheres (1984–2012)*, 103, 32141-32157.
- ADOLT, R., MADĚRA, P., ABRAHAM, J., ČUPA, P., SVÁTEK, M., MATULA, R., ŠEBESTA, J., ČERMÁK, M., VOLAŘÍK, D. & KOUTECKÝ, T. 2013. Field survey of *Dracaena cinnabari* populations in Firmihin, Socotra Island: methodology and preliminary results. *Journal of Landscape Ecology*, 6, 7-34.
- ADOLT, R. & PAVLIS, J. 2004. Age structure and growth of *Dracaena cinnabari* populations on Socotra. *Trees*, 18, 43-53.
- AGUIAR, M. R., PARUELO, J. M., SALA, O. E. & LAUENROTH, W. K. 1996. Ecosystem responses to changes in plant functional type composition: an example from the Patagonian steppe. *Journal of Vegetation Science*, 381-390.
- AGUIAR, M. R. & SALA, O. E. 1999. Patch structure, dynamics and implications for the functioning of arid ecosystems. *Trends in Ecology & Evolution*, 14, 273-277.
- AL SAGHEIR, O. & PORTER, R. The bird diversity of Soqotra. Proceedings of the First International Symposium on Soqotra Island: Present and Future, 1996. 199-212.
- ALBERTI, M. 2005. The effects of urban patterns on ecosystem function. *International regional science review*, 28, 168-192.
- ALEXANDER, D. & MILLER, A. 1995. Socotra's misty future. *New Scientist*, 147, 32-35.
- ANYAMBA, A. & TUCKER, C. 2005. Analysis of Sahelian vegetation dynamics using NOAA-AVHRR NDVI data from 1981–2003. *Journal of Arid Environments*, 63, 596-614.
- ATTORRE, F., FRANCESCONI, F., DE SANCTIS, M., ALFÒ, M., MARTELLA, F., VALENTI, R. & VITALE, M. 2014. Classifying and mapping potential distribution of forest types using a finite mixture model. *Folia Geobotanica*, 49, 313-335.
- ATTORRE, F., FRANCESCONI, F., TALEB, N., SCHOLTE, P., SAED, A., ALFO, M. & BRUNO, F. 2007. Will dragonblood survive the next period of climate change? Current and future potential distribution of *Dracaena cinnabari* (Socotra, Yemen). *Biological Conservation*, 138, 430-439.
- ATTORRE, F., TALEB, N., DE SANCTIS, M., FARCOMENI, A., GUILLET, A. & VITALE, M. 2011. Developing conservation strategies for endemic tree species when faced with time and data constraints: *Boswellia* spp. on Socotra (Yemen). *Biodiversity and Conservation*, 20, 1483-1499.
- BAILEY, R. G. 1983. Delineation of ecosystem regions. *Environmental Management*, 7, 365-373.
- BALAKRISHNAIAH, G., REDDY, L. & REDDY, R. 2016. Evaluation of Clearness and Diffuse Index at a Semi-Arid Station (Anantapur) using Estimated Global and Diffuse Solar Radiation. *International Journal of Advanced Earth Science and Engineering*, 5, pp. 347-363.
- BALFOUR, I. B. 1888. The Botany of Sokotra, Transactions of the Royal Society of Edinburgh.
- BALL, G. H. & HALL, D. J. 1965. ISODATA, a novel method of data analysis and pattern classification. DTIC Document.
- BALTHAZAR, V., VANACKER, V. & LAMBIN, E. F. 2012. Evaluation and parameterization of ATCOR3 topographic correction method for forest cover mapping in mountain areas. *International Journal of Applied Earth Observation and Geoinformation*, 18, 436-450.
- BANERJEE, B., BOVOLO, F., BHATTACHARYA, A., BRUZZONE, L., CHAUDHURI, S. & MOHAN, B. K. 2015. A New Self-Training-Based Unsupervised Satellite Image Classification Technique Using Cluster Ensemble Strategy. *IEEE Geoscience and Remote Sensing Letters*, 12, 741-745.
- BARALDI, A. & HUMBER, M. L. 2015. Quality Assessment of Preclassification Maps Generated From Spaceborne/Airborne Multispectral Images by the Satellite Image Automatic Mapper and Atmospheric/Topographic Correction-Spectral Classification Software Products: Part 1—Theory. *IEEE Journal of Selected Topics in Applied Earth Observations and Remote Sensing*, 8, 1307-1329.
- BARBERO, M., BONIN, G., LOISEL, R. & QUÉZEL, P. 1990. Changes and disturbances of forest ecosystems caused by human activities in the western part of the Mediterranean basin. *Vegetatio*, 87, 151-



- BARBOSA, H. A., KUMAR, T. V. L. & SILVA, L. R. M. 2015. Recent trends in vegetation dynamics in the South America and their relationship to rainfall. *Natural Hazards*, 77, 883-899.
- BARLOW, M., ZAITCHIK, B., PAZ, S., BLACK, E., EVANS, J. & HOELL, A. 2015. A Review of Drought in the Middle East and Southwest Asia. *Journal of Climate*.
- BATISTA, G. T. 2011. "Ambiente & Água" scientific journal after five years of history. *Ambiente e Agua-An Interdisciplinary Journal of Applied Science*, 6, 3-5.
- BAUDENA, M. & PROVENZALE, A. 2008. Rainfall intermittency and vegetation feedbacks in drylands. *Hydrology and Earth System Sciences*, 12, 679-689.
- BEGUE, A., VINTROU, E., RUELLAND, D., CLADEN, M. & DESSAY, N. 2011. Can a 25-year trend in Soudano-Sahelian vegetation dynamics be interpreted in terms of land use change? A remote sensing approach. *Global Environmental Change*, 21, 413-420.
- BELGIU, M. & DRĂGUȚ, L. 2016. Random forest in remote sensing: A review of applications and future directions. *ISPRS Journal of Photogrammetry and Remote Sensing*, 114, 24-31.
- BENCHERIF, M. A., BAZI, Y., GUESSOUM, A., ALAJLAN, N., MELGANI, F. & ALHICHRI, H. Fusion of extreme learning machine and graph-based optimization methods for active classification of remote sensing images. *IEEE Geoscience and Remote Sensing Letters*, 12, 527-531.
- BEYDOUN, Z. R. & BIGHAN, H. R. 1969. The geology of Socotra island, Gulf of Aden. *Quarterly Journal of the Geological Society*, 125, 413-441.
- BEYHL, F. E. & MIES, B. 1996. Remarks on the vegetation ecology of Socotra. *Proceedings of the First International Symposium on Socotra Island, Aden 24-28 March 1996*, 2, 25-62. Aden.
- BIGING, G., CHRISMAN, N., COLBY, D., CONGALTON, R., DOBSON, J., FERGUSON, R., GOODCHILD, M., JENSEN, J. & MACE, T. 1999. Accuracy assessment of remote sensing-detected change detection. *S. Khorram, American Society for Photogrammetry and Remote Sensing (ASPRS), MD, USA*.
- BIJKER, W. 1997. *Radar for rain forest : a monitoring system for land cover change in the Colombian Amazon*. Proefschrift Wageningen, ITC.
- BIRSE, A., BOTT, W., MORRISON, J. & SAMUEL, M. 1997. The Mesozoic and Early Tertiary tectonic evolution of the Socotra area, eastern Gulf of Aden, Yemen. *Marine and Petroleum Geology*, 14, 675-684.
- BOARD, G. S. A. M. R. 2003. Geological Map of Yemen. Socotra Island. Aden-Yemen: Geological Survey Department.
- BONTEMPS, S., BOGAERT, P., TITEUX, N. & DEFURNY, P. 2008. An object-based change detection method accounting for temporal dependences in time series with medium to coarse spatial resolution. *Remote Sensing of Environment*, 112, 3181-3191.
- BORAK, J., LAMBIN, E. & STRAHLER, A. 2000. The use of temporal metrics for land cover change detection at coarse spatial scales. *International Journal of Remote Sensing*, 21, 1415-1432.
- BOSTAN, P. A. 2013. *ANALYSIS AND MODELING OF SPATIALLY AND TEMPORALLY VARYING METEOROLOGICAL PARAMETER: PRECIPITATION OVER TURKEY*. MIDDLE EAST TECHNICAL UNIVERSITY.
- BOXHALL, P. 1966. Socotra:'Island of Bliss'. *Geographical Journal*, 213-222.
- BRACKEN, L. J. & CROKE, J. 2007. The concept of hydrological connectivity and its contribution to understanding runoff-dominated geomorphic systems. *Hydrological Processes*, 21, 1749-1763.
- BRANDT, M., GRAU, T., MBOW, C. & SAMIMI, C. 2014. Modeling soil and woody vegetation in the Senegalese Sahel in the context of environmental change. *Land*, 3, 770-792.
- BROWN, G. 1966. Social and economic conditions and possible development of Socotra. *Report Royal Geographic Society. Royal Geographic Society*.
- BROWN, G. & MIES, B.-A. 2012a. *Vegetation ecology of socotra*, Springer.
- BROWN, G. & MIES, B. 2012b. *Vegetation ecology of Socotra*, Springer Science & Business Media.
- BROWN, K. 2003. Integrating conservation and development: a case of institutional misfit. *Frontiers in Ecology and the Environment*, 1, 479-487.
- BROWN, M. E. & DE BEURS, K. M. 2008. Evaluation of multi-sensor semi-arid crop season parameters based on NDVI and rainfall. *Remote Sensing of Environment*, 112, 2261-2271.

- BRUGGEMAN, H. 1997. Agro-climatic resources of Yemen. Part 1. Agro-climatic inventory. Yemen: Agricultural Research and Extension Authority, Ministry of Agriculture and Water Resources Dhamar, Republic of Yemen.
- BRUZZONE, L. & PRIETO, D. F. 2001. Unsupervised retraining of a maximum likelihood classifier for the analysis of multitemporal remote sensing images. *IEEE Transactions on Geoscience and Remote Sensing*, 39, 456-460.
- BRYANT, R. B., ARNOLD, R. W., SOIL SCIENCE SOCIETY OF AMERICA. DIVISION S-5. & SOIL SCIENCE SOCIETY OF AMERICA. DIVISION S-9. 1994. *Quantitative modeling of soil forming processes : proceedings of a symposium sponsored by Divisions S-5 and S-9 of the Soil Science Society of America in Minneapolis, Minnesota, 2 Nov. 1992*, Madison, Wis., SSSA.
- BURNS, S. J. *The History of the Monsoon in Arabia A Speleothem-based Paleoclimate Study* [Online]. Department of Geosciences University of Massachusetts. Available: <http://www.geo.umass.edu/climate/speleo.html> [Accessed].
- BYSTROEM, K. 1960. *Dracaena draco* L. in the Cape Verde Islands. *Acta Horti Gotobg*, 23, 179-214.
- CAMARGO, M. N., KLAMT, E. & KAUFFMAN, J. H. 1986. Soil classification as used in Brazilian soil surveys. *Annual Report, International Soil Reference and Information Centre, Wageningen*.
- CARDILLE, J. A. & FOLEY, J. A. 2003. Agricultural land-use change in Brazilian Amazonia between 1980 and 1995: Evidence from integrated satellite and census data. *Remote Sensing of Environment*, 87, 551-562.
- CARLEER, A. & WOLFF, E. 2004. Exploitation of Very High Resolution Satellite Data for Tree Species Identification. *Photogrammetric Engineering & Remote Sensing*, 70, 135-140.
- CARLSON, T. N. & RIPLEY, D. A. 1997. On the relation between NDVI, fractional vegetation cover, and leaf area index. *Remote sensing of Environment*, 62, 241-252.
- CASSOLA, F. & WRANIK, W. 1998. A Remarkable New Tiger Beetle from Socotra Island, Republic of Yemen (Coleoptera, Cicindelidae). *Deutsche Entomologische Zeitschrift*, 45, 265-268.
- CASTILLO-SANTIAGO, M. Á., GHILARDI, A., OYAMA, K., HERNÁNDEZ-STEFANONI, J. L., TORRES, I., FLAMENCO-SANDOVAL, A., FERNÁNDEZ, A. & MAS, J.-F. 2013. Estimating the spatial distribution of woody biomass suitable for charcoal making from remote sensing and geostatistics in central Mexico. *Energy for Sustainable Development*, 17, 177-188.
- CHEHBOUNI, A., ESCADAFAL, R., DUCHEMIN, B., BOULET, G., SIMONNEAUX, V., DEDIEU, G., MOUGENOT, B., KHABBA, S., KHARROU, H., MAISONGRANDE, P., MERLIN, O., CHAPONNIERE, A., EZZAHAR, J., ER-RAKI, S., HOEDJES, J., HADRIA, R., ABOURIDA, A., CHEGGOUR, A., RAIBI, F., BOUDHAR, A., BENHADJ, I., HANICH, L., BENKADDOUR, A., GUEMOURIA, N., CHEHBOUNI, A. H., LAHROUNI, A., OLIOSO, A., JACOB, F., WILLIAMS, D. G. & SOBRINO, J. A. 2008. An integrated modelling and remote sensing approach for hydrological study in arid and semi-arid regions: the SUDMED programme. *International Journal of Remote Sensing*, 29, 5161-5181.
- CHEN, J., GU, S., SHEN, M., TANG, Y. & MATSUSHITA, B. 2009. Estimating aboveground biomass of grassland having a high canopy cover: an exploratory analysis of in situ hyperspectral data. *International journal of Remote sensing*, 30, 6497-6517.
- CHEN, K. 2002. An approach to linking remotely sensed data and areal census data. *International Journal of Remote Sensing*, 23, 37-48.
- CHEN, Z.-J., LI, J.-B., FANG, K.-Y., DAVI, N. K., HE, X.-Y., CUI, M.-X., ZHANG, X.-L. & PENG, J.-J. 2012. Seasonal dynamics of vegetation over the past 100 years inferred from tree rings and climate in Hulunbei'er steppe, northern China. *Journal of Arid Environments*, 83, 86-93.
- CHEN, Z., BABIKER, I. S., CHEN, Z., KOMAKI, K., MOHAMED, M. A. & KATO, K. 2004. Estimation of interannual variation in productivity of global vegetation using NDVI data. *International Journal of Remote Sensing*, 25, 3139-3159.
- CHENG, X., AN, S., CHEN, J., LI, B., LIU, Y. & LIU, S. 2007. Spatial relationships among species, above-ground biomass, N, and P in degraded grasslands in Ordos Plateau, northwestern China. *Journal of Arid Environments*, 68, 652-667.
- CHEUNG, C., DE VANTIER, L. & VAN DAMME, K. 2006. Socotra. *A Natural History of the Islands and their People*.

- CHO, M. A., SKIDMORE, A., CORSI, F., VAN WIEREN, S. E. & SOBHAN, I. 2007. Estimation of green grass/herb biomass from airborne hyperspectral imagery using spectral indices and partial least squares regression. *International Journal of Applied Earth Observation and Geoinformation*, 9, 414-424.
- CINGOLANI, A. M., CABIDO, M. R., RENISON, D. & SOLÍS NEFFA, V. 2003. Combined effects of environment and grazing on vegetation structure in Argentine granite grasslands. *Journal of Vegetation Science*, 14, 223-232.
- CISSÉ, S., EYMARD, L., OTTLÉ, C., NDIONE, J. A., GAYE, A. T. & PINSARD, F. 2016. Rainfall Intra-Seasonal Variability and Vegetation Growth in the Ferlo Basin (Senegal). *Remote Sensing*, 8, 66.
- COHEN, W. B. & FIORELLA, M. 1998. Comparison of methods for detecting conifer forest change with Thematic Mapper imagery. *Remote sensing change detection: Environmental monitoring methods and applications*, 89-102.
- COHEN, W. B. & GOWARD, S. N. 2004. Landsat's role in ecological applications of remote sensing. *Bioscience*, 54, 535-545.
- COHEN, W. B., YANG, Z. & KENNEDY, R. 2010. Detecting trends in forest disturbance and recovery using yearly Landsat time series: 2. TimeSync—Tools for calibration and validation. *Remote Sensing of Environment*, 114, 2911-2924.
- COMMISSION, I. S. S. 2001. *IUCN Red List Categories and Criteria*, IUCN.
- CONGALTON, R. G. & GREEN, K. 2008. *Assessing the accuracy of remotely sensed data: principles and practices*, CRC press.
- CONGALTON, R. G., ODERWALD, R. G. & MEAD, R. A. 1983. Assessing Landsat classification accuracy using discrete multivariate analysis statistical techniques. *Photogrammetric Engineering and Remote Sensing*.
- COPPIN, P., JONCKHEERE, I., NACKAERTS, K., MUYS, B. & LAMBIN, E. 2004. Review Article Digital change detection methods in ecosystem monitoring: a review. *International journal of remote sensing*, 25, 1565-1596.
- CRONK, Q. 1985. Botanical survey of Socotra for conservation and plant genetic resources. *WWF conservation yearbook*, 1986.
- CRONK, Q. C. B. 1992. Relict floras of Atlantic islands: patterns assessed. *Biological Journal of the Linnean Society*, 46, 91-103.
- CUMBERLIDGE, N. & WRANIK, W. 2002. A new genus and new species of freshwater crab (Potamoidea, Potamidae) from Socotra Island, Yemen. *Journal of Natural History*, 36, 51-64.
- DA SILVA RODRIGUES, A. 2014. Analysis of vegetation dynamics using time-series vegetation index data from Earth Observation Satellites.
- DAMME, K. V. & BANFIELD, L. 2011. Past and present human impacts on the biodiversity of Socotra Island (Yemen): implications for future conservation. *Zoology in the Middle East*, 54, 31-88.
- DARVISHZADEH, R., SKIDMORE, A., SCHLERF, M. & ATZBERGER, C. 2008. Inversion of a radiative transfer model for estimating vegetation LAI and chlorophyll in a heterogeneous grassland. *Remote Sensing of Environment*, 112, 2592-2604.
- DAVENPORT, M. L. & NICHOLSON, S. E. 1993. ON THE RELATION BETWEEN RAINFALL AND THE NORMALIZED DIFFERENCE VEGETATION INDEX FOR DIVERSE VEGETATION TYPES IN EAST-AFRICA. *International Journal of Remote Sensing*, 14, 2369-2389.
- DE BEURS, K. & HENEBRY, G. 2005. A statistical framework for the analysis of long image time series. *International Journal of Remote Sensing*, 26, 1551-1573.
- DE KLERK, H. M., GILBERTSON, J., LÄCK-VOGEL, M., KEMP, J. & MUNCH, Z. Using remote sensing in support of environmental management: A framework for selecting products, algorithms and methods. *Journal of Environmental Management*, 182, 564-573.
- DE SANCTIS, M., ADEEB, A., FARCOMENI, A., PATRIARCA, C., SAED, A. & ATTORRE, F. 2013. Classification and distribution patterns of plant communities on Socotra Island, Yemen. *Applied Vegetation Science*, 16, 148-165.
- DINIZ-FILHO, J. A. F., BARBOSA, A. C. O., COLLEVATTI, R. G., CHAVES, L. J., TERRIBILE, L. C., LIMA-RIBEIRO, M. S. & TELLES, M. P. 2016. Spatial autocorrelation analysis and ecological niche modelling

- allows inference of range dynamics driving the population genetic structure of a Neotropical savanna tree. *Journal of Biogeography*, 43, 167-177.
- DIOUF, A. & LAMBIN, E. F. 2001. Monitoring land-cover changes in semi-arid regions: remote sensing data and field observations in the Ferlo, Senegal. *Journal of Arid Environments*, 48, 129-148.
- DONG, C., LOY, C. C., HE, K. & TANG, X. 2014. Learning a Deep Convolutional Network for Image Super-Resolution. In: FLEET, D., PAJDLA, T., SCHIELE, B. & TUYTELAARS, T. (eds.) *Computer Vision – ECCV 2014: 13th European Conference, Zurich, Switzerland, September 6-12, 2014, Proceedings, Part IV*. Cham: Springer International Publishing.
- DREGNE, H. E. 2011. *Soils of arid regions*, Elsevier.
- EHLERS, B. K., DAVID, P., DAMGAARD, C. F. & LENORMAND, T. 2016. Competitor relatedness, indirect soil effects, and plant co-existence. *Journal of Ecology*.
- ELIE, S. D. 2014. Pastoralism in Soqotra: external entanglements and communal mutations. *Pastoralism*, 4, 1-19.
- ENGLER, A. 1910. *Die Pflanzenwelt Afrikas, insbesondere seiner tropischen Gebiete : Grundzge der Pflanzenverbreitung im Afrika und die Charakterpflanzen Afrikas / von A. Engler*, Leipzig :, W. Engelmann.
- ERIKSSON, L. E., SANTORO, M., WIESMANN, A. & SCHMULLIUS, C. C. 2003. Multitemporal JERS repeat-pass coherence for growing-stock volume estimation of Siberian forest. *Geoscience and Remote Sensing, IEEE Transactions on*, 41, 1561-1570.
- ESCADAFAL, R., MULDER, M. A. & THIOMBIANO, L. (eds.) 1996. *Surveillance des sols dans l'environnement par télédétection et systèmes d'information géographiques: Monitoring soils in the environment with remote sensing and GIS*, Paris: ORSTOM.
- FAN, Y., LI, X., WU, X., LI, L., LI, W. & HUANG, Y. 2016. Divergent responses of vegetation aboveground net primary productivity to rainfall pulses in the Inner Mongolian Plateau, China. *Journal of Arid Environments*, 129, 1-8.
- FENSHOLT, R., RASMUSSEN, K., NIELSEN, T. T. & MBOW, C. 2009. Evaluation of earth observation based long term vegetation trends—Intercomparing NDVI time series trend analysis consistency of Sahel from AVHRR GIMMS, Terra MODIS and SPOT VGT data. *Remote Sensing of Environment*, 113, 1886-1898.
- FERWERDA, J. G., SKIDMORE, A. K. & MUTANGA, O. 2005. Nitrogen detection with hyperspectral normalized ratio indices across multiple plant species. *International Journal of Remote Sensing*, 26, 4083-4095.
- FETENE, A., HILKER, T., YESHITELA, K., PRASSE, R., COHEN, W. & YANG, Z. 2016. Detecting Trends in Landuse and Landcover Change of Nech Sar National Park, Ethiopia. *Environmental management*, 57, 137-147.
- FITZPATRICK-LINS, K. 1980. *The accuracy of selected land use and land cover maps at scales of 1: 250,000 and 1: 100,000*, Geological Survey.
- FLEITMANN, D., BURNS, S. J., MANGINI, A., MUDELSEE, M., KRAMERS, J., VILLA, I., NEFF, U., AL-SUBBARY, A. A., BUETTNER, A. & HIPPLER, D. 2007. Holocene ITCZ and Indian monsoon dynamics recorded in stalagmites from Oman and Yemen (Socotra). *Quaternary Science Reviews*, 26, 170-188.
- FLEITMANN, D., MATTER, A., BURNS, S. J., AL-SUBBARY, A. & AL-AOWAH, M. A. 2004. Geology and Quaternary climate history of Socotra. *Fauna of Arabia*, 20, 27-44.
- FOODY, G. 2008. GIS: biodiversity applications. *Progress in Physical Geography*, 32, 223-235.
- FOODY, G. M. 2003. Geographical weighting as a further refinement to regression modelling: An example focused on the NDVI-rainfall relationship. *Remote Sensing of Environment*, 88, 283-293.
- FOODY, G. M. & ATKINSON, P. M. 2002. *Uncertainty in remote sensing and GIS*, Wiley Online Library.
- FORKEL, M., CARVALHAIS, N., VERBESSELT, J., MAHECHA, M. D., NEIGH, C. S. R. & REICHSTEIN, M. 2013. Trend Change Detection in NDVI Time Series: Effects of Inter-Annual Variability and Methodology. *Remote Sensing*.
- FOTHERINGHAM, A. S., BRUNSDON, C. & CHARLTON, M. 2003. *Geographically weighted regression: the analysis of spatially varying relationships*, John Wiley & Sons.

- FOURNIER, M., HUCHON, P., KHANBARI, K. & LEROY, S. 2007. Segmentation and along-strike asymmetry of the passive margin in Socotra, eastern Gulf of Aden: Are they controlled by detachment faults? *Geochemistry, Geophysics, Geosystems*, 8.
- FOWECA. FAO WORKSHOP ON FORESTRY OUTLOOK STUDY FOR WESTERN AND CENTRAL ASIA (FOWECA). 1st Sub-regional Workshop for Central Asia and the Caucasus 2004 Beirut, Lebanon.
- FRANCH, B., VERMOTE, E., SOBRINO, J. & FÉDÈLE, E. 2013. Analysis of directional effects on atmospheric correction. *Remote Sensing of Environment*, 128, 276-288.
- FRIIS, I. 1992. *Forests and forest trees of northeast tropical Africa: their natural habitats and distribution patterns in Ethiopia, Djibouti and Somalia*, London (UK), Her Majesty's Stationery Office, 1992.
- FRITZ, H. M. & OKAL, E. A. 2008. Socotra island, yemen: Field survey of the 2004 indian ocean tsunami. *Natural Hazards*, 46, 107-117.
- FUCHS, M. & BUERKERT, A. 2008. A 20 ka sediment record from the Hajar Mountain range in N-Oman, and its implication for detecting arid-humid periods on the southeastern Arabian Peninsula. *Earth and Planetary Science Letters*, 265, 546-558.
- FUYI, T., MOHAMMED, S., ABDULLAH, K., LIM, H. & ISHOLA, K. A comparison of atmospheric correction techniques for environmental applications. Space Science and Communication (IconSpace), 2013 IEEE International Conference on, 2013. IEEE, 233-237.
- GANG, C., ZHOU, W., CHEN, Y., WANG, Z., SUN, Z., LI, J., QI, J. & ODEH, I. 2014. Quantitative assessment of the contributions of climate change and human activities on global grassland degradation. *Environmental Earth Sciences*, 72, 4273-4282.
- GAO, B.-C., MONTES, M. J., DAVIS, C. O. & GOETZ, A. F. 2009. Atmospheric correction algorithms for hyperspectral remote sensing data of land and ocean. *Remote Sensing of Environment*, 113, S17-S24.
- GAO, B., PAN, Y., CHEN, Z., WU, F., REN, X. & HU, M. 2016. A Spatial Conditioned Latin Hypercube Sampling Method for Mapping Using Ancillary Data. *Transactions in GIS*.
- GAO, J. 2009. Bathymetric mapping by means of remote sensing: methods, accuracy and limitations. *Progress in Physical Geography*, 33, 103-116.
- GARCIA-HARO, F. J., SOMMER, S. & KEMPER, T. 2005. A new tool for variable multiple endmember spectral mixture analysis (VMESMA). *International Journal of Remote Sensing*, 26, 2135-2162.
- GHAZANFAR, S. A. & FISHER, M. 2013. *Vegetation of the Arabian peninsula*, Springer Science & Business Media.
- GHIMIRE, B., ROGAN, J. & MILLER, J. 2010. Contextual land-cover classification: incorporating spatial dependence in land-cover classification models using random forests and the Getis statistic. *Remote Sensing Letters*, 1, 45-54.
- GIORDANO, L. 2007. Mediterranean vegetation monitoring by remotely sensed data: LAI retrieval and vegetation trend analysis within two forested areas in southern Italy.
- GÓMEZ-HERNÁNDEZ, J., CASSIRAGA, E., GUARDIOLA-ALBERT, C. & RODRÍGUEZ, J. Á. 2001. Incorporating information from a digital elevation model for improving the areal estimation of rainfall. *geoENV III—Geostatistics for Environmental Applications*. Springer.
- GONG, W., YUAN, L., FAN, W., WANG, X. & STOTT, P. 2016. Comparison to Supervised Classification Modelling in Land Use Cover Using Landsat 8 OLI Data: An Example in Miyun County of North China. *Nature Environment and Pollution Technology*, 15, 243.
- GOOVAERTS, P. 1997. *Geostatistics for natural resources evaluation*, Oxford university press.
- GOOVAERTS, P. 2011. A coherent geostatistical approach for combining choropleth map and field data in the spatial interpolation of soil properties. *European journal of soil science*, 62, 371-380.
- GRAETZ, R. D., PECH, R. P. & DAVIS, A. W. 1988. THE ASSESSMENT AND MONITORING OF SPARSELY VEGETATED RANGELANDS USING CALIBRATED LANDSAT DATA. *International Journal of Remote Sensing*, 9, 1201-1222.
- GREGORIO, A. D. & JANSEN, L. J. M. A new concept for a land cover classification system. Proceedings of the Earth Observation and Environmental Information, 1997 Alexandria, Egypt. 13-16.
- GRIFFITH, D. & CHUN, Y. 2014. Spatial autocorrelation and spatial filtering. *Handbook of Regional Science*. Springer.

- GRIFFITH, D. A. 2013. *Spatial autocorrelation and spatial filtering: gaining understanding through theory and scientific visualization*, Springer Science & Business Media.
- GUO, X., ZHANG, H., YUAN, T., ZHAO, J. & XUE, Z. 2015. Detecting the Temporal Scaling Behavior of the Normalized Difference Vegetation Index Time Series in China Using a Detrended Fluctuation Analysis. *Remote Sensing*, 7, 12942-12960.
- GWET, K. 2002. Inter-rater reliability: dependency on trait prevalence and marginal homogeneity. *Statistical Methods for Inter-Rater Reliability Assessment Series*, 2, 1-9.
- HAAKE, B., RIXEN, T. & ITTEKKOT, V. 1993. Variability of monsoonal upwelling signals in the deep western Arabian Sea. *SCOPE/UNEP Sonderband*, 76, 85-96.
- HABROVÁ, H. 2004. Geobiocoenological differentiation as a tool for sustainable land-use of Socotra Island. *Ekologia(Bratislava)/Ecology(Bratislava)*, 23, 47-57.
- HABROVA, H., CERMAK, Z. & PAVLIS, J. 2009. Dragon's blood tree – Threatened by overmaturity, not by extinction: Dynamics of a *Dracaena cinnabari* woodland in the mountains of Soqotra. *Biological Conservation*, 142, 772-778.
- HABROVA, H., KRAL, K. & MADERA, P. THE WEATHER PATTERN IN ONE OF THE OLDEST FOREST ECOSYSTEMS ON EARTH—DRAGONS BLOOD TREE FOREST (*Dracaena cinnabari*) ON FIRMIHIN–SOQOTRA ISLAND. *Klima lesa. Sborník referátů z mezinárodní vědecké konference. Křtiny*, 2007. 2007.
- HAN, M., SUN, Y. N. & XU, S. G. 2007. Characteristics and driving factors of marsh changes in Zhalong wetland of China. *Environmental Monitoring and Assessment*, 127, 363-381.
- HANAFI, A. & JAUFFRET, S. 2008. Are long-term vegetation dynamics useful in monitoring and assessing desertification processes in the arid steppe, southern Tunisia. *Journal of Arid Environments*, 72, 557-572.
- HANSEN, A. J., PIEKIELEK, N., DAVIS, C., HAAS, J., THEOBALD, D. M., GROSS, J. E., MONAHAN, W. B., OLLIFF, T. & RUNNING, S. W. 2014. Exposure of US National Parks to land use and climate change 1900-2100. *Ecological Applications*, 24, 484-502.
- HANTSON, S. & CHUVIECO, E. 2011. Evaluation of different topographic correction methods for Landsat imagery. *International Journal of Applied Earth Observation and Geoinformation*, 13, 691-700.
- HEALEY, S. P., COHEN, W. B., ZHIQIANG, Y. & KRANKINA, O. N. 2005. Comparison of Tasseled Cap-based Landsat data structures for use in forest disturbance detection. *Remote Sensing of Environment*, 97, 301-310.
- HELMER, E. & RUEFENACHT, B. 2005. Cloud-free satellite image mosaics with regression trees and histogram matching. *Photogrammetric engineering and remote sensing*, 71, 1079.
- HELMER, E. H., KENNAWAY, T. A., PEDREROS, D. H., CLARK, M. L., MARCANO-VEGA, H., TIESZEN, L. L., RUZYCKI, T. R., SCHILL, S. R. & SEAN CARRINGTON, C. M. 2008. Land Cover and Forest Formation Distributions for St. Kitts, Nevis, St. Eustatius, Grenada and Barbados from Decision Tree Classification of Cloud-Cleared Satellite Imagery. *Caribbean Journal of Science*, 44, 175-198.
- HEMMING, C. F. The vegetation of the northern region of the Somali Republic. *Proceedings of the Linnean Society of London*, 1966. Wiley Online Library, 173-250.
- HEROLD, M., MAYAUX, P., WOODCOCK, C., BACCINI, A. & SCHMULLIUS, C. 2008. Some challenges in global land cover mapping: An assessment of agreement and accuracy in existing 1 km datasets. *Remote Sensing of Environment*, 112, 2538-2556.
- HERRMANN, S. M., ANYAMBA, A. & TUCKER, C. J. 2005. Recent trends in vegetation dynamics in the African Sahel and their relationship to climate. *Global Environmental Change*, 15, 394-404.
- HERRMANN, S. M. & HUTCHINSON, C. F. 2005. The changing contexts of the desertification debate. *Journal of Arid Environments*, 63, 538-555.
- HESE, S., LUCHT, W., SCHMULLIUS, C., BARNESLEY, M., DUBAYAH, R., KNORR, D., NEUMANN, K., RIEDEL, T. & SCHRÖTER, K. 2005a. Global biomass mapping for an improved understanding of the CO<sub>2</sub> balance—the Earth observation mission Carbon-3D. *Remote Sensing of Environment*, 94, 94-104.
- HESE, S., LUCHT, W., SCHMULLIUS, C., BARNESLEY, M., DUBAYAH, R., KNORR, D., NEUMANN, K., RIEDEL, T. & SCHRÖTER, K. 2005b. Global biomass mapping for an improved understanding of the CO<sub>2</sub>

- balance—the Earth observation mission Carbon-3D. *Remote Sensing of Environment*, 94, 94-104.
- HEUVELINK, G. B. M., PEBESMA, E. & GRÄHLER, B. Space-Time Geostatistics. In: SHEKHAR, S., XIONG, H. & ZHOU, X. (eds.) *Encyclopedia of GIS*. Cham: Springer International Publishing.
- HEVESI, J. A., FLINT, A. L. & ISTOK, J. D. 1992a. Precipitation estimation in mountainous terrain using multivariate geostatistics. Part II: Isohyetal maps. *Journal of Applied Meteorology*, 31, 677-688.
- HEVESI, J. A., ISTOK, J. D. & FLINT, A. L. 1992b. Precipitation estimation in mountainous terrain using multivariate geostatistics. Part I: structural analysis. *Journal of applied meteorology*, 31, 661-676.
- HIERS, J. K., MITCHELL, R. J., BARNETT, A., WALTERS, J. R., MACK, M., WILLIAMS, B. & SUTTER, R. 2012. The dynamic reference concept: measuring restoration success in a rapidly changing no-analogue future. *Ecological Restoration*, 30, 27-36.
- HIRT, C., FILMER, M. & FEATHERSTONE, W. 2010. Comparison and validation of the recent freely available ASTER-GDEM ver1, SRTM ver4. 1 and GEODATA DEM-9S ver3 digital elevation models over Australia. *Australian Journal of Earth Sciences*, 57, 337-347.
- HOBBS, R. J., RICHARDSON, D. M. & DAVIS, G. W. 1995. Opportunities and constraints for studying the function of biodiversity. In: DAVIS, G. W. & RICHARDSON, D. M. (eds.) *Ecological studies-Mediterranean-type ecosystems : the function of biodiversity*. Berlin ; [New York]: Springer-Verlag.
- HOCKING, M. & KELLY, B. F. 2016. Groundwater recharge and time lag measurement through Vertosols using impulse response functions. *Journal of Hydrology*, 535, 22-35.
- HOLMGREN, C. A., BETANCOURT, J. L. & RYLANDER, K. A. 2006. A 36,000-yr vegetation history from the Peloncillo Mountains, southeastern Arizona, USA. *Palaeogeography Palaeoclimatology Palaeoecology*, 240, 405-422.
- HOUNTONDJI, Y. C., SOKPON, N. & OZER, P. 2006. Analysis of the vegetation trends using low resolution remote sensing data in Burkina Faso (1982-1999) for the monitoring of desertification. *International Journal of Remote Sensing*, 27, 871-884.
- HUANG, C., GOWARD, S. N., SCHLEWEIS, K., THOMAS, N., MASEK, J. G. & ZHU, Z. 2009a. Dynamics of national forests assessed using the Landsat record: Case studies in eastern United States. *Remote sensing of Environment*, 113, 1430-1442.
- HUANG, J., CHEN, D. & COSH, M. 2009b. Sub-pixel reflectance unmixing in estimating vegetation water content and dry biomass of corn and soybeans cropland using normalized difference water index (NDWI) from satellites. *International Journal of Remote Sensing*, 30, 2075-2104.
- HUBÁLKOVÁ, I., MADĚRA, P. & VOLAŘÍK, D. 2015. Growth dynamics of *Dracaena cinnabari* under controlled conditions as the most effective way to protect endangered species. *Saudi Journal of Biological Sciences*.
- HUETE, A. R. & TUCKER, C. J. 1991. INVESTIGATION OF SOIL INFLUENCES IN AVHRR RED AND NEAR-INFRARED VEGETATION INDEX IMAGERY. *International Journal of Remote Sensing*, 12, 1223-1242.
- HULME, P. E. 2005. Adapting to climate change: is there scope for ecological management in the face of a global threat? *Journal of Applied ecology*, 42, 784-794.
- HUSSAIN, M., CHEN, D., CHENG, A., WEI, H. & STANLEY, D. 2013. Change detection from remotely sensed images: From pixel-based to object-based approaches. *ISPRS Journal of Photogrammetry and Remote Sensing*, 80, 91-106.
- HUTABARAT, I. M., SAEFUDDIN, A., DJURAIHAH, A. & MANGKU, I. W. 2013. Estimating the Parameters Geographically Weighted Regression (GWR) with Measurement Error. *Open Journal of Statistics*, Vol.03No.06, 5.
- IMRAN, M., STEIN, A. & ZURITA-MILLA, R. 2015. Using geographically weighted regression kriging for crop yield mapping in West Africa. *International Journal of Geographical Information Science*, 29, 234-257.
- ISLAM, K., JASHIMUDDIN, M., NATH, B. & NATH, T. K. 2016. Quantitative Assessment of Land Cover Change Using Landsat Time Series Data: Case of Chunut Wildlife Sanctuary (CWS), Bangladesh. *International Journal of Environment and Geoinformatics*, 3, 45-55.

- IUCN. 2008. *The IUCN World Heritage Outlook* [Online]. Available: <http://www.worldheritageoutlook.iucn.org/search-sites/-/wdpaid/en/903138#> [Accessed].
- IUCN 2010. Guidelines for using the IUCN Red list categories and criteria. Version 8.1. Prepared by the Standards and Petitions Subcommittee in March 2010.
- JENSEN, J. L. R., HUMES, K. S., VIERLING, L. A. & HUDAK, A. T. 2008. Discrete return lidar-based prediction of leaf area index in two conifer forests. *Remote Sensing of Environment*, 112, 3947-3957.
- JENSEN, J. R. 2005. *Introductory digital image processing: A remote sensing perspective*, Pearson College Division.
- JI, L. & PETERS, A. 2004. A spatial regression procedure for evaluating the relationship between AVHRR-NDVI and climate in the northern Great Plains. *International Journal of Remote Sensing*, 25, 297-311.
- JIANG, L., SHANG, S., YANG, Y. & GUAN, H. 2016. Mapping interannual variability of maize cover in a large irrigation district using a vegetation index-phenological index classifier. *Computers and Electronics in Agriculture*, 123, 351-361.
- JIN, Q., ZHANG, J., SHI, M. & HUANG, J. 2016. Estimating Loess Plateau Average Annual Precipitation with Multiple Linear Regression Kriging and Geographically Weighted Regression Kriging. *Water*, 8, 266.
- JOSHI, P. K. K., ROY, P. S., SINGH, S., AGRAWAL, S. & YADAV, D. 2006. Vegetation cover mapping in India using multi-temporal IRS Wide Field Sensor (WiFS) data. *Remote Sensing of Environment*, 103, 190-202.
- JUPP, D. L., KIRK, J. T. & HARRIS, G. P. 1994. Detection, identification and mapping of cyanobacteria—using remote sensing to measure the optical quality of turbid inland waters. *Marine and Freshwater Research*, 45, 801-828.
- KANGALAWA, R. Y. & LYIMO, J. G. 2013. Climate change, adaptive strategies and rural livelihoods in semiarid Tanzania.
- KASZTA, A., MARINO, J., RAMOELO, A. & WOLFF, E. O. 2016. Bulk feeder or selective grazer: African buffalo space use patterns based on fine-scale remotely sensed data on forage quality and quantity. *Ecological Modelling*, 323, 115-122.
- KAUFMAN, Y. J. & TANRE, D. 1992. Atmospherically resistant vegetation index (ARVI) for EOS-MODIS. *Geoscience and Remote Sensing, IEEE Transactions on*, 30, 261-270.
- KERR, R. 2004. *A General History and Collection of Voyages and Travels (Complete) Arranged in Systematic Order: Forming a Complete History of the Origin and Progress of Navigation, Discovery and Commerce by Sea and Land from the Earliest Ages to the Present Time*, Library of Alexandria.
- KHORRAM, S. 1999. *Accuracy assessment of remote sensing-derived change detection*, Asprs Publications.
- KHORRAM, S., VAN DER WIELE, C. F., KOCH, F. H., NELSON, S. A. & POTTS, M. D. 2016. *Principles of Applied Remote Sensing*, Springer.
- KIBRET, K. S., MAROHN, C. & CADISCH, G. 2016. Assessment of land use and land cover change in South Central Ethiopia during four decades based on integrated analysis of multi-temporal images and geospatial vector data. *Remote Sensing Applications: Society and Environment*, 3, 1-19.
- KILIAN, N. & HEIN, P. 2006. New and noteworthy records for the vascular plant flora of Socotra Island, Yemen. *Englera*, 57-77.
- KNAPP, R. 1968. Höhere Vegetationseinheiten von Äthiopien, Somalia, Natal, Transvaal, Kapland und einigen Nachbargebieten. *Geobotanische Mitteilungen*, 56, 1-36.
- KOUTSODENDRIS, A., BRAUER, A., ZACHARIAS, I., PUTYRSKAYA, V., KLEMT, E., SANGIORGI, F. & PROSS, J. 2015. Ecosystem response to human-and climate-induced environmental stress on an anoxic coastal lagoon (Etoliko, Greece) since 1930 AD. *Journal of Paleolimnology*, 53, 255-270.
- KRÁL, K. & PAVLIŠ, J. 2006. The first detailed land-cover map of Socotra Island by Landsat/ETM+ data. *International Journal of Remote Sensing*, 27, 3239-3250.
- KRULL, E. S., SKJEMSTAD, J. O., BURROWS, W. H., BRAY, S. G., WYNN, J. G., BOL, R., SPOUNCER, L. & HARMS, B. 2005. Recent vegetation changes in central Queensland, Australia: Evidence from  $\delta^{13}C$  and  $\delta^{14}C$  analyses of soil organic matter. *Geoderma*, 126, 241-259.



- KRUPP, F. 2004. Socotra. Fauna of Arabia. 2ed ed.
- KURSCHNER, H. & OCHYRA, R. 2004. Remarkable new records to the bryophyte flora of Yemen (al-Mahra and Socotra Island). Additions to the Bryophyte Flora of the Arabian Peninsula and Socotra 6. *Cryptogamie Bryologie*, 25, 69-81.
- LANDIS, J. R. & KOCH, G. G. 1977a. The Measurement of Observer Agreement for Categorical Data. *Biometrics*, 33, 159-174.
- LANDIS, J. R. & KOCH, G. G. 1977b. The measurement of observer agreement for categorical data. *biometrics*, 159-174.
- LÁZARO, R., RODRIGO, F., GUTIÉRREZ, L., DOMINGO, F. & PUIGDEFÁBREGAS, J. 2001. Analysis of a 30-year rainfall record (1967–1997) in semi–arid SE Spain for implications on vegetation. *Journal of arid environments*, 48, 373-395.
- LE BRIS, A., TASSIN, F. & CHEHATA, N. Contribution of texture and red-edge band for vegetated areas detection and identification. 2013 IEEE International Geoscience and Remote Sensing Symposium-IGARSS, 2013. IEEE, 4102-4105.
- LE HOUEROU, H. N. 2003. Bioclimatology and phytogeography of the Red Sea and Aden Gulf Basins: A monograph (with a particular reference to the Highland Evergreen Sclerophylls and Lowland Halophytes). *Arid Land Research and Management*, 17, 177-256.
- LEE, M., LEE, S., EO, Y., PYEON, M., MOON, K. & HAN, S. Analysis on the effect of Landsat NDVI by atmospheric correction methods. Advances in Civil, Architectural, Structural and Constructional Engineering: Proceedings of the International Conference on Civil, Architectural, Structural and Constructional Engineering, Dong-A University, Busan, South Korea, August 21-23, 2015, 2016. CRC Press, 375.
- LEENDERS, J. K., VISSER, S. M. & STROOSNIJDER, L. 2005. Farmers' perceptions of the role of scattered vegetation in wind erosion control on arable land in Burkina Faso. *Land Degradation & Development*, 16, 327-337.
- LI, J., LEWIS, J., ROWLAND, J., TAPPAN, G. & TIESZEN, L. 2004. Evaluation of land performance in Senegal using multi-temporal NDVI and rainfall series. *Journal of Arid Environments*, 59, 463-480.
- LI, X., LI, R., LI, G., WANG, H., LI, Z., LI, X. & HOU, X. 2016a. Human-induced vegetation degradation and response of soil nitrogen storage in typical steppes in Inner Mongolia, China. *Journal of Arid Environments*, 124, 80-90.
- LI, X., ZHANG, Y., LUO, J., JIN, X., XU, Y. & YANG, W. 2016b. Quantification winter wheat LAI with HJ-1CCD image features over multiple growing seasons. *International Journal of Applied Earth Observation and Geoinformation*, 44, 104-112.
- LI, Z., HUFFMAN, T., MCCONKEY, B. & TOWNLEY-SMITH, L. 2013. Monitoring and modeling spatial and temporal patterns of grassland dynamics using time-series MODIS NDVI with climate and stocking data. *Remote Sensing of Environment*, 138, 232-244.
- LI, Z., WU, W., LIU, X., FATH, B. D., SUN, H., LIU, X., XIAO, X. & CAO, J. 2016c. Land use/cover change and regional climate change in an arid grassland ecosystem of Inner Mongolia, China. *Ecological Modelling*.
- LI, Z. G., WANG, Y. L., ZHOU, Q. B., WU, J. S., PENG, J. & CHANG, H. F. 2008. Spatiotemporal variability of land surface moisture based on vegetation and temperature characteristics in Northern Shaanxi Loess Plateau, China. *Journal of Arid Environments*, 72, 971-982.
- LIANG, E., SHAO, X. & HE, J. 2005. Relationships between tree growth and NDVI of grassland in the semi-arid grassland of north China. *International Journal of Remote Sensing*, 26, 2901-2908.
- LIN, C.-H., TSAI, P.-H., LAI, K.-H. & CHEN, J.-Y. 2013. Cloud removal from multitemporal satellite images using information cloning. *Geoscience and Remote Sensing, IEEE Transactions on*, 51, 232-241.
- LISA M. BANFIELD, K. V. D., MILLER, A. G., BANFIELD, L. M., KAY VAN DAMME, & MILLER., A. G. 2011. *Evolution and biogeography of the flora of the Socotra archipelago (Yemen)The Biology of Island Floras*, Cambridge University Press.
- LIU, J.-H., WU, J.-J., WU, Z.-T., LU, A.-F. & YUE, J.-W. Interactions between climate change and human activities in dryland degradation in Beijing-Tianjin sand-storm source region, China. Geoscience and Remote Sensing Symposium (IGARSS), 2012 IEEE International, 2012. IEEE, 6416-6419.

- LIU, S., WANG, B., ZHANG, J., CAI, D., TIAN, G. & ZHANG, G. 2016. Predicting the Seasonal NDVI Change by GIS Geostatistical Analyst and Study on Driver Factors of NDVI Change in Hainan Island, China. *Journal of Geoscience and Environment Protection*, 4, 92.
- LLOYD, C. D. 2002. Increasing the accuracy of predictions of monthly precipitation in Great Britain using kriging with an external drift. *Uncertainty in remote sensing and GIS*, 243-269.
- LOBO, A., LEGENDRE, P., REBOLLAR, J. L. G., CARRERAS, J. & NINOT, J. M. 2004. Land cover classification at a regional scale in Iberia: separability in a multi-temporal and multi-spectral data set of satellite images. *International Journal of Remote Sensing*, 25, 205-213.
- LOOG, M. 2016. Contrastive Pessimistic Likelihood Estimation for Semi-Supervised Classification. *IEEE Transactions on Pattern Analysis and Machine Intelligence*, 38, 462-475.
- LU, D., MAUSEL, P., BATISTELLA, M. & MORAN, E. 2005. Land-cover binary change detection methods for use in the moist tropical region of the Amazon: a comparative study. *International Journal of Remote Sensing*, 26, 101-114.
- LU, D., MAUSEL, P., BRONDIZIO, E. & MORAN, E. 2004. Change detection techniques. *International journal of remote sensing*, 25, 2365-2401.
- LU, D. & WENG, Q. 2007. A survey of image classification methods and techniques for improving classification performance. *International journal of Remote sensing*, 28, 823-870.
- LUNETTA, R. S., KNIGHT, J. F., EDIRIWICKREMA, J., LYON, J. G. & WORTHY, L. D. 2006. Land-cover change detection using multi-temporal MODIS NDVI data. *Remote sensing of environment*, 105, 142-154.
- MACQUEEN, J. Some methods for classification and analysis of multivariate observations. Proceedings of the fifth Berkeley symposium on mathematical statistics and probability, 1967. Oakland, CA, USA., 281-297.
- MADIN, E. M., DILL, L. M., RIDLON, A. D., HEITHAUS, M. R. & WARNER, R. R. 2016. Human activities change marine ecosystems by altering predation risk. *Global change biology*, 22, 44-60.
- MAGDEFRAU, K. 1975. AGE OF LARGE DRACAENA SPECIMENS OF TENERIFE. *Flora*, 164, 347-357.
- MAHI, H., FARHI, N. & LABED, K. 2015. Remotely Sensed Data Clustering Using K-Harmonic Means Algorithm and Cluster Validity Index. *Computer Science and Its Applications*. Springer.
- MAJID, M. R., JAFFAR, A. R., MAN, N. C., VAZIRI, M. & SULEMANA, M. 2016. MAPPING POVERTY HOT SPOTS IN PENINSULAR MALAYSIA USING SPATIAL AUTOCORRELATION ANALYSIS. *PLANNING MALAYSIA JOURNAL*, 14.
- MAJOR, D. J., BARET, F. & GUYOT, G. 1990. A RATIO VEGETATION INDEX ADJUSTED FOR SOIL BRIGHTNESS. *International Journal of Remote Sensing*, 11, 727-740.
- MALATESTA, L., ATTORRE, F., ALTOBELLI, A., ADEEB, A., DE SANCTIS, M., TALEB, N. M., SCHOLTE, P. T. & VITALE, M. 2013. Vegetation mapping from high-resolution satellite images in the heterogeneous arid environments of Socotra Island (Yemen). *Journal of Applied Remote Sensing*, 7, 073527-073527.
- MANCINO, G., NOLÈ, A., RIPULLONE, F. & FERRARA, A. 2014. Landsat TM imagery and NDVI differencing to detect vegetation change: assessing natural forest expansion in Basilicata, southern Italy. *iForest-Biogeosciences and Forestry*, 7, 75.
- MAO, Z., PAN, D., HE, X., CHEN, J., TAO, B., CHEN, P., HAO, Z., BAI, Y., ZHU, Q. & HUANG, H. 2016. A Unified Algorithm for the Atmospheric Correction of Satellite Remote Sensing Data over Land and Ocean. *Remote Sensing*, 8, 536.
- MARKOS, A. & YOUSSEF, R. QUANTITATIVE ASSESSMENT OF FOREST COVER CHANGE OF FOGERA WOREDA USING NDVI TECHNIQUE.
- MARTIN, H. 2006. Cenozoic climatic change and the development of the arid vegetation in Australia. *Journal of Arid Environments*, 66, 533-563.
- MARTÍNEZ, B. & GILABERT, M. A. 2009. Vegetation dynamics from NDVI time series analysis using the wavelet transform. *Remote Sensing of Environment*, 113, 1823-1842.
- MARTINUZZI, S., GOULD, W. A. & GONZÁLEZ, O. M. R. 2007. *Creating cloud-free Landsat ETM+ data sets in tropical landscapes: cloud and cloud-shadow removal*, US Department of Agriculture, Forest Service, International Institute of Tropical Forestry Río Piedras, Puerto Rico.

- MARTINY, N., CAMBERLIN, P., RICHARD, Y. & PHILIPPON, N. 2006. Compared regimes of NDVI and rainfall in semi-arid regions of Africa. *International Journal of Remote Sensing*, 27, 5201-5223.
- MAS, J.-F. 1999. Monitoring land-cover changes: a comparison of change detection techniques. *International journal of remote sensing*, 20, 139-152.
- MATHER, P. & TSO, B. 2016. *Classification methods for remotely sensed data*, CRC press.
- MCCALLUM, I., WAGNER, W., SCHMULLIUS, C., SHVIDENKO, A., OBERSTEINER, M., FRITZ, S. & NILSSON, S. 2010. Comparison of four global FAPAR datasets over Northern Eurasia for the year 2000. *Remote Sensing of Environment*, 114, 941-949.
- MIEBACH, A., NIESTRATH, P., ROESER, P. & LITT, T. 2016. Impacts of climate and humans on the vegetation in northwestern Turkey: palynological insights from Lake Iznik since the Last Glacial. *Climate of the Past*, 12, 575-593.
- MIES, B. 1993. Socotra - botanically as curious as neglected. *International lichenological newsletter*, 26, 51-52.
- MIES, B. 1999. Neue Pflanzenassoziationen des Crotonion socotrani Mi. 1999 von der Insel Soqotra (Jemen, Indischer Ozean). *Acta Biologica Benrodis*, 10, 27-48.
- MIES, B. & ZIMMER, H. 1993. Die Vegetation der Insel Sokotra im Indischen Ozean. *Natur und Museum*, 123, 253-264.
- MIES, B. A. 1995. On the comparison of the flora and vegetation of the island groups of Socotra and Macaronesia.
- MIES, B. A. 2001. Flora und Vegetationsökologie der Insel Soqotra. *Essener Ökologische Schriften*.
- MIES BA, B. F. 1996. The vegetation ecology of Soqotra. *Proceedings of the first international symposium on Soqotra Island*, I UN Publications, 48.
- MILLER, A. & BAZARA, A. M. (1998): The conservation status of the flora of the Soqotran archipelago. Proc. First Int. Symp. Soqotra Island: Present and Future, Aden, 1996. 15-34.
- MILLER, A. & MORRIS, M. 2001. Conservation and Sustainable Use of the Biodiversity of the Soqotra Archipelago. Final Report. GEF. YEM/96.
- MILLER, A. & MORRIS, M. Ethnoflora of the Sqotra archipelago. 2004a The Royal Botanic Garden Edinburgh, UK.
- MILLER, A. G., COPE, T. A., NYBERG, J. A., ROYAL BOTANIC GARDEN EDINBURGH. & ROYAL BOTANIC GARDENS KEW. 1996. *Flora of the Arabian Peninsula and Socotra*, Edinburgh, Edinburgh University Press in association with Royal Botanic Garden, Edinburgh, Royal Botanic Gardens, Kew.
- MILLER, A. G. & MORRIS, M. 1988. Plants of Dhofar: the southern region of Oman, traditional, economic and medicinal uses. *Oman: Office of the Adviser for Conservation of the Environment, Diwan of Royal Court Sultanate of Oman xxvii, 361p.-col. illus. ISBN, 715708082*.
- MILLER, A. G. & MORRIS, M. 2004b. Ethnoflora of the Soqotra Archipelago. Royal Botanical Garden: Edinburgh, UK.
- MILLER, J. & ROGAN, J. 2007. Using GIS and remote sensing for ecological mapping and monitoring. *Integration of GIS and remote sensing*.
- MITHAL, V., KHANDELWAL, A., BORIAH, S., STEINHAEUSER, K. & KUMAR, V. Change detection from temporal sequences of class labels: application to land cover change mapping. SIAM International Conference on Data mining, Austin, TX, USA, 2013. Citeseer, 2-4.
- MIURA, T., HUETE, A., LEEUWEN, W. & DIDAN, K. 1998. Vegetation detection through smoke-filled AVIRIS images: An assessment using MODIS band passes. *Journal of Geophysical Research: Atmospheres (1984–2012)*, 103, 32001-32011.
- MOFFETT, K., NARDIN, W., SILVESTRI, S., WANG, C. & TEMMERMAN, S. 2015. Multiple Stable States and Catastrophic Shifts in Coastal Wetlands: Progress, Challenges, and Opportunities in Validating Theory Using Remote Sensing and Other Methods. *Remote Sensing*, 7, 10184.
- MOLEELE, N., RINGROSE, S., ARNBERG, W., LUNDEN, B. & VANDERPOST, C. 2001. Assessment of vegetation indexes useful for browse (forage) prediction in semi-arid rangelands. *International Journal of Remote Sensing*, 22, 741-756.
- MORISSETTE, J. T. & KHORRAM, S. 2000. Accuracy assessment curves for satellite-based change detection. *Photogrammetric Engineering and Remote Sensing*, 66, 875-880.

- MORRIS, M. 2002. Manual of traditional land use practices in the Soqotra Archipelago. *Unpublished Report. YEM/96 G*, 32.
- MUBEA, K., NGIGI, T. & MUNDIA, C. 2016. ASSESSING APPLICATION OF MARKOV CHAIN ANALYSIS IN PREDICTING LAND COVER CHANGE.
- MULLER, C. 2007. Soil of dry Tropics. Process and structure indicator-supported analysis of layered, polygenetic and degraded soil of island Socotra (Jemen). *Erdkunde*, 61, 387-388.
- MURWIRA, A. & SKIDMORE, A. K. 2005. The response of elephants to the spatial heterogeneity of vegetation in a Southern African agricultural landscape. *Landscape Ecology*, 20, 217-234.
- MUSAOGLU, N., COSKUN, M. & KOCABAS, V. 2005. Land use change analysis of Beykoz-Istanbul by means of satellite images and GIS. *Water Science and Technology*, 51, 245-251.
- MUTANGA, O., PRINS, H. H. T., SKIDMORE, A. K., WIEREN, S., HUIZING, H., GRANT, R., PEEL, M. & BIGGS, H. 2004. Explaining grass-nutrient patterns in a savanna rangeland of southern Africa. *Journal of Biogeography*, 31, 819-829.
- MUTANGA, O. & SKIDMORE, A. K. 2004. Narrow band vegetation indices overcome the saturation problem in biomass estimation. *International Journal of Remote Sensing*, 25, 3999-4014.
- MWE-EPA 2004. YEMEN FIRST NATIONAL REPORT TO THE CONVENTION ON BIOLOGICAL DIVERSITY. Sana'a: Ministry of Water and Environment - Environment Protection Authority.
- MYERS, N., MITTERMEIER, R. A., MITTERMEIER, C. G., DA FONSECA, G. A. & KENT, J. 2000. Biodiversity hotspots for conservation priorities. *Nature*, 403, 853-858.
- MYNENI, R. B., DONG, J., TUCKER, C., KAUFMANN, R., KAUPPI, P., LISKI, J., ZHOU, L., ALEXEYEV, V. & HUGHES, M. 2001. A large carbon sink in the woody biomass of northern forests. *Proceedings of the National Academy of Sciences*, 98, 14784-14789.
- NANGENDO, G., SKIDMORE, A. K. & VAN OOSTEN, H. 2007. Mapping East African tropical forests and woodlands - A comparison of classifiers. *Isprs Journal of Photogrammetry and Remote Sensing*, 61, 393-404.
- NATH, B. 2014. Quantitative Assessment of Forest Cover Change of a Part of Bandarban Hill Tracts Using NDVI Techniques. *Journal of Geosciences and Geomatics*, 2, 21-27.
- NAUMKIN, V. 1993. Island of the phoenix. An ethnographic study of the people of Socotra. *Ithaca Press*.
- NEMANI, R. R., KEELING, C. D., HASHIMOTO, H., JOLLY, W. M., PIPER, S. C., TUCKER, C. J., MYNENI, R. B. & RUNNING, S. W. 2003. Climate-driven increases in global terrestrial net primary production from 1982 to 1999. *science*, 300, 1560-1563.
- NICHOLSON, S. E., DAVENPORT, M. L. & MALO, A. R. 1990a. A COMPARISON OF THE VEGETATION RESPONSE TO RAINFALL IN THE SAHEL AND EAST-AFRICA, USING NORMALIZED DIFFERENCE VEGETATION INDEX FROM NOAA AVHRR. *Climatic Change*, 17, 209-241.
- NICHOLSON, S. E., DAVENPORT, M. L. & MALO, A. R. 1990b. A comparison of the vegetation response to rainfall in the Sahel and East Africa, using normalized difference vegetation index from NOAA AVHRR. *Climatic Change*, 17, 209-241.
- NICHOLSON, S. E., TUCKER, C. J. & BA, M. B. 1998. Desertification, drought, and surface vegetation: An example from the West African Sahel. *Bulletin of the American Meteorological Society*, 79, 815-829.
- NIDUMOLU, U. B., DE BIE, C., VAN KEULEN, H., SKIDMORE, A. K. & HARMSSEN, K. 2006. Review of a land use planning programme through the soft systems methodology. *Land Use Policy*, 23, 187-203.
- NOOMEN, M. F., SMITH, K. L., COLLS, J. J., STEVEN, M. D., SKIDMORE, A. K. & VAN DER MEER, F. D. 2008. Hyperspectral indices for detecting changes in canopy reflectance as a result of underground natural gas leakage. *International Journal of Remote Sensing*, 29, 5987-6008.
- OBA, G., WELADJI, R. B., LUSIGI, W. J. & STENSETH, N. C. 2003. Scale-dependent effects of grazing on rangeland degradation in northern Kenya: A test of equilibrium and non-equilibrium hypotheses. *Land Degradation & Development*, 14, 83-94.
- OKIN, G. S. & GU, J. 2015. The impact of atmospheric conditions and instrument noise on atmospheric correction and spectral mixture analysis of multispectral imagery. *Remote Sensing of Environment*, 164, 130-141.
- OLDFIELD, S. & SHEPPARD, C. 1997. Conservation of biodiversity and research needs in the UK Dependent Territories. *Journal of Applied Ecology*, 1111-1121.

- OLSSON, L., EKLUNDH, L. & ARDÖ, J. 2005. A recent greening of the Sahel—trends, patterns and potential causes. *Journal of Arid Environments*, 63, 556-566.
- ORGANISATION, C. S. 2007. "Final Census Results 2004: The General Frame of the Population Final Results (First Report)". *The General Population Housing and Establishment Census 2004*. ed. Sana'a, Yemen: Central Statistical Organization.
- PADILLA, M., STEHMAN, S. V., RAMO, R., CORTI, D., HANTSON, S., OLIVA, P., ALONSO-CANAS, I., BRADLEY, A. V., TANSEY, K. & MOTA, B. 2015. Comparing the accuracies of remote sensing global burned area products using stratified random sampling and estimation. *Remote Sensing of Environment*, 160, 114-121.
- PARUELO, J. M. & LAUENROTH, W. K. 1998. Interannual variability of NDVI and its relationship to climate for North American shrublands and grasslands. *Journal of Biogeography*, 25, 721-733.
- PAUL REICH, H. E., SELIM KAPUR , ERHAN AKCA. 2001. LAND DEGRADATION AND DESERTIFICATION IN DESERT MARGINS. Available: [http://www.toprak.org.tr/isd/isd\\_36.htm](http://www.toprak.org.tr/isd/isd_36.htm).
- PAULAY, G. 1994. Biodiversity on oceanic islands: its origin and extinction1. *American Zoologist*, 34, 134-144.
- PETERSEN, S. L. & STRINGHAM, T. K. 2008. Development of GIS-based models to predict plant community structure in relation to western juniper establishment. *Forest Ecology and Management*, 256, 981-989.
- PETIT, C. & LAMBIN, E. 2001. Integration of multi-source remote sensing data for land cover change detection. *International Journal of Geographical Information Science*, 15, 785-803.
- PHUA, M. H., TSUYUKI, S., FURUYA, N. & LEE, J. S. 2008. Detecting deforestation with a spectral change detection approach using multitemporal Landsat data: A case study of Kinabalu Park, Sabah, Malaysia. *Journal of Environmental Management*, 88, 784-795.
- PIAO, S., FANG, J., ZHOU, L., GUO, Q., HENDERSON, M., JI, W., LI, Y. & TAO, S. 2003. Interannual variations of monthly and seasonal normalized difference vegetation index (NDVI) in China from 1982 to 1999. *Journal of Geophysical Research: Atmospheres (1984–2012)*, 108.
- PICHI-SERMOLLI, R. 1955. Tropical East Africa (Ethiopia, Somaliland, Kenya, Tanganyika). *Arid Zone Res*, 6, 302-360.
- PICHI-SERMOLLI, R. E. 1957. Una carta geobotanica dell'Africa Orientale (Eritrea, Etiopia, Somalia). *Webbia*, 13, 15-132.
- PICKUP, G. 1998. Desertification and climate change - the Australian perspective. *Climate Research*, 11, 51-63.
- PICKUP, G. & CHEWINGS, V. H. 1988. ESTIMATING THE DISTRIBUTION OF GRAZING AND PATTERNS OF CATTLE MOVEMENT IN A LARGE ARID ZONE PADDOCK - AN APPROACH USING ANIMAL DISTRIBUTION MODELS AND LANDSAT IMAGERY. *International Journal of Remote Sensing*, 9, 1469-1490.
- PIETSCH, D. 2007. Structure- and process-related indicators for dry-Tropical soil development, Socotra Island (Yemen). *Geophysical Research Abstracts*, 9.
- PIETSCH, D. & KÜHN, P. 2009. Soil developmental stages of layered Cambisols and Calcisols on Socotra Island, Yemen. *Soil Science*, 174, 292-302.
- PIETSCH, D. & LUCKE, B. 2008. Soil substrate classification and the FAO and World Reference Base systems: examples from Yemen and Jordan. *European Journal of Soil Science*, 59, 824-834.
- PIETSCH, D. & MORRIS, M. 2010. Modern and ancient knowledge of conserving soils in Socotra Island, Yemen. *Land Degradation and Desertification: Assessment, Mitigation and Remediation*. Springer.
- PINZON, J. E. & TUCKER, C. J. 2014. A non-stationary 1981–2012 AVHRR NDVI3g time series. *Remote Sensing*, 6, 6929-6960.
- PLUTZAR, C., KROISLEITNER, C., FETZEL, T. & ERB, K.-H. 2016. Method PrÃ©cis: Using Geographic Information Systems in Social Ecology. *Social Ecology: Society-Nature Relations across Time and Space*, 5, 311.
- POLYAKOVA, M. A. 2016. Trends in the formation of cenotic diversity of steppe vegetation in mountain steppe landscapes of Khakassia. *Russian Journal of Ecology*, 47, 207-210.

- POPOV, G. 1957. The vegetation of Socotra. *Journal of the Linnean Society of London, Botany*, 55, 706-720.
- POTTER, J. 1984. The channel correlation method for estimating aerosol levels from multispectral scanner data: the errors in this method are small enough to make it useful for such applications as monitoring smoke plumes. *Photogrammetric engineering and remote sensing*, 50, 43-52.
- PROPASTIN, P. 2007. *Remote Sensing Based Study on Vegetation Dynamics in Dry Lands of Kazakhstan*, Ibidem-Verlag.
- PROPASTIN, P., KAPPAS, M. & MURATOVA, N. 2008. A remote sensing based monitoring system for discrimination between climate and human-induced vegetation change in Central Asia. *Management of Environmental Quality: An International Journal*, 19, 579-596.
- PU, R. L., GONG, P., TIAN, Y., MIAO, X., CARRUTHERS, R. I. & ANDERSON, G. L. 2008. Using classification and NDVI differencing methods for monitoring sparse vegetation coverage: a case study of saltcedar in Nevada, USA. *International Journal of Remote Sensing*, 29, 3987-4011.
- QU, B., ZHU, W., JIA, S. & LV, A. 2015. Spatio-Temporal Changes in Vegetation Activity and Its Driving Factors during the Growing Season in China from 1982 to 2011. *Remote Sensing*, 7, 13729-13752.
- RAJA, S. K. S., DAS, J. A. B. & KUMAR, K. D. 2016. Image Enhancement by Image Fusion for Crime Investigation. *International Journal of Image Processing (IJIP)*, 10, 85.
- RAP-CMO 2004. DRAFT SECTORAL ENVIRONMENTAL ASSESSMENT-TECHNIPLAN In: SERVICES, S. E. (ed.) *Yemen. Rural Access Program*. Rome: Rural Access Project - Central Management Office (RAP CMO).
- RASMUSSEN, M. S. 1998. Developing simple, operational, consistent NDVI-vegetation models by applying environmental and climatic information: Part I. Assessment of net primary production. *International Journal of Remote Sensing*, 19, 97-117.
- RATHJENS, C., RATHJENS, C. & SAMLENSKI, E. 1956. *Beiträge zur Klimakunde Südwest-Arabiens: das Klima von Sana: das Klima von Jemen*, Dt. Wetterdienst, Seewetteramt.
- REED, M. S., DOUGILL, A. J. & TAYLOR, M. J. 2007. Integrating local and scientific knowledge for adaptation to land degradation: Kalahari rangeland management options. *Land Degradation & Development*, 18, 249-268.
- REY, S. J., STEPHENS, P. & LAURA, J. 2016. An evaluation of sampling and full enumeration strategies for Fisher Jenks classification in big data settings. *Transactions in GIS*.
- REYNOLDS, J. F., STAFFORD SMITH, D. M., LAMBIN, E. F., TURNER, B. L., MORTIMORE, M., BATTERBURY, S. P. J., DOWNING, T. E., DOWLATABADI, H., FERNANDEZ, R. J., HERRICK, J. E., HUBER-SANNWALD, E., JIANG, H., LEEMANS, R., LYNAM, T., MAESTRE, F. T., AYARZA, M. & WALKER, B. 2007. Global desertification: Building a science for dryland development. *Science*, 316, 847-851.
- RICHARD, Y. & POCCARD, I. 1998. A statistical study of NDVI sensitivity to seasonal and interannual rainfall variations in Southern Africa. *International Journal of Remote Sensing*, 19, 2907-2920.
- RICHTER, R. 1996. A spatially adaptive fast atmospheric correction algorithm. *International Journal of Remote Sensing*, 17, 1201-1214.
- RICHTER, R., KELLENBERGER, T. & KAUFMANN, H. 2009. Comparison of topographic correction methods. *Remote Sensing*, 1, 184-196.
- RICHTER, R. & SCHLÄPFER, D. 2011. Atmospheric/topographic correction for airborne imagery. *ATCOR-4 user guide*, 565-02.
- RICHTER, R. & SCHLÄPFER, D. 2014. Atmospheric/Topographic Correction for Satellite Imagery. Version 8.3.1 ed. Germany: DLR: Wessling.
- RICHTER, R. & SCHLÄPFER, D. 2016. Atmospheric/topographic correction for satellite imagery. *DLR report DLR-IB, ATCOR-2/3 User Guide*, 565-01.
- RICKLEFS, R. E. 1987. Community diversity: relative roles of local and regional processes. *Science*, 235, 167-171.
- RIETKERK, M., DEKKER, S. C., DE RUITER, P. C. & VAN DE KOPPEL, J. 2004. Self-organized patchiness and catastrophic shifts in ecosystems. *Science*, 305, 1926-1929.
- RITZEMA, H. 2006. Mission to support the development of the course module on integrated coastal zone management. Wageningen University.

- RODER, A., KUEMMERLE, T., HILL, J., PAPANASTASIS, V. P. & TSIOURLIS, G. M. 2007. Adaptation of a grazing gradient concept to heterogeneous Mediterranean rangelands using cost surface modelling. *Ecological Modelling*, 204, 387-398.
- RODER, A., UDELHOVEN, T., HILL, J., DEL BARRIO, G. & TSIOURLIS, G. 2008. Trend analysis of Landsat-TM and -ETM+ imagery to monitor grazing impact in a rangeland ecosystem in Northern Greece. *Remote Sensing of Environment*, 112, 2863-2875.
- ROFF, A., LYONS, M., JONES, H. & THONELL, J. 2016. Reliability of map accuracy assessments: A comment on Hunter et al.(2016). *Ecological Management & Restoration*, 17, 124-127.
- RÖSSLER, M. 2006. World heritage cultural landscapes: a UNESCO flagship programme 1992–2006. *Landscape Research*, 31, 333-353.
- ROTENBERG, E. & YAKIR, D. 2010. Contribution of semi-arid forests to the climate system. *Science*, 327, 451-454.
- RUELLAND, D., DEZETTER, A., PUECH, C. & ARDOIN-BARDIN, S. 2008. Long-term monitoring of land cover changes based on Landsat imagery to improve hydrological modelling in West Africa. *International Journal of Remote Sensing*, 29, 3533-3551.
- SAHU, K. C. 2007. *Textbook of remote sensing and geographical information systems*, Atlantic Publishers & Dist.
- SANTOS, A. R. O., DA SILVA, A. A. M., LAMY FILHO, F., BATISTA, R. F. L., DE BRITTO, M. T. S. S., ROCHA, L. J. L. F., LAMY, Z. C. & DE CARVALHO RODRIGUES, M. 2014. RELAÇÕES DE PODER NO PROCESSO DE TRABALHO DAS AÇÕES DE CONTROLE DA DENGUE/RELATIONS OF POWER IN THE WORKING PROCESS OF DENGUE CONTROL ACTIVITIES. *Revista de Pesquisa em Saúde*, 15.
- SARKAR, S. & KAFATOS, M. 2004. Interannual variability of vegetation over the Indian sub-continent and its relation to the different meteorological parameters. *Remote Sensing of Environment*, 90, 268-280.
- SCHEFFER, M. & CARPENTER, S. R. 2003. Catastrophic regime shifts in ecosystems: linking theory to observation. *Trends in Ecology & Evolution*, 18, 648-656.
- SCHEFFER, M., STRAILE, D., VAN NES, E. H. & HOSPER, H. 2001. Climatic warming causes regime shifts in lake food webs. *Limnology and Oceanography*, 46, 1780-1783.
- SCHMIDT, K. S., SKIDMORE, A. K., KLOOSTERMAN, E. H., VAN OOSTEN, H., KUMAR, L. & JANSSEN, J. A. M. 2004. Mapping coastal vegetation using an expert system and hyperspectral imagery. *Photogrammetric Engineering and Remote Sensing*, 70, 703-715.
- SCHNEIDER, U., BECKER, A., FINGER, P., MEYER-CHRISTOFFER, A., ZIESE, M. & RUDOLF, B. 2014. GPCC's new land surface precipitation climatology based on quality-controlled in situ data and its role in quantifying the global water cycle. *Theoretical and Applied Climatology*, 115, 15-40.
- SCHOLTE, P., AL-OKAISHI, A. & SULEYMAN, A. S. 2011. When conservation precedes development: a case study of the opening up of the Socotra archipelago, Yemen. *Oryx*, 45, 401-410.
- SCHOLTE, P. & DE GEEST, P. 2010. The climate of Socotra Island (Yemen): A first-time assessment of the timing of the monsoon wind reversal and its influence on precipitation and vegetation patterns. *Journal of Arid Environments*, 74, 1507-1515.
- SCHOLTE, P., MILLER, A., SHAMSAN, A., SULEIMAN, A. S., TALEB, N., MILROY, T., ATTORRE, F., PORTER, R., CARUGATI, C. & PELLA, F. 2008. Goats: part of the problem or the solution to biodiversity conservation on Socotra. *Report to UNESCO-IUCN to Support Socotra's Listing as World Heritage Site*.
- SCHOLTE, S., VASILEIADOU, E. & PETERSEN, A. C. 2013. Opening up the societal debate on climate engineering: how newspaper frames are changing. *Journal of Integrative Environmental Sciences*, 10, 1-16.
- SCHULTZ, P. & HALPERT, M. 1995. Global analysis of the relationships among a vegetation index, precipitation and land surface temperature. *Remote Sensing*, 16, 2755-2777.
- SCHWANTES, A. M., SWENSON, J. J. & JACKSON, R. B. 2016. Quantifying drought-induced tree mortality in the open canopy woodlands of central Texas. *Remote Sensing of Environment*, 181, 54-64.
- SCHWEIK, C. M. & GREEN, G. M. 1999. The use of spectral mixture analysis to study human incentives, actions, and environmental outcomes. *Social Science Computer Review*, 17, 40-63.

- SENAN, A., TOMASETTO, F., FARCOMENI, A., SOMASHEKAR, R. & ATTORRE, F. 2012. Determinants of plant species invasions in an arid island: evidence from Socotra Island (Yemen). *Plant Ecology*, 213, 1381-1392.
- SHEN, B., FANG, S. & LI, G. 2014. Vegetation Coverage Changes and Their Response to Meteorological Variables from 2000 to 2009 in Naqu, Tibet, China. *Canadian Journal of Remote Sensing*, 00-00.
- SHOSHANY, M. 2000. Satellite remote sensing of natural Mediterranean vegetation: a review within an ecological context. *Progress in Physical Geography*, 24, 153-178.
- SHOSHANY, M., LAVEE, H. & KUTIEL, P. 1995. SEASONAL VEGETATION COVER CHANGES AS INDICATORS OF SOIL TYPES ALONG A CLIMATOLOGICAL GRADIENT - A MUTUAL STUDY OF ENVIRONMENTAL PATTERNS AND CONTROLS USING REMOTE-SENSING. *International Journal of Remote Sensing*, 16, 2137-2151.
- SINDACO, R., METALLINO, M., PUPIN, F., FASOLA, M. & CARRANZA, S. 2012. Forgotten in the ocean: systematics, biogeography and evolution of the *Trachylepis* skinks of the Socotra Archipelago. *Zoologica Scripta*, 41, 346-362.
- SINGH, A. 1989. Review article digital change detection techniques using remotely-sensed data. *International journal of remote sensing*, 10, 989-1003.
- SKIDMORE, A. & PRINS, H. 2002. *Environmental modelling with GIS and remote sensing*, London ; New York, Taylor & Francis.
- SKIDMORE, A. K., TURNER, B. J., BRINKHOF, W. & KNOWLES, E. 1997. Performance of a neural network: Mapping forests using GIS and remotely sensed data. *Photogrammetric Engineering and Remote Sensing*, 63, 501-514.
- SKOLE, D. & TUCKER, C. 1993. TROPICAL DEFORESTATION AND HABITAT FRAGMENTATION IN THE AMAZON - SATELLITE DATA FROM 1978 TO 1988. *Science*, 260, 1905-1910.
- SMITS, P., DELLEPIANE, S. & SCHOWENGERDT, R. 1999. Quality assessment of image classification algorithms for land-cover mapping: a review and a proposal for a cost-based approach. *International journal of remote sensing*, 20, 1461-1486.
- SONG, C., WOODCOCK, C. E., SETO, K. C., LENNEY, M. P. & MACOMBER, S. A. 2001. Classification and change detection using Landsat TM data: when and how to correct atmospheric effects? *Remote sensing of Environment*, 75, 230-244.
- SONG, M. & CIVCO, D. L. A knowledge-based approach for reducing cloud and shadow. Proceedings of the American Society of Photogrammetry and Remote Sensing annual convention, 2002 Washington, DC: American Society of Photogrammetry and Remote Sensing., 22-26.
- SOUTHWORTH, J., MUNROE, D. & NAGENDRA, H. 2004. Land cover change and landscape fragmentation - comparing the utility of continuous and discrete analyses for a western Honduras region. *Agriculture Ecosystems & Environment*, 101, 185-205.
- SQUIRES, V. R. & SIDAHMED, A. 1997. Livestock management in dryland pastoral systems: Prospects and problems. *Annals of Arid Zone*, 36, 79-96.
- STEWART FOTHERINGHAM, A., CHARLTON, M. & BRUNSDON, C. 1996. The geography of parameter space: an investigation of spatial non-stationarity. *International Journal of Geographical Information Systems*, 10, 605-627.
- STÖCKLI, R. & VIDALE, P. L. 2004. European plant phenology and climate as seen in a 20-year AVHRR land-surface parameter dataset. *International Journal of Remote Sensing*, 25, 3303-3330.
- STOSIC, T., TELESKA, L., DA COSTA, S. L. L. & STOSIC, B. 2016. Identifying drought-induced correlations in the satellite time series of hot pixels recorded in the Brazilian Amazon by means of the detrended fluctuation analysis. *Physica A: Statistical Mechanics and its Applications*, 444, 660-666.
- SUEPA, T., QI, J., LAWAWIROJWONG, S. & MESSINA, J. P. 2016. Understanding spatio-temporal variation of vegetation phenology and rainfall seasonality in the monsoon Southeast Asia. *Environmental research*, 147, 621-629.
- SULLIVAN, S. & ROHDE, R. 2002. On non-equilibrium in arid and semi-arid grazing systems. *Journal of Biogeography*, 29, 1595-1618.
- SUZUKI, R., XU, J. & MOTOYA, K. 2006. Global analyses of satellite-derived vegetation index related to climatological wetness and warmth. *International journal of climatology*, 26, 425-438.















- SWAN, A. R. & SANDILANDS, M. Introduction to geological data analysis. *International Journal of Rock Mechanics and Mining Sciences and Geomechanics Abstracts*, 1995. 387A.
- SYMON, D. E. 1974. The growth of *Dracaena draco* "dragon's blood tree". *J Arnold Arbor*, 55, 51-58.
- TAN, B., HU, J. N., HUANG, D., YANG, W. Z., ZHANG, P., SHABANOV, N. V., KNYAZIKHIN, Y., NEMANI, R. R. & MYNENI, R. B. 2005. Assessment of the broadleaf crops leaf area index product from the Terra MODIS instrument. *Agricultural and Forest Meteorology*, 135, 124-134.
- TEILLET, P. & FEDOSEJEVS, G. 1995. On the dark target approach to atmospheric correction of remotely sensed data. *Canadian Journal of Remote Sensing*, 21, 374-387.
- THOMPSON, D. R., ROBERTS, D. A., GAO, B. C., GREEN, R. O., GUILD, L., HAYASHI, K., KUDELA, R. & PALACIOS, S. 2016. Atmospheric correction with the Bayesian empirical line. *Optics express*, 24, 2134-2144.
- TIAN, H., CAO, C., CHEN, W., BAO, S., YANG, B. & MYNENI, R. B. 2015. Response of vegetation activity dynamic to climatic change and ecological restoration programs in Inner Mongolia from 2000 to 2012. *Ecological Engineering*, 82, 276-289.
- TODD, S. W., HOFFER, R. M. & MILCHUNAS, D. G. 1998. Biomass estimation on grazed and ungrazed rangelands using spectral indices. *International Journal of Remote Sensing*, 19, 427-438.
- TOURRE, Y., JARLAN, L., LACAUX, J., ROTELA, C. & LAFAYE, M. 2008. Spatio-temporal variability of NDVI-precipitation over southernmost South America: possible linkages between climate signals and epidemics. *Environmental Research Letters*, 3, 044008.
- TOUTIN, T. 2004. Review article: Geometric processing of remote sensing images: models, algorithms and methods. *International Journal of Remote Sensing*, 25, 1893-1924.
- TOWNSHEND, J. R. G., JUSTICE, C. O., GURNEY, C. & MCMANUS, J. 1992. The impact of misregistration on change detection. *IEEE Transactions on Geoscience and Remote Sensing*, 30, 1054-1060.
- TRODD, N. M. & DOUGILL, A. J. 1998. Monitoring vegetation dynamics in semi-arid African rangelands - Use and limitations of Earth observation data to characterize vegetation structure. *Applied Geography*, 18, 315-330.
- TSAI, H. P. & YANG, M.-D. Relating Vegetation Dynamics to Climate Variables in Taiwan Using 1982–2012 NDVI3g Data.
- TUCKER, C. J., DREGNE, H. E. & NEWCOMB, W. W. 1991. EXPANSION AND CONTRACTION OF THE SAHARA DESERT FROM 1980 TO 1990. *Science*, 253, 299-301.
- TUCKER, C. J., SLAYBACK, D. A., PINZON, J. E., LOS, S. O., MYNENI, R. B. & TAYLOR, M. G. 2001. Higher northern latitude normalized difference vegetation index and growing season trends from 1982 to 1999. *International journal of biometeorology*, 45, 184-190.
- TURNBULL, L., WAINWRIGHT, J. & BRAZIER, R. E. 2008a. A conceptual framework for understanding semi-arid land degradation: ecohydrological interactions across multiple-space and time scales. *Ecohydrology*, 1, 23-34.
- TURNBULL, L., WAINWRIGHT, J. & BRAZIER, R. E. 2008b. A conceptual framework for understanding semi-arid land degradation: ecohydrological interactions across multiple-space and time scales.
- TURNER, D. P., RITTS, W. D., COHEN, W. B., MAEIRSPERGER, T. K., GOWER, S. T., KIRSCHBAUM, A. A., RUNNING, S. W., ZHAO, M., WOFYSY, S. C. & DUNN, A. L. 2005. Site-level evaluation of satellite-based global terrestrial gross primary production and net primary production monitoring. *Global Change Biology*, 11, 666-684.
- UNCCD 1994. United Nations convention to combat desertification in countries experiencing serious drought and/or desertification, particularly in Africa. Permanent Secretariat UNCCD, Bonn: UNCCD.
- UNDP/UNEP. INTERGOVERNMENTAL NEGOTIATING COMMITTEE FOR THE ELABORATION OF AN INTERNATIONAL CONVENTION TO COMBAT DESERTIFICATION IN THOSE COUNTRIES EXPERIENCING SERIOUS DROUGHT AND/OR DESERTIFICATION. *In: SECRETARIAT, N. B. T., ed. ELABORATION OF AN INTERNATIONAL CONVENTION TO COMBAT DESERTIFICATION IN COUNTRIES EXPERIENCING SERIOUS DROUGHT AND/OR DESERTIFICATION, PARTICULARLY IN AFRICA*, 1994 Paris. 4.
- UNESCO 2008. Socotra Archipelago.

- VAN AUKEN, O. W. 2000. Shrub invasions of North American semiarid grasslands. *Annual Review of Ecology and Systematics*, 197-215.
- VANBREEMEN, N. 1993. SOILS AS BIOTIC CONSTRUCTS FAVORING NET PRIMARY PRODUCTIVITY. *Geoderma*, 57, 183-211.
- VERBESSELT, J., HYNDMAN, R., NEWNHAM, G. & CULVENOR, D. 2010. Detecting trend and seasonal changes in satellite image time series. *Remote sensing of Environment*, 114, 106-115.
- VERHEYE, W. 2006. Dry lands and desertification. *Land use, land cover and soil sciences*.
- VIBHUTE, A. D., DHUMAL, R. K., NAGNE, A. D., RAJENDRA, Y. D., KALE, K. & MEHROTRA, S. Analysis, Classification, and Estimation of Pattern for Land of Aurangabad Region Using High-Resolution Satellite Image. Proceedings of the Second International Conference on Computer and Communication Technologies, 2016. Springer, 413-427.
- VILLWOCK, G. 1991. *Beiträge zur physischen Geographie und Landschaftsgliederung des südlichen Jemen (ehemals VDRJ)*, Reichert.
- VINTON, M. A. & BURKE, I. C. 1995. INTERACTIONS BETWEEN INDIVIDUAL PLANT-SPECIES AND SOIL NUTRIENT STATUS IN SHORTGRASS STEPPE. *Ecology*, 76, 1116-1133.
- VOLCANI, A., KARNIELI, A. & SVORAY, T. 2005. The use of remote sensing and GIS for spatio-temporal analysis of the physiological state of a semi-arid forest with respect to drought years. *Forest Ecology and Management*, 215, 239-250.
- WACKERNAGEL, H. 1998. Multivariate Geostatistics. Berlin, Springer-Verlag.
- WAGNER, W., LUCKMAN, A., VIETMEIER, J., TANSEY, K., BALZTER, H., SCHMULLIUS, C., DAVIDSON, M., GAVEAU, D., GLUCK, M. & LE TOAN, T. 2003. Large-scale mapping of boreal forest in SIBERIA using ERS tandem coherence and JERS backscatter data. *Remote Sensing of Environment*, 85, 125-144.
- WAINWRIGHT, J., PARSONS, A. J., SCHLESINGER, W. H. & ABRAHAMMS, A. D. 2002. Hydrology-vegetation interactions in areas of discontinuous flow on a semi-arid bajada, Southern New Mexico. *Journal of Arid Environments*, 51, 319-338.
- WANG, G. L. & ELTAHIR, E. A. B. 2000a. Biosphere-atmosphere interactions over West Africa. II: Multiple climate equilibria. *Quarterly Journal of the Royal Meteorological Society*, 126, 1261-1280.
- WANG, G. L. & ELTAHIR, E. A. B. 2000b. Role of vegetation dynamics in enhancing the low-frequency variability of the Sahel rainfall. *Water Resources Research*, 36, 1013-1021.
- WANG, J., MENG, J. J. & CAI, Y. L. 2008a. Assessing vegetation dynamics impacted by climate change in the southwestern karst region of China with AVHRR NDVI and AVHRR NPP time-series. *Environmental Geology*, 54, 1185-1195.
- WANG, S., HUANG, C., ZHANG, L., LIN, Y., CEN, Y. & WU, T. 2016. Monitoring and Assessing the 2012 Drought in the Great Plains: Analyzing Satellite-Retrieved Solar-Induced Chlorophyll Fluorescence, Drought Indices, and Gross Primary Production. *Remote Sensing*, 8, 61.
- WANG, T.-C., XIONG, Y.-C., GE, J.-P., WANG, S.-M., LI, Y., YUE, D.-X., WANG, T.-M. & WANG, G. 2008b. Four-year dynamic of vegetation on mounds created by zokors (*Myospalax baileyi*) in a subalpine meadow of the Qinghai-Tibet Plateau. *Journal of arid environments*, 72, 84-96.
- WEISS, J. L., GUTZLER, D. S., COONROD, J. E. A. & DAHM, C. N. 2004. Long-term vegetation monitoring with NDVI in a diverse semi-arid setting, central New Mexico, USA. *Journal of Arid Environments*, 58, 249-272.
- WESTERN, A. W., ZHOU, S. L., GRAYSON, R. B., MCMAHON, T. A., BLOSCHL, G. & WILSON, D. J. 2004. Spatial correlation of soil moisture in small catchments and its relationship to dominant spatial hydrological processes. *Journal of Hydrology*, 286, 113-134.
- WHITE, F. 1983. The vegetation of Africa, a descriptive memoir to accompany the UNESCO/AETFAT/UNSO vegetation map of Africa (3 Plates, Northwestern Africa, Northeastern Africa, and Southern Africa, 1: 5,000,000). Unesco, Paris.
- WIENS, J., SUTTER, R., ANDERSON, M., BLANCHARD, J., BARNETT, A., AGUILAR-AMUCHASTEGUI, N., AVERY, C. & LAINE, S. 2009. Selecting and conserving lands for biodiversity: the role of remote sensing. *Remote Sensing of Environment*, 113, 1370-1381.
- WIENS, J. A. & HOBBS, R. J. 2015. Integrating Conservation and Restoration in a Changing World. *BioScience*, 65, 302-312.

- WIERSEMA, J. H. & LEON, B. 2016. *World economic plants: a standard reference*, CRC press.
- WILLIS, K. S. 2015. Remote sensing change detection for ecological monitoring in United States protected areas. *Biological Conservation*, 182, 233-242.
- WRANIK, W. Faunistic notes on Soqotra island. Proceedings of the First International Symposium on Soqotra island: present & future, Aden, 1996. 135-198.
- WRANIK, W. 2003. *Fauna of the Socotra Archipelago: field guide*, Univ.-Dr.
- XIAO, P., ZHANG, X., WANG, D., YUAN, M., FENG, X. & KELLY, M. 2016. Change detection of built-up land: A framework of combining pixel-based detection and object-based recognition. *ISPRS Journal of Photogrammetry and Remote Sensing*, 119, 402-414.
- XIAO, X., BOLES, S., LIU, J., ZHUANG, D., FROLKING, S., LI, C., SALAS, W. & MOORE III, B. 2005. Mapping paddy rice agriculture in southern China using multi-temporal MODIS images. *Remote Sensing of Environment*, 95, 480-492.
- XIE, Y., SHA, Z. & YU, M. 2008. Remote sensing imagery in vegetation mapping: a review. *Journal of Plant Ecology*, 1, 9-23.
- YANG, L., WYLIE, B. K., TIESZEN, L. L. & REED, B. C. 1998. An analysis of relationships among climate forcing and time-integrated NDVI of grasslands over the US northern and central Great Plains. *Remote Sensing of Environment*, 65, 25-37.
- YU, Q., GONG, P., CLINTON, N., BIGING, G., KELLY, M. & SCHIROKAUER, D. 2006. Object-based detailed vegetation classification with airborne high spatial resolution remote sensing imagery. *Photogrammetric Engineering & Remote Sensing*, 72, 799-811.
- YU, W., ZHOU, W., QIAN, Y. & YAN, J. 2016. A new approach for land cover classification and change analysis: Integrating backdating and an object-based method. *Remote Sensing of Environment*, 177, 37-47.
- YUAN, X., LI, L., CHEN, X. & SHI, H. 2015. Effects of precipitation intensity and temperature on NDVI-based grass change over Northern China during the period from 1982 to 2011. *Remote Sensing*, 7, 10164-10183.
- ZHANG, P., ANDERSON, B., BARLOW, M., TAN, B. & MYNENI, R. B. 2004. Climate-related vegetation characteristics derived from Moderate Resolution Imaging Spectroradiometer (MODIS) leaf area index and normalized difference vegetation index. *Journal of Geophysical Research: Atmospheres (1984–2012)*, 109.
- ZHANG, P., GONG, M., SU, L., LIU, J. & LI, Z. 2016. Change detection based on deep feature representation and mapping transformation for multi-spatial-resolution remote sensing images. *ISPRS Journal of Photogrammetry and Remote Sensing*, 116, 24-41.
- ZHENG, D. L., HEATH, L. S. & DUCEY, M. J. 2008. Satellite detection of land-use change and effects on regional forest aboveground biomass estimates. *Environmental Monitoring and Assessment*, 144, 67-79.
- ZHOU, D., ZHAO, X., HU, H., SHEN, H. & FANG, J. 2015. Long-term vegetation changes in the four mega-sandy lands in Inner Mongolia, China. *Landscape Ecology*, 30, 1613-1626.
- ZHOU, Y. & LEUNG, Y. 2010. Multifractal temporally weighted detrended fluctuation analysis and its application in the analysis of scaling behavior in temperature series. *Journal of Statistical Mechanics: Theory and Experiment*, 2010, P06021.
- ŽLIOBAITĖ, I., BIFET, A., READ, J., PFAHRINGER, B. & HOLMES, G. 2015. Evaluation methods and decision theory for classification of streaming data with temporal dependence. *Machine Learning*, 98, 455-482.
- ZUNZUNEGUI, M., BARRADAS, M. D., AIN-LHOUT, F., CLAVIJO, A. & NOVO, F. G. 2005. To live or to survive in Doñana dunes: adaptive responses of woody species under a Mediterranean climate. *Plant and soil*, 273, 77-89.

## Supplementary Appendixes

### Appendix 1. cloud cover of Socotra Island though the last 40 years

	Preview Image	Show Footprint	Show All Fields	Exclude	Order Qty	Price	 DOWNLOADS	Landsat Scene Identifier	Date Acquired
1		<a href="#">Show</a>	<a href="#">Show</a>	<input type="checkbox"/>		N/A	<a href="#">Download now</a>	LM11710511972279AAA03	1972/10/05
2		<a href="#">Show</a>	<a href="#">Show</a>	<input type="checkbox"/>		N/A	<a href="#">Download now</a>	LM11710511972351AAA04	1972/12/16
3		<a href="#">Show</a>	<a href="#">Show</a>	<input type="checkbox"/>		N/A	<a href="#">Download now</a>	LM11710511973021AAA01	1973/01/21
4		<a href="#">Show</a>	<a href="#">Show</a>	<input type="checkbox"/>		N/A	<a href="#">Download now</a>	LM11710511973039AAA01	1973/02/08
5		<a href="#">Show</a>	<a href="#">Show</a>	<input type="checkbox"/>		N/A	<a href="#">Download now</a>	LM11710511973057AAA01	1973/02/26
6		<a href="#">Show</a>	<a href="#">Show</a>	<input type="checkbox"/>		N/A	<a href="#">Download now</a>	LM11710511973183AAA03	1973/07/02
7		<a href="#">Show</a>	<a href="#">Show</a>	<input type="checkbox"/>		N/A	<a href="#">Download now</a>	LM11710511973273AAA01	1973/09/30
8		<a href="#">Show</a>	<a href="#">Show</a>	<input type="checkbox"/>		N/A	<a href="#">Download now</a>	LM11710521973003AAA03	 1973/01/03
9		<a href="#">Show</a>	<a href="#">Show</a>	<input type="checkbox"/>	<input type="checkbox"/>	5.00	Available by ordering	LM11710521973021AAA01	1973/01/21
10		<a href="#">Show</a>	<a href="#">Show</a>	<input type="checkbox"/>		N/A	<a href="#">Download now</a>	LM31710511978229AAA04	1978/08/17

	Preview Image	Show Footprint	Show All Fields	Exclude	Order Qty	Price	 DOWNLOADS	Landsat Scene Identifier	Date Acquired
1		<a href="#">Show</a>	<a href="#">Show</a>	<input type="checkbox"/>		N/A	<a href="#">Download now</a>	LE71590512006069ASN00	2006/03/10
2		<a href="#">Show</a>	<a href="#">Show</a>	<input type="checkbox"/>		N/A	<a href="#">Download now</a>	LE71590512006085ASN00	2006/03/26
3		<a href="#">Show</a>	<a href="#">Show</a>	<input type="checkbox"/>		N/A	<a href="#">Download now</a>	LE71590512006117ASN00	2006/04/27
4		<a href="#">Show</a>	<a href="#">Show</a>	<input type="checkbox"/>		N/A	<a href="#">Download now</a>	LE71590512006293ASN00	2006/10/20
5		<a href="#">Show</a>	<a href="#">Show</a>	<input type="checkbox"/>		N/A	<a href="#">Download now</a>	LE71590512006309ASN00	2006/11/05
6		<a href="#">Show</a>	<a href="#">Show</a>	<input type="checkbox"/>		N/A	<a href="#">Download now</a>	LE71590512007264ASN00	2007/09/21
7		<a href="#">Show</a>	<a href="#">Show</a>	<input type="checkbox"/>		N/A	<a href="#">Download now</a>	LE71590512007280ASN00	2007/10/07
8		<a href="#">Show</a>	<a href="#">Show</a>	<input type="checkbox"/>		N/A	<a href="#">Download now</a>	LE71590512003285ASN01	2003/10/12
9		<a href="#">Show</a>	<a href="#">Show</a>	<input type="checkbox"/>		N/A	<a href="#">Download now</a>	LE71590512004144ASN01	2004/05/23
10		<a href="#">Show</a>	<a href="#">Show</a>	<input type="checkbox"/>		N/A	<a href="#">Download now</a>	LE71590512004176ASN01	2004/06/24

**Appendix 2. Illumination of clouds with clouds shadows and SLC-off image gaps and adjusted image (down).**

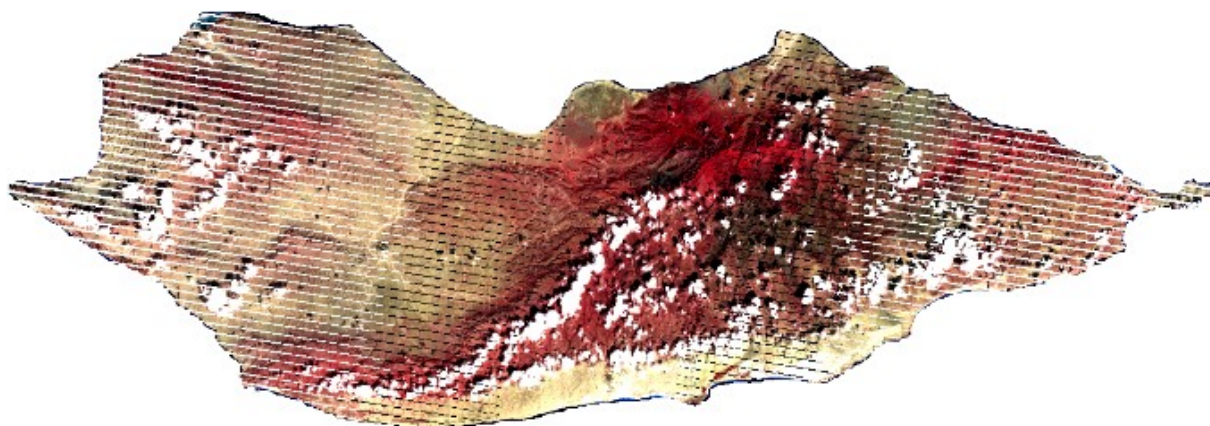


Image before cloud elimination.

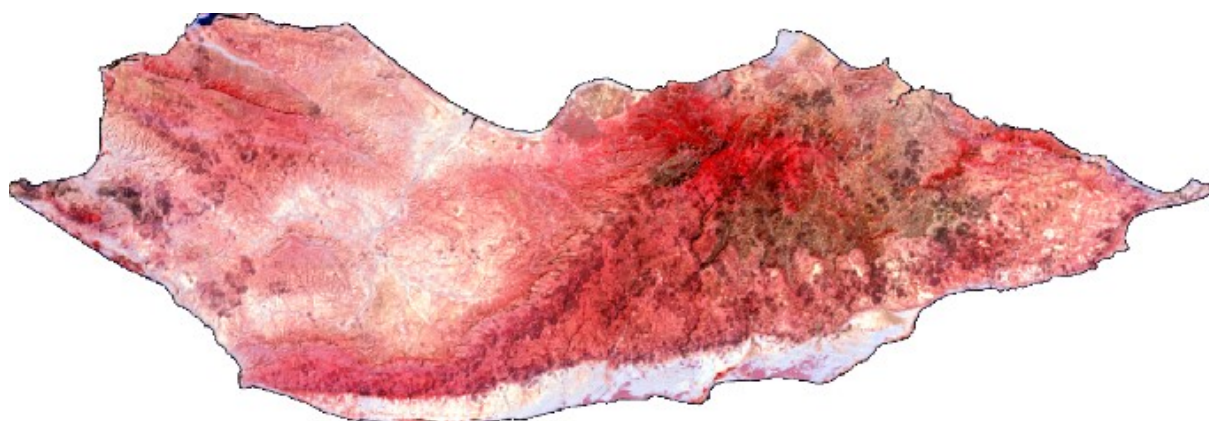
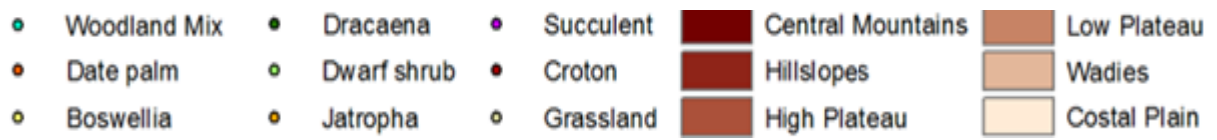
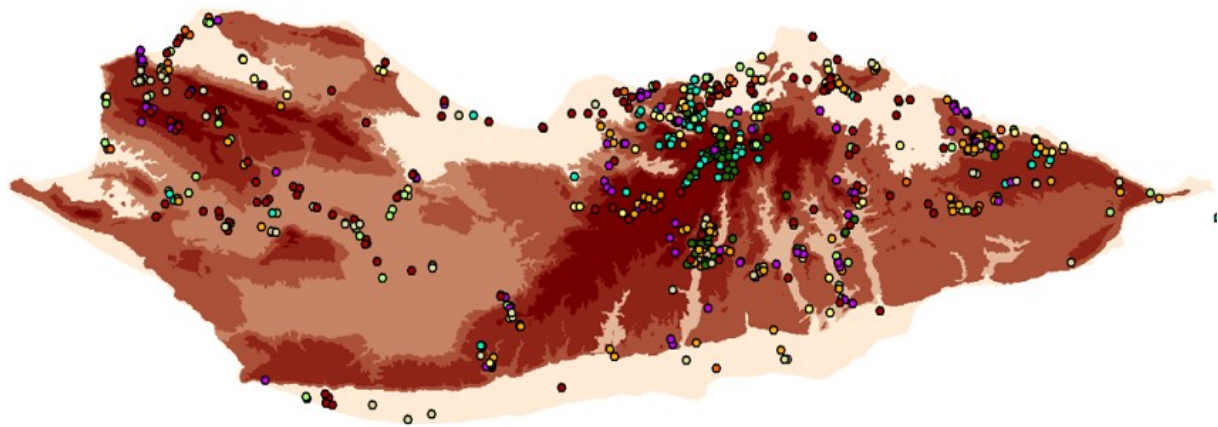
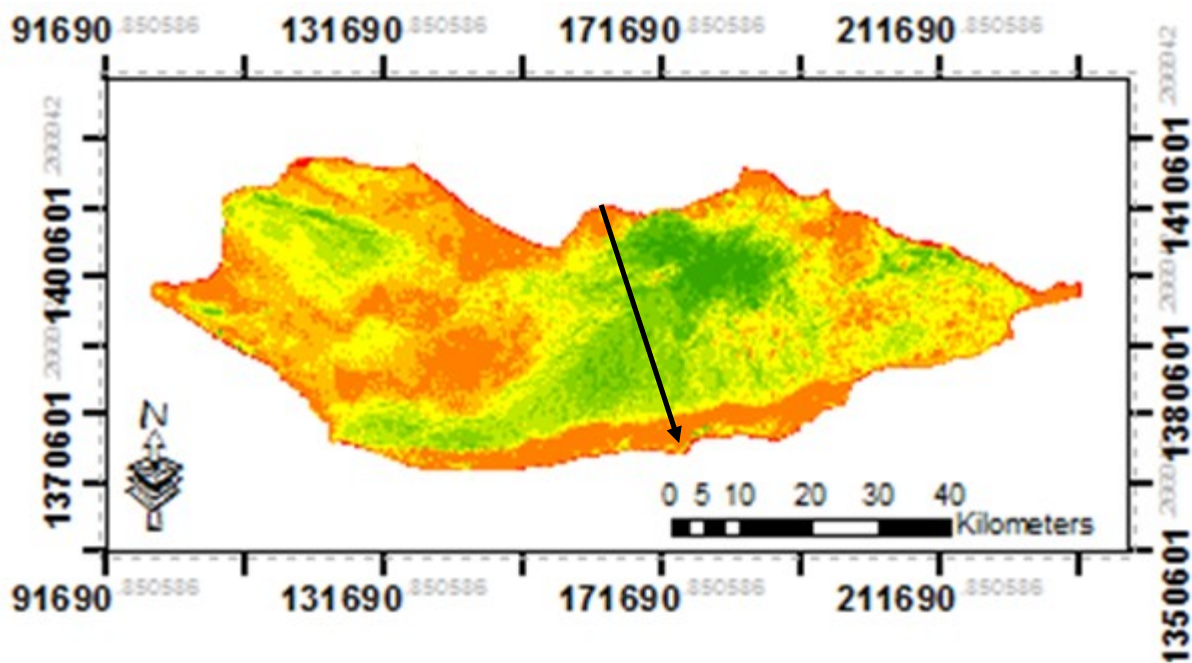
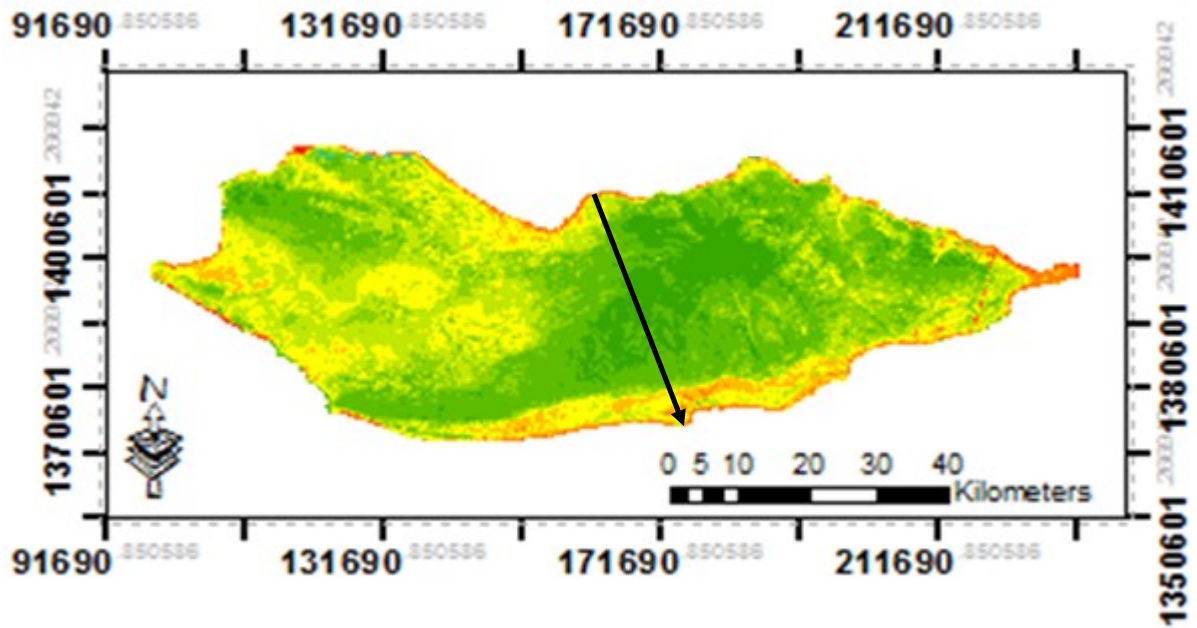


Image after cloud elimination.

Appendix 3. Training sites per ecological zones.

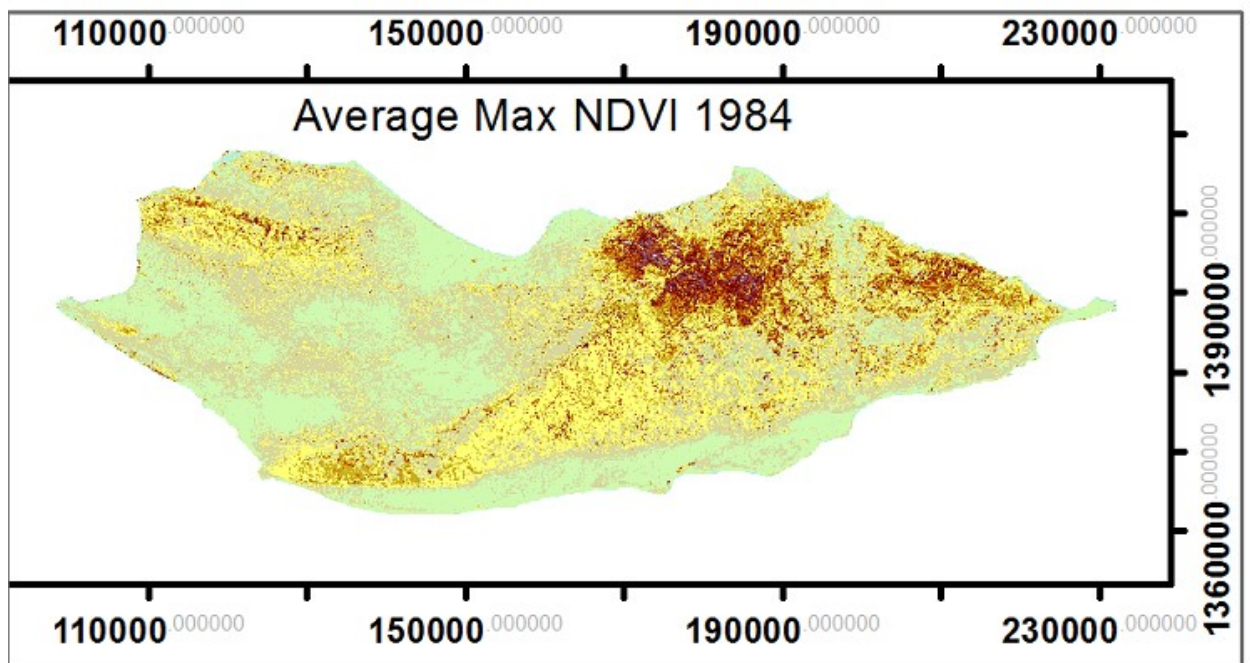
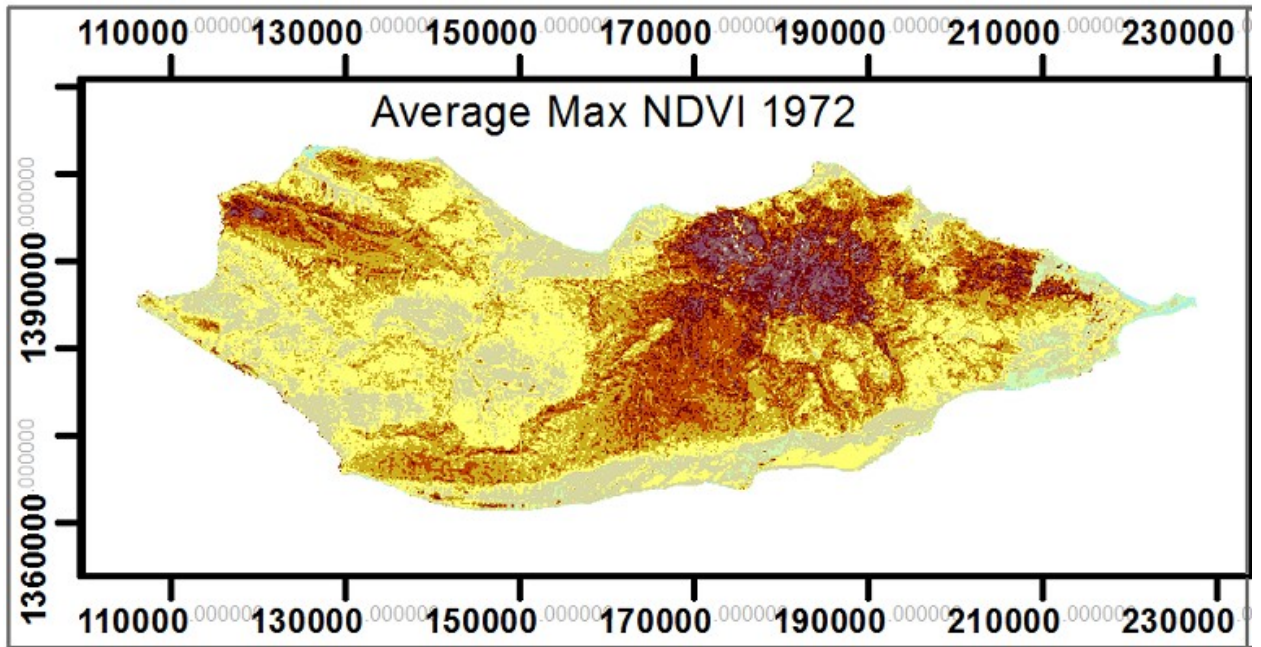


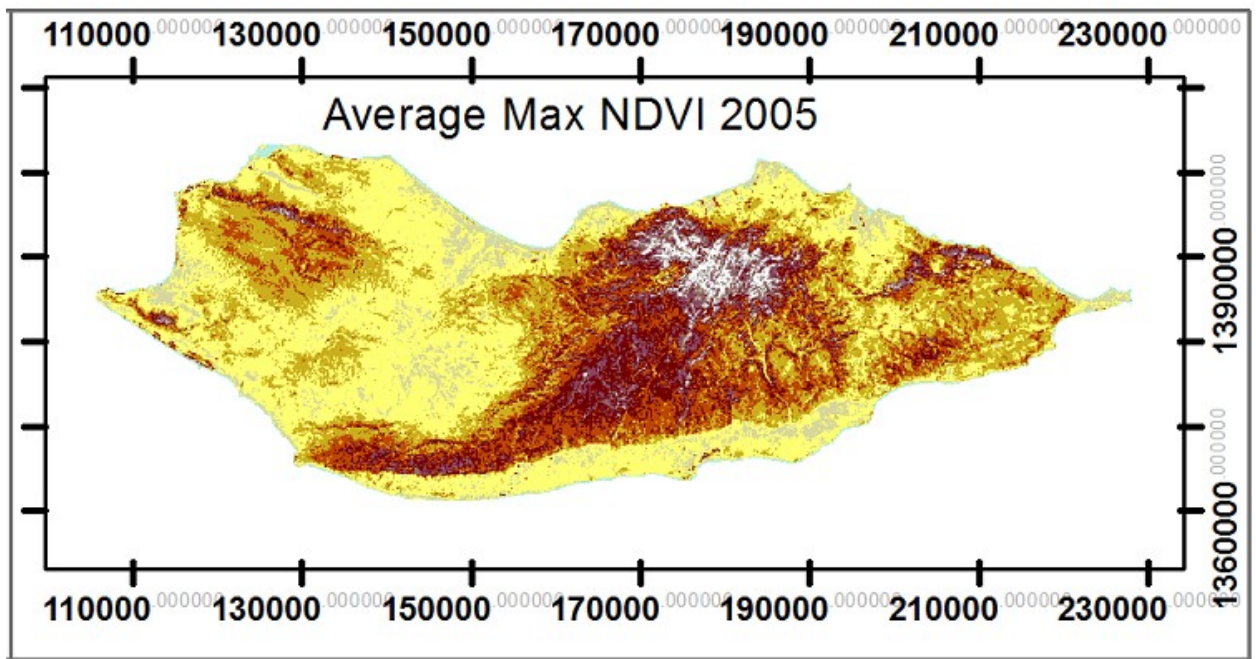
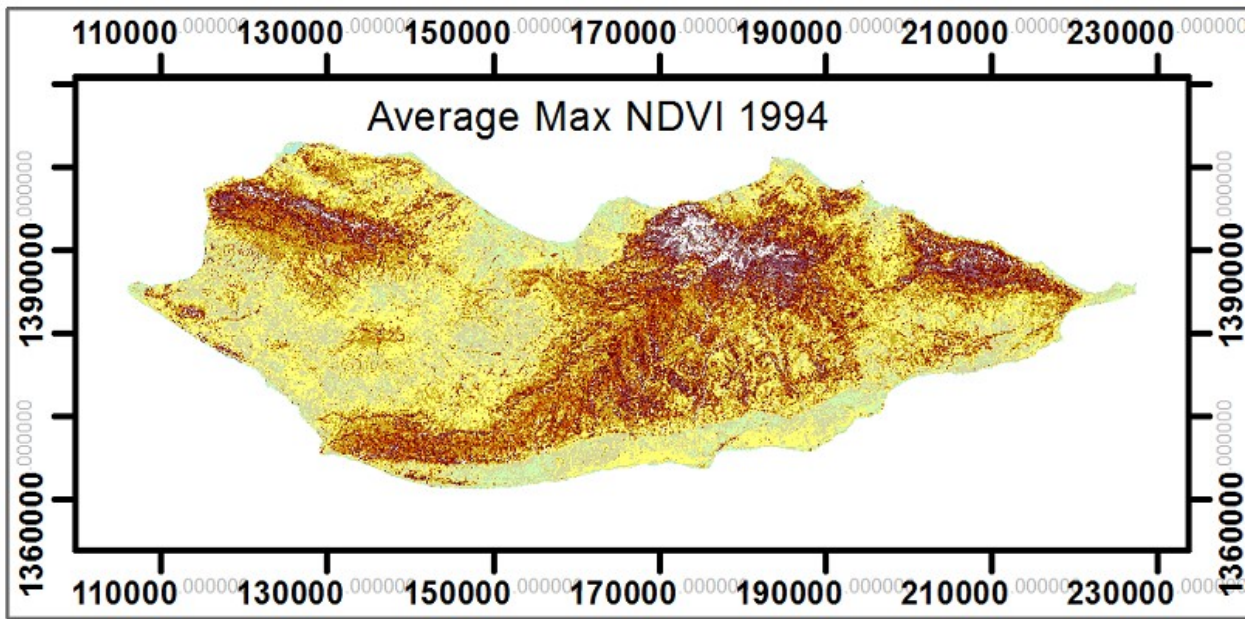
Appendix 4. Spatial distribution of NDVI series and North-South spatial profiles in 1972 and 2005

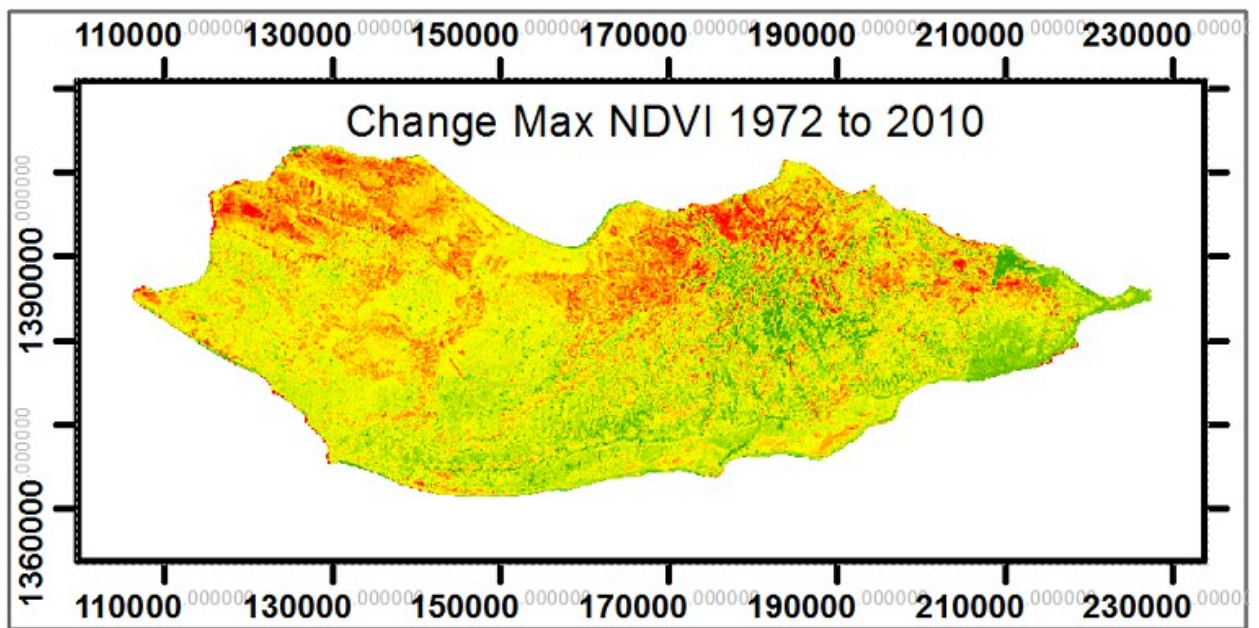
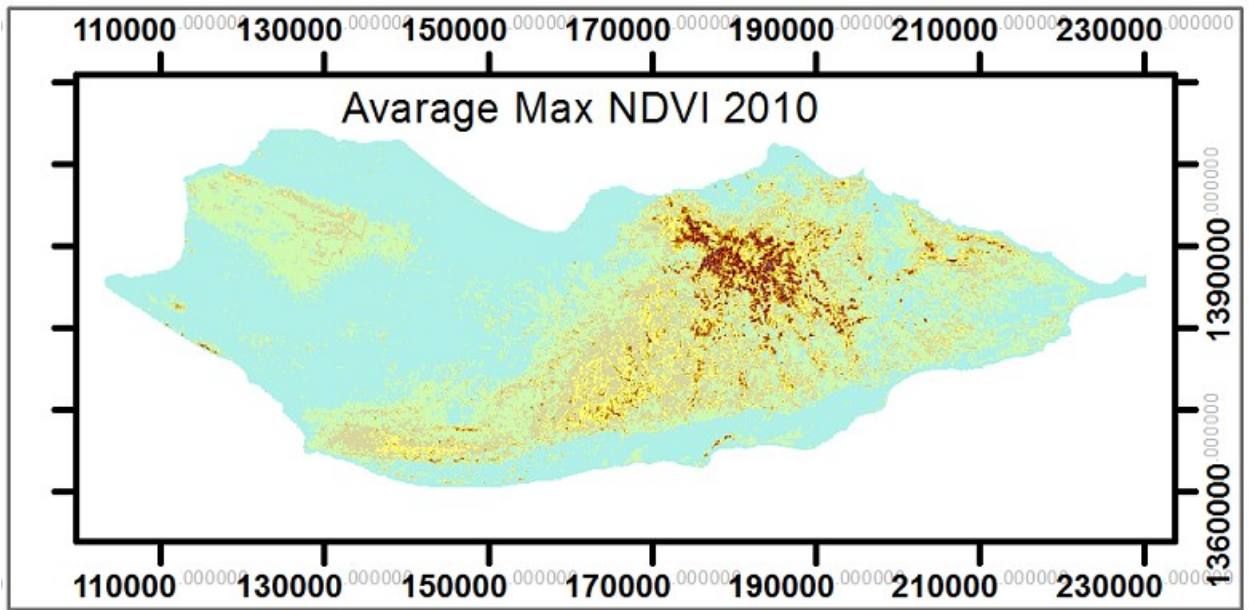




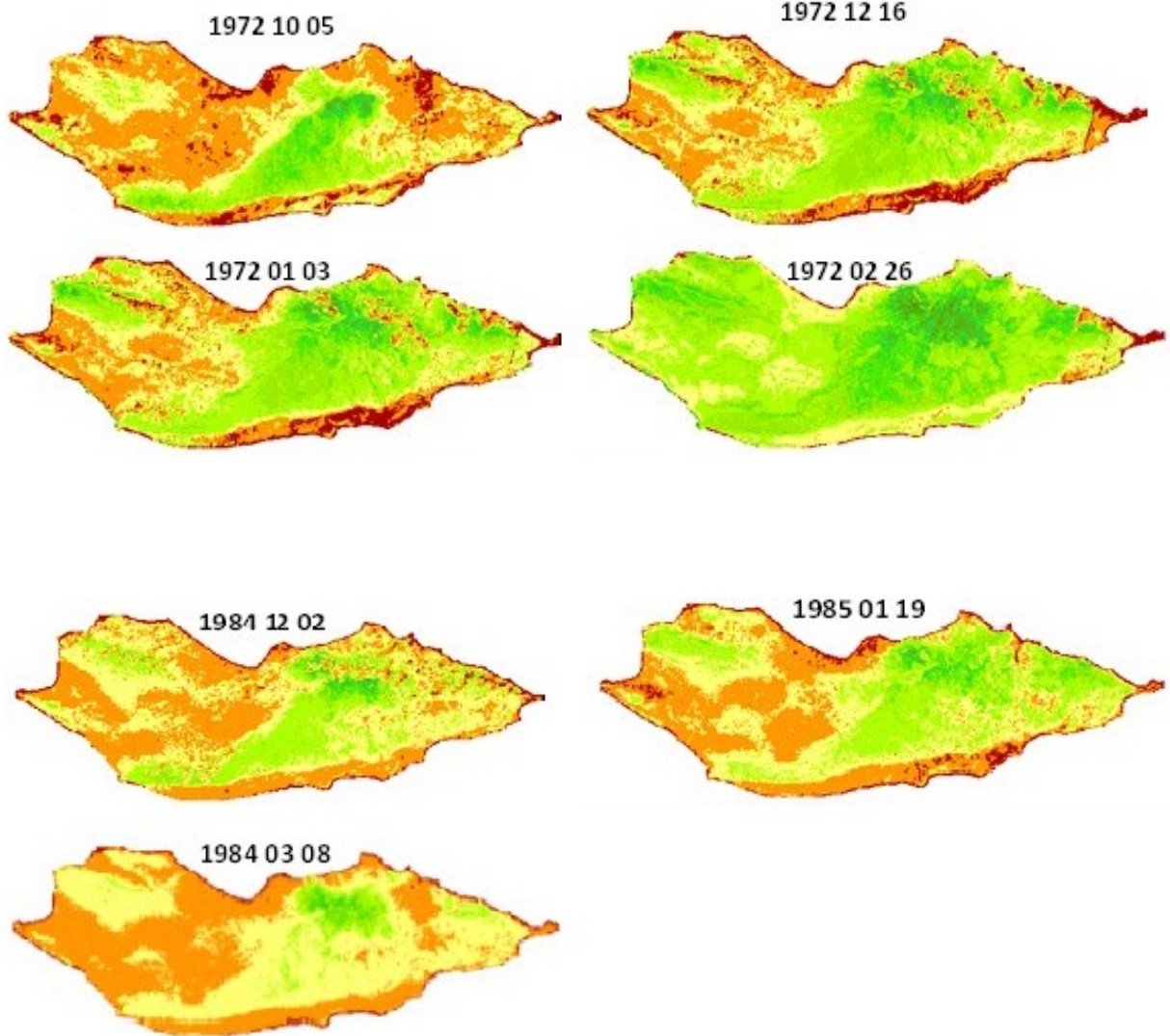
Appendix 5: Maps of time-integrated NDVI from 1972 to 2010 (mean maximum within seasons)

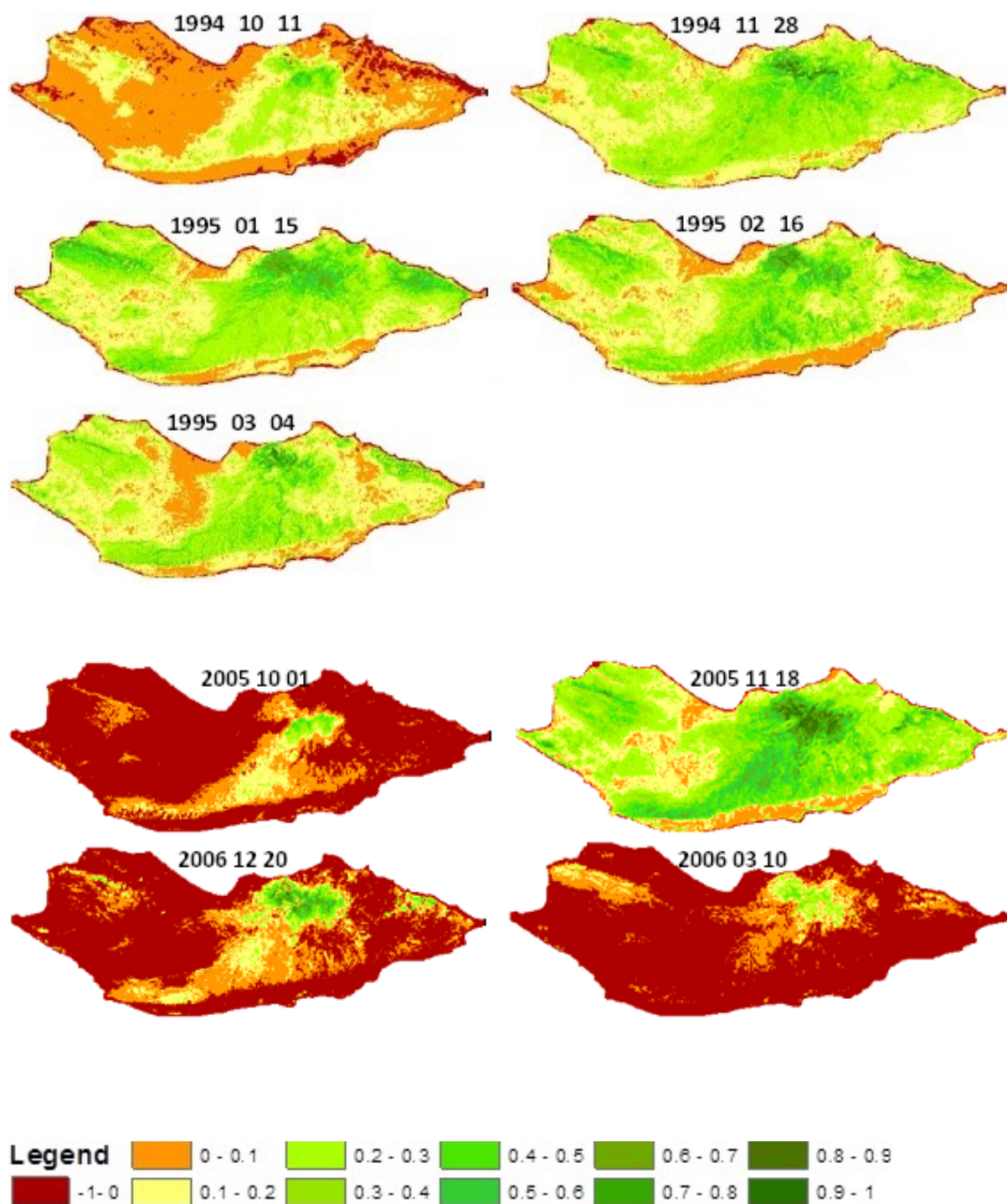






Appendix 6. Within-season NDVI variation (a) for 70s, (b) 80s, (c) 90s and (d) 00s, respectively.





## Acknowledgments

Foremost, I would like to express my sincere gratitude to my family, my wife and my children for their patience and supporting me spiritually throughout my life and during my study. I also want to thank my Father for his spiritually support and all my family members.

O God, who hast commanded us to honor our father and our mother; in Thy mercy have pity on the soul of my mother, and forgive her, her trespasses; and make me to see her again in the Paradise. Ameen.

My sincere thanks goes to my incredible patient supervisor Gottfried Jetschke for his guidance and continuous support, patience, motivation, enthusiasm, and immense knowledge. Especially the fieldwork of this research wouldn't have been possible without his generous financial support. Besides my supervisor, I would like to thank Dr. Sören Hese for his kind guidance and help in all the time of research, enlightening me and who never got tired of answering my questions. In fact, I acknowledge him as my second supervisor.

My deepest gratitude of course, to my Chiefs in the Agriculture Research and Extension Authority and my Department in Yemen. I would like to thank my colleagues in the Renewable Natural Resources Research Centre, without their patience and support this project would never have been started.

I am also deeply grateful to all my friends and colleagues from the Institute of Ecology and Institute for Geography for their helpful discussions and fruitful support.

These acknowledgments would not be completed without mentioning the people who accompanied and help me during the fieldworks on Socotra Island. All people from SCDP and EPA specially my field accompany Ahmed Adeeb.

Finally, all my best regards go to all those people whom I not listed and were helping me in all the time of research and talking with me and were always interested in the work.

Abdulmaged Alhemiary



## Declaration of Honour (Selbständigkeitserklärung)

Herewith, I myself declare

that I have composed and written the dissertation myself, that the material presented here is the result of my original research and that I have not used any sections of text from a third party or from dissertations of others without identifying them as such, and have acknowledged all assistance, personal communication, and sources within the work.

The thesis has been prepared under the supervision of PD Dr. Gottfried Jetschke and PD Dr. Sören Hese, who have assisted with the choice and assessment of materials and with some support while writing the manuscript.

Jena, 28. 10. 2016

(Abdulmaged Alhemiary)

A handwritten signature in blue ink, appearing to read 'Alhemiary', is written on a small white rectangular piece of paper.

Name  
Address



Telephone(s)

E-mail

Nationality

Date of birth

Dates

Occupation

Name and address of employer

Type of business or sector

Dates

Occupation or position held

Main activities

Name and address of employer

Type of business or sector

Dates

Occupation or position

Main activities

### Education and training

Dates

Title of qualification awarded

Principal subjects/occupational skills covered

Name and type of organisation providing education and training

Dates

Title of qualification awarded

Principal subjects/occupational skills covered

Name and type of organisation providing education and training

## Alhemiary, Abdulmaged Abdulraqueeb Farhan

Institute for Ecology

Dornburger Str. 159

D-07743, Jena Tel: (03641) 940404 Mobile: (+49) 176 21851968

malhemiary@yahoo.co.uk

Yemeni

1/1/1968

From June 2005 till March 2008.

**Technical Director for the Natural Resource Research Centre (RNRRC).**

**Agricultural Research and Extension Authority, Renewable Natural Resources Research Centre, Dhamar, Yemen.**

Government.

From 1997 to 2001

**Head of Remote sensing and GIS Department.**

Supervising all section activities.

Agricultural Research and Extension Authority, Renewable Natural Resources Research Centre, Dhamar, Yemen.

Government.

From 1991 to 1995

**Head of Database Management Department and Acting Soil Survey and Land Evaluation Project Manager.**

Database manager.

Sep. 2009 till now (with 4 times interruption = 32 months due to financial, political and social problems in Yemen);

8. Aug 2009 – 22. Jul. 2010	12. Jul. 2012 – 26. Dec 2012
10. Apr 2013 – 28. Dec. 2013	28 Jun 2014 – 13. Jan 2015

**PhD student.**

Time Series Analysis of High Resolution Remote Sensing Data to Assess Degradation of Vegetation Cover of the Island of Socotra (Yemen).

**Institut für Ökologie, Biologisch-Pharmazeutische Fakultät, Friedrich-Schiller-Universität Jena**

1/4/2008 to 5/4/2009

**Visitor researcher**

Attend module courses in photogrammetric, GIS, Remote Sensing, Geo-Informatics and conducting literature review for my PhD proposal.

**International Institute for Geo-Information Science and Earth Observation (ITC) Netherlands.**



Dates  
 Title of qualification awarded  
 Principal subjects/occupational skills covered  
 Occupational:  
 Name and type of organisation providing education and training

From 1996 to 1998  
**MSc. LAND and Water Management (LAND RESOURCES MANAGEMENT OPTION).**  
 Geographic Information Systems (GIS) Technology / Applications, Aerial photograph Interpretation, Applied Remote Sensing, Resources Survey, Hydrology and Water resources, Surveying, Soil Conservation, Economics of Resource Management, Introduction to Management, Multivariate Analysis, Ecology and Range Land Management.  
 Science applied to land resources management and use planning.  
**Faculty of Agricultural Engineering, Food Production and Rural Land Use,**  
**Silsoe, Cranfield University**  
**Bedfordshire**  
**United Kingdom.**

Dates  
 Title of qualification awarded  
 Principal subjects/occupational skills covered  
 Name and type of organisation providing education and training  
 Personal skills and competences

From 1982 to 1986  
**B.Sc. Agricultural Engineering- (SOIL SCIENCE)**  
 Science applied to plants, water and land resources management.  
**Faculty of Agriculture**  
**Cairo University**  
**Cairo**  
**Egypt.**

Mother tongue(s)

Arabic

Other language(s)

Self-assessment  
 European level (\*)

Understanding				Speaking				Writing	
Listening		Reading		Spoken interaction		Spoken production			
C1	Proficient user	B2	Independent user	C1	Proficient user	B2	Independent user	B2	Independent user
C2	Proficient user	C2	Proficient user	C2	Proficient user	C2	Proficient user	C2	Proficient user
B2	Independent user	B2	Independent user	B2	Independent user	B1	Independent user	B2	Independent user

**English**

**Arabic**

**German**